GALERKIN APPROXIMATION OF A NONLINEAR PARABOLIC INTERFACE PROBLEM ON FINITE AND SPECTRAL ELEMENTS

BY

MATTHEW OLAYIWOLA, ADEWOLE
MATRIC NO: 161396

B.Tech. Pure and Applied Maths. (LAUTECH), M.Sc. Maths. (Ibadan)

A Thesis in the Department of Mathematics,

Submitted to the Faculty of Sciences

in partial fulfilment of the requirements for the Degree of

DOCTOR OF PHILOSOPHY

of the

UNIVERSITY OF IBADAN

MAY 2017

Abstract

Nonlinear parabolic interface problems are frequently encountered in the modelling of physical processes which involved two or more materials with different properties. Research had focused largely on solving linear parabolic interface problems with the use of Finite Element Method (FEM). However, Spectral Element Method (SEM) for approximating nonlinear parabolic interface problems is scarce in literature. This work was therefore designed to give a theoretical framework for the convergence rates of finite and spectral element solutions of a nonlinear parabolic interface problem under certain regularity assumptions on the input data.

A nonlinear parabolic interface problem of the form

$$u_t - \nabla \cdot (a(x,u)\nabla u) = f(x,u) \quad \text{in} \quad \Omega \times (0,T]$$

with initial and boundary conditions

$$u(x,0) = u_0(x) \,, \qquad u(x,t) = 0 \qquad \text{on} \quad \partial\Omega \times [0,T]$$

and interface conditions

$$[u]_\Gamma = 0, \qquad \left[a(x,u)\frac{\partial u}{\partial n}\right]_\Gamma = g(x,t)$$

was considered on a convex polygonal domain $\Omega \in \mathbb{R}^2$ with the assumption that the unknown function $u(x,t)$ is of low regularity across the interface, where $f : \Omega \times \mathbb{R} \to \mathbb{R}$, $a : \Omega \times \mathbb{R} \to \mathbb{R}$ are given functions and $g : [0,T] \to H^2(\Gamma) \cap H^{1/2}(\Gamma)$ is the interface function. Galerkin weak formulation was used and the solution domain was discretised into quasi-uniform triangular elements after which the unknown function was approximated by piecewise linear functions on the finite elements. The time discretisation was based on Backward Difference Schemes (BDS). The implementation of this was based on predictor-corrector method due to the presence of nonlinear terms. A four-step linearised FEM-BDS was proposed and analysed to ease the computational stress and improve on the accuracy of the

time-discretisation. On spectral elements, the formulation was based on Legendre polynomials evaluated at Gauss-Lobatto-Legendre points. The integrals involved were evaluated by numerical quadrature. The linear theories of interface and non-interface problems as well as Sobolev imbedding inequalities were used to obtain the a priori and the error estimates. Other tools used to obtain the error estimates were approximation properties of linear interpolation operators and projection operators.

The a priori estimates of the weak solution were obtained with low regularity assumption on the solution across the interface, and almost optimal convergence rates of $O\left(h\left(1+\frac{1}{|\log h|}\right)^{1/2}\right)$ and $O\left(h^2\left(1+\frac{1}{|\log h|}\right)\right)$ in the $L^2(0,T;H^1(\Omega))$ and $L^2(0,T;L^2(\Omega))$ norms respectively were established for the spatially discrete scheme. Almost optimal convergence rates of $O\left(k+h\left(1+\frac{1}{|\log h|}\right)\right)$ and $O\left(k+h^2\left(1+\frac{1}{|\log h|}\right)\right)$ in the $L^2(0,T;H^1(\Omega))$ and $L^2(0,T;L^2(\Omega))$ norms were obtained for the fully discrete scheme based on the backward Euler scheme, respectively for small mesh size h and time step k. Similar error estimates were obtained for two-step implicit scheme and four-step linearised FEM-BDS. The solution by SEM was found to converge spectrally in the $L^2(0,T;L^2(\Omega))$-norm as the degree of the Legendre polynomial increases.

Convergence rates of almost optimal order in the $L^2(0,T;H^1(\Omega))$ and $L^2(0,T;L^2(\Omega))$ norms for finite element approximation of a nonlinear parabolic interface problem were established when the integrals involved were evaluated by numerical quadrature.

Keywords: Finite element, Spectral element, Nonlinear parabolic problem
Word count: 438

ACKNOWLEDGEMENTS

CERTIFICATION

I certify that this work was carried out by Mr. M.O. Adewole in the Department of Mathematics, University of Ibadan.

_____

Supervisor

V.F. Payne,

B.Sc., M.Sc., Ph.D. (Ibadan)

Professor, Department of Mathematics,

University of Ibadan, Nigeria.

DEDICATION

The project is dedicated to Almighty God.

Contents

List of Figures

List of Tables

Chapter 1

INTRODUCTION

Partial Differential Equations (PDEs) have variety of applications to mechanics, electrostatics, quantum mechanics and many other fields of physics as well as to finance. In the linear theory, solutions obey the principle of linear superposition, if certain convergence requirements are satisfied, and they often have representation formulas. However, superposition is not available for nonlinear PDEs and therefore methods needed to study nonlinear equations are quite different from those of the linear theory (Debnath, 2012). Nonlinear PDEs appear for example in non-Newtonian fluids, glaceology, rheology, nonlinear elasticity, flow through a porous medium, and image processing (Haberman, 2005 & Debnath, 2012).

In order to understand the dynamics of nature, we need to consider time evolution which often leads to parabolic partial differential equations. The most well-known linear parabolic partial differential equation is the heat equation, however, the heat equation has some unphysical features like the infinite speed of propagation. Nonlinear generalizations of the heat equation often behave more realistically. Furthermore, nonlinear models introduce new interesting phenomena from intrinsic behaviour to extinction in finite time.

Interface problems are differential equations in which the input data are either non-smooth, discontinuous or singular across one or more interfaces in the solution

domain (Kumar and Joshi, 2012). Parabolic interface problems are frequently encountered in scientific computing and industrial applications. A typical example is provided in the modelling of physical processes which involve two or more materials with different properties such as the conductivities of steel and bronze in heat diffusion (Feistauer and Sobotikova, 1990). However, the solutions of interface problems may have higher regularities in each individual material region than in the entire physical domain because of the discontinuities across the interface (Ladyzhenskaya *et al.*, 1966 and Chen & Zou, 1998). In this case, achieving higher order accuracy may be difficult using the classical method, hence there is need to find the solution to the problem by variational formulation. In what follows, we give an overview of the Finite Element Method FEM which is the fundamental method used for solving partial differential equations.

1.1   Finite Element Method

Finite element method is an approximate technique where differential equations are solved in a weak sense (in most cases). The weak form gives rises to desirable flexibilities in enforcing boundary and interface conditions. The domain under consideration is effectively discretised into smaller pieces (called elements) and an approximate piecewise polynomial solution found on each of these pieces. The dependent variable is approximated by a function that is mathematically simple (piecewise linear or other polynomial forms), on a finite set of elements, approximating the domain of the differential equation (Gockenbach, 2006 and Brenner & Scott, 2008).

In contrast with the finite element method, the finite difference method (which is the classical numerical method for solving partial differential equations) involves replacing the derivatives with difference quotients of the unknown at certain (finitely many) points to obtain the corresponding discrete problem whereas the discretisation process using the finite element method involves, basically, the

following steps (Johnson 1987, Knabner and Angermann 2002, Gockenback 2006, Kumar & Joshi 2012):

- Variationally formulation of the given problem.

- Discretisation (ie construction of the finite element space)

- Solution of the discrete problem

- Implementation of the method

The advantage of finite element method over finite difference method is that complicated geometry, general boundary conditions and variable or non-linear material properties can be handled easily. In addition, the finite element method has a solid theoretical foundation which facilitates mathematical analysis and estimation of error in the approximate finite element solution and thus makes it more reliable (Johnson, 1987).

1.1.1 Basic Concept of FEM

Finite element method (FEM) involves a sequence of steps as given earlier. When applied to a differential equation, the equation is first approximated by a piecewise polynomial function u_h which is expanded in a basis of test functions ϕ_i, and then the residual function is tested against all the basis functions. The procedure yields a linear system $KU = F$ for which the components of U are the values of u_h at the nodes. K is the stiffness matrix and F is the load vector.

For clarity, we explain this procedure using a one-dimensional elliptic problem with discontinuous coefficients:

$$\begin{cases} -\dfrac{d}{dx}\left(a(x)\dfrac{du}{dx}\right) = f(x) \\ u(0) = u(5) = 0 \end{cases} \tag{1.1.1}$$

where

$$a(x) = \begin{cases} 1 & 0 \le x < 3 \\ x & 3 \le x \le 5 \end{cases}$$

3

$$f(x) = \begin{cases} 2x^3 - \frac{18}{5}x^2 & 0 \le x < 3 \\ 8 - 4x & 3 \le x \le 5 \end{cases}$$

with interface parameters

$$[u]_{x=3} = 0 \qquad \left[a(x)\frac{du}{dx}\right]_{x=3} = -2.1$$

The exact solution to (1.1.1) is

$$u(x) = \begin{cases} \frac{1}{10}x^4(3-x) & 0 \le x < 3 \\ x^2 - 8x + 15 & 3 \le x \le 5 \end{cases}$$

$\mathcal{T}_h = \{[0,1],[1,2],[2,3],[3,4],[4,5]\}$ and S_h denotes the space of piecewise polynomial functions.

The four basis functions in S_h are illustrated in Fig 1.1 and are given as

$$v_1 = \begin{cases} x & x \in [0,1) \\ 2-x & x \in [1,2) \\ 0 & \text{elsewhere} \end{cases} \qquad v_3 = \begin{cases} x-2 & x \in [2,3) \\ 4-x & x \in [3,4) \\ 0 & \text{elsewhere} \end{cases}$$

$$v_2 = \begin{cases} x-1 & x \in [1,2) \\ 3-x & x \in [2,3) \\ 0 & \text{elsewhere} \end{cases} \qquad v_4 = \begin{cases} x-3 & x \in [3,4) \\ 5-x & x \in [4,5] \\ 0 & \text{elsewhere} \end{cases}$$

Multiply (1.1.1) by $\phi = v_1 + v_2 + v_3 + v_4$ to obtain the weak form, then integrate over $\mathcal{T}_h$ to obtain the algebraic system

$$\begin{pmatrix} a(v_1,v_1) & a(v_1,v_2) & a(v_1,v_3) & a(v_1,v_4) \\ a(v_2,v_1) & a(v_2,v_2) & a(v_2,v_3) & a(v_2,v_4) \\ a(v_3,v_1) & a(v_3,v_2) & a(v_3,v_3) & a(v_3,v_4) \\ a(v_4,v_1) & a(v_4,v_2) & a(v_4,v_3) & a(v_4,v_4) \end{pmatrix} \begin{pmatrix} u_1 \\ u_2 \\ u_3 \\ u_4 \end{pmatrix} = \begin{pmatrix} L(v_1) \\ L(v_2) \\ L(v_3) \\ L(v_4) \end{pmatrix} \qquad (1.1.2)$$
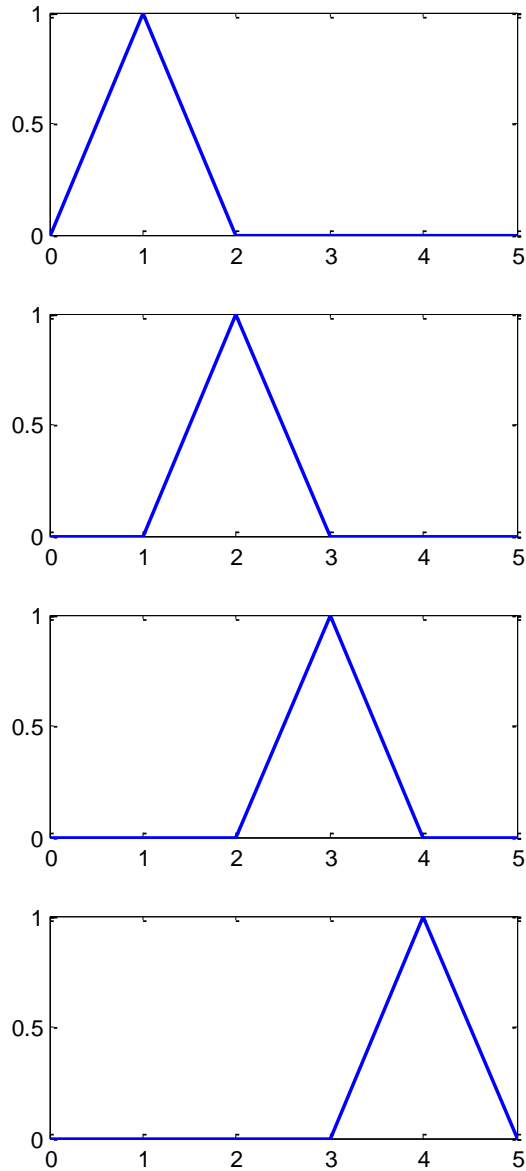
Figure 1.1: Basis functions v_1, v_2 v_3 and v_4

where

$$a(v_1, v_1) = \int_0^5 a(x) \frac{dv_1}{dx} \frac{dv_1}{dx}\ dx$$

$$= \int_0^2 (1 \cdot 1)\ dx$$

$$= 2$$

In a like manner,

$$a(v_1, v_2) = -1$$

$$a(v_1, v_3) = 0$$

$$a(v_1, v_4) = 0$$

$$a(v_2, v_2) = 2$$

$$a(v_2, v_3) = -1$$

$$a(v_2, v_4) = 0$$

$$a(v_3, v_3) = 4.5$$

$$a(v_3, v_4) = -3.5$$

$$a(v_4, v_4) = 8$$

Other components of the (4×4) matrix follow from the symmetric nature of the matrix.

$$L(v_1) = \int_0^5 f(x)v_1\ dx$$

$$= \int_0^1 \left(2x^3 - \frac{18}{5}x^2\right) x\ dx + \int_1^2 \left(2x^3 - \frac{18}{5}x^2\right)(2 - x)\ dx$$

$$= -1.2$$

$$L(v_2) = 3$$

$$L(v_3) = \int_0^5 f(x)v_3\ dx$$

$$= \int_2^3 \left(2x^3 - \frac{18}{5}x^2\right)(x - 2)\ dx + \int_3^4 (8 - 4x)(4 - x)\ dx$$

$$= 3.83333$$

$$L(v_4) = -8$$

System (1.1.2) becomes

$$
\begin{pmatrix}
2 & -1 & 0 & 0 \\
-1 & 2 & -1 & 0 \\
0 & -1 & 4.5 & -3.5 \\
0 & 0 & -3.5 & 8
\end{pmatrix}
\begin{pmatrix}
u_1 \\
u_2 \\
u_3 \\
u_4
\end{pmatrix}
=
\begin{pmatrix}
-1.2 \\
3 \\
3.83333 \\
-8
\end{pmatrix}
+
\begin{pmatrix}
0 \\
0 \\
-2.1 \\
0
\end{pmatrix}
\qquad (1.1.3)
$$

Solving (1.1.3), we obtain

$$
\begin{pmatrix}
u_1 \\
u_2 \\
u_3 \\
u_4
\end{pmatrix}
=
\begin{pmatrix}
0.1759 \\
1.5517 \\
-0.0724 \\
-1.0317
\end{pmatrix}
$$

Therefore the finite element solution to (1.1.1) is

$$
u_h(x) = 0.1759v_1 + 1.5517v_2 - 0.0724v_3 - 1.0317v_4
$$

see Fig 1.2 for the graph of u_h and the exact solution u.

The solution u_h is only an approximation of the exact solution u and can be improved on by dividing the domain into more intervals (ie. having several basis functions) see Fig 1.3.

In what follows, we discuss the development of the method.

1.2 Historical Setup

According to Thomee (2001) and Kantorovich & Krylov (1958), the idea of using variational formulation for the numerical solution of a boundary value problem can be traced back to Lord Rayleigh (in 1894 and 1896) and Ritz (in 1908). Ritz approximated the exact solution with a linear combination of simple functions (like polynomials and trigonometrical polynomials). The idea to express the variational form as a minimization of a quadratic functional problem was attributed
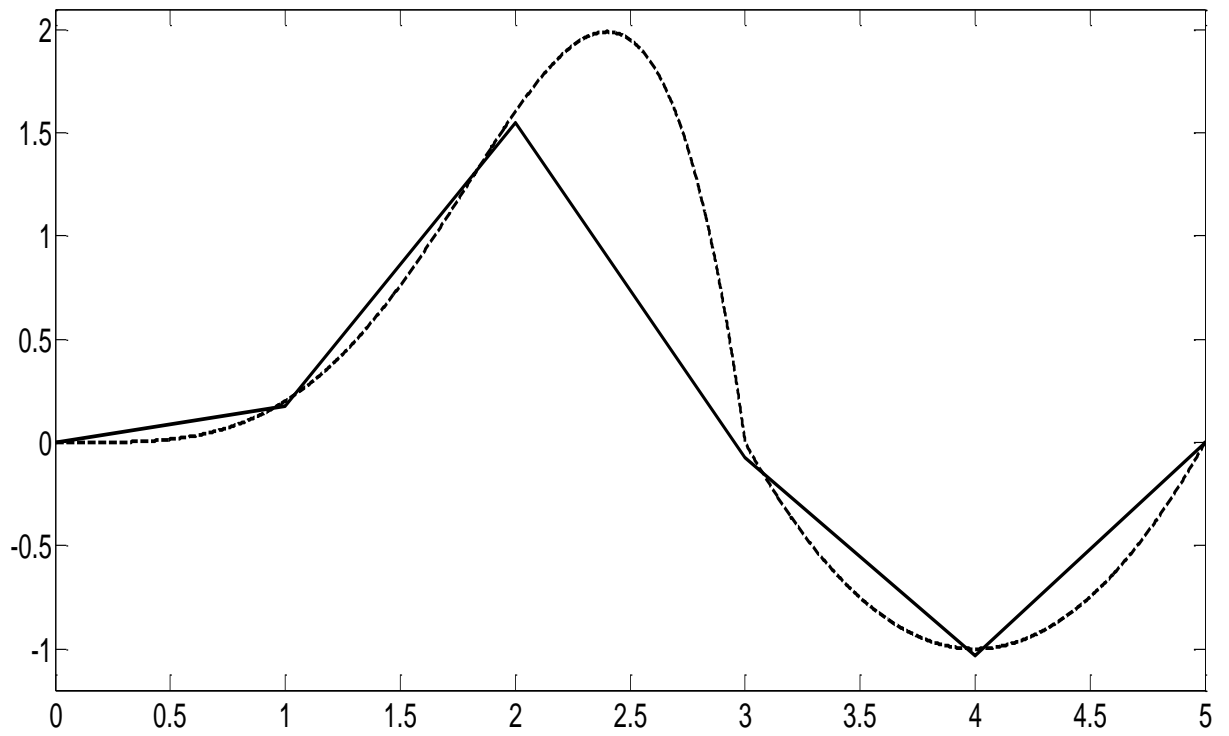
Figure 1.2: The exact solution u (with broken lines) and the FE solution u_h (with a thick line)
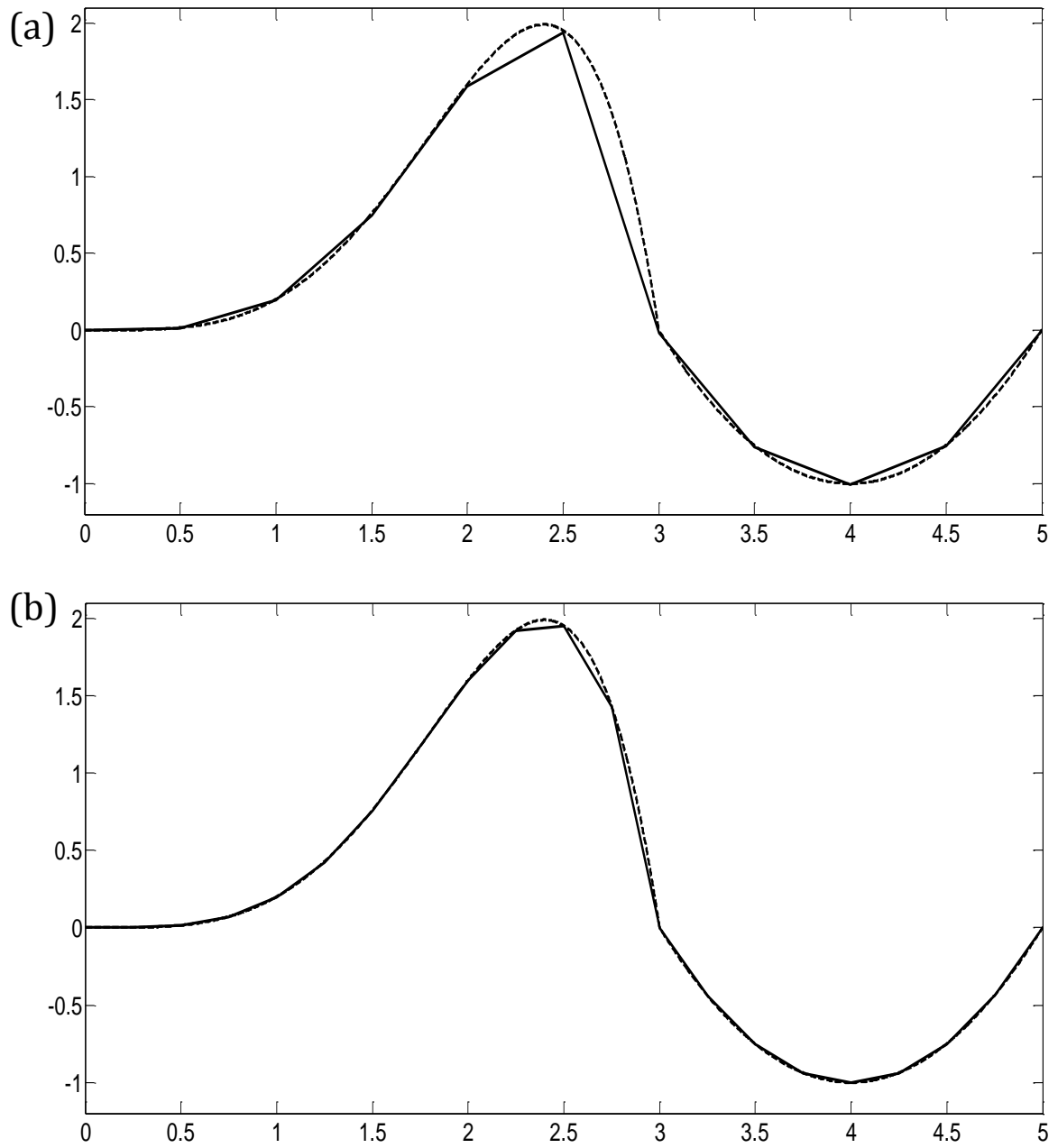
Figure 1.3: The exact solution u (with broken lines) and the FE solution u_h (with a thick line) when $h = 0.5$ and 0.25

to Ritz while the use of orthogonality condition was attributed to Galerkin in 1915 (Siddiqi, 2004).

The method of discretising the domain into finite subdomains and the use of approximating functions on these subdomains was first proposed by Courant in 1943, these subdomains were called "Courant elements". This is often thought of as the starting point of FEM. Courant solved the St. Venant's torsion of a square hollow box of (2×2) with wall thickness of $\frac{1}{4}$ by expressing the problem as a minimization of a functional. He then used linear approximation over Courant elements with values being specified at discrete points (now called nodal points) (Babuska 1994, Gupta & Meek 1996).

A remarkable contribution was contained in a paper by Turner *et al.* (1956), where the local approximation of the partial differential equation of linear elasticity by the usage of assembly strategies was discussed. They used rectangular and triangular elements and wrote "*The triangle is not only simpler to handle than the rectangle but later it will be used as the basic building block for calculating stiffness matrices for plates of arbitrary shape*".

Engineer Argyris in 1960, used the technique of dividing certain structures into small structures (called elements) with locally defined strains and stresses. He developed the concept of using stiffness matrix and flexibility matrix and in 1960, Clough termed these technique as "Finite Element Methods" (Gupta *et al.* 1996, Sididqqi 2004).

In 1965, the minimization technique by Courant was extended and clarified by Zienkiewicz and Chaung to analyze heat transfer and St. Venant's torson of prismatic shafts (Zienkiewicz and Chaung 1965). The mathematical theory of the *a* priori error analysis due to interpolation properties of a class of triangular elements was given by Zlámal (1968). His work is considered as the first most significant mathematically based analysis of FEM (Thomee 2001, Siddiqi 2004).

One of the difficulties faced by FEM is to effectively approximate functions on irregular domains. It is not possible, in general, to approximate the boundary

conditions of a domain with curved boundary. To deal with this difficulty, Ciarlet (1978 and 1991) reported the use of curved elements as proposed and analysed by that Argyris, Fried *et al.*, Zienkiewicz, Felipa and Clough. The idea was to define a polynomial map between a curved boundary and a reference element (called isoparametric elements).

Another method of dealing with this difficulty was proposed by Nitsche (1971). He introduced a bilinear form (Thomee 2001 and 2006)

$$N_\gamma(u, \chi) := (\nabla u, \nabla \chi) - \left\langle \frac{\partial u}{\partial n}, \chi \right\rangle - \left\langle u, \frac{\partial \chi}{\partial n} \right\rangle + \gamma h^{-1} \langle u, \chi \rangle$$

and showed that the variational form for

$$-\Delta u = f$$

can be expressed as

$$N_\gamma(u, \chi) = (f, \chi) \qquad \forall \, \chi \in S_h$$

where S_h is the finite element space.

Books by Brenner and Scott (2008), Ciarlet (1978,1991) and Thomee (2006) have provided a good mathematical foundation for the method. Besides books by Zienkiewics and Cheung (1965), Zienkiewics and Taylor (1989,1991) have enriched the applications of FEM in Engineering.

In practice, FEM is most suitable for diffusion-dominated problems and has been critised for its weakness in handling convection-dominated problems (Pozrikidis, 2014). However, modification can be made to overcome this limitation. In the past decades, researchers have concentrated their efforts on the improvement of FEM to achieve high accuracy. This lead to adaptive refinement and hp-refinement techniques as well as FEM with functions different from polynomials and spectral element method. In this work, we study the finite element method as well as its combination with spectral method.

1.3 Spectral Element Method

The fundamental idea of spectral method is to approximate solutions of PDEs by finite series of orthogonal functions such as the complex exponentials, Chebyshev or Legendre polynomials (Boyd, 1999). The main advantage of the spectral method relies on the exponential convergence property as soon as the orthogonal functions are carefully chosen, but the main drawback is its inability to handle complex geometries (Pasquetti and Rapetti 2004, Boyd 1999). Furthermore, spectral methods are appropriate for problems in which high-order regularity is guaranteed due to their high-order character. Thus if the regularity of the solution is very low, the result obtained from spectral methods might not be different from other low-order methods (Timmermans *et al.*, 1994).

Spectral Element Method (SEM) combines the geometric flexibilities of the FEM with the rapid convergence of the spectral technique. It is an advanced implementation of the finite element method in which the solution over each element is expressed in terms of *a* priori unknown values at carefully selected spectral nodes (Pasquetti and Rapetti 2004, Pozrikidis 2014). The advantage of the spectral element method is that stable solution algorithms and high accuracy can be achieved with a low number of elements under a broad range of conditions (Pozrikidis 2014).

Spectral element method does not mean selecting extremely high-order expansions in the largest elements compatible with a given geometry. Rather, element boundaries are chosen to provide optimal convergence of low-order spectral (but high-order finite element) expansions. In fact a well formulated spectral element problem (ie. one that is not overly global at the expense of a great loss in efficiency) should not require an excessive number of collocation points/element (Patera 1984).

In what follows, we give the basic concept of SEM.

1.3.1 Basic Concept of SEM

Spectral element method involves a sequence of steps just as the FEM. When applied to a differential equation, the domain is first discretised into elements and the unknown is approximated by linear combination of basis functions ϕ with each basis function passing through spectral nodes on each element. The procedure yields a linear system $KU = F$ for which the components of u are the values of u_h at the nodes. K is the stiffness matrix and F is the load vector.

For clarity, we explain this procedure using the one-dimensional elliptic problem (1.1.1). The basis function is taken as fourth degree Lagrange polynomial with Gauss-Lobatto-Legendre (GLL) collocation points.
The GLL points is given as

$$
\begin{aligned}
z_0 &= -1 \\
P'_N(z_i) &= 0 \qquad i = 1, \ldots, N-1 \\
z_N &= +1
\end{aligned}
$$

where $P_N(z)$ is the Legendre polynomial of degree N. In this example, $N = 4$ which implies

$$
\begin{aligned}
P_4(z) &= \frac{1}{8}(35z^4 - 30z^2 + 3) \\
P'_4(z) &= \frac{1}{2}(35z^3 - 15z) = 0
\end{aligned}
$$

Therefore, for a bi-unit domain $[-1, 1]$, the nodes are

$$
-1, \quad -\sqrt{\frac{3}{7}}, \quad 0, \quad +\sqrt{\frac{3}{7}}, \quad +1
$$

As a matter of choice we use

$$
-1, \quad -0.66, \quad 0, \quad +0.66, \quad +1
$$

For simplicity, we map nth element $(n = 1, \ldots, 5)$ to the standard interval of the dimensionless x-axis $[-1, 1]$. The mapping is governed by the function

$$
x(\xi) = \frac{1}{2}\left(x_2^{(n)} + x_1^{(n)}\right) + \frac{1}{2}\left(x_2^{(n)} - x_1^{(n)}\right)\xi
$$

13

It follows that $dx = \frac{1}{2}h_n\, d\xi$ where $h_n = x_2^{(n)} - x_1^{(n)}$ is the element size. We make use of the fourth degree Lagrange basis functions

$$\psi_1(\xi) = \frac{(\xi - \xi_2)(\xi - \xi_3)(\xi - \xi_4)(\xi - \xi_5)}{(\xi_1 - \xi_2)(\xi_1 - \xi_3)(\xi_1 - \xi_4)(\xi_1 - \xi_5)}$$

$$\psi_2(\xi) = \frac{(\xi - \xi_1)(\xi - \xi_3)(\xi - \xi_4)(\xi - \xi_5)}{(\xi_2 - \xi_1)(\xi_2 - \xi_3)(\xi_2 - \xi_4)(\xi_2 - \xi_5)}$$

$$\psi_3(\xi) = \frac{(\xi - \xi_1)(\xi - \xi_2)(\xi - \xi_4)(\xi - \xi_5)}{(\xi_3 - \xi_1)(\xi_3 - \xi_2)(\xi_3 - \xi_4)(\xi_3 - \xi_5)}$$

$$\psi_4(\xi) = \frac{(\xi - \xi_1)(\xi - \xi_2)(\xi - \xi_3)(\xi - \xi_5)}{(\xi_4 - \xi_1)(\xi_4 - \xi_2)(\xi_4 - \xi_3)(\xi_4 - \xi_5)}$$

$$\psi_5(\xi) = \frac{(\xi - \xi_1)(\xi - \xi_2)(\xi - \xi_3)(\xi - \xi_4)}{(\xi_5 - \xi_1)(\xi_5 - \xi_2)(\xi_5 - \xi_3)(\xi_5 - \xi_4)}$$

Fourth degree element contains five nodal points, thus $\mathcal{T}_h$ contains 21 nodal points. The approximate solution can be expressed as

$$u_h(x) = \sum_{j=1}^{21} u_j \psi_j(x)$$

From the weak form of (1.1.1), we obtain

$$\sum_{j=1}^{21} \left(\sum_{n=1}^{5} \int_{E_n} a(x)\frac{d\psi_i}{dx}\frac{d\psi_j}{dx}\, dx \right) u_j = \sum_{n=1}^{5} \int_{E_n} f(x)\psi_i\, dx + \text{interface parameter}$$

$$(1.3.1)$$

for $i = 1, \ldots, 21$. E_n denotes nth element. Now

$$A_{ij}^{(n)} = \int_{E_n} a(x)\frac{d\psi_i(x)}{dx}\frac{d\psi_j(x)}{dx}\, dx$$

$$= \frac{2}{h_n}\int_{-1}^{1} a(\xi)\frac{d\psi_i(\xi)}{d\xi}\frac{d\psi_j(\xi)}{d\xi}\, d\xi$$

The Dirichlet boundary conditions require that $\psi_1 = \psi_{21} = 0$. After a simple

14

(a)

(b)
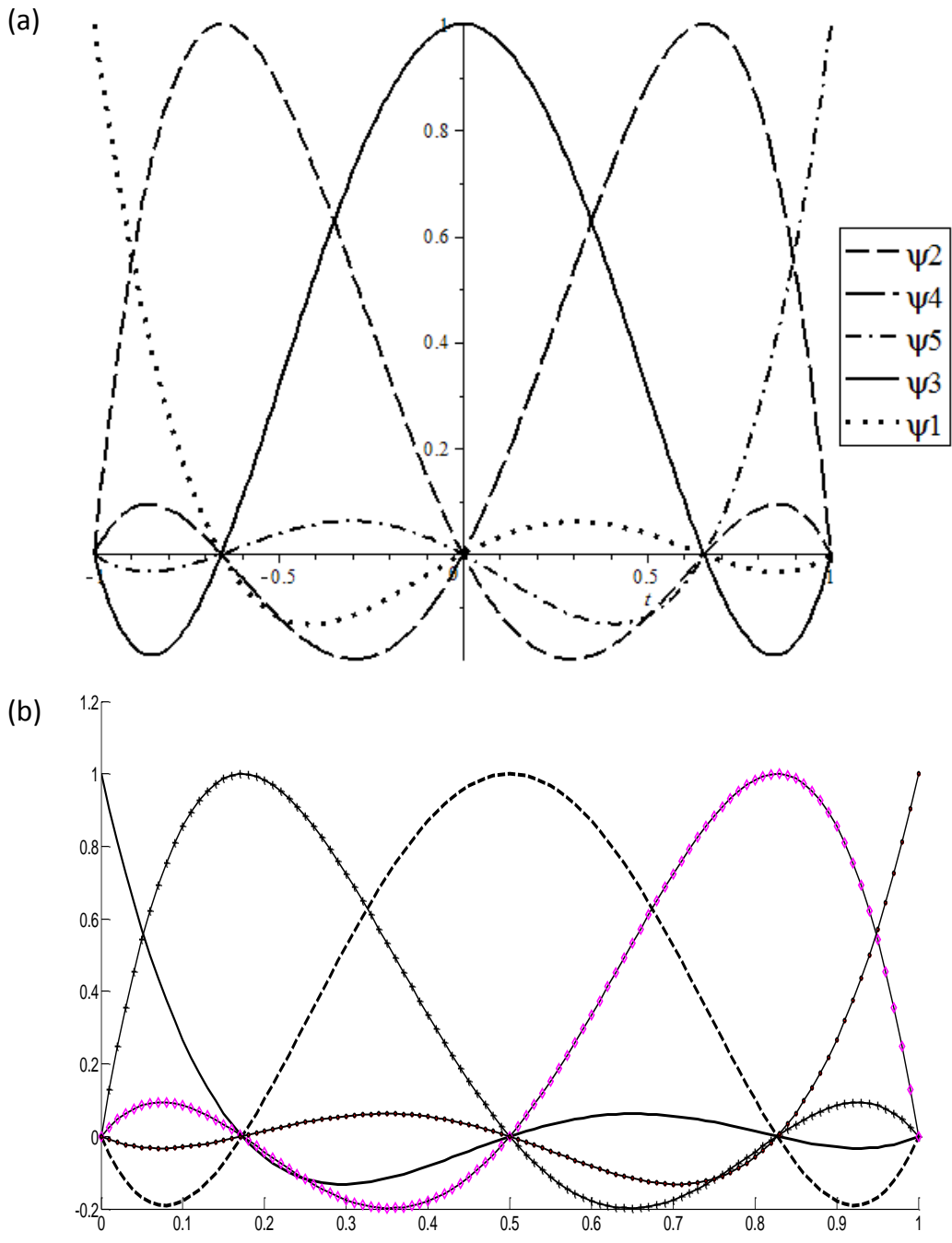
Figure 1.4: (a) The basis functions on the bi-unit domain $[-1, 1]$. (b) The basis functions on the element $[0, 1]$

computation, we obtain

$$
A^{(1)} = \begin{pmatrix}
0 & 0 & 0 & 0 & 0 \\
0 & 12.6983 & -5.6565 & 1.1675 & -0.3018 \\
0 & -5.6565 & 9.2697 & -5.6565 & 1.0297 \\
0 & 1.1675 & -5.6565 & 12.6982 & -7.9719 \\
0 & -0.3018 & 1.0297 & -7.9719 & 7.2173
\end{pmatrix}
$$

$$
A^{(2)} = A^{(3)} = \begin{pmatrix}
7.2173 & -7.9719 & 1.0297 & -0.3018 & 0.0837 \\
-7.9719 & 12.6983 & -5.6565 & 1.1675 & -0.3018 \\
1.0667 & -5.8074 & 9.4815 & -5.8074 & 1.0667 \\
-0.3018 & 1.1675 & -5.6565 & 12.6983 & -7.9719 \\
0.0837 & -0.3018 & 1.0297 & -7.9719 & 7.2173
\end{pmatrix}
$$

$$
A^{(4)} = \begin{pmatrix}
22.1687 & -24.6103 & 3.3581 & -1.0342 & 0.2929 \\
-24.6103 & 40.2842 & -18.8818 & 4.0862 & -1.0786 \\
3.3581 & -18.8818 & 32.4439 & -20.7138 & 3.8497 \\
-1.0342 & 4.0862 & -20.7138 & 48.6036 & -31.1931 \\
0.2929 & -1.0786 & 3.8499 & -31.1931 & 22.1687
\end{pmatrix}
$$

$$
A^{(5)} = \begin{pmatrix}
35.5695 & -32.5822 & 4.3878 & -1.3360 & 0 \\
-32.5823 & 52.9824 & -24.5383 & 5.2537 & 0 \\
4.3878 & -24.5383 & 41.7135 & -26.3703 & 0 \\
-1.3360 & 5.2537 & -26.3703 & 61.3019 & 0 \\
0 & 0 & 0 & 0 & 0
\end{pmatrix}
$$

Similarly,

$$
\begin{aligned}
L_i^{(n)} &= \int_{E_n} f(x)\psi_i(x)\, dx \\
&= \frac{h_n}{2} \int_{-1}^{1} f(\xi)\psi_i(\xi)\, d\xi
\end{aligned}
$$

After a simple calculation,

$$L^{(1)} = \begin{pmatrix} 0 \\ -0.02494 \\ -0.23470 \\ -0.36243 \\ -0.07820 \end{pmatrix} \qquad L^{(2)} = \begin{pmatrix} -0.07737 \\ -0.46997 \\ -0.48387 \\ 0.05160 \\ 0.07962 \end{pmatrix} \qquad L^{(3)} = \begin{pmatrix} 0.08046 \\ 0.93978 \\ 3.16116 \\ 4.46803 \\ 1.05945 \end{pmatrix}$$

$$L^{(4)} = \begin{pmatrix} -0.19571 \\ -1.26905 \\ -2.16345 \\ -1.98493 \\ -0.39142 \end{pmatrix} \qquad L^{(5)} = \begin{pmatrix} -0.39144 \\ -2.35371 \\ -3.60575 \\ -3.06959 \\ 0 \end{pmatrix}$$

The system of equations becomes

$$AU = L \tag{1.3.2}$$

where

$$A = \begin{pmatrix}
12.6983 & -5.6565 & 1.1675 & -0.3018 & 0 & 0 & 0 & 0 & 0 & 0 & 0 \\
-5.6565 & 9.2697 & -5.6565 & 1.0297 & 0 & 0 & 0 & 0 & 0 & 0 & 0 \\
1.1675 & -5.6565 & 12.6982 & -7.9719 & 0 & 0 & 0 & 0 & 0 & 0 & 0 \\
-0.3018 & 1.0297 & -7.9719 & 14.4346 & -7.9719 & 1.0297 & -0.3018 & 0.0837 & 0 & 0 & 0 \\
0 & 0 & 0 & -7.9719 & 12.6983 & -5.6565 & 1.1675 & -0.3018 & 0 & 0 & 0 \\
0 & 0 & 0 & 1.0667 & -5.8074 & 9.4815 & -5.8074 & 1.0667 & 0 & 0 & 0 \\
0 & 0 & 0 & -0.3018 & 1.1675 & -5.6565 & 12.6983 & -7.9719 & 0 & 0 & 0 \\
0 & 0 & 0 & 0.0837 & -0.3018 & 1.0297 & -7.9719 & 14.4346 & -7.9719 & 1.0297 & -0.3018 \\
0 & 0 & 0 & 0 & 0 & 0 & 0 & -7.9719 & 12.6983 & -5.6565 & 1.1675 \\
0 & 0 & 0 & 0 & 0 & 0 & 0 & 1.0667 & -5.8074 & 9.4815 & -5.8074 \\
0 & 0 & 0 & 0 & 0 & 0 & 0 & -0.3018 & 1.1675 & -5.6565 & 12.6983 \\
0 & 0 & 0 & 0 & 0 & 0 & 0 & 0.0837 & -0.3018 & 1.0297 & -7.9719 \\
0 & 0 & 0 & 0 & 0 & 0 & 0 & 0 & 0 & 0 & 0 \\
0 & 0 & 0 & 0 & 0 & 0 & 0 & 0 & 0 & 0 & 0 \\
0 & 0 & 0 & 0 & 0 & 0 & 0 & 0 & 0 & 0 & 0 \\
0 & 0 & 0 & 0 & 0 & 0 & 0 & 0 & 0 & 0 & 0 \\
0 & 0 & 0 & 0 & 0 & 0 & 0 & 0 & 0 & 0 & 0 \\
0 & 0 & 0 & 0 & 0 & 0 & 0 & 0 & 0 & 0 & 0
\end{pmatrix}$$

$$
\begin{pmatrix}
0 & 0 & 0 & 0 & 0 & 0 & 0 & 0 \\
0 & 0 & 0 & 0 & 0 & 0 & 0 & 0 \\
0 & 0 & 0 & 0 & 0 & 0 & 0 & 0 \\
0 & 0 & 0 & 0 & 0 & 0 & 0 & 0 \\
0 & 0 & 0 & 0 & 0 & 0 & 0 & 0 \\
0 & 0 & 0 & 0 & 0 & 0 & 0 & 0 \\
0 & 0 & 0 & 0 & 0 & 0 & 0 & 0 \\
0.0837 & 0 & 0 & 0 & 0 & 0 & 0 & 0 \\
-0.3018 & 0 & 0 & 0 & 0 & 0 & 0 & 0 \\
1.0297 & 0 & 0 & 0 & 0 & 0 & 0 & 0 \\
-7.9719 & 0 & 0 & 0 & 0 & 0 & 0 & 0 \\
29.3860 & -24.6103 & 3.3581 & -1.0342 & 0.2929 & 0 & 0 & 0 \\
-24.6103 & 40.2842 & -18.8818 & 4.0862 & -1.0786 & 0 & 0 & 0 \\
3.3581 & -18.8818 & 32.4439 & -20.7138 & 3.8497 & 0 & 0 & 0 \\
-1.0342 & 4.0862 & -20.7138 & 48.6036 & -31.1931 & 0 & 0 & 0 \\
0.2929 & -1.0786 & 3.8499 & -31.1931 & 57.7382 & -32.5822 & 4.3878 & -1.3360 \\
0 & 0 & 0 & 0 & -32.5823 & 52.9824 & -24.5383 & 5.2537 \\
0 & 0 & 0 & 0 & 4.3878 & -24.5383 & 41.7135 & -26.3703 \\
0 & 0 & 0 & 0 & -1.3360 & 5.2537 & -26.3703 & 61.3019
\end{pmatrix}
$$

$$
U = \begin{pmatrix}
U_2 \\ U_3 \\ U_4 \\ U_5 \\ U_6 \\ U_7 \\ U_8 \\ U_9 \\ U_{10} \\ U_{11} \\ U_{12} \\ U_{13} \\ U_{14} \\ U_{15} \\ U_{16} \\ U_{17} \\ U_{18} \\ U_{19} \\ U_{20}
\end{pmatrix}
\quad \text{and} \quad
L = \begin{pmatrix}
-0.02494 \\ -0.23470 \\ -0.36243 \\ -0.15557 \\ -0.46997 \\ -0.48387 \\ 0.05160 \\ 0.16009 \\ 0.93978 \\ 3.16116 \\ 4.46803 \\ 0.86374 \\ -1.26905 \\ -2.16345 \\ -1.98493 \\ -0.78286 \\ -2.35371 \\ -3.60575 \\ -3.06959
\end{pmatrix}
+
\begin{pmatrix}
0 \\ 0 \\ 0 \\ 0 \\ 0 \\ 0 \\ 0 \\ 0 \\ 0 \\ 0 \\ 0 \\ -2.1 \\ 0 \\ 0 \\ 0 \\ 0 \\ 0 \\ 0 \\ 0
\end{pmatrix}
$$

The solution to (1.3.2), with the implementation of the boundary conditions, is

$$
U = (0.00000, 0.00065, 0.01681, 0.10495, 0.20080, 0.34572, 0.76295, 1.31652,
$$
$$
1.59225, 1.84560, 1.95908, 1.09715, 0.00709, -0.30472, -0.74501,
$$
$$
-0.96737, -0.98911, -0.96856, -0.74853, -0.31062, 0.00000)
$$

It can be seen from Fig 1.5 and Fig 1.3(b) that SEM provides a better result than FEM with the same number of collocation points

18
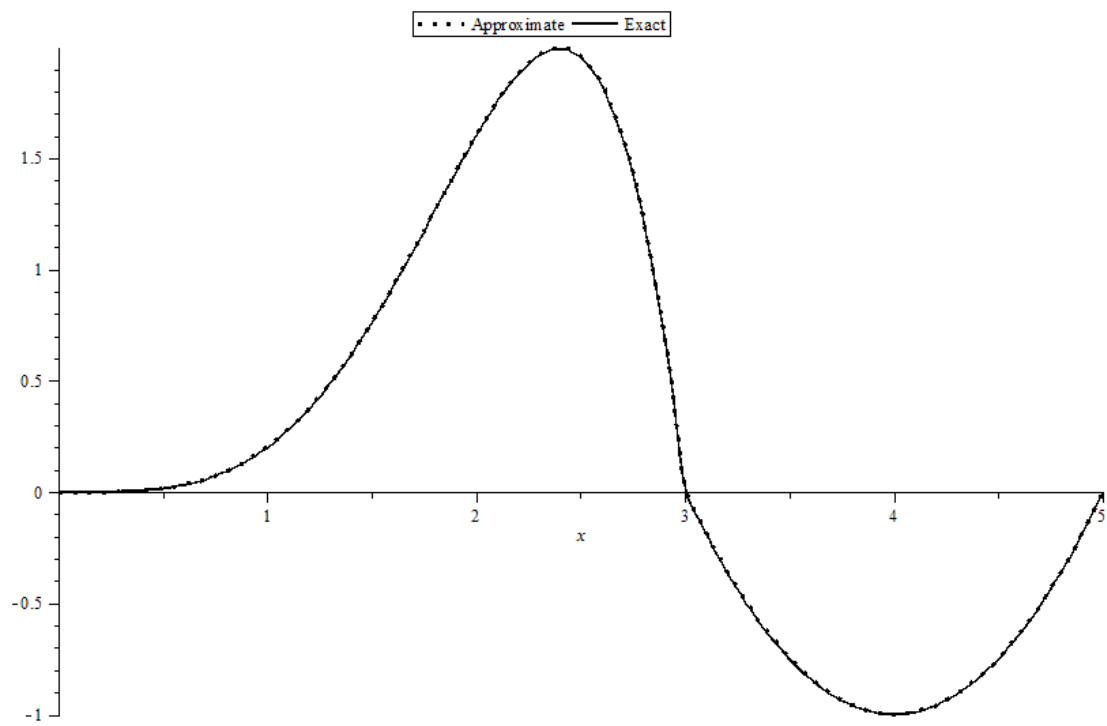
Figure 1.5: The exact solution and the SE solution

1.4   Knowledge Gap

FEM and SEM have been successfully applied to a wide variety of interface problems (see Chapter 2). It is therefore of interest to extend these methods to nonlinear parabolic interface problems.

Finite Element solution of nonlinear parabolic interface problems with time discretisation based on θ method has been discussed by Farago *et al.*, (2012). With necessary assumptions that guarantee the uniqueness of solutions, they showed that the scheme preserves the discrete maximum principle. Their results were based on the algebraic discrete maximum principle for suitable ODE systems. The authors focused on the discrete maximum principle of the scheme however, the authors were silent on the convergence of the scheme. Due to the presence of the nonlinear coefficients, the mass and stiffness matrices cannot be obtained in the usual way, however, the authors did not give a definite technique on how to obtain the mass and stiffness matrices.

Finite element solution of a nonlinear parabolic interface problem with a linear source term has been studied by Yang (2015). She proposed a fully-discrete scheme with time discretisation based on a linearised 2-step implicit scheme. Under certain regularity assumptions on the input data, she proved the stability of the scheme and obtained suboptimal convergence rate in the $L^2(\Omega)$-norm. The author was silent on the semi-discrete scheme and the use of higher order polynomials on the elements.

The convergence of the FE solution of the parabolic interface problem of the form $(1.5.1) - (1.5.3)$ has not been considered and considering the high spatial accuracy of the spectral element method, it is natural to extend the technique to the treatment of $(1.5.1) - (1.5.3)$.

1.5   Problem Specification

Let Ω be a convex polygonal domain in $\mathbb{R}^2$ with boundary $\partial\Omega$ and $\Omega_1 \in \Omega$ be an open domain with smooth boundary $\Gamma = \partial\Omega_1$. Let $\Omega_2 = \Omega \setminus \bar{\Omega}_1$ be another open domain contained in Ω with boundary $\Gamma \cup \partial\Omega$ (see Fig 1.6).

We consider the parabolic interface problem

$$u_t - \nabla \cdot (a(x,u)\nabla u) = f(x,u) \quad \text{in} \quad \Omega \times (0,T] \qquad (1.5.1)$$

with initial and boundary conditions

$$\begin{cases} u(x,0) & = & u_0(x) & \text{in } \Omega \\ u(x,t) & = & 0 & \text{on } \partial\Omega \times [0,T] \end{cases} \qquad (1.5.2)$$

and interface conditions

$$\begin{cases} [u]_\Gamma & = & 0 \\ \left[a(x,u)\dfrac{\partial u}{\partial n} \right]_\Gamma & = & g(x,t) \end{cases} \qquad (1.5.3)$$

where $0 < T < \infty$, the symbol $[u]$ is a jump of a quantity u across the interface Γ and n is the unit outward normal to the boundary $\partial\Omega_i$, $(i = 1,2)$.

The interface conditions are defined as the difference of the limiting values from each side of the interface ie

$$[u]_{m\in\Gamma} := \lim_{x\to m^+} u_2(x,t) - \lim_{x\to m^-} u_1(x,t)$$

and

$$\left[a(x,u)\frac{\partial u}{\partial n} \right]_{m\in\Gamma} := \left[\lim_{x\to m^+} a_2\nabla u_2(x,t) - \lim_{x\to m^-} a_1\nabla u_1(x,t) \right] \cdot n$$

The coefficient function $a(x,u)$ is assumed piecewise across Γ ie $a(x,u) = a_i(x,u)$ for $u \in \mathbb{R}$ and $x \in \Omega$, $i = 1,2$.

This kind of problems arises in various branches of material science, population growth, nonlinear problems of heat and mass transfer biochemistry, multiphase flow in porous media, etc. (Fisher 1936, Canosa 1973, Sinha and Deka 2009,
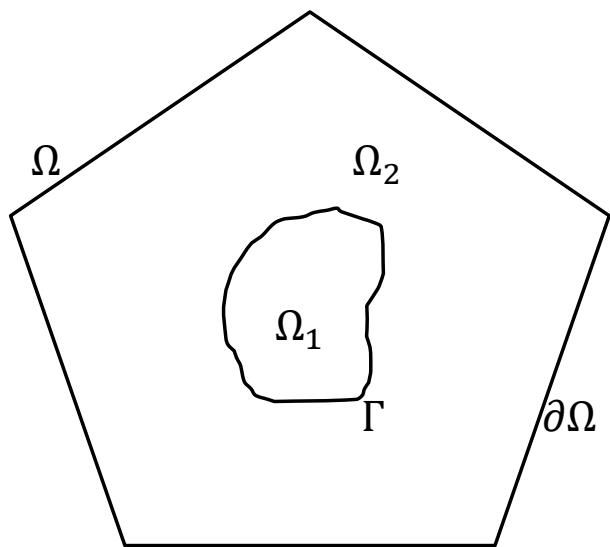
Figure 1.6: A polygonal domain $\Omega = \Omega_1 \cup \Omega_2$ with interface Γ

Polyanin and Zaitsev 2012) often when two or more different materials are involved with different conductivities or densities. In discrete element modelling, Fig 1.1 may represent solid structures (such as rocks, metals, ceramics etc.) with fractures, fragmentation or other extensive material damage (Munijiza, 2004).

Assumption 1.1

A_1 Ω is a bounded convex polygonal domain in $\mathbb{R}^2$, the interface $\Gamma \in \Omega$ and the boundary $\partial\Omega$ are piecewise smooth, Lipschitz continuous and 1-dimensional.

A_2 The functions $a : \Omega \times \mathbb{R} \to \mathbb{R}$, $f : \Omega \times \mathbb{R} \to \mathbb{R}$ are measurable and bounded with respect to their first variable $x \in \Omega$ and continuously differentiable with respect to their second variable $\eta \in \mathbb{R}$ on Ω_i, $i = 1, 2$.
$g(x, t) \in L^2(0, T; H^2(\Gamma) \cap H^{1/2}(\Gamma))$.

A_3 Functions a and f satisfy

$$0 < \mu_1 \leq a(x, \xi) \leq \mu_2, \qquad \left|\frac{\partial a}{\partial \xi}(x, \xi)\right| + \left|\frac{\partial f}{\partial \xi}(x, \xi)\right| \leq \mu_3 \,,$$

for $\xi \in \mathbb{R}$, $x \in \Omega$ with positive constants μ_1, μ_2 and μ_3 independent of (x, ξ).

Definition 1.1 For a given Banach space B, we define, for $1 \leq p < \infty$,

$$W^{m,p}(0, T; B) = \left\{ u(t) \in B \text{ for a.e } t \in (0, T) \text{ and } \sum_{i=0}^{m} \int_0^T \left\|\frac{\partial^i u}{\partial t^i}(t)\right\|_B^p \, dt < 0 \right\}$$

equipped with the norm

$$\|u\|_{W^{m,p}(0,T;B)} = \left[\sum_{i=0}^{m} \int_0^T \left\|\frac{\partial^i u}{\partial t^i}(t)\right\|_B^p \, dt\right]^{1/p}$$

We write $L^2(0, T; B) = W^{0,2}(0, T; B)$ and $H^m(0, T; B) = W^{m,2}(0, T; B)$.
We shall need the following spaces

$$X = H^1(\Omega) \cap H^2(\Omega_1) \cap H^2(\Omega_2) \,, \quad Y = L^2(\Omega) \cap H^1(\Omega_1) \cap H^1(\Omega_2)$$

equipped with the norms

$$\|v\|_X = \|v\|_{H^1(\Omega)} + \|v\|_{H^2(\Omega_1)} + \|v\|_{H^2(\Omega_2)} \quad \forall \, v \in X$$

$$\|v\|_Y = \|v\|_{L^2(\Omega)} + \|v\|_{H^1(\Omega_1)} + \|v\|_{H^1(\Omega_2)} \quad \forall \, v \in Y$$

1.5.1 Guiding Questions

(i) Nonlinear PDEs are prone to blow-ups. Thus, how can this be prevented?

(ii) What are the conditions that guarantee the stability and convergence of the scheme?

(iii) What is the convergence rate?

(iv) How can we improve on the accuracy of the FEM solutions?

1.5.2 Research Objectives

The main objectives of the study are to

- obtain regularity estimates which will be used to establish the existence and uniqueness of the solution to $(1.5.1) - (1.5.3)$ in the weak sense

- obtain almost optimal order error estimates in the $L^2(0,T;H^1(\Omega))$-norm and $L^2(0,T;L^2(\Omega))$-norm for the spatially discrete scheme;

- obtain almost optimal order error estimates in the $L^2(0,T;H^1(\Omega))$-norm and $L^2(0,T;L^2(\Omega))$-norm for the fully discrete scheme with time descretisation based on backward Euler method;

- obtain almost optimal order error estimates in the $L^2(0,T;L^2(\Omega))$-norm for the fully discrete scheme with time descretisation based on implicit linear multistep method;

- combine FEM with spectral method and obtain appropriate error estimate in the $L^2(\Omega)$-norm for discrete time discretisation.

The first objective answers the first guiding question. The second and third objectives answer the second and third questions while the fourth and fifth objects answer the fourth question.

1.5.3   Research Methodology

The finite element discretisation is done by partitioning the domain into quasi-uniform triangular elements and the interface approximated by a polygon. The unknown function is approximated by piecewise linear functions on each element. On spectral elements, our formulation is based on Lagrange polynomials evaluated at Gauss-Lobatto-Legendre points. In both cases, the time discretisation is based on backward Euler scheme. To improve on the time discretisation, we consider a two-point implicit method and a linearised scheme. The integrals involved are evaluated by numerical quadrature and it is assumed that the mesh cannot be fitted to the arbitrary interface.

The linear theories of interface and non-interface problems as well as Sobolev imbedding inequalities were used. *a* priori estimates of the weak solution were used to establish error estimates. Other tools used in this work are approximation properties of linear interpolation operator and other projection operators.

To confirm the theoretical analysis, a good number of versions of problem $(1.5.1) - (1.5.3)$ were considered as test problems for our numerical experiment. The mesh generation and computation are done in MATLAB®, FreeFEM++ (F.Hecht, 2012) and Nektar++ (Cantwell *et al.*, 2015) environments.

1.6   Notation

Unless otherwise stated, the symbol Ω refers to some connected region in $\mathbb{R}^2$, with $\partial\Omega$ referring to its boundary. $\bar{\Omega}$ denotes the closure of Ω (ie $\bar{\Omega} = \Omega \cup \partial\Omega$). Points in $\mathbb{R}^2$ are denoted by $x = (x_1, x_2)$.

For the sake of notational convenience, we introduce multi-index.

Definition 1.2   Let $\mathbb{Z}_+$ denote the set of non-negative integers. An n-tuple $\alpha = (\alpha_1, ..., \alpha_n) \in \mathbb{Z}_+^n$ is called a multi-index. The non-negative integer $|\alpha| := \alpha_1 + \cdots + \alpha_n$ is referred to as the length of the multi-index α. We denote $(0, ..., 0)$ by 0; clearly $|0| = 0$. We also define

$$D^\alpha := \left(\frac{\partial}{\partial x_1}\right)^{\alpha_1} \cdots \left(\frac{\partial}{\partial x_n}\right)^{\alpha_n} = \frac{\partial^\alpha}{\partial x_1^{\alpha_1} \cdots \partial x_n^{\alpha_n}}$$

1.7 Basic Definitions and Some Auxiliary Results of Function Spaces

The accuracy of finite element method for solving partial differential equations depends on the smoothness of the analytical solution of the equation under consideration, and this hinges on the smoothness of the data (Ciarlet 1978, Brenner and Scott 2008).

Precise assumptions about the regularity of the solution and the data can be conveniently formulated in terms of the choice of function spaces. Next a brief overview of basic definitions and simple results from the theory of functions spaces are presented.

1.7.1 The Space of Continuous Functions

Definition 1.3 We denote by $C^k(\Omega)$ the set of all continuous real-valued functions defined on Ω such that $D^\alpha u$ is continuous on Ω for all $\alpha = (\alpha_1, ..., \alpha_n) \in \mathbb{Z}_+^n$ with $|\alpha| \le k$. $C^k(\bar{\Omega})$ denotes the set of all u in $C^k(\Omega)$ such that $D^\alpha u$ can be extended from Ω to a continuous function defined on $\bar{\Omega}$ for all $\alpha = (\alpha_1, ..., \alpha_n)$, $|\alpha| \le k$. $C^k(\Omega)$ can be equipped with the norm

$$\|u\|_{C^k(\Omega)} := \sum_{|\alpha| \le k} \sup_{x \in \Omega} |D^\alpha u(x)|$$

When $k = 0$ we shall write $C(\bar{\Omega})$ instead of $C^0(\bar{\Omega})$ to denote the set of all continuous functions defined on $\bar{\Omega}$.

Definition 1.4 The support of a function $\phi : \Omega \to \mathbb{R}$ is the closure of the set of

points in Ω for which ϕ is non-zero. ie

$$Supp\, \phi := \overline{\{x \in \Omega : \phi(x) \neq 0\}}$$

Thus, $Supp\, \phi$ is the smallest closed subset of Ω such that $u = 0$ in $\Omega \backslash Supp\, \phi$.

Definition 1.5 $C_0^k(\Omega)$ denotes the set of all functions u contained in $C^k(\Omega)$ whose support is a bounded subset of Ω. Also we have

$$C_0^\infty(\Omega) := \bigcap_{k \geq 0} C_0^k(\Omega)$$

1.7.2 L^p-Space

Definition 1.6 Let $\Omega \subset \mathbb{R}^n$ and $1 \leq p < \infty$, $L^p(\Omega)$ denotes the class of all measurable functions u, defined on Ω, for which

$$\int_\Omega |u(x)|^p \, \mathrm{d}x < \infty \tag{1.7.1}$$

$L^p(\Omega)$ functions are identified with almost everywhere defined functions on Ω. The elements of $L^p(\Omega)$ are thus actually equivalence classes of measurable functions satisfying (1.7.1), two functions being equivalent if they are equal almost everywhere in Ω. This space is endowed with the norm

$$\|u\|_{L^p(\Omega)} = \left(\int_\Omega |u(x)|^p \, \mathrm{d}x \right)^{1/p}$$

Definition 1.7 A function u, measurable on Ω, is said to be essentially bounded on Ω provided there exists a constant M for which $|u(x)| \leq M$ almost everywhere on Ω. The greatest lower bound of such constants is called the essential supremum of u on Ω and is denoted by $\mathrm{esssup}_{x \in \Omega} |u(x)|$.

Definition 1.8 $L^\infty(\Omega)$ denotes the vector space consisting of all functions u that are essentially bounded on Ω, functions being once again identified if they are equal almost everywhere in Ω. $L^\infty(\Omega)$ is equipped with the norm

$$\|u\|_{L^\infty(\Omega)} = \mathrm{ess} \sup_{x \in \Omega} |u(x)|$$

$L^p(\Omega)$ is a Banach space for all $1 \leq x \leq \infty$ (Adams 1975).

Definition 1.9 Let $\Omega \subset \mathbb{R}^n$, $u,v \in L^p(\Omega)$ and α be a multi-index. Then v is the weak α-th partial derivatives of u if

$$\int_\Omega u D^\alpha \phi \, \mathrm{d}x = (-1)^{|\alpha|} \int_\Omega v\phi \, \mathrm{d}x \qquad \forall \quad \phi \in C_0^\infty(\Omega)$$

Since this definition relies on integration, we can only talk about the weak derivatives of a function up to a set of measure zero. A weak α^{th}-partial derivative of a function, if it exists, is unique up to a set of measure zero (Adams 1975).

1.7.3 Sobolev Spaces of Integral Order

Definition 1.10 Let Ω be an open set in $\mathbb{R}^n$. Define $W^{m,p}(\Omega)$ as the set of all functions in $L^p(\Omega)$ whose weak partial derivatives, up to order m are also in $L^p(\Omega)$, $p \geq 1$. This space is equipped with the norm

$$\|u\|_{W^{m,p}(\Omega)} := \left(\sum_{|\alpha| \leq m} \|D^\alpha u\|_{L^p(\Omega)}^p \right)^{1/p} \qquad , \qquad 1 \leq p < \infty$$

and

$$\|u\|_{W^{m,\infty}(\Omega)} := \sum_{|\alpha| \leq m} \|D^\alpha u\|_{L^\infty(\Omega)}$$

$W_0^{m,p}(\Omega)$ denotes the closure of $C_0^\infty(\Omega)$ in $W^{m,p}(\Omega)$. $W_0^{m,p}(\Omega)$ comprises of functions $u \in W^{m,p}(\Omega)$ such that

$$D^\alpha u = 0 \qquad \text{on} \qquad \partial\Omega \qquad \forall \quad |\alpha| \leq m-1$$

It is obvious that $W^{0,p}(\Omega) = L^p(\Omega)$. For any $m \in \mathbb{N}$, the chain of imbedding

$$W_0^{m,p}(\Omega) \subset W^{m,p}(\Omega) \subset L^p(\Omega)$$

holds (Adams 1975). $W^{m,p}(\Omega)$ is a Banach space (Adams 1975, Evans 1997). An important special case of $W^{m,p}(\Omega)$ corresponds to taking $p = 2$; the space

$W_0^{m,2}(\Omega)$ is then a Hilbert space with the inner product

$$(u, v)_{W^{k,2}(\Omega)} := \sum_{|\alpha| \leq k} (D^\alpha u, D^\alpha v)$$

We shall usually write $H^k(\Omega)$ instead of $W^{k,2}(\Omega)$. $H_0^m(\Omega)$ is a closed subspace of $H^m(\Omega)$, which is the closure of $C_0^\infty(\Omega)$ in the norm of $\| \cdot \|_{H^m(\Omega)}$.

Theorem 1.1 (Atkinson and Han, 2009) Let $\Omega \subset \mathbb{R}^n$ be bounded along the direction of one axis, $p \in [0, \infty)$. Then there exists a constant c, depending only on Ω and p , so that, for every function $u \in W_0^{1,p}(\Omega)$,

$$\|u\|_{L^p(\Omega)} \leq c\|\nabla u\|_{L^p(\Omega)}$$

This result is called Poincaré inequality.

Definition 1.11 Let V and W be two Banach spaces with $V \subset W$. We say the space V s continuously embedded in W and write $V \hookrightarrow W$, if there is a $c > 0$ such that

$$\|u\|_W \leq c\|u\|_V \qquad \forall\, u \in V$$

If $V \hookrightarrow W$, the functions in V are more smooth than the remaining functions in W (Atkinson *et al.* 2009).

Theorem 1.2 (Atkinson and Han, 2009)   Let $\Omega \subset \mathbb{R}^d$ be a Lipschitz domain. Then the following statements are valid.

a. If $k < \dfrac{d}{p}$, then $W^{k,p}(\Omega) \hookrightarrow L^q(\Omega)$ for any $q \leq p^\star$, where $p^\star$ is defined by
$$\frac{1}{p^\star} = \frac{1}{p} - \frac{k}{d}.$$

b. If $k = \dfrac{d}{p}$ then $W^{k,p}(\Omega) \hookrightarrow L^q(\Omega)$ for any $q < \infty$

c. If $k > \dfrac{d}{p}$, then
$$W^{k,p}(\Omega) \hookrightarrow C^{k-[d/p]-1,\beta}(\Omega)$$

where

$$\beta = \begin{cases} [d/p] + 1 - d/p & \text{if} \quad d/p \neq \text{integer} \\ \text{any positive number} < 1 & \text{if} \quad d/p = \text{integer} \end{cases}$$

$[x]$ denotes the integer part of x, i.e. the largest integer less than or equal to x.

1.7.4   Duality; The Space $W^{-m,p}(\Omega)$

Definition 1.12   We denote by $W^{-m,p}(\Omega)$, $(1 \leq p < \infty)$ the dual space of $W^{m,p}(\Omega)$. In other words f belongs to $W^{-m,p}(\Omega)$ provided f is a bounded linear functional on $W^{m,p}(\Omega)$. We shall write $(\cdot, \cdot)$ to denote the pairing between $W^{-m,p}(\Omega)$ and $W^{m,p}(\Omega)$. If $f \in W^{-m,p}(\Omega)$, we define the norm

$$\|f\|_{W^{-m,p}(\Omega)} := \sup\{\langle f, u \rangle : u \in W^{m,p}(\Omega), \|u\|_{W^{m,p}(\Omega)} \leq 1\}$$

$W^{-m,p}(\Omega)$ is complete (Adams 1975).

1.7.5   Fractional Order Spaces

We now define spaces $W^{s,p}(\Omega)$ for arbitrary domains Ω in $\mathbb{R}^n$, arbitrary values of s, and $1 < p < \infty$. These spaces coincide for integral values of s with the space $W^{m,p}(\Omega)$ and $W^{-m,p}(\Omega)$ defined earlier (Adams 1975). For $s \geq 0$, the definitions can be extended to $p = 1$ and $p = \infty$ (Adams 1975),

Definition 1.13 Let $s = k + \sigma$ with $k \geq 0$ an integer and $\sigma \in (0,1)$. Then we define the Sobolev space $W^{s,p}(\Omega)$ to be the set

$$\left\{ v \in W^{k,p}(\Omega) \mid \frac{|D^\alpha v(x) - D^\alpha v(y)|^p}{\|x - y\|^{\sigma p + n}} < \infty \ \forall \ \alpha : |\alpha| = k \right\}$$

with the norm

$$\|u\|_{W^{s,p}(\Omega)} = \left[\|v\|^p_{W^{k,p}(\Omega)} + \sum_{|\alpha|=k} \int_{\Omega \times \Omega} \frac{|D^\alpha v(x) - D^\alpha v(y)|^p}{\|x - y\|^{\sigma p + n}} \ dx dy \right]^{1/p}$$

30

The space $W^{s,p}(\Omega)$ is a Banach space (Atkinson and Han 2009). It is reflexive if and only if $p \in (1, \infty)$. It is Hilbert when $p = 2$. From this definition, $H^{1/2}(\partial\Omega)$ is the space

$$\left\{ v \in L^p(\partial\Omega) \mid \frac{|v(x) - v(y)|^2}{\|x - y\|^{1+n}} < \infty \right\}$$

with the norm

$$\|u\|_{H^{1/2}(\partial\Omega)} = \left[\|v\|_{L^p(\partial\Omega)}^2 + \int_{\partial\Omega \times \partial\Omega} \frac{|v(x) - v(y)|^2}{\|x - y\|^{1+n}} \, dxdy \right]^{1/2}$$

1.7.6 Trace Operator

Sobolev spaces are defined through $L^p(\Omega)$ spaces and therefore, a typical function $u \in W^{1,p}(\Omega)$ is only defined almost everywhere in Ω. The boundary value of a Sobolev function is not well defined since the $\partial\Omega$ has Lebesgue measure zero. This problem is resolved by trace operators. For a Sobolev function which is continuous up to the boundary, its trace coincides with its boundary value (Atkinson and Han 2009, Evans 1997).

Theorem 1.3 (Atkinson and Han 2009, Evans 1997) Assume Ω is bounded and $\partial\Omega$ is C^1. Then there exists a bounded linear operator

$$T : W^{1,p}(\Omega) \to L^p(\partial\Omega)$$

such that

(a) $Tu = u|_{\partial\Omega}$ if $u \in W^{1,p}(\Omega) \cap C(\bar{\Omega})$

(b) $\|Tu\|_{L^p(\partial\Omega)} \le C\|u\|_{W^{1,p}(\Omega)}$ for each $u \in W^{1,p}(\Omega)$, with the constant C depending only on p and Ω.

The operator T is called the trace operator, and Tu can be called the generalized boundary value of u.

The trace operator is neither an injection nor a surjection from $W^{1,p}(\Omega)$ to $L^p(\partial\Omega)$. Specifically, the range $T(W^{1,p}(\Omega)) = W^{1-1/p,p}(\partial\Omega) \subset L^p(\partial\Omega)$ (Atkinson *et al.*,

2009). In this work, we use traces of the $H^1(\Omega)$ functions. These traces form the space $H^{1/2}(\partial\Omega)$ and therefore we have

$$\|z\|_{H^{1/2}(\partial\Omega)} \leq C\|z\|_{H^1(\Omega)} \quad \forall\, z \in H^1(\Omega) \qquad (1.7.2)$$

Similarly, the trace space on the interface Γ is $H^{1/2}(\Gamma)$. More information on trace operators can be found in the books by Adams (1975) and Evans (1997).

1.8 The Finite Element Interpolation Theorem for C^k Functions

Theorem 1.4 (Oden & Reddy, 1976) Let $u(\mathbf{x})$ denote any function with the properties

(i) $u(\mathbf{x}) \in C^k(M) \qquad M \subset \mathbb{R}^n$

(ii) $\mathfrak{D}^{k+1}u(\mathbf{x})$ exists $\quad \forall\, \mathbf{x} \in M$

where k is a fixed integer ≥ 0, and M is an $\mathfrak{L}_e$−admissible set for some collection of nodal points $\mathfrak{L}_e$ in $\mathbb{R}^n$. Let

$$C_{k+1} \;=\; \sup_{\mathbf{x}\in\Omega_e} \|\mathfrak{D}^{k+1}u(\mathbf{x})\| \;<\; \infty$$

where $\|\mathfrak{D}^k u(\mathbf{x})\| = \sup\left\{|\mathfrak{D}^k u(\mathbf{x})\cdot(\xi_1,\xi_2,\ldots,\xi_n)|,\ |\xi_i|\leq 1; i = 1,2,\ldots,n\right\}$. In addition, let either the following two sets of conditions hold:

(I) (Lagrange finite elements)

$$\mathfrak{L}_e \;=\; \left\{\mathbf{x}_e^N\right\}_{N=1}^{N_e}$$

is a k−unisolvent set of nodal points of a finite element $\Omega_e \subset \mathbb{R}^n$, and $U_e(\mathbf{x})$ is the unique interpolating polynomial of degree $\leq k$ of $u(\mathbf{x})$.

(II) (Hermite finite elements)

$$\mathfrak{L}_e = \bigcup_{\mu=0}^{\nu} \Sigma^{(\mu)} \qquad \Sigma^{(\mu)} = \left\{ {}_{(\mu)}\mathbf{x}_e^N \right\}_{N=1}^{N_e}$$

is a $k-$unisolvent nodes of an $\mathfrak{L}_e-$admissible finite element Ω_e such that ${}_{(\mu)}\mathbf{x}_e^N$ is associated with a subset χ_μ^N of $\prod^\mu \mathbb{R}^n \equiv (\mathbb{R}^n)^\mu$, $1 \le N \le N_\mu$, $0 \le \mu \le \nu$, and $U_e(\mathbf{x})$ is the unique interpolating polynomial in $\mathcal{P}_k(M)$ such that

$$\left. \begin{array}{c} U_e({}_{(0)}X^N) = u({}_{(0)}X^N) \qquad 1 \le N \le N_0 \\ \mathfrak{D}^\mu U_e({}_{(\mu)}X^N) \cdot (\xi_1, \xi_2, \ldots, \xi_\mu) = \mathfrak{D}^\mu u({}_{(\mu)}X^N) \cdot (\xi_1, \xi_2, \ldots, \xi_\mu) \end{array} \right\}$$

$$\forall \, (\xi_1, \xi_2, \ldots, \xi_\mu) \in \chi_\mu^N, \quad 1 \le N \le N_\mu, 0 \le \mu \le \nu.$$

Then there exist positive constants $C = C(n, k, m, \hat{\mathfrak{L}}_M)$ depending on n, k, m and $\hat{\mathfrak{L}}_M$ but not on u, h or ρ such that, for any integer m, $0 \le m \le k$, we have

$$\sup_{\mathbf{x} \in \Omega_e} \|\mathfrak{D}^m u(\mathbf{x}) - \mathfrak{D}^m U_e(\mathbf{x})\| \le CC_{k+1} \frac{h^{k+1}}{\rho^m}$$

For regular refinement,

$$\sup_{\mathbf{x} \in \Omega_e} \|\mathfrak{D}^m u(\mathbf{x}) - \mathfrak{D}^m U_e(\mathbf{x})\| \le CC_{k+1} h^{k+1-m} \tag{1.8.1}$$

The remaining part of this thesis is organised as follows: Chapter 2 is devoted to the review of relevant results and methods necessary for this research.

In chapter 3, we first establish the boundedness of $(1.5.1) - (1.5.3)$ in the L^2, H^1, and X norms, and state the FE discretisation. We then define interpolation and projection operators and obtain necessary estimates in L^2 and H^1 norms. Lastly, we give the analysis of the error estimates of the semi-discrete and fully discrete schemes of the FEM solution of $(1.5.1) - (1.5.3)$.

In chapter 4, we propose the use of spectral element method for $(1.5.1)-(1.5.3)$. We define the spectral element discretisation and establish an optimal convergence rate for a linearised backward Euler scheme. We discuss our results and conclude in chapter 5.

Chapter 2

LITERATURE REVIEW

Solution of nonlinear parabolic interface problems by FEM has been discussed by few authors. In the sequel, we shall give the existing methods and results of FEM and SEM as discussed in relevant literature.

2.1 Finite Element Method

Although interface problems have been studied by Ja (1966) using difference schemes, the use of FEM for interface problems started with the work of Babuska (1970) on elliptic interface problem. He studied finite element approximation to elliptic interface problem

$$-\sum_{i=1}^{n} \frac{\partial}{\partial x_i} \left[a(x) \frac{\partial u}{\partial x_i} \right] = f \qquad \text{on} \quad \Omega$$

with Dirichlet boundary condition on smooth domain $\Omega \subset \mathbb{R}^n$ with C^∞ boundary and interface. He formulated the problem as a minimization problem, defined and analysed a quadratic functional which was used to obtain an error estimate of optimal order in $H^1(\Omega)$-norm

Barrett and Elliot (1987), assuming higher regularity on the solution, analyzed elliptic problems via a penalty method. By choosing the penalty parameter approximately, it was shown that the approximate solution converges to the exact

solution at an optimal rate in both the H^1-norm and L^2-norm, over any interior domain.

Feistauer and Sobotiková (1990) studied the finite element approximation of a nonlinear elliptic problem with discontinuous coefficients across a common part of the boundary of the domain. Conforming piecewise linear elements were used and integrals were evaluated by numerical quadrature. Solvability and convergence of the finite element solution were established with the assumption that the unknown is in $H^1(\Omega)$.

Ženíšek (1990) presented the analysis of the finite element method for nonlinear elliptic equations with discontinuous coefficients

$$-\sum_{i=1}^{2} \frac{\partial}{\partial x_i} a_i(x, u(x), \nabla u(x)) + a_0(x, u(x), \nabla u(x)) = f(x) \quad x \in \Omega$$

with mixed boundary conditions

$$u(x) = u_D(x) \quad \text{on } \partial\Omega_D \quad \text{and} \quad \sum_{i=1}^{2} a_i(x, u(x), \nabla u(x))n_i(x) = q(x) \quad \text{on } \partial\Omega_N$$

where Ω is a two dimensional polygonal domain with Lipschitz continuous boundary. Under suitable assumptions which guarantee that the differential operator is strongly monotone and Lipschitz continuous, he proved that the weak form of the problem has a unique solution and the finite element solution converges at the rate of order $O(h^\varepsilon)$ to the exact solution $u \in H^1(\Omega)$ provided the exact solution is of class $H^{1+\varepsilon}$ ($0 < \varepsilon \leq 1$) and no rate of convergence if $u \in H^1(\Omega)$ only.

Chen and Zou (1998) proposed the finite element method for second order elliptic and parabolic interface problems. They considered an elliptic problem of the form

$$-\nabla \cdot (\beta \nabla u) = f \qquad \text{in } \Omega$$

with boundary and interface conditions

$$u = 0 \quad \text{on } \partial\Omega \qquad \text{and} \quad [u] = 0, \quad \left[\beta \frac{\partial u}{\partial n}\right] = g \quad \text{across } \Gamma$$

They assumed that Ω is a convex polygon in $\mathbb{R}^2$ with C^2 boundary and an interface of arbitrary shape. With the assumption that the solution, coefficients and interface function are of low regularity, they obtained almost optimal convergence rates of $O(h|\log h|^{1/2})$ and $O(h^2|\log h|)$ in energy norm and $L^2(\Omega)$ norm respectively. Linear parabolic interface problem of the form

$$\frac{\partial u}{\partial t} - \nabla \cdot (\beta \nabla u) = f(x,t) \qquad \text{in } \Omega \times (0,T)$$

with initial, boundary and interface conditions

$$u(x,0) = u_0 \text{ in } \Omega; \quad u = 0 \text{ on } \partial\Omega \times (0,T); \text{ and } [u] = 0, \quad \left[\beta \frac{\partial u}{\partial n}\right] = g \text{ across } \Gamma \times (0,T)$$

was studied using backward Euler time discretisation. They proved almost optimal error estimates of $O(k + h^2|\log h|)$ and $O(k + h|\log h|^{1/2})$ in $L^2(0,T; L^2(\Omega))$ and energy norms. Their analysis was based on Sobolev embedding inequality, Sobolev extension theorem, duality arguments, energy norm projection operator and L^2 projection operator.

An unfitted finite element discretisation using an approach due to Nitsche was proposed by Hansbo and Hansbo (2002) for approximating the elliptic interface problem

$$-\nabla \cdot (\alpha \nabla u) = f \qquad \text{in } \Omega_1 \cup \Omega_2$$

with boundary and interface conditions

$$u = 0 \quad \text{on } \partial\Omega \qquad \text{and} \qquad [u] = 0, \quad \left[\alpha \frac{\partial u}{\partial n}\right] = g \quad \text{on } \Gamma$$

It is known that suboptimal convergence behaviour occurs when the mesh is not fitted to the interface (Babuska, 1970). This problem was resolved by allowing the approximating function to be discontinuous inside the elements which intersect the interface. For each interface element K, they introduced the notation

$$\kappa_i|_K = \frac{\text{meas}(K_i)}{\text{meas}(K)} \qquad \text{and} \qquad \{\phi\} = (\kappa_1\phi_1 + \kappa_2\phi_2)_\Gamma$$

and expressed the discrete weak form as

$$a_h(U, \phi) = (f, \phi)_\Omega + (\kappa_2 g, \phi_1)_\Gamma + (\kappa_1 g, \phi_2)_\Gamma$$

where

$$a_h(U, \phi) := (\alpha_i \nabla U_i, \nabla \phi_i)_{\Omega_i \cup \Omega_2} - \left([U], \left\{\alpha \frac{\partial \phi}{\partial n}\right\}\right)_\Gamma - \left(\left\{\alpha \frac{\partial U}{\partial n}\right\}, [\phi]\right)_\Gamma + (\lambda[U], [\phi])_\Gamma$$

with λ sufficiently large.

Although their method is more computationally complex than the standard FEM, it gives a better approximation because an optimal order of convergence is guaranteed in the L^2-norm. The analysis of the method was based on Sobolev embedding inequalities and linear interpolation operator on quasi-uniform triangular elements.

Based on cartesian triangulations, Li *et al.* (2003) discussed elliptic interface problems and established the optimal rate of convergence in the energy norm for a conforming FEM.

Olshankii and Reusken (2004) treated a stationary Stokes problem on a bounded connected domain in which the viscosity coefficient is piecewise constant and with different values on the subdomains. With velocity $u \in H_0^1(\Omega)^d$ and pressure $p \in L_0^2(\Omega)$ (ie. $p \in L^2(\Omega)$ and $\int_\Omega p \ dx = 0$), they established a well posedness result. Analysis of the discretisation was based on conforming finite element spaces and stability as well as convergence results were proved with respect to the jump in the viscosity coefficient.

Sinha and Deka (2005) discussed FEM for a linear parabolic interface problem with the use of curved elements across the interface instead of triangle elements. They employed the Linear theories of interface problems and Aubstin Nitsche duality argument and show that the finite element solutions approximate the true solutions with an optimal order of $O(h)$ and $O(h^2)$ in $L^2(0, T; H^1(\Omega))$ and $L^2(0, T; L^2(\Omega))$ norms respectively. Their time discretisation was based on discontinuous Galerkin method and also obtained optimal order of convergence.

Karatson and Korotov (2005) investigated the discrete maximum principles for finite element solutions of nonlinear elliptic problems. They presented several vari-

ants of the maximum principles and their discrete counterparts for second order nonlinear elliptic problems with mixed boundary conditions. The problems considered were numerically solved by the continuous piecewise linear finite element approximations built on simplicial meshes.

Sinha and Deka (2007) proposed and analyzed an unfitted finite element discretisation for both elliptic and parabolic problems with discontinuous coefficients. They considered the interface problems first considered by Chen and Zou (1998) but on unfitted finite element. An optimal order error estimate of $O(h)$ in the H^1-norm was shown to be obtainable and almost optimal order error estimate $O(h^2|\log h|)$ in the L^2-norm was derived for elliptic interface problems. An extension to parabolic interface problems was also discussed and estimates in $L^2(H^1)$-norm and $L^2(L^2)$-norm were derived for the spatially discrete scheme. A fully discrete scheme based on the backward Euler method was analyzed and an optimal order error estimates in $L^2(H^1)$-norm was derived.

Sinha and Deka (2009) studied the FEMs for second order semilinear elliptic interface problem

$$-\nabla \cdot (\beta(x)\nabla u(x)) + u(x) = f(u) \qquad \text{in } \Omega$$

with boundary and interface conditions

$$u = 0 \quad \text{on } \partial\Omega \quad \text{and} \quad [u] = 0, \quad \left[\beta\frac{\partial u}{\partial n}\right] = 0 \quad \text{along } \Gamma$$

They assumed that Ω is a convex polygon in $\mathbb{R}^2$ with C^2 boundary and the mesh can be fitted exactly to the arbitrary interface, however, it is very difficult to generate a grid which exactly follows the actual interface in practice. They obtained optimal convergence rate of $O(h)$ in $H^1(\Omega)$ norm.

An extension to the semilinear parabolic interface problem of the form

$$\frac{\partial u}{\partial t} - \nabla \cdot (\beta(x)\nabla u) + u(x) = f(u) \qquad \text{in } \Omega \times (0,T]$$

with initial, boundary and interface conditions

$$u(x,0) = u_0 \text{ in } \Omega; \ \ u = 0 \text{ on } \partial\Omega \times (0,T); \text{ and } [u] = 0, \ \left[\beta\frac{\partial u}{\partial n}\right] = 0 \ \text{ along } \Gamma \times (0,T)$$

was also considered. The convergence of the semidiscrete solution to the exact solution was of order $O(h)$ in the $L^2(0, T; H^1(\Omega))$-norm. A similar error estimate was obtained for fully discrete scheme based on backward Euler method. Their analysis was based on the linear theory of interface problems and the approximation theory of Brezzi-Rappaz-Raviart, Sobolev embedding inequality and auxiliary projections.

Karatson and Korotov (2009) proved discrete maximum principles for finite element discretisations of nonlinear elliptic interface problems with jumps of the normal derivatives. This work is an extension of thier work in 2005 to a class of such problems, and relies on a similar technique using positivity that ensure well-posedness. The jump was allowed for normal derivatives but not for the solution itself.

Deka and Ahmed (2012) improved on the works of Chen and Zou (1998) and Sinha and Deka (2006) and also confirmed the optimal error estimates in $L^2(0, T; L^2(\Omega))$-norm. Optimal error estimates in the $L^2(L^2)$ and $L^2(H^1)$ norms were established for linear semi discrete scheme and a similar error estimates was also extended to semilinear interface problems.

Mu *et al.* (2013) developed a weak Galerkin finite element method for elliptic interface problems. An algorithm based on the work by Wang and Ye (2013) was presented and analyzed. The uniqueness as well as the convergence of the algorithm was established. Convergence of $O(h^{1.75})$ was established numerically in the L^∞-norm.

Payne *et al.* (2012) employed the regularity assumption on the true solution of an elliptic interface problem as well as interface and domain approximation technique made popular by Chen and Zou (1998) in the finite element method for elliptic problems with smooth interfaces. The result of the work showed that optimal order of convergence in the L^2 and H^1-norms are possible even if the solution has a low regularity.

Minimal dissipation local discontinuous Galerkin method for linear parabolic

interface problem on two dimensional polygonal domain was proposed by Zhang & Yu (2015). They considered the interface problem

$$\frac{\partial u}{\partial t} - \nabla \cdot (\beta \nabla u) = f(x,t) \qquad \text{in } \Omega \times (0,T)$$

with initial, boundary and interface conditions

$$u(x,0) = u_0 \text{ in } \Omega; \ \ u = 0 \text{ on } \partial\Omega \times (0,T); \text{ and } [u] = 0, \ \left[\beta \frac{\partial u}{\partial n}\right] = 0 \ \text{ along } \Gamma \times (0,T)$$

They introduced auxiliary variables and recast the problem in a way suitable for mathematical analysis. The method was proved to be L^2-stable and converges at a rate proportional to $h|\log h|^{1/2}$ however, they showed numerically that the convergence rates are higher than the theoretical result.

Yang (2015) studied the convergence of the finite element solution of a nonlinear parabolic interface problem with a linear source term:

$$\begin{cases} \dfrac{\partial u}{\partial t} - \nabla \cdot (\sigma_0(u)\nabla u) = f(x,t) & \text{in } \Omega_0 \\ \dfrac{\partial u}{\partial t} - \nabla \cdot (\sigma_1(u)\nabla u) = f(x,t) & \text{in } \Omega_1 \end{cases}$$

with initial, boundary and interface conditions

$$u(x,0) = u_0(x) \text{ in } \Omega; \ \ u = 0 \text{ on } \partial\Omega \times (0,T); \text{ and } [u] = 0, \ \left[-\sigma \frac{\partial u}{\partial n}\right] = g \ \text{ on } \Gamma$$

The author focused on the fully discrete approximation and used a linearized 2-step backward difference scheme for the time discretisation while piecewise linear interpolation was used to approximate the interface. With the assumption that the coefficient $\sigma(u)$ is positive and smooth with respect to $u \in \mathbb{R}$ but not continuous across the interface, the author proved a convergence rate of almost optimal order $O(k^2 + h^2|\ln(2 + 1/h)|^2)$ in the L^2-norm. Her mathematical analysis was carried out using body fitted triangulation, error splitting technique, and some projection operators under certain regularity conditions that guaranteed a unique solution.

2.2 Spectral Element Method

Spectral element method was first presented by Patera (1984). He proposed a spectral element method for the solution of the incompressible Navier-Stokes equations

$$\frac{\partial \mathbf{v}}{\partial t} + (\mathbf{v} \cdot \nabla)\mathbf{v} = -\nabla p + \nu \nabla^2 \mathbf{v}$$

with

$$\nabla \cdot \mathbf{v} = 0$$

The unknown function was represented as high order Langrangian interpolant through Chebyshev collocation points for the spatial discretisation. For the time discretisation, operator splitting technique was employed with second order Adams-Bashforth explicit scheme for the wave operator and Crank-Nicolson method for the diffusion term. He implemented the technique on a one-dimensional inflow-outflow advection-diffusion equation

$$\frac{\partial u}{\partial t} + \frac{\partial u}{\partial x} = \nu \frac{\partial^2 u}{\partial x^2} \qquad -\infty < x < \infty$$

and simulated laminar flow on two-dimensional domain. He showed numerically that the spectral element solution converges exponentially to the exact solution in the L^∞-norm. Extensions and improvements to the SEM which will allow it to be used in greater generality were also suggested.

The study of interface problem by SEM was first carried out by Ronquist and Patera in 1987. They presented a Legendre spectral element method for multi-dimensional unsteady change-of-phase (Stefan) problem

$$
\begin{aligned}
k\frac{\partial T_1}{\partial t} &= \kappa_1 \nabla^2 T_1 \quad \text{in} \quad D_1 \\
k\frac{\partial T_2}{\partial t} &= \kappa_2 \nabla^2 T_1 \quad \text{in} \quad D_2
\end{aligned}
$$

with mixed boundary conditions and a moving interface. The moving interface was captured by interface-local transformations and consistent flux evaluation.

The analysis of the method was given for a 1-dimensional problem and the result was extended to a 2-dimensional problem. Quadrilateral elements were used for the spatial discretisation and the unknown was approximated using Legendre polynomials on Gauss-Lobatto-Legendre collocation points. For computational simplification, tensor product mapping was used to map each element in the physical domain to a local (mathematical) domain.

The analysis of the rapid convergence rate and stability based on Gauss-Lobatto Legendre quadrature was provided. Exponential convergence of the numerical solution to the exact solution as the polynomial order increases was established for fixed element.

Timmermans *et al.* (1994) combined Taylor-Galekin method (a method based on Taylor series of the time derivative) with a spectral element spatial discretisation for the approximation of convection-diffusion problems. Operator splitting method is used to decouple the problem into a pure convection problem and a pure diffusion problem. Convergence of the approximate solution to the exact solution was established numerically in the L^∞-norm. The result of the this work was established by computation.

In the paper by Yoseph *et al.* (1995), the spectral element technique proposed by Patera (1984) was implemented on a one-dimensional nonlinear advection-diffusion equations. Time discretisations based on one-step implicit-explicit method, Adams-Bashforth multistep method and a subcycling method (a technique in which several convective steps are taken for each time step) were compared and stability as well as convergence analysis were carried out. From the result of their computation, subcycling method showed the best convergence rate and thus they concluded that higher-order time scheme should be used with spectral finite element. The result of the this work was established by computation.

Taylor *et al.* (1997), Komatitsch *et al.* (1999), Liquan (1999), Meng *et al.* (2003) Pasquetti & Rapetti (2004) and Deng & Cai (2005) have all contributed to the growth of SEM.

Simulation of two- and three-dimensional moving boundary problems such as free-surface flows or fluid structure interaction was presented by Bodard *et al.* (2008). A moving boundary fitted technique was used for the simulation of the unsteady part of the boundary. This was achieved by using arbitrary Lagrangian-Eulerian (ALE) technique to avoid mesh distortion. The moving boundary incompressible Newtonian fluid flows considered are governed by the Navier-Stokes equation

$$\frac{\partial \mathbf{u}}{\partial t}\bigg|_{\mathbf{x}} + \mathbf{u} \cdot \nabla_{\mathbf{x}} \mathbf{u} = -\nabla_{\mathbf{x}} p + 2\nu \nabla_{\mathbf{x}} \cdot \mathbf{D}_{\mathbf{x}}(\mathbf{u}) + \mathbf{f}, \qquad \forall\, (\mathbf{x}, t) \in \Omega_t \times I$$

with $\nabla_{\mathbf{x}} \cdot \mathbf{u} = 0$ where $\mathbf{u}$ is the velocity field, p the pressure field, ν the kinematic viscosity of the fluid, $\mathbf{D}_{\mathbf{x}}(\mathbf{u}) = \frac{1}{2}(\nabla_{\mathbf{x}} \mathbf{u} + \nabla_{\mathbf{x}} \mathbf{u}^T)$ the rate of deformation tensor and $\mathbf{f}$ the body force per unit mass. Under suitable transformation, the Navier-Stokes equation was written in ALE strong form as

$$\frac{\partial \mathbf{u}}{\partial t}\bigg|_{\mathbf{Y}} + (\mathbf{u} - \mathbf{w}) \cdot \nabla_{\mathbf{x}} \mathbf{u} = -\nabla_{\mathbf{x}} p + 2\nu \nabla_{\mathbf{x}} \cdot \mathbf{D}_{\mathbf{x}}(\mathbf{u}) + \mathbf{f}, \qquad \forall\, (\mathbf{x}, t) \in \Omega_t \times I$$

where $\mathbf{w}$ is the ALE velocity, $\mathbf{x}$ position of a point in the current fluid domain Ω_t and $\mathbf{Y}$ is the position of a point in the reference (ALE) coordinate.

Galerkin method was used to obtain the weak form in the ALE frame and quadrilateral elements were used for the spectral element discretisation with most of the integrals evaluated numerically by Gauss-Lobatto-Legendre quadrature rule. The velocity and pressure were approximated by GLL Lagrangian interpolation basis of degrees N and $N - 2$ respectively on the each element. A combination of implicit difference scheme and extrapolation method of order 2 were used for the time discretisation. This work is purely computational and the results obtained are very good with the theoretical results when available.

Gerritsma *et al.* (2008) investigated the application of the least square SEM to compressible flow problems. They demonstrated that the least square SEM has optimal convergence and that it is better used for functions with oscillation than the ordinary SEM.

Comparison of SEM with Radial Basis Function (RBF) method has been carried out by Shin & Jung (2011). In their methods, it was assumed that the the locations of the interfaces inside the given domain are known a priori. With the position of the interface fixed, the domain was discretised into intervals and Lagrange polynomials on collocation points were used for spectral element descretisation. This resulted to an overdetermined system of linear equations which was solved by Least square method. The shape parameters needed for the RBF method, were chosen to increase the accuracy of the method while keeping the system well-conditioned.

The methods were implemented on a first order differential equation

$$\frac{du}{dx} = f(x), \quad x \in (0,1) \qquad \text{with } u(0) = c_0 \in \mathbb{R}$$

and interfaces at several points within $(0,1)$. Solution by SEM was found on Chebyshev-Gauss-Lobatto collocation points and two different shape functions (uniform and weighted functions) for RBF. The methods were further implemented on a second order differential equations with singular functions:

$$-(\beta u_x)_x + ru = f + \nu \delta_0, \quad x \in (0,1) \qquad u(0) = u(1) = 0$$

where β and r are smooth and piecewise across the interface. Galerkin method was used to obtain the weak form and the solution by SEM was found on Chebyshev and Legendre collocation points. The solution by RBF was based on two different shape functions (ie uniform and weighted).

The authors concluded that for both spectral and RBF methods, least squares collocation method is efficient and yields accurate results for the interface problems. The authors also noted that SEM is superior to RBF method in that boundary effect related to Runge phenomenon is better treated with SEM.

Dehghan & Sabouri (2013) developed the Legendre spectral element method

(LSEM) for a predator-prey model

$$\begin{aligned}
\frac{\partial u}{\partial t} &= D_u \Delta u + F(u) - E(u,v) \\
\frac{\partial v}{\partial t} &= D_v \Delta v + \kappa E(u,v) - G(u)
\end{aligned}$$

with Neuman boundary condition on a one dimensional domain. See Dehghan & Sabouri (2013) for the meanings of the parameters $D_u, D_v, \kappa, F(u), G(u)$ and $E(u,v)$. The domain was partitioned into intervals and the unknown was approximated by Lagrange polynomials on each element with Gauss-Lobatto-Legendre collocation points. For computational conveniences, the domain was transformed to a bi-unit domain and the model was converted to a system of initial value ordinary differential equations. The time discretisation was based on implicit method to ensure numerical stability. The maximum norm errors generated from LSEM were compared with that from Lagrange Pseudo-Spectral Method (LPSM) and the FEM with quadratic bases. It was shown that high accuracy could be achieved from LSEM with less computational effort and time than the LPSM and FEM. The integrals involved were numerically evaluated using Gauss-Lobatto quadrature rule. The emphasis of the authors was on the accuracy of the spatial discretisation using the LSEM.

Dutt *et al.* (2014) presented results of numerical experiments for a number of test problems on non-smooth domains with analytic as well as singular solutions to validate the theoretical error estimates obtained in their earlier work for a non-conforming $h - p$ SEM. Several examples on elliptic PDE of the form

$$\sum_{ij=1}^{3} -\frac{\partial}{\partial x_i}(a_{ij}w_{x_i}) + cw = F \quad \text{in} \quad \Omega$$

on different geometrical 3-d domains containing different types of singularities namely, vertex, edge and vertex-edge, were considered with different types of boundary conditions. To overcome the singularities, the authors used local systems of coordinates (which were modified versions of spherical and cylindrical coordinate systems) together with geometric meshes which become finer near corners

and edges. The domains were discretised into hexahedrons and the spectral element solution was obtained on Gauss-Lobatto-Legendre collocation points. It was demonstrated numerically that the sum of regular error and the errors at the singularity points decreases exponentially in $H^1(\Omega)$-norm.

In the work by Claus *et al.* (2015), the motion of an incompressible fluid governed by the Navier-Stokes equation

$$Re\left(\frac{\partial \mathbf{u}}{\partial t} + (\mathbf{u} \cdot \nabla)\mathbf{u}\right) = -\nabla p + 2\nabla \cdot \mathbf{D} \quad \text{in} \quad \Omega_t, \ t \in I$$

with $\nabla \cdot \mathbf{u} = 0$ in Ω_t and Dirichlet boundary condition was studied numerically using SEM, where $\mathbf{u}$ is the velocity, p is the pressure, $\mathbf{D} = \frac{1}{2}(\nabla \mathbf{u} + \nabla \mathbf{u}^T)$ is the rate of deformation tensor and Re is the Reynolds number. The method was capable of approximating the infinite stress values with an exponential increase in the extreme values of the pressure with p-refinement. To avoid computational crime, the grid points of the computational mesh at the free surface were moved with the normal fluid velocity and arbitrary Lagrangian-Eulerian technique was used to avoid mesh distortion. The result of this work is compared with existing results with several numerical examples. Moreover, the impact of each parameter of the model on the solution was investigated numerically. Exponential convergence rate of the approximate solution to the exact solution was numerically established.

Sabouri & Dehghan (2015) presented an implicit spectral element approximation using the method-of-lines (MoL) to solve nonlinear parabolic differential equations with smooth coefficients. Naturally, solutions by SEM are only C-functions, hence the their derivatives are not continuous across the elements in general and as a result, the arising expansion for the spatial derivative is no longer a nodal one. To overcome this limitation, the authors proposed the use of nodal expansion for the spatial derivative. The nodal points used are the Gauss-Lobatto-Legendre and Fakete points and the numerical quadrature points are chosen to coincide with these point to increase the accuracy of the numerical integration. The authors

demonstrated the method for the nonlinear problem

$$\frac{\partial u}{\partial t} = \nabla \cdot (F(u, \nabla u)\nabla u) + f(x) \ .$$

Use was made of the cardinality property of the Lagrange polynomials for the MoL formulation in terms of the differentiation matrix and the Jacobian matrix. In contrast with the stiffness matrix, the differentiation matrix is computationally simple as it is independent of time.

The efficiency of the method was illustrated with a good number of numerical simulations - cell motion model, tumor angiogenesis model, 2 and 3 dimensional p-Laplacian equation. In each case the solutions from the method were compared with other methods and it was concluded that the SEM is an efficient and convenient technique for time dependent nonlinear diffusion equation in complex geometries if the unknown function, its derivatives and deformed elements are represented by the nodal expansion.

Chapter 3

APPROXIMATION BY FEM

This chapter is devoted to the analysis of the error estimates, which is preceded by variational formulation of the specified interface problem, finite element discretisation and the approximation properties of the unknown function across the interface as well as the prove of some auxiliary estimates necessary for the error analysis.

3.1 Regularity Estimates

The accuracy of FEM for differential equations depends on the smoothness of the analytic solution to the equation under consideration, and this depends on the smoothness of the data (Ciarlet 1978, Brenner & Scott 2008). Due to the low regularity of the solution across the interface, sufficient conditions for the solvability of $(1.5.1) - (1.5.3)$ will be discussed in the weak form.

In what follows, we find the weak form and prove the a priori estimates for the solution of $(1.5.1) - (1.5.3)$ under appropriate regularity conditions on a, f and g. We multiply $(1.5.1)$ by a test function $v \in L^2(0, T; H_0^1(\Omega))$ and use the Green's identity to obtain

$$(u_t, v) + A(u : u, v) = (f, v) + \langle g, v \rangle_\Gamma \quad \forall \, v(t) \in H_0^1(\Omega), \text{ a.e } t \in [0, T] \quad (3.1.1)$$

where

$$(\phi, \psi) = \int_\Omega \phi\psi \, dx \qquad A(\xi : \phi, \psi) = \int_\Omega a(x, \xi)\nabla\phi \cdot \nabla\psi \, dx \qquad \langle\phi, \psi\rangle_\Gamma = \int_\Gamma \phi\psi \, d\Gamma$$

It is known that $u_t \in L^2(0, T; H^{-1}(\Omega))$ (cf Evans, 1997) and $g \in L^2(0, T; H^{1/2}(\Gamma) \cap H^2(\Gamma))$ (cf Ladyzhenskaya *et al.*, 1966 and Chen & Zou 1998). We have the following estimates:

Lemma 3.1 Suppose that the conditions of Assumption 1.1 are satisfied for every $a : \Omega \times \mathbb{R} \to \mathbb{R}$, $f : \Omega \times \mathbb{R} \to \mathbb{R}$ and $g \in L^2(0, T; H^{1/2}(\Gamma))$, there exists a constant C depending on μ_1, μ_2, μ_3, T and Ω such that

$$\|u\|_{L^\infty(0,T;L^2(\Omega))} + \|u\|_{L^2(0,T;H^1(\Omega))} + \|u_t\|_{L^2(0,T;H^{-1}(\Omega))}$$
$$\leq C\left(\|g\|_{L^2(0,T;H^{1/2}(\Gamma))} + \|u_0\|_{L^2(\Omega)}\right) \quad (3.1.2)$$

Proof Let $v = u$ in (3.1.1), we have for $t \in [0, T]$

$$\frac{1}{2}\frac{d}{dt}\|u\|^2_{L^2(\Omega)} + \mu_1\|\nabla u\|^2_{L^2(\Omega)} \leq (f, u) + \langle g, u\rangle_\Gamma$$

Using Cauchy inequality, Young's inequality and (1.6.2) we obtain, for γ (which depends on meas(Ω))

$$\frac{1}{2}\frac{d}{dt}\|u\|^2_{L^2(\Omega)} + \mu_1\|\nabla u\|^2_{L^2(\Omega)} \leq (\mu_3 + \gamma)\|u\|^2_{L^2(\Omega)} + \frac{C}{4\varepsilon}\|g\|^2_{H^{1/2}(\Gamma)} + \varepsilon\|u\|^2_{H^1(\Omega)}$$

with $\varepsilon = \frac{\mu_1}{2}$, it follows that

$$\frac{1}{2}\frac{d}{dt}\|u\|^2_{L^2(\Omega)} - \beta\|u\|^2_{L^2(\Omega)} + \frac{\mu_1}{2}\|u\|^2_{H^1(\Omega)} \leq C\|g\|^2_{H^{1/2}(\Gamma)}$$

where $\beta = \gamma + \mu_1 + \mu_3$. We multiply both sides by the integrating factor $\exp(-2\beta t) > 0$

$$e^{-2\beta t}\frac{1}{2}\frac{d}{dt}\|u\|^2_{L^2(\Omega)} - e^{-2\beta t}\beta\|u\|^2_{L^2(\Omega)} + \frac{\mu_1}{2}e^{-2\beta t}\|u\|^2_{H^1(\Omega)} \leq Ce^{-2\beta t}\|g\|^2_{H^{1/2}(\Gamma)}$$

which implies

$$\frac{1}{2}\frac{d}{dt}\left[e^{-2\beta t}\|u\|^2_{L^2(\Omega)}\right] + \frac{\mu_1}{2}e^{-2\beta t}\|u\|^2_{H^1(\Omega)} \leq Ce^{-2\beta t}\|g\|^2_{H^{1/2}(\Gamma)}$$

49

For $t \in [0, T]$, we have

$$e^{-2\beta t}\|u\|_{L^2(\Omega)}^2 + \mu_1 \int_0^t e^{-2\beta s}\|u\|_{H^1(\Omega)}^2 \, ds \leq C \int_0^t e^{-2\beta s}\|g\|_{H^{1/2}(\Gamma)}^2 \, ds + \|u_0\|_{L^2(\Omega)}^2$$

(3.1.3)

Taking the supremum of (3.1.3) with respect to t over $[0, T]$, there is a constant C which depends on $\mu_1, \mu_3, \text{meas}(\Omega)$, and T such that

$$\|u\|_{L^\infty(0,T;L^2(\Omega))}^2 + \|u\|_{L^2(0,T;H^1(\Omega))}^2 \leq C\left(\|g\|_{L^2(0,T;H^{1/2}(\Gamma))}^2 + \|u_0\|_{L^2(\Omega)}^2\right) \quad (3.1.4)$$

For $u_t(t)$ we have with $t \in [0, T]$

$$\|u_t\|_{H^{-1}(\Omega)} = \sup_{v \in H^1(\Omega)} \frac{(u_t, v)}{\|v\|_{H^1(\Omega)}}, \qquad v \neq 0$$

It follows from (3.1.1) and (3.1.4) (and Assumption 1.1 in mind) that

$$(u_t, v) \leq C\left(\|u(t)\|_{H^1(\Omega)} + \|g(t)\|_{H^{1/2}(\Gamma)}\right)\|v\|_{H^1(\Omega)}$$

where C depends on μ_2, Ω and μ_3. Thus for all $v \in H^1(\Omega)$,

$$\|u_t\|_{H^{-1}(\Omega)} \leq C\left(\|u(t)\|_{H^1(\Omega)} + \|g(t)\|_{H^{1/2}(\Gamma)}\right)$$

Integrating this with respect to t from 0 to T, we have

$$\|u_t\|_{L^2(0,T;H^{-1}(\Omega))} \leq C\left(\|u(t)\|_{L^2(0,T;H^1(\Omega))} + \|g(t)\|_{L^2(0,T;H^{1/2}(\Gamma))}\right) \quad (3.1.5)$$

(3.1.2) follows from (3.1.4) and (3.1.5). $\qquad\qquad\qquad\qquad\qquad\qquad\square$

Remark 3.1 Suppose the conditions of Lemma 3.1 are satisfied with $f(x, u) = f_1(u) + f_2(x)$ then (3.1.2) becomes

$$\|u\|_{L^\infty(0,T;L^2(\Omega))} + \|u\|_{L^2(0,T;H^1(\Omega))} + \|u_t\|_{L^2(0,T;H^{-1}(\Omega))}$$
$$\leq C\left(\|g\|_{L^2(0,T;H^{1/2}(\Gamma))} + \|f_2\|_{H^{-1}(\Omega)} + \|u_0\|_{L^2(\Omega)}\right)$$

Lemma 3.2 In Lemma 3.1, it is assumed that the solution $u \in L^2(0, T; H_0^1(\Omega))$. However, if $u(t) \in X \cap H_0^1(\Omega)$ for $t \in (0, T]$, we have

$$\|u\|_{L^2(0,T;X)} \leq C\left(\|g\|_{L^2(0,T;H^{1/2}(\Gamma))} + \|u_0\|_{L^2(\Omega)}\right) \quad (3.1.6)$$

Proof Multiply (1.5.1) by $v \in X \cap H_0^1(\Omega)$ and integrate over Ω_1

$$\int_{\Omega_1} u_t v - \int_{\Gamma} a(x,u)\frac{\partial u}{\partial n_1} v + \int_{\Omega_1} a(x,u)\nabla u \cdot \nabla v = \int_{\Omega_1} f(x,u)v \qquad (3.1.7)$$

where n_1 is the unit outward normal to the interface. Let $v = u_t$ in (3.1.7) and using (1.5.1)

$$-\int_{\Omega_1} a\nabla u \cdot \nabla[\nabla \cdot (a\nabla u)] = \|u_t\|_{L^2(\Omega_1)}^2 - \int_{\Gamma} gu_t - \int_{\Omega_1} fu_t + \int_{\Omega_1} a\nabla u \cdot \nabla f \quad (3.1.8)$$

Using the notation $\partial_i u$ for $\frac{\partial u}{\partial x_i}$ $(i = 1,2)$, we have the expression

$$\begin{aligned}
-\int_{\Omega_1} a\nabla u \cdot \nabla[\nabla \cdot (a\nabla u)] &\equiv -\sum_{i,j=1}^{2} \int_{\Omega_1} (a\partial_i u)(\partial_i \partial_j (a\partial_j u)) \\
&= \sum_{i,j=1}^{2} \left[\int_{\Omega_1} \partial_j(a\partial_i u)(\partial_i(a\partial_j u)) \right. \\
&\quad \left. - \int_{\Gamma} (a\partial_i u)(\partial_i(a\partial_j u)) \right] \qquad (3.1.9)
\end{aligned}$$

Substitute (3.1.9) into (3.1.8)

$$\begin{aligned}
\sum_{i,j=1}^{2} \int_{\Omega_1} \partial_j(a\partial_i u)(\partial_i(a\partial_j u)) &= \|u_t\|_{L^2(\Omega_1)}^2 - \int_{\Gamma} gu_t - \int_{\Omega_1} fu_t + \int_{\Omega_1} a\nabla u \cdot \nabla f \\
&\quad + \sum_{i,j=1}^{2} \int_{\Gamma} (a\partial_i u)(\partial_i(a\partial_j u))
\end{aligned}$$

By Assumption 1.1, Schwartz and Young's inequalities, we have for γ, depending on $\mathrm{meas}(\Omega_1)$,

$$\begin{aligned}
\mu_1^2 \sum_{i,j=1}^{2} (\partial_i \partial_j u)^2 &\leq \frac{3}{2}\|u_t\|_{L^2(\Omega)}^2 + \frac{1}{2}\|g\|_{H^{1/2}(\Gamma)}^2 + \frac{\mu_3}{2}\frac{d}{dt}\|u\|_{L^2(\Omega_1)}^2 + \gamma\|u_t\|_{L^2(\Omega_1)}^2 \\
&\quad + \frac{\mu_2^4}{\mu_1^2} \sum_{i=1}^{2} \int_{\Gamma} (\partial_i u)^2 + \frac{\mu_1^2}{2} \sum_{i,j=1}^{2} \int_{\Omega_1} (\partial_i \partial_j u)^2 + \mu_3 \int_{\Omega_1} |\nabla u|^2
\end{aligned}$$

which implies

$$\sum_{i,j=1}^{2} (\partial_i \partial_j u)^2 \leq C \left[\|u_t\|_{L^2(\Omega_1)}^2 + \|g\|_{H^{1/2}(\Gamma)}^2 + \frac{d}{dt}\|u\|_{L^2(\Omega_1)}^2 + \|u\|_{H^1(\Omega_1)}^2 \right]$$

51

Now, we have

$$
\begin{aligned}
\|u\|_{H^2(\Omega_1)}^2 &= \sum_{\alpha=2} \|D^\alpha u\|_{L^2(\Omega_1)}^2 + \|u\|_{H^1(\Omega_1)}^2 \\
&= \sum_{i,j=1}^2 (\partial_i \partial_j u)^2 + \|u\|_{H^1(\Omega_1)}^2 \\
&\leq C \left[\|u_t\|_{L^2(\Omega_1)}^2 + \|g\|_{H^{1/2}(\Gamma)}^2 + \frac{d}{dt}\|u\|_{L^2(\Omega_1)}^2 + \|u\|_{H^1(\Omega_1)}^2 \right]
\end{aligned}
$$

Integrating with respect to t from 0 to T then using (3.1.2), we have

$$
\|u\|_{L^2(0,T;H^2(\Omega_1))} \leq C \left[\|g\|_{L^2(0,T;H^{1/2}(\Gamma))} + \|u_0\|_{L^2(\Omega)} \right] \tag{3.1.10}
$$

Following the same argument as above, we have

$$
\|u\|_{L^2(0,T;H^2(\Omega_2))} \leq C \left[\|g\|_{L^2(0,T;H^{1/2}(\Gamma))} + \|u_0\|_{L^2(\Omega)} \right] \tag{3.1.11}
$$

(3.1.6) follows from (3.1.2), (3.1.10) and (3.1.11). $\qquad\square$

3.2 Finite Element Discretisation and Auxiliary Results

$\mathcal{T}_h$ denotes a partition of Ω into disjoint triangles K (called elements) such that no vertex of any triangle lies on the interior or side of another triangle. The domain Ω_1 is approximated by a domain Ω_1^h with a polygonal boundary Γ_h whose vertices all lie on the interface Γ. Ω_2^h represents the domain with $\partial\Omega$ and Γ_h as its exterior and interior boundaries respectively.

Let h_K be the diameter of an element $K \in \mathcal{T}_h$ and $h = \max_{K \in \mathcal{T}_h} h_K$. Let $\mathcal{T}_h^\star$ denote the set of all elements that are intersected by the interface Γ;

$$
\mathcal{T}_h^\star = \{K \in \mathcal{T}_h : K \cap \Gamma \neq \phi\}
$$

$K \in \mathcal{T}_h^\star$ is called an interface element and we write $\Omega_h^\star = \bigcup_{K \in \mathcal{T}_h^\star} K$.
The triangulation $\mathcal{T}_h$ of the domain Ω satisfies the following conditions

(i) $\bar{\Omega} = \bigcup_{K \in \mathcal{T}_h} \bar{K}$

(ii) If $\bar{K}_1, \bar{K}_2 \in \mathcal{T}_h$ and $\bar{K}_1 \neq \bar{K}_2$, then either $\bar{K}_1 \cap \bar{K}_2 = \emptyset$ or $\bar{K}_1 \cap \bar{K}_2$ is a common vertex or a common edge.

(iii) Each $K \in \mathcal{T}_h$ is either in Ω_1^h or Ω_2^h, and has at most two vertices lying on Γ_h.

(iv) For each element $K \in \mathcal{T}_h$, let r_K and $\bar{r}_K$ be the diameters of its inscribed and circumscribed circles respectively. It is assumed that, for some fixed $h_0 > 0$, there exists two positive constants C_0 and C_1, independent of h, such that

$$C_0 r_K \leq h \leq C_1 \bar{r}_K \quad \forall\, h \in (0, h_0)$$

For any interface element $K \in \mathcal{T}_h^\star$, let $K_1 = K \cap \Omega_1$ and $K_2 = K \cap \Omega_2$, it was shown by Chen & Zou (1998) that

$$\text{either} \quad \text{meas}(K_1) \leq Ch_K^3 \quad \text{or} \quad \text{meas}(K_2) \leq Ch_K^3$$

To correct the discontinuities that might occur at the corners, we make the elements at the corners finer (see Fig 3.1).

Let S_h denote the space of continuous piecewise linear functions on $\mathcal{T}_h$ which vanish on $\partial \Omega$. To describe a function $\omega \in S_h$, we will use the values $\omega(N_i)$ of ω as parameter, where N_i, $(i = 1, 2, ..., M)$ are nodes (see figure 3.3) of triangles in $\mathcal{T}_h$. Since $\omega = 0$ on $\partial \Omega$, we exclude the nodes on the boundary $\partial \Omega$. The basis function for the space S_h is ϕ_j which is given for $i = 1, .., M$ as

$$\phi_j(N_i) = \delta_{ij} = \begin{cases} 1 & \text{if } i = j \\ 0 & \text{if } i \neq j \end{cases}$$

The support of ϕ_j consists of the triangles with common nodes N_j. A function $w \in S_h$ has the representation

$$\omega(x) = \sum_{j=1}^{M} \xi_j \phi_j(x) \qquad \text{for} \quad x \in \Omega \cup \partial \Omega$$

53
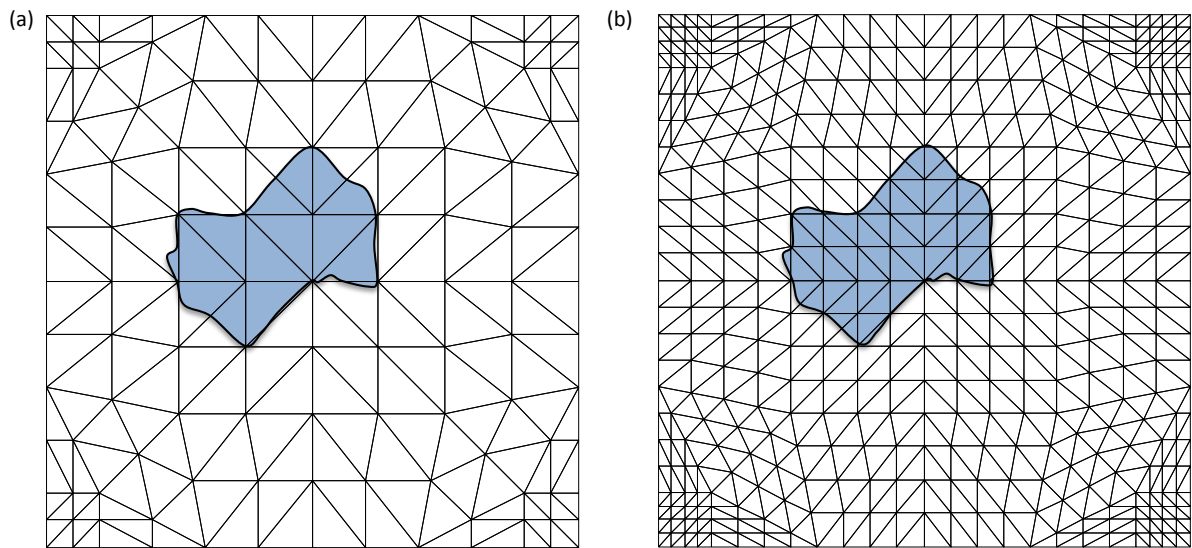
Figure 3.1: A body fitted triangulation of a rectangular domain with one refinement
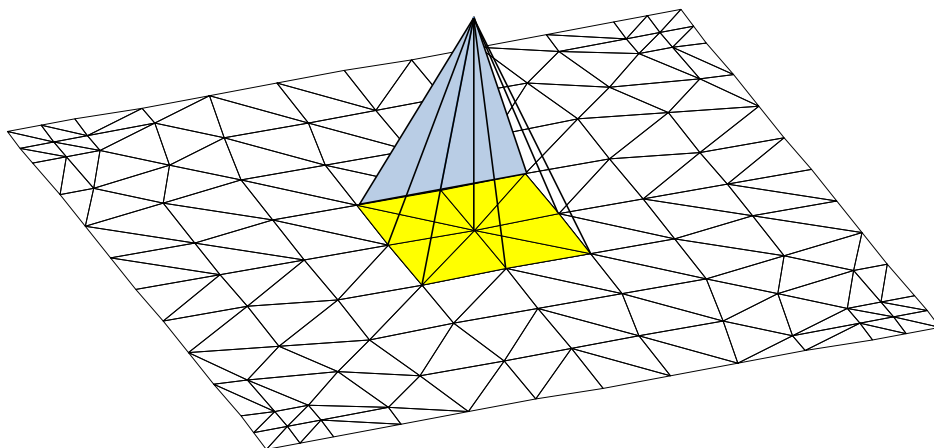
Figure 3.2: Basis function ϕ_j

where $\xi_j = \omega(N_j)$

Let $\pi_h : C(\bar{\Omega}) \to S_h$ be the Lagrange interpolation operator corresponding to the space S_h. The standard interpolation theory can not be applied due to the low regularity of the solution across the interface. We follow Chen and Zou (1998) for the proof of the following result.

Lemma 3.3 For the linear interpolation operator $\pi_h : C(\bar{\Omega}) \to S_h$, we have, for $m = 0, 1$, and $0 < h < 1$

$$\|u - \pi_h u\|_{H^m(\Omega)} \leq Ch^{2-m}\left(1 + \frac{1}{|\ln h|}\right)^{1/2} \|u\|_X \qquad \forall\, u \in X \qquad (3.2.1)$$

Proof By standard finite element interpolation theory [Ciarlet (1978),Evans (1997), Brenner & Scott (2008)], for any triangle $K \in \mathcal{T}_h \backslash \mathcal{T}_h^*$,

$$\|u - \pi_h u\|_{H^m(K)} \leq Ch^{2-m}\|u\|_{H^2(K)} \qquad \text{for} \quad m = 0, 1 \qquad (3.2.2)$$

Now, for any element $K \in \mathcal{T}_h^*$, using Hölder's inequality and the fact that $meas(K_1) \leq Ch^3$, we have

$$
\begin{aligned}
\|u - \pi_h u\|_{H^m(K_1)}^2 &\leq \sum_{|\alpha| \leq m} \|D^\alpha(u - \pi_h u)\|_{L^2(K_1)}^2 \\
&\leq [meas(K_1)]^{\frac{p-2}{p}} \left(\sum_{|\alpha| \leq m} \|D^\alpha(u - \pi_h u)\|_{L^2(K_1)}^p\right)^{2/p} \\
&\leq Ch^{3\left(\frac{p-2}{p}\right)} \left(\sum_{|\alpha| \leq m} \|D^\alpha(u - \pi_h u)\|_{L^2(K_1)}^p\right)^{2/p} \qquad \text{for} \quad p > 2
\end{aligned}
$$

Therefore

$$
\begin{aligned}
\|u - \pi_h u\|_{H^m(K_1)} &\leq Ch^{3\left(\frac{p-2}{2p}\right)}\|u - \pi_h u\|_{W^{m,p}(K_i)} \\
&\leq Ch^{3\left(\frac{p-2}{2p}\right)}\|u - \pi_h u\|_{W^{m,p}(K)}
\end{aligned}
$$

Using the standard finite element interpolation theory,

$$\|u - \pi_h u\|_{H^m(K_1)} \leq Ch^{\frac{3p-6}{2p}+1-m}\|u\|_{W^{1,p}(K)} \quad \text{for any } p > 2, \, m = 0, 1$$

55

Recall the Sobolev embedding inequality for two dimensions [Ren & Wei (1994), Evans (1997)]

$$\|\phi\|_{L^p(\Omega_i)} \leq Cp^{1/2}\|\phi\|_{H^1(\Omega_i)} \quad \forall\, p > 2, \ \ \phi \in H^1(\Omega_i), \ \ i = 1, 2$$

therefore,

$$\|u - \pi_h u\|_{H^m(K_1)} \leq Ch^{\frac{3p-6}{2p}+1-m}p^{1/2}\|u\|_{H^1(K)} \quad \text{for any } p > 2, \ m = 0, 1 \quad (3.2.3)$$

By means of extensions [Stein (1971)],

$$\|u - \pi_h u\|_{H^m(K_2)} \leq Ch^{2-m}\|u\|_{H^2(K)} , \quad m = 0, 1 \qquad (3.2.4)$$

It follows from (3.2.3) and (3.2.4) that

$$\sum_{K \in \mathcal{T}_h^*} \|u - \pi_h u\|_{H^m(K)}^2 \ \leq \ Ch^{4-2m}\left[1 + ph^{1-6/p}\right]\|u\|_X^2 \qquad (3.2.5)$$

From (3.2.2) and (3.2.5), we have

$$\|u - \pi_h u\|_{H^m(\Omega)}^2 \ \leq \ Ch^{4-2m}\|u\|_X^2 + Ch^{4-2m}ph^{1-6/p}\|u\|_X^2 , \qquad m = 0, 1 \quad p > 2$$

Since $p > 2$, we take

$$p = 2\left(1 + \frac{1}{|\ln h|}\right) > 2 \qquad \text{for } 0 < h < 1$$

and (3.2.1) follows.

For the approximation property of g_h to the interface function g, we have the following (cf Chen & Zou, 1998)

Lemma 3.4 Assume that $g \in H^2(\Gamma)$. Then we have

$$|\langle g, v_h\rangle_\Gamma - \langle g_h, v_h\rangle_{\Gamma_h}| \leq Ch^{3/2}\|g\|_{H^2(\Gamma)}\|v_h\|_{H^1(\Omega_h^\star)} \qquad \forall\, v_h \in S_h \qquad (3.2.6)$$

The following result is one of the instruments used to establish the error estimates.

Lemma 3.5 For all $\nu_h, \omega_h \in S_h$, we have

$$|A(u : \nu_h, \omega_h) - A_h(u_h : \nu_h, \omega_h)| \leq \mu_3 \|\nabla \nu_h\|_{L^\infty(\Omega)} \|u - u_h\|_{L^2(\Omega)} \|\omega_h\|_{H^1(\Omega)}$$
$$+ Ch \|\nu_h\|_{H^1(\Omega_h^\star)} \|\omega_h\|_{H^1(\Omega_h^\star)}$$

Proof Let $\tilde{K}$ denote one of K_1 or K_2, ie $\mathrm{supp}(a(x,u) - a(x,u_h)) \cap K = \tilde{K} \;\; \forall \, K \in \mathcal{T}_h^\star$. See Fig 3.3.

$$
\begin{aligned}
|A(u : \nu_h, \omega_h) - A_h(u_h : \nu_h, \omega_h)| &\leq \sum_{K \in \mathcal{T}_h} \int_K |a(x,u) - a(x,u_h)||\nabla \nu_h \cdot \nabla \omega_h| \\
&= \sum_{K \in \mathcal{T}_h} \int_{K \setminus \tilde{K}} |a(x,u) - a(x,u_h)||\nabla \nu_h \cdot \nabla \omega_h| \\
&\quad + \sum_{K \in \mathcal{T}_h^\star} \int_{\tilde{K}} |a(x,u) - a(x,u_h)||\nabla \nu_h \cdot \nabla \omega_h|
\end{aligned}
$$

Mean value theorem cannot be applied on $\tilde{K}$ due to the discontinuity across the interface and therefore we have

$$
\begin{aligned}
|A(u : \nu_h, \omega_h) - A_h(u_h : \nu_h, \omega_h)| &\leq \mu_3 \sum_{K \in \mathcal{T}_h} \int_{K \setminus \tilde{K}} |u - u_h||\nabla \nu_h||\nabla \omega_h| \\
&\quad + |\mu_2 - \mu_1| \sum_{K \in \mathcal{T}_h^\star} \int_{\tilde{K}} |\nabla \nu_h \cdot \nabla \omega_h| \\
&\leq \mu_3 \|\nabla \nu_h\|_{L^\infty(\Omega)} \|u - u_h\|_{L^2(\Omega)} \|\nabla \omega_h\|_{L^2(\Omega)} \\
&\quad + Ch \|\nabla \nu_h\|_{L^2(\Omega_h^\star)} \|\nabla \omega_h\|_{L^2(\Omega_h^\star)} \\
&\leq \mu_3 \|\nabla \nu_h\|_{L^\infty(\Omega)} \|u - u_h\|_{L^2(\Omega)} \|\omega_h\|_{H^1(\Omega)} \\
&\quad + Ch \|\nu_h\|_{H^1(\Omega_h^\star)} \|\omega_h\|_{H^1(\Omega_h^\star)}
\end{aligned}
$$

We have made use of the fact that $\nabla \nu_h$ and $\nabla \omega_h$ are constant in $K \in \mathcal{T}_h$ and $\mathrm{meas}(\tilde{K}) \leq Ch^3$.
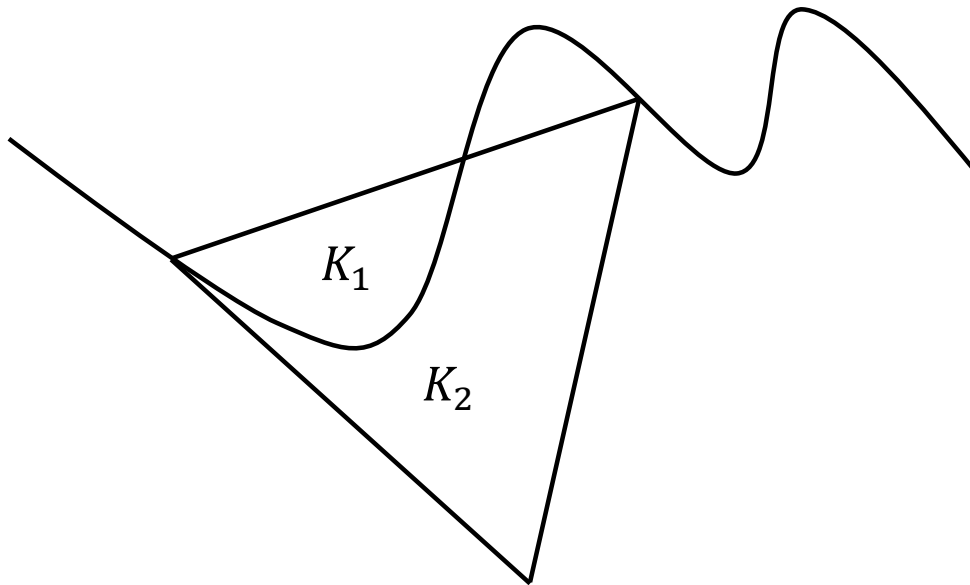
Figure 3.3: A typical interface element showing $\tilde{K}$

Remark 3.2 If a is independent of u, we obtain the result by Chen and Zou (1998)

$$|A(\nu_h, \omega_h) - A_h(\nu_h, \omega_h)| \le Ch \|\nu_h\|_{H^1(\Omega_h^\star)} \|\omega_h\|_{H^1(\Omega_h^\star)}$$

The following lemma will be used for the error estimation (Sinha and Deka, 2007)

Lemma 3.7 Let $\Omega_h^\star$ be the union of all interface triangles. Then we have

$$\|v\|_{H^1(\Omega_h^\star)} \le Ch^{1/2} \|v\|_X \quad \forall\, v \in X$$

3.3   Continuous Time Error Estimates

This section is devoted to the analysis of the spatially discrete approximation of the nonlinear parabolic interface problem. Almost optimal order error estimates are analysed in $H^1(\Omega)$-norm and $L^2(\Omega)$-norm. The finite element analysis of nonlinear non-interface problems are contained in Thomee (2006) and the references therein.

The semidiscrete problem is to find $u_h : [0,T] \to S_h$ such that $u_h(0) = u_{h,0}$ and satisfying

$$(u_{h,t}, v_h)_h + A_h(u_h : u_h, v_h) = (f(x, u_h), v_h)_h + \langle g_h, v_h \rangle_{\Gamma_h} \quad \forall\, v_h \in S_h, \text{ a.e } t \in [0,T]$$
$$(3.3.1)$$

where $(\psi, \phi)_h : H^1(\Omega) \times H^1(\Omega) \to \mathbb{R}$, $A_h(u_h : \phi, \psi) : H^1(\Omega) \times H^1(\Omega) \to \mathbb{R}$ and $(f(x, u_h), v_h)_h : \mathbb{R} \times H^1(\Omega) \to \mathbb{R}$ are defined as

$$(\psi, \phi)_h = \sum_{K \in \mathcal{T}_h} \int_K \psi\phi \, dx \,, \quad A_h(u_h : \phi, \psi) = \sum_{K \in \mathcal{T}_h} \int_K a(x, u_h)\nabla\phi \cdot \nabla\psi \, dx \,,$$

$$(f(x, u_h), \phi)_h = \sum_{K \in \mathcal{T}_h} \int_K f(x, u_h)\phi \, dx \quad \forall\, \phi, \psi \in H^1(\Omega), \; t \in [0,T]$$

$(\psi, \phi)_h : H^1(\Omega) \times H^1(\Omega) \to \mathbb{R}$, $A_h(\phi, \psi) : H^1(\Omega) \times H^1(\Omega) \to \mathbb{R}$ and $(f(x, u_h), \phi)_h : \mathbb{R} \times H^1(\Omega) \to \mathbb{R}$ are the discrete versions of $(\psi, \phi) : H^1(\Omega) \times H^1(\Omega) \to \mathbb{R}$, $A(u : \phi, \psi) : H^1(\Omega) \times H^1(\Omega) \to \mathbb{R}$ and $(f(x, u), \phi) : \mathbb{R} \times H^1(\Omega) \to \mathbb{R}$ respectively

and are obtained numerically using quadrature schemes. See Germain (2001) and the references therein, for more information on numerical integration in FEM.

The existence of a unique solution to (3.3.1) follows the standard theory of Ordinary Differential Equations (see Thomee (2006) for details). With u_h expressed as $u_h(x,t) = \sum_{j=1}^{N_h} \alpha_j(t)\phi_j(x)$ $(\alpha_j(t) : [0,T] \to \mathbb{R})$ in (3.3.1), this results to a system of nonlinear ODEs. The assumptions on $a(x,u), f(x,u)$ and $g(x,t)$ guarantee a unique bounded solution for $t \in [0,T]$.

It is easy to see that u_h in (3.3.1) satisfies the a priori estimate (3.2.2)

$$\|u_h\|_{L^\infty(0,T;L^2(\Omega))} + \|u_h\|_{L^2(0,T;H^1(\Omega))} + \|u_{h,t}\|_{L^2(0,T;H^{-1}(\Omega))}$$
$$\leq C \left(\|g\|_{L^2(0,T;H^{1/2}(\Gamma))} + \|u_0\|_{L^2(\Omega)} \right) \quad (3.3.2)$$

The convergence of u_h in (3.3.1) to u in (3.1.1) could be established using Banach-Alaoglu theorem (Siddiqi, 2004 Theorem 4.5.1) and the boundedness of u_h, $u_{h,t}$ in $L^2(0,T;H_0^1(\Omega))$ and $L^2(0,T;H_0^{-1}(\Omega))$ respectively.

Let $L_h : L_0^2(\Omega) \to S_h$ be the standard L^2 projection defined by

$$(L_h\omega, \psi) = (\omega, \psi) \qquad \forall\, \omega \in L^2(\Omega),\ \psi \in S_h \quad (3.3.3)$$

Since (3.3.3) holds for all $\psi \in S_h$, it holds particularly for $\psi = L_h\omega$

$$
\begin{aligned}
\Rightarrow \quad \|L_h\omega\|_{L^2(\Omega)}^2 &= (L_h\omega, L_h\omega) \\
&= (\omega, L_h\omega) \\
&\leq \|\omega\|_{L^2(\Omega)}\|L_h\omega\|_{L^2(\Omega)} \\
\Rightarrow \quad \|L_h\omega\|_{L^2(\Omega)} &\leq \|\omega\|_{L^2(\Omega)} \quad (3.3.4)
\end{aligned}
$$

Also, if $\omega \in H^1(\Omega)$ and let $\psi = D^\alpha L_h\omega$ for a multi-index $|\alpha| = 1$,

$$\|D^\alpha L_h\omega\|_{L^2(\Omega)} \leq \|D^\alpha\omega\|_{L^p(\Omega)} \quad (3.3.5)$$

(3.3.4) and (3.3.5) imply

$$\|L_h\omega\|_{H^1(\Omega)} \leq \|\omega\|_{H^1(\Omega)} \quad \forall\, \omega \in H^1(\Omega) \quad (3.3.6)$$

$L_h v \in S_h$ is the best approximation in the L^2-norm to $v \in L^2(\Omega)$. Thus, Lemma 3.3 implies that

$$\|L_h\omega - \omega\|_{L^2(\Omega)} \leq C\|\pi_h\omega - \omega\|_{L^2(\Omega)} \leq Ch^2\left(1 + \frac{1}{|\log h|}\right)^{1/2}\|\omega\|_X \qquad (3.3.7)$$

Now, it follows from Sinha & Deka (2007) and inverse inequality (Ren & Wei 1994) that

$$
\begin{aligned}
\|L_h\omega - \omega\|_{H^1(\Omega)} &\leq \|\pi_h\omega - \omega\|_{H^1(\Omega)} + \|L_h\omega - \pi_h\omega\|_{H^1(\Omega)} \\
&\leq \|\pi_h\omega - \omega\|_{H^1(\Omega)} + Ch^{-1}\|L_h\omega - \pi_h\omega\|_{L^2(\Omega)} \\
&\leq Ch\left(1 + \frac{1}{|\log h|}\right)^{1/2}\|\omega\|_X \\
&\quad + Ch^{-1}\left\{\|\omega - \pi_h\omega\|_{L^2(\Omega)} + \|L_h\omega - \omega\|_{L^2(\Omega)}\right\} \\
&\leq Ch\left(1 + \frac{1}{|\log h|}\right)^{1/2}\|\omega\|_X \\
&\quad + Ch^{-1}\left[Ch^2\left(1 + \frac{1}{|\log h|}\right)^{1/2}\|\omega\|_X\right] \\
&\leq Ch\left(1 + \frac{1}{|\log h|}\right)^{1/2}\|\omega\|_X \qquad (3.3.8)
\end{aligned}
$$

The theorem below gives the convergence result for the spatially discrete scheme in $L^2(0,T;H^1(\Omega))$-norm.

Theorem 3.1 Suppose that the conditions of Assumption 1.1 are satisfied for every $a : \Omega \times \mathbb{R} \to \mathbb{R}$, $f : \Omega \times \mathbb{R} \to \mathbb{R}$ and $g \in L^2(0,T;H^{1/2}(\Gamma) \cap H^2(\Gamma))$ and let u and u_h be the solution of (3.1.1) and (3.3.1) respectively, then for $u_0 \in H_0^1(\Omega)$ there exists a positive constant C, independent of h, such that

$$\|u - u_h\|_{L^2(0,T;H^1(\Omega))}^2 \leq C(u_0, a, f, g)h^2\left(1 + \frac{1}{|\log h|}\right)$$

Proof Subtract (3.3.1) from (3.1.1) to get:

$$
\begin{aligned}
(u_t - u_{h,t}, v_h) + A(u : u, v_h) &= A_h(u_h : u_h, v_h) + (f(x,u), v_h) - (f(x,u_h), v_h)_h \\
&\quad + \langle g, v_h \rangle_\Gamma - \langle g_h, v_h \rangle_{\Gamma_h} \\
&\quad + (u_{h,t}, v_h)_h - (u_{h,t}, v_h) \quad \forall\, v_h \in S_h
\end{aligned}
$$

61

Let $e(t) = u - u_h$, $v_h = L_h u - u_h$ and use (3.3.3)

$$\frac{1}{2}\frac{d}{dt}\|e(t)\|^2_{L^2(\Omega)} + A(u : e, e) = A_h(u_h : u_h, L_h u - u_h) - A(u : u_h, L_h u - u_h)$$
$$+ A(u : u - u_h, u - L_h u) + (f(x, u), L_h u - u_h)$$
$$- (f(x, u_h), L_h u - u_h)_h + \langle g, L_h u - u_h \rangle_\Gamma$$
$$- \langle g_h, L_h u - u_h \rangle_{\Gamma_h} + (u_{h,t}, L_h u - u_h)_h - (u_{h,t}, L_h u - u_h)$$
$$\leq B_1 + B_2 + B_3 + B_4 \qquad (3.3.9)$$

where

$$B_1 = |A_h(u_h : u_h, L_h u - u_h) - A(u : u_h, L_h u - u_h)|$$
$$B_2 = |A(u : u - u_h, u - L_h u)| + |(u_{h,t}, L_h u - u_h)_h - (u_{h,t}, L_h u - u_h)|$$
$$B_3 = |(f(x, u), L_h u - u_h) - (f(x, u_h), L_h u - u_h)_h|$$
$$B_4 = |\langle g, L_h u - u_h \rangle_\Gamma - \langle g_h, L_h u - u_h \rangle_{\Gamma_h}|$$

Using (3.3.8) and the fact that ∇u_h is constant on $K \in \mathcal{T}_h$, $\|\nabla u_h\|_{L^\infty(\Omega)} \leq c$,

$$B_1 \leq \mu_3 \|\nabla u_h\|_{L^\infty(\Omega)} \|e(t)\|_{L^2(\Omega)} \|L_h u - u_h\|_{H^1(\Omega)} + Ch\|u_h\|_{H^1(\Omega)} \|L_h u - u_h\|_{H^1(\Omega)}$$
$$\leq \mu_3 c \|e(t)\|_{L^2(\Omega)} \left[\|e(t)\|_{H^1(\Omega)} + Ch\left(1 + \frac{1}{|\log h|}\right)^{1/2} \|u\|_X \right]$$
$$+ Ch\|u_h\|_{H^1(\Omega)} \left[\|e(t)\|_{H^1(\Omega)} + Ch\left(1 + \frac{1}{|\log h|}\right)^{1/2} \|u\|_X \right]$$
$$\leq (\varepsilon + 1)c^2 \mu_3^2 \|e(t)\|^2_{L^2(\Omega)} + \frac{1}{2\varepsilon}\|e(t)\|^2_{H^1(\Omega)}$$
$$+ Ch^2\left(1 + \frac{1}{|\log h|}\right) [\|u\|^2_X + (\varepsilon + 1)\|u_h\|^2_{H^1(\Omega)}] \qquad (3.3.10)$$

We obtain the last inequality by using Young's inequality (with $\varepsilon > 0$) and fact that $h < 1$.

$$B_2 \leq \mu_2 \|e(t)\|_{H^1(\Omega)} \|u - L_h u\|_{H^1(\Omega)} + Ch\|u_{h,t}\|_{H^{-1}(\Omega_h^\star)} \|L_h u - u_h\|_{H^1(\Omega_h^\star)}$$
$$\leq \frac{1}{2\varepsilon}\|e(t)\|^2_{H^1(\Omega)} + C(\varepsilon)h^2\left(1 + \frac{1}{|\log h|}\right) \|u\|^2_X + (\varepsilon + 1)Ch^2 \|u_{h,t}\|^2_{H^{-1}(\Omega)}$$
$$\leq \frac{1}{2\varepsilon}\|e(t)\|^2_{H^1(\Omega)} + C(\varepsilon)h^2\left(1 + \frac{1}{|\log h|}\right)\left[\|u\|^2_X + \|u_{h,t}\|^2_{H^{-1}(\Omega)}\right] \qquad (3.3.11)$$

$$
\begin{aligned}
B_3 \;\leq\;& |(f(x,u), L_h u - u_h) - (f(x,u), L_h u - u_h)_h| \\
&+ |(f(x,u) - f(x,u_h), L_h u - u_h)_h| \\
\leq\;& Ch\|u\|_{H^1(\Omega_h^\star)}\|L_h u - u_h\|_{H^1(\Omega_h^\star)} + \mu_3\|u - u_h\|_{L^2(\Omega)}\|L_h u - u_h\|_{L^2(\Omega)} \\
\leq\;& Ch^2\left(1 + \frac{1}{|\log h|}\right)\left[(\varepsilon+1)\|u\|_{H^1(\Omega)}^2 + \|u\|_X^2\right] + \frac{1}{4\varepsilon}\|e(t)\|_{H^1(\Omega)}^2 \\
&+ (\mu_3^2 + \mu_3)\|e(t)\|_{L^2(\Omega)}^2 \\
\leq\;& C(\varepsilon)h^2\left(1 + \frac{1}{|\log h|}\right)\|u\|_X^2 + \frac{1}{4\varepsilon}\|e(t)\|_{H^1(\Omega)}^2 + C(\mu_3)\|e(t)\|_{L^2(\Omega)}^2 \quad (3.3.12)
\end{aligned}
$$

Using Lemma 3.4,

$$
\begin{aligned}
B_4 \;\leq\;& Ch^{3/2}\|g\|_{H^2(\Gamma)}\|L_h u - u_h\|_{H^1(\Omega)} \\
\leq\;& Ch^3(\varepsilon+1)\|g\|_{H^2(\Gamma)}^2 + \frac{1}{4\varepsilon}\|e(t)\|_{H^1(\Omega)}^2 + Ch^2\left(1 + \frac{1}{|\log h|}\right)\|u\|_X^2 \quad (3.3.13)
\end{aligned}
$$

Substitute $(3.3.10) - (3.3.13)$ into $(3.3.9)$ and simplify with $\varepsilon = 3/\mu_1$ to obtain, for $h < 1$,

$$
\begin{aligned}
\frac{1}{2}\frac{d}{dt}\|e(t)\|_{L^2(\Omega)}^2 + \frac{\mu_1}{2}\|e(t)\|_{H^1(\Omega)}^2 \;\leq\;& \gamma\|e(t)\|_{L^2(\Omega)}^2 \\
&+ Ch^2\left(1 + \frac{1}{|\log h|}\right)\left(\|g\|_{H^2(\Gamma)}^2 + \|u\|_X^2 + \|u_h\|_{H^1(\Omega)}^2 + \|u_{h,t}\|_{H^{-1}(\Omega)}^2\right)
\end{aligned}
$$

where $\gamma > 0$ depends on c, μ_3 and μ_1. It follows that

$$
\begin{aligned}
e^{-2\gamma t}\frac{3\mu_1}{8}\|e(t)\|_{H^1(\Omega)}^2 + \frac{1}{2}\frac{d}{dt}\left[\|e(t)\|_{L^2(\Omega)}^2 e^{-2\gamma t}\right] \\
\leq Ch^2\left(1 + \frac{1}{|\log h|}\right)e^{-2\gamma t}\left(\|g\|_{H^2(\Gamma)}^2 + \|u\|_X^2 + \|u_h\|_{H^1(\Omega)}^2 + \|u_{h,t}\|_{H^{-1}(\Omega)}^2\right)
\end{aligned}
$$

The result follows by integrating both sides with respect to time from 0 to T and using Lemma 3.1, Lemma 3.2, (3.3.2), Lemma 3.3 with $u_{0,h} = \pi_h u_0$.

Theorem 3.2 Suppose that the conditions of Assumption 1.1 are satisfied for every $a : \Omega \times \mathbb{R} \to \mathbb{R}$, $f : \Omega \times \mathbb{R} \to \mathbb{R}$ and $g \in L^2(0,T; H^2(\Gamma))$ and let u and u_h be the solution of (3.1.1) and (3.3.1) respectively, then for $u_0 \in H_0^1(\Omega)$ there exists a positive constant C, independent of h, such that

$$
\|u - u_h\|_{L^2(0,T;L^2(\Omega))} \;\leq\; h^2\left(1 + \frac{1}{|\log h|}\right)C(u_0, u, g)
$$

63

where

$$C(u_0, u, g) = C \left\{ \|u_0\|_X^2 + \|u\|_{L^\infty(0,T;X)}^2 \right.$$

$$\left. + \int_0^T \exp(-\gamma t) \left(\|g\|_{H^2(\Gamma)}^2 + \|u\|_X^2 + \|u_t\|_X^2 \right) \, dt \right\}^{1/2}$$

The proof of this theorem requires some preparations

Let $P_h : X \cap H^1(\Omega) \to S_h$ be the elliptic projection of the exact solution u in S_h defined by

$$A_h(u : P_h \nu, \phi) = A(u : \nu, \phi) \quad \forall \, \phi \in S_h, \, t \in [0, T] \qquad (3.3.14)$$

From (3.3.14)

$$
\begin{aligned}
\mu_1 \|P_h \nu\|_{H^1(\Omega)}^2 &\leq A_h(u : P_h \nu, P_h \nu) \\
&\leq A(u : \nu, P_h \nu) \\
&\leq \mu_2 \|\nu\|_{H^1(\Omega)} \|P_h \nu\|_{H^1(\Omega)}
\end{aligned}
$$

It follows that, for $C > 0$,

$$\|P_h \nu\|_{H^1(\Omega)} \leq C \|\nu\|_{H^1(\Omega)} \qquad \forall \, \nu \in H^1(\Omega) \qquad (3.3.15)$$

For this projection, we have

Lemma 3.8 Let u be a smooth function in $\Omega \times T$ and $a = a(x, u)$ satisfies Assumption 1.1. Assume that $u \in X \cap H_0^1$ and let $P_h u$ be defined as in (3.3.14), then

$$\|P_h u - u\|_{H^1(\Omega)} \leq Ch \left(1 + \frac{1}{|\log h|} \right)^{1/2} \|u\|_X \qquad (3.3.16)$$

$$\|P_h u - u\|_{L^2(\Omega)} \leq Ch^2 \left(1 + \frac{1}{|\log h|} \right) \|u\|_X \qquad (3.3.17)$$

64

Proof For $\rho > 0$, we have

$$
\begin{aligned}
\rho\|P_h u - u\|_{H^1(\Omega)}^2 &\leq A_h(u : P_h u - u, P_h u - u) \\
&\leq A_h(u : P_h u, P_h u - \phi) - A_h(u : u, P_h u - \phi) \\
&\quad + A_h(u : P_h u - u, \phi - u), \quad \phi \in S_h \\
&\leq |A(u : u, P_h u - \phi) - A_h(u : u, P_h u - \phi)| \\
&\quad + |A_h(u : P_h u - u, \phi - u)|
\end{aligned}
$$

By a similar argument to the proof of Lemma 3.5, we have

$$
\begin{aligned}
\rho\|P_h u - u\|_{H^1(\Omega)}^2 &\leq Ch\|u\|_{H^1(\Omega)}\|P_h u - \phi\|_{H^1(\Omega)} + \|P_h u - u\|_{H^1(\Omega)}\|\phi - u\|_{H^1(\Omega)} \\
&\leq Ch\|u\|_{H^1(\Omega)}\|P_h u - u\|_{H^1(\Omega)} + Ch\|u\|_{H^1(\Omega)}\|u - \phi\|_{H^1(\Omega)} \\
&\quad + \|P_h u - u\|_{H^1(\Omega)}\|\phi - u\|_{H^1(\Omega)} \\
&\leq \varepsilon Ch^2\|u\|_{H^1(\Omega)}^2 + \frac{3}{4\varepsilon}\|P_h u - u\|_{H^1(\Omega)}^2 + \varepsilon\|\phi - u\|_{H^1(\Omega)}^2
\end{aligned}
$$

(3.3.16) follows, using (3.2.1) with $\varepsilon = 2/\rho$ and $\phi = \pi_h u$.

Now consider the dual problem

$$
-\nabla \cdot (a(x, u)\nabla\psi) = P_h u - u \qquad \text{in } \Omega, \ \psi = 0 \text{ on } \partial\Omega
$$

whose weak form is

$$
A(u : \psi, \phi) = (P_h u - u, \phi) \quad \forall \, \phi \in H_0^1(\Omega) \tag{3.3.18}
$$

It follows from a similar argument of Thomee (2006,pg 233) that

$$
\|\psi\|_X \leq C\|P_h u - u\|_{L^2(\Omega)} \tag{3.3.19}
$$

This is because, by Poincare inequality (Atkinson & Han 2009),

$$
\begin{aligned}
\mu_1\|\nabla\psi\|_{L^2(\Omega)}^2 &\leq A(u : \psi, \psi) = (P_h u - u, \psi) \leq \|P_h u - u\|_{L^2(\Omega)}\|\psi\|_{L^2(\Omega)} \\
&\leq C\|P_h u - u\|_{L^2(\Omega)}\|\nabla\psi\|_{L^2(\Omega)} \\
\Rightarrow \quad \|\nabla\psi\|_{L^2(\Omega)} &\leq C\|P_h u - u\|_{L^2(\Omega)} \tag{3.3.20}
\end{aligned}
$$

From the definition of X and the fact that $\psi \in H_0^1(\Omega)$,

$$
\begin{aligned}
\|\psi\|_X &\leq C\|\psi\|_{H^2(\Omega)} \\
&\leq C\|\Delta\psi\|_{L^2(\Omega)} \leq \|a\Delta\psi\|_{L^2(\Omega)} \\
&= C\|P_h u - u + \nabla a \cdot \nabla\psi\|_{L^2(\Omega)} \\
&\leq C\|P_h u - u\|_{L^2(\Omega)}
\end{aligned}
$$

Use is made of (3.3.20) and Assumption 1.1 in the last inequality.
Now, it follows from (3.3.18) that

$$
\begin{aligned}
\|P_h u - u\|_{L^2(\Omega)}^2 &= A(u : P_h u - u, \psi) \\
&= A(u : P_h u - u, \psi - \phi) + A(u : P_h u - u, \phi) \quad \phi \in S_h \\
&\leq C\|P_h u - u\|_{H^1(\Omega)}\|\psi - \phi\|_{H^1(\Omega)} + |A(u : P_h u, \phi) - A_h(u : P_h u, \phi)|
\end{aligned}
$$

Using (3.2.1), (3.3.16) and Lemma 3.5 with $\phi = \pi_h\psi$ we obtain

$$
\begin{aligned}
\|P_h u - u\|_{L^2(\Omega)}^2 &\leq Ch^2\left(1 + \frac{1}{|\log h|}\right)\|u\|_X\|\psi\|_X \\
&\qquad\qquad + Ch\|P_h u\|_{H^1(\Omega_h^\star)}\|\pi_h\psi\|_{H^1(\Omega_h^\star)}
\end{aligned}
$$

It follows from Lemma 3.7 that

$$
\begin{aligned}
\|P_h u - u\|_{L^2(\Omega)}^2 &\leq Ch^2\left(1 + \frac{1}{|\log h|}\right)\|u\|_X\|\psi\|_X \\
&\qquad\qquad + Ch^2\|P_h u\|_{H^1(\Omega)}\|\pi_h\psi\|_{H^1(\Omega)}
\end{aligned}
$$

Using (3.3.15), (3.3.19) and the fact that $\|\pi_h\psi\| \leq C\|\psi\|$, we have

$$
\begin{aligned}
\|P_h u - u\|_{L^2(\Omega)}^2 &\leq Ch^2\left(1 + \frac{1}{|\log h|}\right)\|u\|_X\|\psi\|_X + Ch^2\|u\|_X\|\psi\|_X \\
&\leq Ch^2\left(1 + \frac{1}{|\log h|}\right)\|u\|_X\|P_h u - u\|_{L^2(\Omega)}
\end{aligned}
$$

which implies (3.3.17)

Lemma 3.9 Let u be a smooth function in $\Omega \times T$ and $a = a(x, u)$ satisfies

Assumption 1.1. Assume that $u \in X \cap H_0^1$ and let $P_h u$ be defined as in (3.2.9), then

$$\|(P_h u - u)_t\|_{H^1(\Omega)}^2 \leq Ch^2 \left(1 + \frac{1}{|\log h|}\right)(\|u\|_X^2 + \|u_t\|_X^2) \qquad (3.3.21)$$

$$\|(P_h u - u)_t\|_{L^2(\Omega)}^2 \leq Ch^4 \left(1 + \frac{1}{|\log h|}\right)^2 (\|u\|_X^2 + \|u_t\|_X^2) \qquad (3.3.22)$$

Proof Let $\xi = P_h u - u$, and assume that a_t is uniformly bounded. Following the argument of Thomme (2006), we have

$$
\begin{aligned}
\rho\|\xi_t\|_{H^1(\Omega)}^2 &\leq A(u : \xi_t, \xi_t) \\
&= A(u : \xi_t, \phi - u_t) + A(u : \xi_t, (P_h u)_t - \phi) \\
&= A(u : \xi_t, \phi - u_t) + \int_\Omega \left[\frac{\partial}{\partial t}(a\nabla\xi) - \frac{\partial a}{\partial t}\nabla\xi\right] \cdot \nabla((P_h u)_t - \phi) \, dx \\
&\leq \|\xi_t\|_{H^1(\Omega)}\|\phi - u_t\|_{H^1(\Omega)} + \|\xi\|_{H^1(\Omega)}\|(P_h u)_t - \phi\|_{H^1(\Omega)}
\end{aligned}
$$

Take $\phi = \pi_h u_t$. Using Lemma 3.3, (3.3.16) and Young's inequality, we obtain (3.3.21). Following the duality argument $(3.3.18) - (3.3.20)$, it is easy to see that

$$\|(P_h u - u)_t\|_{L^2(\Omega)}^2 \leq Ch^4 \left(1 + \frac{1}{|\log h|}\right)^2 (\|u\|_X + \|u_t\|_X)$$

Proof of Theorem 3.2 We have

$$
\begin{aligned}
\|u - u_h\|_{L^2(\Omega)}^2 &\leq 2(\|u - P_h u\|_{L^2(\Omega)}^2 + \|P_h u - u_h\|_{L^2(\Omega)}^2) \\
&\leq Ch^4 \left(1 + \frac{1}{|\log h|}\right)^2 \|u\|_X^2 + 2\|P_h u - u_h\|_{L^2(\Omega)}^2 \quad (3.3.23)
\end{aligned}
$$

Using (3.3.14), we have

$$((u_h - P_h u)_t, v_h)_h + A_h(u_h : u_h - P_h u, v_h)$$

$$= (u_{h,t}, v_h)_h - ((P_h u)_t, v_h)_h + A_h(u_h : u_h, v_h) - A_h(u_h : P_h u, v_h)$$

$$= (f(x, u_h), v_h)_h + \langle g_h, v_h \rangle_{\Gamma_h} + ((u - P_h u)_t, v_h) + A_h(u_h : u - P_h u, v_h)$$
$$\quad - (u_t, v_h) - A_h(u_h : u, v_h) + A(u : u, v_h) - A(u : u, v_h)$$
$$\quad + (P_h u_t, v_h) - (P_h u_t, v_h)_h$$

$$= (f(x, u_h), v_h)_h + \langle g_h, v_h \rangle_{\Gamma_h} + ((u - P_h u)_t, v_h) + A_h(u_h : u, v_h)$$
$$\quad - A_h(u_h : P_h u, v_h) - (f(x, u), v_h) - \langle g, v_h \rangle_\Gamma + A(u : u, v_h) - A_h(u_h : u, v_h)$$
$$\quad + (P_h u_t, v_h) - (P_h u_t, v_h)_h$$

$$= ((u - P_h u)_t, v_h) + (f(x, u_h), v_h)_h - (f(x, u), v_h) + \langle g_h, v_h \rangle_{\Gamma_h} - \langle g, v_h \rangle_\Gamma$$
$$\quad + A_h(u : P_h u, v_h) - A_h(u_h : P_h u, v_h) + (P_h u_t, v_h) - (P_h u_t, v_h)_h$$

We take $v_h = u_h - P_h u$ and make use of the fact that $\nabla P_h u$ is constant on $K \in \mathcal{T}_h$, and obtain

$$\frac{1}{2}\frac{d}{dt}\|u_h - P_h u\|^2_{L^2(\Omega)} + \mu_1\|u_h - P_h u\|^2_{H^1(\Omega)}$$

$$\leq \quad \|u_h - P_h u\|_{L^2(\Omega)}\|(u - P_h u)_t\|_{L^2(\Omega)}$$
$$\quad + Ch\|P_h u_t\|_{H^1(\Omega_h^\star)}\|u_h - P_h u\|_{H^1(\Omega_h^\star)}$$
$$\quad + c\mu_3\|u - u_h\|_{L^2(\Omega)}\|u_h - P_h u\|_{H^1(\Omega)} + B_5 + B_6$$

$$\leq \quad C(\mu_1, \mu_3, \varepsilon)\|u_h - P_h u\|^2_{L^2(\Omega)} + C(\mu_3, \varepsilon)\|u - P_h u\|^2_{L^2(\Omega)}$$
$$\quad + \|(u - P_h u)_t\|^2_{L^2(\Omega)} + \frac{1}{4\varepsilon}\|u_h - P_h u\|^2_{H^1(\Omega)}$$
$$\quad + h^2\|P_h u_t\|_{H^1(\Omega)}\|u_h - P_h u\|_{H^1(\Omega)} + B_5 + B_6$$

$$\leq \quad C\|u_h - P_h u\|^2_{L^2(\Omega)} + Ch^4\left(1 + \frac{1}{|\log h|}\right)^2 (\|u\|^2_X + \|u_t\|^2_X)$$
$$\quad + \frac{1}{2\varepsilon}\|u_h - P_h u\|^2_{H^1(\Omega)} + B_5 + B_6 \qquad\qquad (3.3.24)$$

we obtain (3.3.24) using (3.3.15), Lemma 3.7, Lemma 3.8 and Lemma 3.9, where

$$B_5 = |(f(x, u_h), u_h - P_h u)_h - (f(x, u), u_h - P_h u)|$$
$$B_6 = |\langle g_h, u_h - P_h u \rangle_{\Gamma_h} - \langle g, u_h - P_h u \rangle_\Gamma|$$

From Lemma 3.7

$$
\begin{aligned}
B_5 \;\leq\; & |(f(x,u), P_h u - u_h) - (f(x,u), P_h u - u_h)_h| \\
& + |(f(x,u) - f(x,u_h), P_h u - u_h)_h| \\
\leq\; & Ch\|u\|_{H^1(\Omega_h^\star)}\|P_h u - u_h\|_{H^1(\Omega_h^\star)} + \mu_3\|e(t)\|_{L^2(\Omega)}\|P_h u - u_h\|_{L^2(\Omega)} \\
\leq\; & Ch^2\|u\|_X\|P_h u - u_h\|_{H^1(\Omega)} + \mu_3\|e(t)\|_{L^2(\Omega)}\|P_h u - u_h\|_{L^2(\Omega)} \\
\leq\; & C(\mu_3,\varepsilon)h^4\left(1 + \frac{1}{|\log h|}\right)^2 \|u\|_X^2 + \frac{1}{4\varepsilon}\|P_h u - u_h\|_{H^1(\Omega)}^2 \\
& + \frac{5}{4}\|P_h u - u_h\|_{L^2(\Omega)}^2 \qquad\qquad (3.3.25)
\end{aligned}
$$

The last inequality is an implication of Lemma 3.8.

From Lemma 3.4 and Lemma 3.7, and the fact that $P_h u - u_h$ is linear.

$$
\begin{aligned}
B_6 \;\leq\; & Ch^{3/2}\|g\|_{H^2(\Gamma)}\|P_h u - u_h\|_{H^1(\Omega^\star)} \\
\leq\; & Ch^2\|g\|_{H^2(\Gamma)}\|P_h u - u_h\|_{H^1(\Omega)} \\
\leq\; & \varepsilon Ch^4\|g\|_{H^2(\Gamma)}^2 + \frac{1}{4\varepsilon}\|P_h u - u_h\|_{H^1(\Omega)}^2 \qquad (3.3.26)
\end{aligned}
$$

Substitute (3.3.25) and (3.3.26) into (3.3.24), taking $\varepsilon = \mu_1$

$$
\begin{aligned}
\frac{1}{2}\frac{d}{dt}\|P_h u - u_h\|_{L^2(\Omega)}^2 \;\leq\; & \gamma\|P_h u - u_h\|_{L^2(\Omega)}^2 \\
& + Ch^4\left(1 + \frac{1}{|\log h|}\right)^2 \left(\|u\|_X^2 + \|u_t\|_X^2 + \|g\|_{H^2(\Gamma)}^2\right)
\end{aligned}
$$

With $u_{h,0} = \pi_h u_0$, it follows that

$$
\begin{aligned}
\|(P_h u - u_h)(t)\|_{L^2(\Omega)}^2 \;\leq\; & Ch^4\left(1 + \frac{1}{|\log h|}\right)^2 \Bigg[\, \exp(2\gamma t)\|u_0\|_X^2 \\
& + \int_0^t \exp(2\gamma(t-s))(\|u\|_X^2 + \|u_t\|_X^2 + \|g\|_{H^2(\Gamma)}^2)\, ds \Bigg] \quad (3.3.27)
\end{aligned}
$$

The result follows by substituting (3.3.27) into (3.3.23) and taking the supremum with respect to t over $[0,T]$.

3.4 Fully Discrete Scheme

Now we present a fully discrete scheme based on backward difference approximations. Almost optimal order error estimates in the $L^2(0, T; H^1(\Omega))$-norm and $L^2(0, T; L^2(\Omega))$-norm are obtained.

The interval [0,T] is divided into M equally spaced (for simplicity) subintervals:

$$0 = t_0 < t_1 < \ldots < t_M = T$$

with $t_n = nk$, $k = T/M$ being the time step. Let $I_n = (t_{n-1}, t_n]$ be the nth subinterval and let a piecewise constant function U_{hk} be defined by $U_{hk}(x, t) = U_h^n(x)$, $\forall\, t \in I_n$, $n = 1, 2, \ldots, M$.

3.4.1 Backward Euler Time Discretisation

For a given sequence $\{w_n\}_{n=0}^M \subset L^2(\Omega)$, we have the backward difference quotient defined by

$$\partial_k w^n = \frac{w^n - w^{n-1}}{k}$$

The fully discrete finite element approximation to (3.1.1) is defined as follows: Let $U_h^0 = \pi_h u_0$, find $U_h^n \in S_h$, for $n = 1, 2, \ldots, M$, such that

$$(\partial_k U_h^n, v_h)_h + A_h(U_h^n : U_h^n, v_h) = (f(x, U_h^n), v_h)_h + \langle g_h^n, v_h \rangle_{\Gamma_h} \quad \forall\, v_h \in S_h \quad (3.4.1)$$

The result below establishes the convergence of the fully discrete solution to the exact solution in the $L^2(0, T; H^1(\Omega))$-norm.

Theorem 3.3 Let u and U_{hk} be the solutions of (3.1.1) and (3.4.1) respectively. Suppose that the conditions of Assumption 1.1 are satisfied for every $a : \Omega \times \mathbb{R} \to \mathbb{R}$, $f : \Omega \times \mathbb{R} \to \mathbb{R}$ and $g \in L^2(0, T; H^2(\Omega))$. There exists a positive constant C in dependent of h and k such that

$$\|u - U_{hk}\|_{L^2(0,T;H^1(\Omega))} \leq \left[k + h \left(1 + \frac{1}{|\log h|} \right) \right] C(u_0, u, g) \quad (3.4.2)$$

where

$$C(u_0, u, g) = \left\{ \|u_0\|_{H^1(\Omega)}^2 + \int_0^T \left(\|u\|_X^2 + \|u_{h,t}\|_{H^1(\Omega)}^2 + \|g\|_{H^2(\Gamma)}^2 \right. \right.$$
$$\left. \left. + \|u_t\|_Y + \|u_{tt}\|_{L^2(\Omega)} \right) dt \right\}^{1/2}$$

Proof Subtract (3.4.1) from (3.1.1)

$$(u_t^n - \partial_k U_h^n, v_h) + A(u^n : u^n, v_h)$$

$$= A_h(U_h^n : U_h^n, v_h) + (f(x, u^n), v_h) - (f(x, U_h^n), v_h)_h + \langle g^n, v_h \rangle_\Gamma - \langle g_h^n, v_h \rangle_{\Gamma_h}$$
$$+ (\partial_k U_h^n, v_h)_h - (\partial_k U_h^n, v_h) \qquad \forall\, v_h \in S_h$$

Let $v_h = P_h u^n - U_h^n$ and use (3.3.14) with $e^n = u^n - U_h^n$ and $z^n = u^n - P_h u^n$

$$(\partial_k e^n, e^n) + A_h(U_h^n : e^n, e^n)$$

$$= A_h(U_h^n : e^n, z^n) + (\partial_k e^n, z^n) + (\partial_k u^n - u_t^n, P_h u^n - U_h^n)$$
$$+ A_h(U_h^n : u^n, P_h u^n - U_h^n) - A_h(u^n : P_h u^n, P_h u^n - U_h^n)$$
$$+ (f(x, u^n), P_h u^n - U_h^n) - (f(x, U_h^n), P_h u^n - U_h^n)_h + \langle g^n, P_h u^n - U_h^n \rangle_\Gamma$$
$$- \langle g_h^n, P_h u^n - U_h^n \rangle_{\Gamma_h} + (\partial_k U_h^n, P_h u^n - U_h^n)_h - (\partial_k U_h^n, P_h u^n - U_h^n) \quad (3.4.3)$$

It is important to note the following:

i. For $V = H^2(\Gamma)$ or $L^2(\Omega)$ or $H^1(\Omega)$ or X, there exists a constant $C > 0$ independent of k such that

$$k \sum_{n=1}^M \|\omega^n\|_V^2 \leq C \|\omega\|_{L^2(0,T;V)}^2 \qquad \forall\, \omega^n \in V \qquad (3.4.4)$$

ii.

$$\frac{1}{2} \sum_{n=1}^M \|e^n - e^{n-1}\|_{L^2(\Omega)}^2 + \frac{1}{2} \|e^M\|_{L^2(\Omega)}^2 - \frac{1}{2} \|e^0\|_{L^2(\Omega)}^2 = k \sum_{n=1}^M (\partial_k e^n, e^n) \quad (3.4.5)$$

71

To obtain (3.4.5), observe that

$$\sum_{n=1}^{M} \|e^n - e^{n-1}\|_{L^2(\Omega)}^2 = k^2 \sum_{n=1}^{M} \|\partial_k e^n\|_{L^2(\Omega)}^2$$

$$= k^2 \sum_{n=1}^{M} (\partial_k e^n, \partial_k e^n)$$

$$= k \sum_{n=1}^{M} (\partial_k e^n, e^n - e^{n-1})$$

which implies

$$\sum_{n=1}^{M} \|e^n - e^{n-1}\|_{L^2(\Omega)}^2 + k \sum_{n=1}^{M} (\partial_k e^n, e^{n-1}) = k \sum_{n=1}^{M} (\partial_k e^n, e^n) \qquad (3.4.6)$$

and

$$\|e^M\|_{L^2(\Omega)}^2 - \|e^0\|_{L^2(\Omega)}^2 = \sum_{n=1}^{M} \|e^n\|_{L^2(\Omega)}^2 - \sum_{n=1}^{M} \|e^{n-1}\|_{L^2(\Omega)}^2$$

$$= \sum_{n=1}^{M} \int_{\Omega} (e^n - e^{n-1})(e^n + e^{n-1}) \, dx$$

$$= k \sum_{n=1}^{M} \int_{\Omega} \partial_k e^n (e^n + e^{n-1}) \, dx$$

$$= k \sum_{n=1}^{M} (\partial_k e^n, e^n) + k \sum_{n=1}^{M} (\partial_k e^n, e^{n-1}) \qquad (3.4.7)$$

(3.4.5) follows from (3.4.6) and (3.4.7).

We sum (3.4.3) over n from 1 to M and use (3.4.5).

$$\frac{1}{2}\|e^M\|_{L^2(\Omega)}^2 + \frac{1}{2}\sum_{n=1}^{M} \|e^n - e^{n-1}\|_{L^2(\Omega)}^2 + k\sum_{n=1}^{M} A_h(U_h^n : e^n, e^n)$$

$$\leq \frac{1}{2}\|e^0\|_{L^2(\Omega)}^2 + B_7 + B_8 + B_9 + B_{10} + B_{11} \quad (3.4.8)$$

where

$$B_7 \quad = \quad \sum_{n=1}^{M} \left| kA_h(U_h^n : e^n, z^n) + (e^n - e^{n-1}, z^n) \right|$$
$$+ \left| (U_h^n - U_h^{n-1}, P_h u^n - U_h^n)_h - (U_h^n - U_h^{n-1}, P_h u^n - U_h^n) \right|$$

$$B_8 \quad = \quad \sum_{n=1}^{M} k |A_h(U_h^n : u^n, P_h u^n - U_h^n) - A_h(u^n : P_h u^n, P_h u^n - U_h^n)|$$

$$B_9 \quad = \quad \sum_{n=1}^{M} k |(\partial_k u^n - u_t^n, P_h u^n - U_h^n)|$$

$$B_{10} \quad = \quad \sum_{n=1}^{M} k \left| (f(x, u^n), P_h u^n - U_h^n) - (f(x, U_h^n), P_h u^n - U_h^n)_h \right|$$

$$B_{11} \quad = \quad \sum_{n=1}^{M} k \left| \langle g^n, P_h u^n - U_h^n \rangle_\Gamma - \langle g_h^n, P_h u^n - U_h^n \rangle_{\Gamma_h} \right|$$

By (3.3.16), (3.3.17) and Assumption (2.1, A_3), we have, for $\varepsilon > 0$:

$$B_7 \quad \leq \quad \mu_2 \sum_{n=1}^{M} k \|e^n\|_{H^1(\Omega)} \|z^n\|_{H^1(\Omega)} + \sum_{n=1}^{M} \|e^n - e^{n-1}\|_{L^2(\Omega)} \|z^n\|_{L^2(\Omega)}$$

$$+ Ch \sum_{n=1}^{M} \|U_h^n - U_h^{n-1}\|_{H^1(\Omega)} \|P_h u^n - U_h^n\|_{H^1(\Omega)}$$

$$\leq \quad \frac{1}{4\varepsilon} \sum_{n=1}^{M} k \|e^n\|_{H^1(\Omega)}^2 + \mu_2^2 \varepsilon \sum_{n=1}^{M} k \|z^n\|_{H^1(\Omega)}^2 + \frac{1}{2} \sum_{n=1}^{M} \|e^n - e^{n-1}\|_{L^2(\Omega)}^2$$

$$+ \frac{1}{2} \sum_{n=1}^{M} \|z^n\|_{L^2(\Omega)}^2 + Ch^2 \sum_{n=1}^{M} \|U_h^n - U_h^{n-1}\|_{H^1(\Omega)}^2 + \frac{1}{2} \sum_{n=1}^{M} \|P_h u^n - U_h^n\|_{H^1(\Omega)}^2$$

$$\leq \quad \frac{1}{4\varepsilon} \sum_{n=1}^{M} k \|e^n\|_{H^1(\Omega)}^2 + \mu_2^2 \varepsilon Ch^2 \left(1 + \frac{1}{|\log h|} \right) \sum_{n=1}^{M} k \|u^n\|_X^2$$

$$+ \frac{1}{2} \sum_{n=1}^{M} \|e^n - e^{n-1}\|_{L^2(\Omega)}^2 + Ch^4 \left(1 + \frac{1}{|\log h|} \right)^2 \sum_{n=1}^{M} \|u^n\|_X^2$$

$$+ Ch^2 \sum_{n=1}^{M} \int_{t_{n-1}}^{t_n} \|u_{h,t}\|_{H^1(\Omega)}^2 \, dt + \sum_{n=1}^{M} \|e^n\|_{H^1(\Omega)}^2$$

$$\leq \frac{1}{4\varepsilon} \sum_{n=1}^{M} k\|e^n\|_{H^1(\Omega)}^2 + Ch^2\|u_{h,t}\|_{L^2(0,T;H^1(\Omega))}^2 + Ch^2 \left(1 + \frac{1}{|\log h|}\right) \sum_{n=1}^{M} k\|u^n\|_X^2$$

$$+ Ch^4 \left(1 + \frac{1}{|\log h|}\right)^2 \sum_{n=1}^{M} \|u^n\|_X^2 + \frac{1}{2} \sum_{n=1}^{M} \|e^n - e^{n-1}\|_{L^2(\Omega)}^2$$

$$+ \sum_{n=1}^{M} \|e^n\|_{H^1(\Omega)}^2 \qquad\qquad (3.4.9)$$

Using Lemma 3.8 for B_8, we have

$$\begin{aligned}
B_8 &\leq C(\mu_1,\mu_2) \sum_{n=1}^{M} k\|u^n - P_h u^n\|_{H^1(\Omega)} \|P_h u^n - U_h^n\|_{H^1(\Omega)} \\
&\leq C(\mu_1,\mu_2) \sum_{n=1}^{M} k\|u^n - P_h u^n\|_{H^1(\Omega)}^2 \\
&\quad + C(\mu_1,\mu_2) \sum_{n=1}^{M} k\|u^n - P_h u^n\|_{H^1(\Omega)} \|e^n\|_{H^1(\Omega)} \\
&\leq C(\mu_1,\mu_2,\varepsilon) \sum_{n=1}^{M} k\|u^n - P_h u^n\|_{H^1(\Omega)}^2 + \frac{1}{4\varepsilon} \sum_{n=1}^{M} k\|e^n\|_{H^1(\Omega)}^2 \\
&\leq Ch^2 \left(1 + \frac{1}{|\log h|}\right) \sum_{n=1}^{M} k\|u^n\|_X^2 + \frac{1}{4\varepsilon} \sum_{n=1}^{M} k\|e^n\|_{H^1(\Omega)}^2 \qquad (3.4.10)
\end{aligned}$$

For the term B_9, we have

$$\begin{aligned}
B_9 &= \sum_{n=1}^{M} \left(\int_{t_{n-1}}^{t_n} (t_{n-1} - s) u_{ss}(s)\, ds, P_h u^n - U_h^n\right) \\
&\leq \sum_{n=1}^{M} k\|u_{tt}^n\|_{L^2(t_{n-1},t_n:L^2(\Omega))} \|P_h u^n - U_h^n\|_{L^2(\Omega)} \\
&\leq \frac{1}{4} \sum_{n=1}^{M} \|e^n\|_{L^2(\Omega)}^2 + k^2\|u_{tt}\|_{L^2(0,T;L^2(\Omega))}^2 \\
&\quad + Ch^4 \left(1 + \frac{1}{|\log h|}\right)^2 \sum_{n=1}^{M} \|u^n\|_X^2 \qquad (3.4.11)
\end{aligned}$$

A similar approach to the estimation of B_3 shows that

$$
\begin{aligned}
B_{10} \;\leq\;& \varepsilon h^2 \sum_{n=1}^{M} k\|u^n\|_{H^1(\Omega)}^2 + \frac{1}{2\varepsilon}\sum_{n=1}^{M} k\|P_h u^n - U_h^n\|_{H^1(\Omega)}^2 + \varepsilon\mu_3^2 \sum_{n=1}^{M} k\|e^n\|_{L^2(\Omega)}^2 \\
\leq\;& C(\varepsilon)h^2\left(1+\frac{1}{|\log h|}\right)\sum_{n=1}^{M} k\|u^n\|_X^2 + \frac{1}{\varepsilon}\sum_{n=1}^{M} k\|e^n\|_{H^1(\Omega)}^2 \\
& + \varepsilon\mu_3^2 \sum_{n=1}^{M} k\|e^n\|_{L^2(\Omega)}^2
\end{aligned}
\tag{3.4.12}
$$

Using Lemma 3.4,

$$
\begin{aligned}
B_{11} \;\leq\;& k\sum_{n=1}^{M} Ch^{3/2}\|g^n\|_{H^2(\Gamma)}\|P_h u^n - U_h^n\|_{H^1(\Omega)} \\
\leq\;& C(\varepsilon)h^3 \sum_{n=1}^{M} k\|g^n\|_{H^2(\Gamma)}^2 + Ch^2\left(1+\frac{1}{|\log h|}\right)\sum_{n=1}^{M} k\|u\|_X^2 \\
& + \frac{1}{4\varepsilon}\sum_{n=1}^{M} k\|e^n\|_{H^1(\Omega)}^2
\end{aligned}
\tag{3.4.13}
$$

Substituting $(3.4.9) - (3.4.13)$ into $(3.4.8)$ with $\varepsilon = 7$ and $U_h^0 = \pi_h u_0$, we obtain for $h < 1$,

$$
\begin{aligned}
\sum_{n=1}^{M} k\|e^n\|_{H^1(\Omega)}^2 \;\leq\;& Ch^2\left(1+\frac{1}{|\log h|}\right)\|u_0\|_{H^1(\Omega)}^2 + \sum_{n=1}^{M}\left(7\mu_3^2 k + \frac{1}{4}\right)\|e^n\|_{L^2(\Omega)}^2 \\
& + Ch^2\left(1+\frac{1}{|\log h|}\right)^2\left[\sum_{n=1}^{M} k\|u^n\|_X^2 + \sum_{n=1}^{M}\|u^n\|_X^2\right] \\
& + \int_0^T\left(k^2\|u_{tt}\|_{L^2(\Omega)}^2 + Ch^2\|u_{h,t}\|_{H^1(\Omega)}^2\right)dt + Ch^2\sum_{n=1}^{M} k\|g^n\|_{H^2(\Gamma)}^2
\end{aligned}
$$

Applying the discrete version of Gronwall's Lemma and $(3.4.4)$, we have

$$
\begin{aligned}
\sum_{n=1}^{M} k\|e^n\|_{H^1(\Omega)}^2 \;\leq\;& Ch^2\left(1+\frac{1}{|\log h|}\right)^2\left[\|u_0\|_{H^1(\Omega)}^2 + \|u\|_{L^2(0,T;X)}^2 + \|u_{h,t}\|_{L^2(0,T;H^1(\Omega))}^2 \right.\\
& \left. + \|g\|_{L^2(0,T;H^2(\Gamma))}^2\right] + k^2\|u_{tt}\|_{L^2(0,T;L^2(\Omega))}^2
\end{aligned}
\tag{3.4.14}
$$

It was shown by Chen and Zou (1998), that

$$
\|u - U_{hk}\|_{L^2(0,T;H^1(\Omega))} \leq Ck\|u_t\|_{L^2(0,T;Y)} + C\left[\sum_{n=1}^{M} k\|e^n\|_{H^1(\Omega)}^2\right]^{1/2}
\tag{3.4.15}
$$

The result follows from (3.4.14) and (3.4.15).

The result below establishes the convergence of the fully discrete solution to the exact solution in the $L^2(0, T; L^2(\Omega))$-norm.

Theorem 3.4 Let u and U_h^n be the solutions of (3.1.1) and (3.4.1) respectively. Suppose that the conditions of Assumption 1.1 are satisfied for every $a : \Omega \times \mathbb{R} \to \mathbb{R}$, $f : \Omega \times \mathbb{R} \to \mathbb{R}$ and $g \in L^2(0, T; H^2(\Omega))$. There exists a positive constant C in dependent of h and k such that

$$\|u^n - U_h^n\|_{L^2(\Omega)} \leq \left[k + h^2 \left(1 + \frac{1}{|\log h|} \right) \right] C(u_0, u, g) \qquad (3.4.16)$$

where

$$C(u_0, u, g) = C \left[\|u_0\|_X^2 + \|u^n\|_X^2 + \int_0^{t_n} \left(\|u\|_X^2 + \|u_t\|_X^2 + \|g\|_{H^2(\Gamma)}^2 \right. \right.$$
$$\left. \left. + \|u_{tt}\|_{L^2(\Omega)}^2 \right) dt \right]^{1/2}$$

for $n = 1, \dots, M$, and

$$\|u - U_{hk}\|_{L^2(0, T; L^2(\Omega))} \leq \left[k + h^2 \left(1 + \frac{1}{|\log h|} \right) \right] D(u_0, u, g) \quad (3.4.17)$$

$$D(u_0, u, g) = C \left[\|u_0\|_X^2 + \int_0^T \left(\|u\|_X^2 + \|u_t\|_X^2 + \|g\|_{H^2(\Gamma)}^2 + \|u_{tt}\|_{L^2(\Omega)}^2 \right) dt \right]^{1/2}$$

Proof We establish this using error splitting technique (Thomee, 2006). Let $z^n = P_h u^n - U_h^n$, then

$(\partial_k z^n, v_h)_h + A_h(U_h^n : z^n, v_h)$

$$= (\partial_k P_h u^n, v_h)_h - (\partial_k U_h^n, v_h)_h + A_h(U_h^n : P_h u^n, v_h) - A_h(U_h^n : U_h^n, v_h)$$

$$= (\partial_k P_h u^n, v_h)_h - (f(x, U_h^n), v_h)_h - \langle g_h^n, v_h \rangle_{\Gamma_h} + A_h(U_h^n : P_h u^n, v_h)$$

$$= (\partial_k P_h u^n, v_h)_h + A_h(U_h^n : P_h u^n, v_h) - A_h(u^n : P_h u^n, v_h)$$

$$+ (f(x, u^n), v_h) - (f(x, U_h^n), v_h)_h + \langle g^n, v_h \rangle_\Gamma - \langle g_h^n, v_h \rangle_{\Gamma_h}$$

$$- (u_t^n, v_h) \qquad (3.4.18)$$

We made use of (3.1.1), (3.3.14) and (3.4.1) to obtain (3.4.18). It follows from (3.4.18) that

$$(\partial_k z^n, v_h)_h + A_h(U_h^n : z^n, v_h)$$

$$= (\partial_k(P_h u^n - u^n), v_h)_h + A_h(U_h^n : P_h u^n, v_h) - A_h(u^n : P_h u^n, v_h)$$

$$+ (f(x, u^n), v_h) - (f(x, U_h^n), v_h)_h + \langle g^n, v_h \rangle_\Gamma - \langle g_h^n, v_h \rangle_{\Gamma_h}$$

$$+ (\partial_k u^n - u_t^n, v_h) + (\partial_k u^n, z^n)_h - (\partial_k u^n, z^n)$$

$$= B_{12} + B_{13} + B_{14} \tag{3.4.19}$$

where

$$B_{12} = (\partial_k(P_h u^n - u^n), v_h)_h + (\partial_k u^n - u_t^n, v_h) + (\partial_k u^n, z^n)_h - (\partial_k u^n, z^n)$$

$$B_{13} = A_h(U_h^n : P_h u^n, v_h) - A_h(u^n : P_h u^n, v_h)$$

$$B_{14} = (f(x, u^n), v_h) - (f(x, U_h^n), v_h)_h + \langle g^n, v_h \rangle_\Gamma - \langle g_h^n, v_h \rangle_{\Gamma_h}$$

Now, using Young's inequality, Lemma 3.7 with the fact that $\|z^n\|_{H^2(\Omega)} = 0$, we obtain

$$B_{12} \leq \|\partial_k(P_h u^n - u^n)\|_{L^2(\Omega)} \|z^n\|_{L^2(\Omega)} + \|\partial_k u^n - u_t^n\|_{L^2(\Omega)} \|z^n\|_{L^2(\Omega)}$$

$$+ Ch\|\partial_k u^n\|_{H^1(\Omega_h^\star)} \|z^n\|_{H^1(\Omega_h^\star)}$$

$$\leq \|\partial_k(P_h u^n - u^n)\|_{L^2(\Omega)}^2 + \frac{1}{2}\|z^n\|_{L^2(\Omega)}^2 + \|\partial_k u^n - u_t^n\|_{L^2(\Omega)}^2$$

$$+ \gamma Ch^4\|\partial_k u^n\|_X^2 + \frac{1}{4\gamma}\|z^n\|_{H^1(\Omega)}^2 \tag{3.4.20}$$

Using Young's inequality, Lemma 3.8, we obtain

$$B_{13} \leq C\mu_3\|U_h^n - u^n\|_{L^2(\Omega)} \|z^n\|_{H^1(\Omega)}$$

$$\leq C\|z^n\|_{L^2(\Omega)} \|z^n\|_{H^1(\Omega)} + C\|P_h u^n - u^n\|_{L^2(\Omega)} \|z^n\|_{H^1(\Omega)}$$

$$\leq \gamma C\|z^n\|_{L^2(\Omega)}^2 + \frac{1}{2\gamma}\|z^n\|_{H^1(\Omega)}^2 + C(\gamma)h^4\left(1 + \frac{1}{|\log h|}\right)^2 \|u^n\|_X^2 \tag{3.4.21}$$

Using Lemma 3.4, Lemma 3.7, Lemma 3.8 with the fact that $D^\alpha z^n = 0$ for $|\alpha| = 2$, we have

$$
\begin{aligned}
B_{14} &\leq Ch\|u^n\|_{H^1(\Omega_h^\star)}\|z^n\|_{H^1(\Omega_h^\star)} + \mu_3\|u^n - U_h^n\|_{L^2(\Omega)}\|z^n\|_{L^2(\Omega)} \\
&\quad + Ch^{3/2}\|g^n\|_{H^2(\Gamma)}\|z^n\|_{H^1(\Omega_h^\star)} \\
&\leq Ch^2\|u^n\|_X\|z^n\|_{H^1(\Omega)} + C\|z^n\|_{L^2(\Omega)}^2 + C\|P_h u^n - u^n\|_{L^2(\Omega)}^2 \\
&\quad + Ch^2\|g^n\|_{H^2(\Gamma)}\|z^n\|_{H^1(\Omega)} \\
&\leq C(\gamma)h^4\left(1 + \frac{1}{|\log h|}\right)^2 \left(\|u^n\|_X^2 + \|g^n\|_{H^2(\Gamma)}^2\right) + \frac{1}{2\gamma}\|z^n\|_{H^1(\Omega)}^2 \\
&\quad + C\|z^n\|_{L^2(\Omega)}^2 \quad\quad\quad\quad\quad\quad\quad\quad\quad\quad\quad\quad\quad\quad\quad (3.4.22)
\end{aligned}
$$

Substituting $(3.4.20) - (3.4.22)$ into $(3.4.19)$, we have

$$
\begin{aligned}
\frac{1}{k}\|z^n\|_{L^2(\Omega)}^2 + \mu_1\|\nabla z^n\|_{L^2(\Omega)}^2 &\leq \frac{1}{k}\|z^n\|_{L^2(\Omega)}\|z^{n-1}\|_{L^2(\Omega)} + \|\partial_k(P_h u^n - u^n)\|_{L^2(\Omega)}^2 \\
&\quad + C\|z^n\|_{L^2(\Omega)}^2 + \|\partial_k u^n - u_t^n\|_{L^2(\Omega)}^2 + Ch^4\|\partial_k u^n\|_X^2 \\
&\quad + Ch^4\left(1 + \frac{1}{|\log h|}\right)^2 \left(\|u^n\|_X^2 + \|g^n\|_{H^2(\Gamma)}^2\right) \\
&\quad + \frac{5}{4\gamma}\|z^n\|_{H^1(\Omega)}^2 \quad\quad\quad\quad\quad\quad\quad\quad\quad (3.4.23)
\end{aligned}
$$

With $\gamma = \dfrac{5}{4\mu_1}$, we obtain

$$
\begin{aligned}
(1 - Ck)\|z^n\|_{L^2(\Omega)}^2 &\leq \|z^{n-1}\|_{L^2(\Omega)}^2 + C\Big[k\|\partial_k(P_h u^n - u^n)\|_{L^2(\Omega)}^2 \\
&\quad + k\|\partial_k u^n - u_t^n\|_{L^2(\Omega)}^2 + kh^4\|\partial_k u^n\|_X^2 \\
&\quad + kh^4\left(1 + \frac{1}{|\log h|}\right)^2 \left(\|u^n\|_X^2 + \|g^n\|_{H^2(\Gamma)}^2\right)\Big] (3.4.24)
\end{aligned}
$$

For k sufficiently small, $(3.4.24)$ becomes

$$
\begin{aligned}
\|z^n\|_{L^2(\Omega)}^2 &\leq (1 + Ck)\|z^{n-1}\|_{L^2(\Omega)}^2 + Ck\Big[\|\partial_k(P_h u^n - u^n)\|_{L^2(\Omega)}^2 \\
&\quad + \|\partial_k u^n - u_t^n\|_{L^2(\Omega)}^2 + h^4\|\partial_k u^n\|_X^2 \\
&\quad + h^4\left(1 + \frac{1}{|\log h|}\right)^2 \left(\|u^n\|_X^2 + \|g^n\|_{H^2(\Gamma)}^2\right)\Big] \quad (3.4.25)
\end{aligned}
$$

78

for $n = 1, \ldots, M$.

By iteration on n, we have

$$
\begin{aligned}
\|z^n\|^2_{L^2(\Omega)} &\leq \|z^0\|^2_{L^2(\Omega)} \sum_{i=1}^{n}(1+Ck)^i + Ck \sum_{i=1}^{n}(1+Ck)^{n-i} \Big[\|\partial_k(P_h u^i - u^i)\|^2_{L^2(\Omega)} \\
&\quad + \|\partial_k u^i - u^i_t\|^2_{L^2(\Omega)} + h^4 \|\partial_k u^i\|^2_X \\
&\quad + h^4 \left(1 + \frac{1}{|\log h|}\right)^2 \left(\|u^i\|^2_X + \|g^i\|^2_{H^2(\Gamma)} \right) \Big] \\
&\leq C\|z^0\|^2_{L^2(\Omega)} + Ck \sum_{i=1}^{n} \Big[\|\partial_k(P_h u^i - u^i)\|^2_{L^2(\Omega)} + \|\partial_k u^i - u^i_t\|^2_{L^2(\Omega)} \\
&\quad + h^4 \|\partial_k u^i\|^2_X + h^4 \left(1 + \frac{1}{|\log h|}\right)^2 \left(\|u^i\|^2_X + \|g^i\|^2_{H^2(\Gamma)} \right) \Big] \\
&\leq C\|z^0\|^2_{L^2(\Omega)} + C \int_0^{t_n} \Big[\|(P_h u - u)_t\|^2_{L^2(\Omega)} + k^2 \|u_{tt}\|^2_{L^2(\Omega)} \\
&\quad + h^4 \|u_t\|^2_X + h^4 \left(1 + \frac{1}{|\log h|}\right)^2 \left(\|u\|^2_X + \|g\|^2_{H^2(\Gamma)} \right) \Big] \, dt \qquad (3.4.26)
\end{aligned}
$$

We have made use of (3.4.4) to obtain (3.4.26). Therefore

$$
\begin{aligned}
\|z^n\|^2_{L^2(\Omega)} &\leq C\|z^0\|^2_{L^2(\Omega)} + C \left[h^4 \left(1 + \frac{1}{|\log h|}\right)^2 \int_0^{t_n} \left(\|u\|^2_X + \|u_t\|^2_X + \|g\|^2_{H^2(\Gamma)} \right) \, dt \right. \\
&\quad \left. + k^2 \int_0^{t_n} \|u_{tt}\|^2_{L^2(\Omega)} \, dt \right]
\end{aligned}
$$

With $U_h^0 = \pi_h u_0$, we have

$$
\begin{aligned}
\|z^n\|^2_{L^2(\Omega)} &\leq C \left[h^4 \left(1 + \frac{1}{|\log h|}\right)^2 \left(\|u_0\|^2_X + \int_0^{t_n} \left(\|u\|^2_X + \|u_t\|^2_X + \|g\|^2_{H^2(\Gamma)} \right) \, dt \right) \right. \\
&\quad \left. + k^2 \int_0^{t_n} \|u_{tt}\|^2_{L^2(\Omega)} \, dt \right]
\end{aligned}
$$

79

Now,

$$
\begin{aligned}
\|u^n - U_h^n\|_{L^2(\Omega)}^2 &\leq 2\|u^n - P_h u^n\|_{L^2(\Omega)}^2 + 2\|z^n\|_{L^2(\Omega)}^2 \\
&\leq C\left[h^4 \left(1 + \frac{1}{|\log h|}\right)^2 \left(\|u_0\|_X^2 + \|u^n\|_X^2 \right.\right. \\
&\qquad \left. + \int_0^{t_n} \left(\|u\|_X^2 + \|u_t\|_X^2 + \|g\|_{H^2(\Gamma)}^2 \right) dt \right) \\
&\qquad \left. + k^2 \int_0^{t_n} \|u_{tt}\|_{L^2(\Omega)}^2 \, dt \right] \qquad\qquad (3.4.27)
\end{aligned}
$$

(3.4.16) follows from (3.4.27).

Summing (3.4.27) over n from 1 to M, we have

$$
\begin{aligned}
\sum_{n=1}^M k\|u^n - U_h^n\|_{L^2(\Omega)}^2 &\leq C\left[h^4 \left(1 + \frac{1}{|\log h|}\right)^2 \sum_{n=1}^M k \left(\|u_0\|_X^2 + \|u^n\|_X^2 \right.\right. \\
&\qquad \left. + \int_0^{t_n} \left(\|u\|_X^2 + \|u_t\|_X^2 + \|g\|_{H^2(\Gamma)}^2 \right) dt \right) \\
&\qquad \left. + k^2 \sum_{n=1}^M k \int_0^{t_n} \|u_{tt}\|_{L^2(\Omega)}^2 \right] \\
&\leq Ch^4 \left(1 + \frac{1}{|\log h|}\right)^2 \left[Mk \left(\|u_0\|_X^2 + \|u\|_{L^2(0,T;X)}^2 \right.\right. \\
&\qquad \left. + \|u_t\|_{L^2(0,T;X)}^2 + \|g\|_{L^2(0,T;H^2(\Gamma))}^2 \right) + \|u\|_{L^2(0,T;X)}^2 \bigg] \\
&\qquad + Ck^2 Mk \|u_{tt}\|_{L^2(0,T;L^2(\Omega))}^2
\end{aligned}
$$

but $Mk = T$ and therefore

$$
\begin{aligned}
\sum_{n=1}^M k\|u^n - U_h^n\|_{L^2(\Omega)}^2 &\leq C\left[h^4 \left(1 + \frac{1}{|\log h|}\right)^2 \left(\|u_0\|_X^2 \right.\right. \\
&\qquad \left. + \int_0^T \left(\|u\|_X^2 + \|u_t\|_X^2 + \|g\|_{H^2(\Gamma)}^2 \right) dt \right) \\
&\qquad \left. + k^2 \int_0^T \|u_{tt}\|_{L^2(\Omega)}^2 \, dt \right] \qquad\qquad (3.4.28)
\end{aligned}
$$

It was shown by Chen and Zou (1998) that

$$
\|u - U_{hk}\|_{L^2(0,T;L^2(\Omega))} \leq Ck\|u_t\|_{L^2(0,T;L^2(\Omega))} + \left(\sum_{n=1}^M k\|u^n - U_h^n\|_{L^2(\Omega)}^2 \right)^{1/2} \qquad (3.4.29)
$$

80

(3.4.17) follows from (3.4.28) and (3.4.29).

3.4.2 One-Step Numerical Experiment

The results of the finite element error estimates are verified using globally continuous piecewise linear finite element functions based on the quasi-uniform triangulation described in section 3.2. The mesh parameter $h = \max_{K \in \mathcal{T}_h} h_K$ where h_K is the longest side of an element $K \in \mathcal{T}_h$.

The numerical experiments of this section are based on fully-discrete scheme (3.4.1).

We represent the solution as $u_h(x, t) = \sum_{j=1}^{N_h} \alpha_j(t) \phi_j(x)$, where each basis function ϕ_j, $(j = 1, 2, \ldots, N_h)$ is a pyramid function with unit height. Thus, (3.3.1) becomes

$$\mathfrak{A}\alpha'(t) + \mathfrak{B}(\alpha)\alpha(t) = \hat{f}(\alpha) + \hat{g}(t) \quad \text{for } t \in (0, T], \text{ with } \alpha(0) = \alpha_0 = \pi_h u_0 \quad (3.4.30)$$

where $\alpha(t) = (\alpha_1(t), \alpha_2(t), \ldots, \alpha_{N_h}(t))^T$, $\mathfrak{A} = (a_{jk})$, $\mathfrak{B}(\alpha) = (b_{jk}(\alpha))$, $\hat{f}(\alpha) = (\hat{f}_1(\alpha), \hat{f}_2(\alpha), \ldots, \hat{f}_{N_h}(\alpha))^T$ with

$$
\begin{aligned}
a_{jk} &= (\phi_j, \phi_k) \\
b_{jk}(\alpha) &= \left(a\left(x, \sum_{i=1}^{N_h} \alpha_i \phi_i \right) \nabla \phi_j, \nabla \phi_k \right) \\
\hat{f}_j(\alpha) &= \left(f\left(x, \sum_{i=1}^{N_h} \alpha_i(t) \phi_i \right), \phi_j \right)
\end{aligned}
$$

For the approximation $\hat{g}(t)$, let $\{z_j\}_{j=1}^{n_h}$ be the set of all nodes of the triangulation $\mathcal{T}_h$ that lie on the interface Γ and $\{\psi_j\}_{j=1}^{n_h}$ be the hat functions corresponding to $\{z_j\}_{j=1}^{n_h}$ in the space S_h. Then we have, for $g \in C(\Gamma) \times (0, T]$, $\hat{g}(t) = (\hat{g}_1(t), \hat{g}_2(t), \ldots, \hat{g}_{n_h}(t))$ with $\hat{g}_j(t) = \langle g(z_j, t), \psi_j \rangle_{\Gamma_h}$, $j = 1, \ldots, n_h$.

The fully discrete version of (3.4.30) is

$$(\mathfrak{A} + k\mathfrak{B}(\alpha^n))\alpha^n = \mathfrak{A}\alpha^{n-1} + k\hat{f}(\alpha^n) + \hat{g}_n \quad \text{for } t_n \in (0, T], \text{ with } \alpha_0 = \pi_h u_0 \quad (3.4.31)$$

The iterative scheme for (3.4.1) could be expressed as

$$(U_h^n - U_h^{n-1}, v_h) + k(a(x, U_h^n)\nabla U_h^n, \nabla v_h)_h = k(f(x, U_h^n), v_h)_h + k\langle g_h, v_h\rangle_{\Gamma_h}$$

$$v_h \in S_h, \; n = 1, 2, \ldots$$

$$(3.4.32)$$

Implementation of (5.0.3) will result to a system of nonlinear algebraic equations as a result of $a(x, U_h^n)$ and $f(x, U_h^n)$ in (5.3). To avoid this difficulty, we use predictor-corrector method. For $n = 1, 2, \ldots$,

$$\begin{cases} (X_h^n - U_h^{n-1}, v_h) + k(a(x, U_h^{n-1})\nabla X_h^n, \nabla v_h)_h \\ \qquad = k(f(x, U_h^{n-1}), v_h)_h + k\langle g_h, v_h\rangle_{\Gamma_h} \quad v_h \in S_h \\ (U_h^n - U_h^{n-1}, v_h) + k(a(x, X_h^n)\nabla U_h^n, \nabla v_h)_h \\ \qquad = k(f(x, X_h^n), v_h)_h + k\langle g_h, v_h\rangle_{\Gamma_h} \qquad v_h \in S_h \end{cases} \tag{3.4.33}$$

The mesh generation and computation are done in MATLAB® and FreeFEM++ (Hecht, 2012) environments.

Example 1 We discuss the result of a two-dimensional non-linear parabolic interface problem in the domain $\Omega = (-1, 1) \times (-1, 1)$ where Ω_1 is a circle centered at $(0, 0)$ with radius $r = \sqrt{x^2 + y^2} = 0.5$, $\Omega_2 = \Omega \setminus \Omega_1$ and the interface Γ is a circle of radius 0.5 and therefore $\Gamma \neq \Gamma_h$.

On $\Omega \times (0, 50]$, consider the nonlinear problem

$$\begin{cases} u_t - \nabla \cdot (a_i \nabla u) &= f_i & \text{in} \quad \Omega_i \times (0, 50], \quad i = 1, 2 \\ u(x, y, 0) &= u_0(x, y) & \text{in} \quad \Omega \\ u(x, y, t) &= 0 & \text{on} \quad \partial\Omega \times (0, 50] \\ u_1|_\Gamma &= u_2|_\Gamma \\ \left[a(u)\dfrac{\partial u}{\partial n}\right]_\Gamma &= g \end{cases}$$

where n_i denotes the unit normal vector on Ω_1 $(i = 1, 2)$. For the exact solution, we choose

$$u = \begin{cases} \dfrac{1}{8}(1 - 4r^2)\sin(t) & \text{in} \quad \Omega_1 \times (0, 50] \\ \dfrac{1}{4}(1 - x^2)(1 - y^2)(1 - 4r^2)\sin(2t) & \text{in} \quad \Omega_2 \times (0, 50] \end{cases}$$

82

The source function f, interface function g and the initial data u_0 are determined from the choice of u with

$$a = \begin{cases} \dfrac{u^2}{1+u^2} & \text{in } \Omega_1 \times (0,50] \\ \dfrac{1}{1+u^2} & \text{in } \Omega_2 \times (0,50] \end{cases}$$

Errors in L^2-norm and H^1-norm at $t=5$ for various step size h time step k are presented in Tables 3.1 and 3.2 respectively.

The error entries in Tables 3.1 and 3.2 show that

$$\|\text{Error}\|_{L^2(\Omega)} = O\left(k^{1.063} + h^{2.097}\left(1 + \frac{1}{|\ln h|}\right)\right)$$

$$\|\text{Error}\|_{H^1(\Omega)} = O\left(k^{0.989} + h^{2.281}\left(1 + \frac{1}{|\ln h|}\right)\right)$$

Example 2 We discuss the result of a two-dimensional non-linear parabolic interface problem in the domain $\Omega = (-1,1) \times (-1,1)$ where Ω_1 is the ellipse $4x^2 + 16y^2 < 1$, $\Omega_2 = \Omega \setminus \Omega_1$ and the interface Γ is the ellipse $4x^2 + 16y^2 = 1$ and therefore $\Gamma \neq \Gamma_h$.

On $\Omega \times (0,10]$, consider the nonlinear problem

$$\begin{cases} u_t - \nabla \cdot (a_i \nabla u) = f_i & \text{in } \Omega_i \times (0,10], \quad i = 1,2 \\ u(x,y,0) = u_0(x,y) & \text{in } \Omega \\ u(x,y,t) = 0 & \text{on } \partial\Omega \times (0,10] \\ u_1|_\Gamma = u_2|_\Gamma \\ \left[a(u)\dfrac{\partial u}{\partial n}\right]_\Gamma = g \end{cases}$$

where n_i denotes the unit normal vector on Ω_1 ($i = 1,2$). For the exact solution, we choose

$$u = \begin{cases} \dfrac{1}{8}(1 - 4x^2 - 16y^2)t\exp(\sin t) & \text{in } \Omega_1 \times (0,10] \\ \dfrac{1}{2}(1 - x^2)(1 - y^2)(4x^2 16y^2 - 1)\sin t & \text{in } \Omega_2 \times (0,10] \end{cases}$$

83

Table 3.1: Error estimates in L^2-norm for Example 1

h	Error ($k = 0.005$)	k	Error ($h = 0.0606786$)
0.404061	2.91025×10^{-2}	0.125	4.57222×10^{-3}
0.217242	7.20502×10^{-3}	0.1	3.81943×10^{-3}
0.113497	1.80574×10^{-3}	0.05	2.19672×10^{-3}
0.0711493	8.44232×10^{-4}	0.01	7.07933×10^{-4}
0.0543104	5.38294×10^{-4}	0.005	5.36616×10^{-4}

Table 3.2: Error estimates in H^1-norm for Example 1

h	Error ($k = 0.005$)	k	Error ($h = 0.0606786$)
0.404061	7.97666×10^{-2}	0.125	1.30663×10^{-1}
0.217242	4.17718×10^{-2}	0.1	1.07278×10^{-1}
0.113497	1.88953×10^{-2}	0.05	6.39467×10^{-2}
0.0711493	1.40793×10^{-2}	0.01	1.94120×10^{-2}
0.0543104	1.41391×10^{-2}	0.005	1.37051×10^{-2}
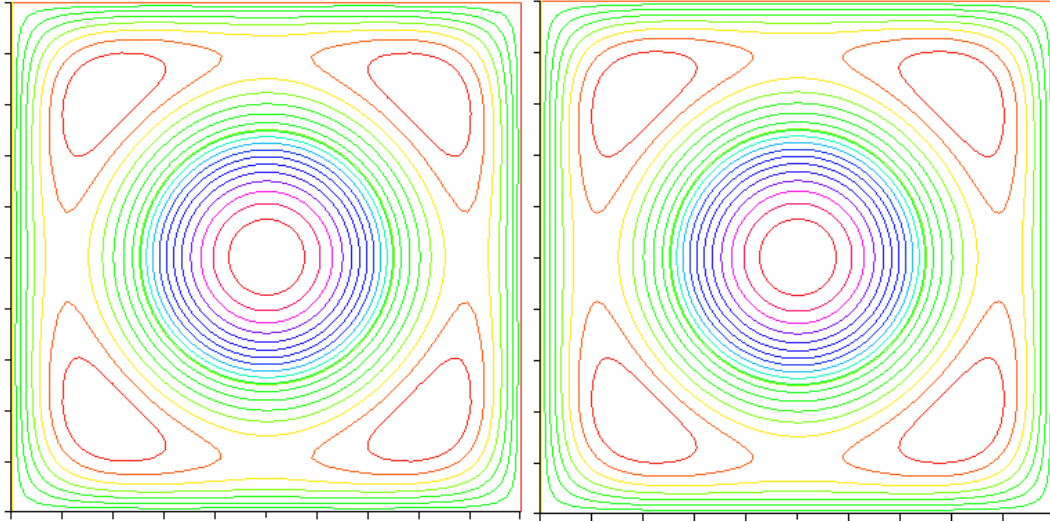
Figure 3.4: Contour plot of the finite element solution Example 1 at $h = 0.0619$ and 0.03266 respectively.
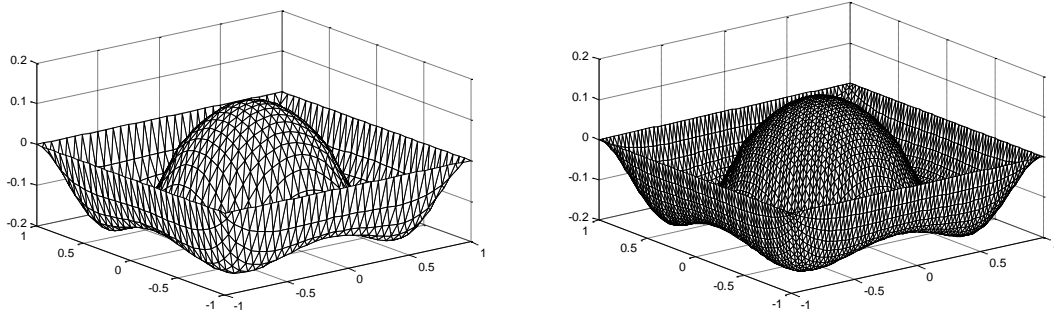
Figure 3.5: The graph showing the finite element solutions of Example 1 at $t = 0.01$ $(h_x, h_y) = \left(\frac{1}{32}, \frac{1}{32}\right)$ & $\left(\frac{1}{64}, \frac{1}{64}\right)$

The source function f, interface function g and the initial data u_0 are determined from the choice of u with

$$
a = \begin{cases}
5 & \text{in} \quad \Omega_1 \times (0, 10] \\[2mm]
\dfrac{1}{1 + u^2} & \text{in} \quad \Omega_2 \times (0, 10]
\end{cases}
$$

Errors in L^2-norm and H^1-norm at $t = 5$ for various step size h time step k are presented in Tables 3.3 and 3.4 respectively.

The error entries in Tables 3.3 and 3.3 show that

$$
\begin{aligned}
\|\text{Error}\|_{L^2(\Omega)} &= O\left(k^{1.209} + h^{2.13}\left(1 + \frac{1}{|\ln h|}\right)\right) \\
\|\text{Error}\|_{H^1(\Omega)} &= O\left(k^{1.313} + h^{1.558}\left(1 + \frac{1}{|\ln h|}\right)\right)
\end{aligned}
$$

In the above examples, the mesh cannot be fitted exactly to the interface. However, convergence rate of almost optimal order could still be obtained when the mesh fits exactly to the interface. We demonstrate this with the example below.
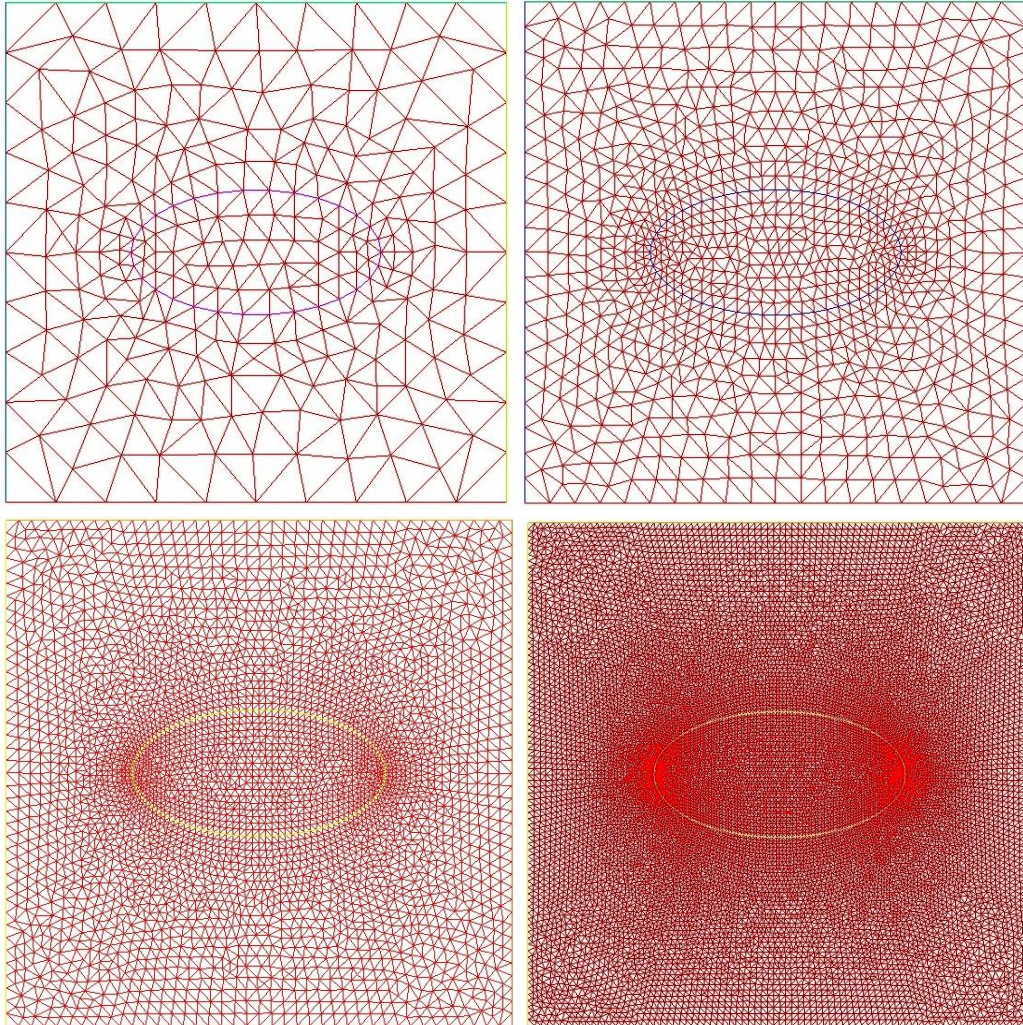
Figure 3.6: Discretisation of the domain of Example 2 with three refinements.
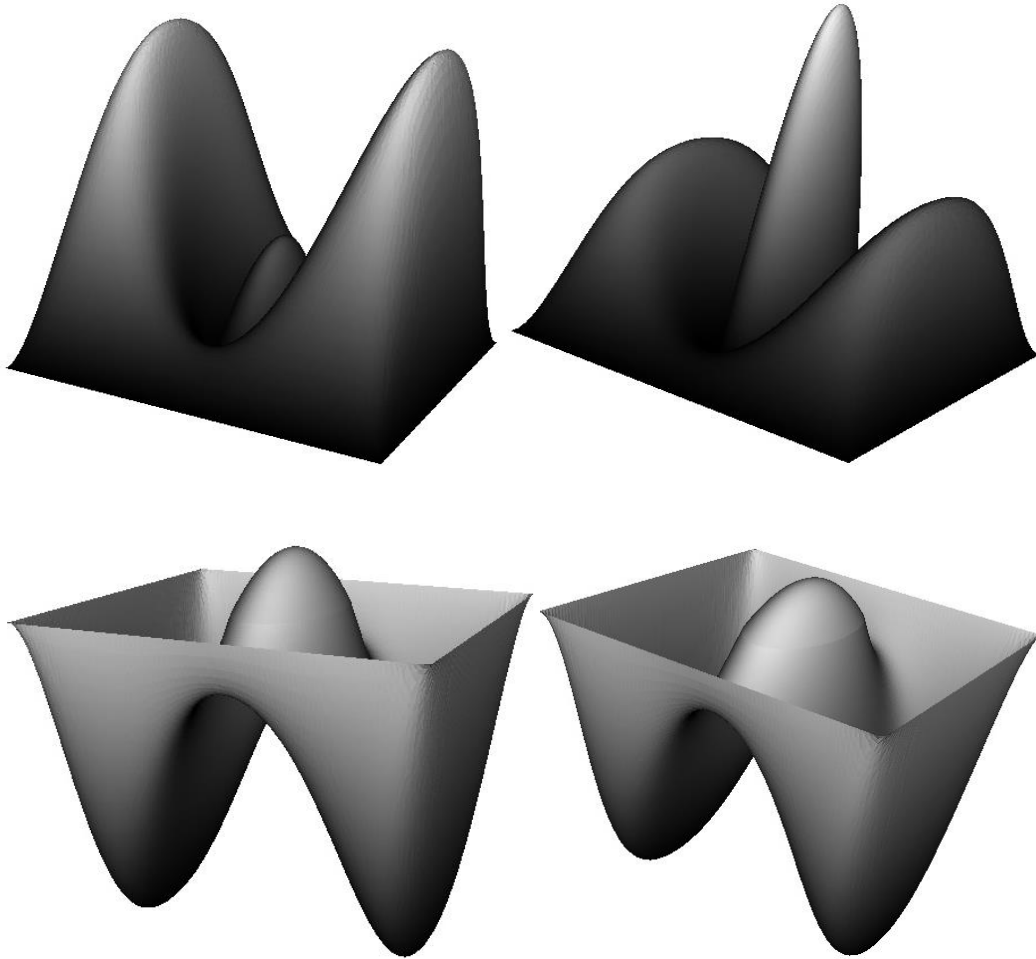
Figure 3.7: Finite element solutions of Example 2 at $t = 2, 3, 4, 5$ respectively with $h = 0.0387774$ and $k = 0.01$.

Table 3.3: Error estimates in L^2-norm for Example 2

h	Error ($k = 0.01$)	k	Error ($h = 0.0285903$)
0.205602	1.11369×10^{-1}	0.5	1.17166×10^{-1}
0.110793	2.85504×10^{-2}	0.25	5.58821×10^{-2}
0.0724138	1.47834×10^{-2}	0.125	2.13369×10^{-2}
0.0550215	9.81734×10^{-3}	0.0625	6.71479×10^{-3}
0.0273063	5.68978×10^{-3}	0.01	5.69057×10^{-3}

Table 3.4: Error estimates in H^1-norm for Example 2

h	Error ($k = 0.01$)	k	Error ($h = 0.0285903$)
0.205602	3.89808×10^{-1}	0.5	6.19003×10^{-1}
0.110793	1.43536×10^{-1}	0.25	2.83365×10^{-1}
0.0724138	9.70718×10^{-2}	0.125	1.05819×10^{-1}
0.0550215	6.06143×10^{-2}	0.0625	4.28184×10^{-2}
0.037129	4.70875×10^{-2}	0.01	3.88477×10^{-2}

Example 3 Consider the following parabolic boundary value problem in $\Omega = (-1, 1) \times (-1, 1)$. The interface $\Gamma = \bar{\Omega}_1 \cap \bar{\Omega}_2$ is the line $x = 0$ where Ω_1 is the rectangle $[-1, 0) \times [-1, -1]$, Ω_2 is the triangle $(0, 1] \times [-1, -1]$.

$$\begin{cases} u_t - \nabla \cdot (a_i \nabla u) = f_i & \text{in} \quad \Omega_i \times (0, 20] \; i = 1, 2 \\ u(x, y, 0) = u_0(x, y) & \text{in} \quad \Omega \\ u(x, y, t) = 0 & \text{on} \quad \partial\Omega \times (0, 20] \\ u_1|_\Gamma = u_2|_\Gamma \\ (\alpha_1 \nabla u_1 \cdot n_1)|_\Gamma - (\alpha_2 \nabla u_2 \cdot n_2)|_\Gamma = g \end{cases}$$

where n_i denotes the unit normal vector on Ω_1 $(i = 1, 2)$. We choose a problem with a known solution as follows:

$$u = \begin{cases} t(1 + x)(1 - y^2) & \text{in} \quad \Omega_1 \times (0, 20] \\ t(1 - x)(1 - y^2) & \text{in} \quad \Omega_2 \times (0, 20] \end{cases}$$

The source function f, interface function g and the initial data u_0 are determined from the choice of u with

$$a = \begin{cases} \dfrac{1}{1 + u^2} & \text{in} \quad \Omega_1 \times (0, 20] \\ 1 - x^2 y^2 & \text{in} \quad \Omega_2 \times (0, 20] \end{cases}$$

Errors in L^2-norm and H^1-norm at $t = 2$ for various step size h time step k are presented in Tables 3.5 and 3.6 respectively.

The data presented in Tables 3.5 and 3.6 indicate that

$$\|u - u_h\|_{L^2(\Omega)} = O\left(k^{0.915} + h^{1.996}\left(1 + \frac{1}{|\ln h|}\right)\right) \quad \text{and}$$

$$\|u - u_h\|_{H^1(\Omega)} = O\left(k^{1.106} + h^{1.715}\left(1 + \frac{1}{|\ln h|}\right)\right)$$

These numerical results match the convergence rates as given in Theorem 3.3 and Theorem 3.4 respectively.

Table 3.5: Error estimates in L^2-norm for Example 3

h	Error ($k = 0.001$)	k	Error ($h = 0.0967333$)
0.35912	2.42799×10^{-2}	0.05	9.27316×10^{-2}
0.286896	6.05176×10^{-3}	0.04	7.48363×10^{-2}
0.179911	2.73589×10^{-3}	0.02	3.80558×10^{-2}
0.0967333	2.97570×10^{-3}	0.01	1.91958×10^{-2}
0.0646608	2.99729×10^{-3}	0.001	2.97570×10^{-3}

Table 3.6: Error estimates in H^1-norm for Example 3

h	Error ($k = 0.001$)	k	Error ($h = 0.0967333$)
0.35912	1.37141×10^{-1}	0.05	6.64483×10^{-1}
0.286896	5.67485×10^{-2}	0.04	5.32124×10^{-1}
0.179911	2.10261×10^{-2}	0.02	2.65937×10^{-1}
0.0959059	1.34518×10^{-2}	0.01	1.32882×10^{-1}
0.0646608	1.34375×10^{-2}	0.001	1.34518×10^{-2}

3.4.3 Two-Step Time Discretisation

Now we discuss a fully discrete scheme based on 2-step backward difference approximation. Almost optimal order error estimate in the $L^2(0,T;L^2(\Omega))$-norm is derived.

For a given sequence $\{w_n\}_{n=0}^M \subset L^2(\Omega)$, we have the backward difference quotient defined by

$$\partial_k^2 w^n = \frac{3w^n - 4w^{n-1} + w^{n-2}}{2k}$$

The 2-step fully discrete finite element approximation to (3.1.1) is defined as follows:

Let $U_h^0 = \pi_h u_0$, find $U_h^n \in S_h$, for $n = 1, 2, \ldots, M$, such that

$$(\partial_k^2 U_h^n, v_h) + A_h(U_h^n, v_h) = (f(x, U_h^n), v_h)_h + \langle g_h^n, v_h \rangle_{\Gamma_h} \quad \forall\, v_h \in S_h \qquad (3.4.34)$$

We have the following stability result:

Lemma 3.10 Suppose the conditions of Assumption 1.1 are satisfied, there exists a constant C independent of h and k such that for the solution of (3.4.34)

$$\|U_h^n\|^2 \le C \left(\|U_h^0\|^2 + \|U_h^1\|^2 \right) + Ck \sum_{i=2}^n \|g_h^i\|_{H^{1/2}(\Gamma)}^2 \quad n = 2, 3, \ldots, M \qquad (3.4.35)$$

Proof Taking $v_h = U_h^n$ in (3.4.34), we obtain by simple calculation

$$\|U_h^n\|_{L^2(\Omega)}^2 - Ck\|U_h^n\|_{L^2(\Omega)}^2 \le C \left[\|U_h^{n-2}\|_{L^2(\Omega)}^2 + \|U_h^{n-1}\|_{L^2(\Omega)}^2 + k\|g_h^n\|_{H^{1/2}(\Gamma)}^2 \right]$$

For k sufficiently small,

$$\|U_h^n\|_{L^2(\Omega)}^2 \le C(1+k) \left[\|U_h^{n-2}\|_{L^2(\Omega)}^2 + \|U_h^{n-1}\|_{L^2(\Omega)}^2 \right] + Ck\|g_h^n\|_{H^{1/2}(\Gamma)}^2$$

By iteration on n we have

$$\|U_h^n\|_{L^2(\Omega)}^2 \le C \left[\|U_h^0\|_{L^2(\Omega)}^2 + \|U_h^1\|_{L^2(\Omega)}^2 \right] \sum_{i=2}^n (1+k)^i + Ck \sum_{i=2}^n (1+k)^{n-i} \|g_h^i\|_{H^{1/2}(\Omega)}^2$$

$$\le C \left[\|U_h^0\|_{L^2(\Omega)}^2 + \|U_h^1\|_{L^2(\Omega)}^2 \right] + Ck \sum_{i=2}^n \|g_h^i\|_{H^{1/2}(\Omega)}^2$$
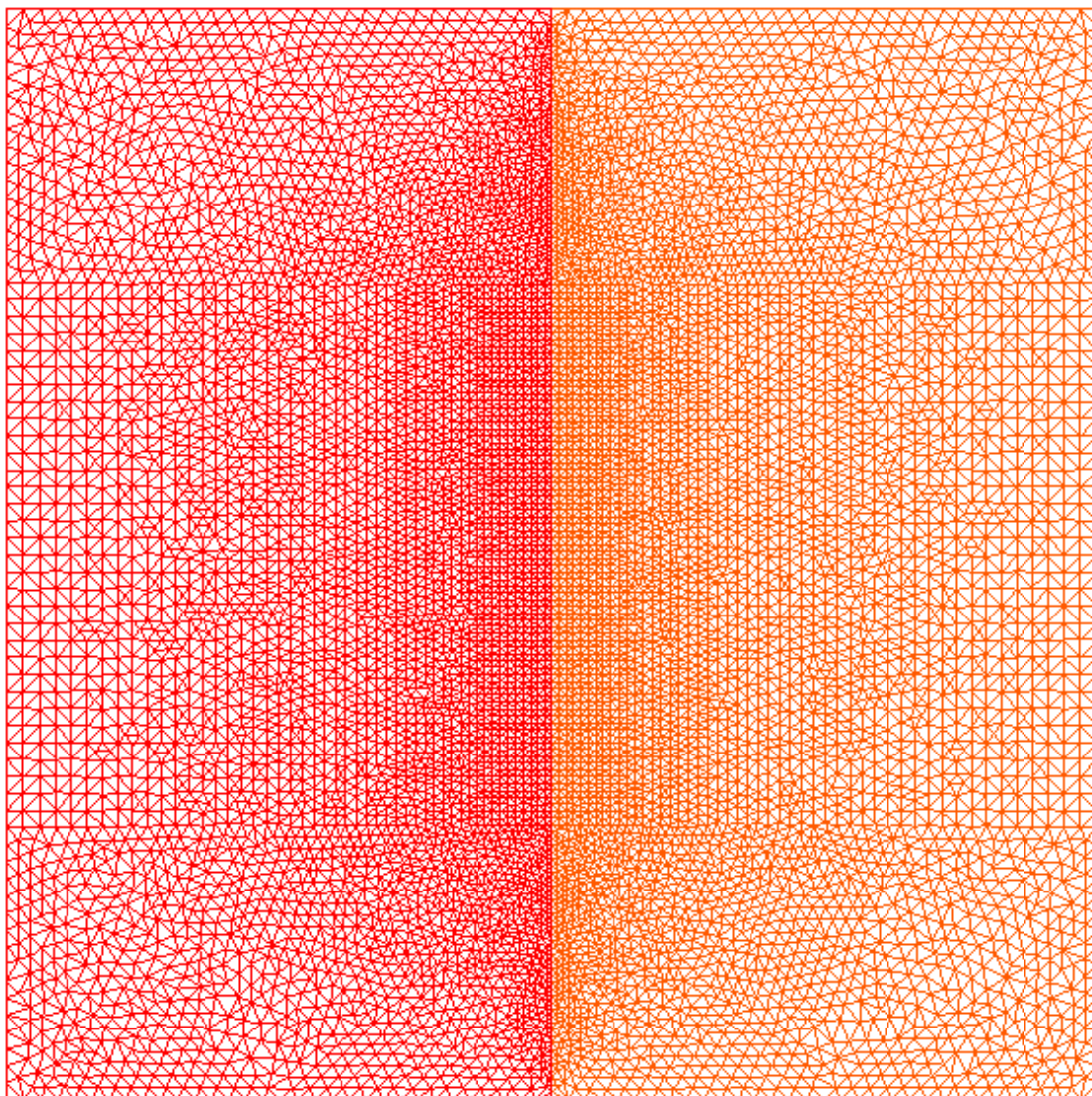
Figure 3.8: Computational domain of Example 3

The result below establishes the convergence of the fully discrete solution to the exact solution in the $L^2(0,T;L^2(\Omega))$-norm.

Theorem 3.5 Let u and U_h^n be the solutions of (3.1.1) and (3.4.34) respectively. Suppose that the conditions of Assumption 1.1 are satisfied for every $a : \Omega \times \mathbb{R} \to \mathbb{R}$, $f : \Omega \times \mathbb{R} \to \mathbb{R}$, $g(x,t)$, and u_{ttt} is defined for $\Omega \times [0,T]$. There exists a positive constant C independent of h and k such that

$$\|u^n - U_h^n\|_{L^2(\Omega)} \leq \left[k^2 + h^2 \left(1 + \frac{1}{|\log h|} \right) \right] C(u_0, u, g) \qquad (3.4.36)$$

where

$$
\begin{aligned}
C(u_0, u, g) = \; & C \Big\{ \|u_0\|_X^2 + \|u^n\|_X^2 \\
& + \int_0^{t_n} \left(\|u\|_X^2 + \|u_t\|_X^2 + \|g\|_{H^2(\Gamma)}^2 + \|u_{ttt}\|_{L^2(\Omega)}^2 \right) dt \Big\}^{1/2}
\end{aligned}
$$

and

$$\|u^n - U_{hk}\|_{L^2(\Omega)} \leq \left[k^2 + h^2 \left(1 + \frac{1}{|\log h|} \right) \right] D(u_0, u, g) \qquad (3.4.37)$$

where

$$
\begin{aligned}
D(u_0, u, g) = \; & C \Big\{ \|u_0\|_X^2 \\
& + \int_0^{T} \left(\|u\|_X^2 + \|u_t\|_X^2 + \|u_{tt}\|_{L^2(\Omega)}^2 + \|g\|_{H^2(\Gamma)}^2 + \|u_{ttt}\|_{L^2(\Omega)}^2 \right) dt \Big\}^{1/2}
\end{aligned}
$$

Proof Let $z^n = U_h^n - P_h u^n$ then following the argument that led to (3.4.19), we have

$$(\partial_k^2 z^n, v_h) + A_h(U_h^n : z^n, v_h) = B_{15} + B_{13} + B_{14} \qquad (3.4.38)$$

where

$$B_{15} = (\partial_k^2(P_h u^n - u^n), v_h)_h + (\partial_k^2 u^n - u_t^n, v_h) + (\partial_k^2 u^n, z^n)_h - (\partial_k^2 u^n, z^n)$$

With $v_h = z^n$, we have

$$
\begin{aligned}
B_{15} \leq \; & \|\partial_k^2(P_h u^n - u^n)\|_{L^2(\Omega)}^2 + \frac{1}{2}\|z^n\|_{L^2(\Omega)}^2 + \|\partial_k^2 u^n - u_t^n\|_{L^2(\Omega)}^2 \\
& + \gamma C h^4 \|\partial_k^2 u^n\|_X^2 + \frac{1}{4\gamma}\|z^n\|_{H^1(\Omega)}^2 \qquad (3.4.39)
\end{aligned}
$$

94

Following the argument that led to (3.4.35) using (3.4.21), (3.4.22) and (3.4.39), we have

$$
\begin{aligned}
\|z^n\|^2_{L^2(\Omega)} \;\leq\;& C\left[\|z^0\|^2_{L^2(\Omega)} + \|z^1\|^2_{L^2(\Omega)}\right] + Ck\sum_{j=2}^{n}\|\partial_k^2(u^j - P_h u^j)\|^2_{L^2(\Omega)} \\
&+ Ch^4\left(1 + \frac{1}{|\log h|}\right)^2 k\sum_{j=2}^{n}(\|u^j\|^2_X + \|g^j\|^2_{H^2(\Gamma)}) \\
&+ Ck\sum_{j=2}^{n}\|\partial_k^2 u^j - u_t^j\|^2_{L^2(\Omega)} + Ch^4 k\sum_{j=2}^{n}\|\partial_k^2 u^j\|^2_X \\
\leq\;& C\left[\|z^0\|^2_{L^2(\Omega)} + \|z^1\|^2_{L^2(\Omega)}\right] + Ck\sum_{j=2}^{n}\|\partial_k(u^j - P_h u^j)\|^2_{L^2(\Omega)} \\
&+ Ck\sum_{j=2}^{n}\|\partial_k(u^{j-1} - P_h u^{j-1})\|^2_{L^2(\Omega)} \\
&+ Ch^4\left(1 + \frac{1}{|\log h|}\right)^2 k\sum_{j=2}^{n}(\|u^j\|^2_X + \|g^j\|^2_{H^2(\Gamma)}) \\
&+ Ck^4 k\sum_{j=2}^{n}\|u_{ttt}^j\|^2_{L^2(\Omega)} + Ch^4 k\sum_{j=2}^{n}\|\partial_k u^j\|^2_X + Ch^4 k\sum_{j=2}^{n}\|\partial_k u^{j-1}\|^2_X \\
\leq\;& C\left[\|z^0\|^2_{L^2(\Omega)} + \|z^1\|^2_{L^2(\Omega)}\right] + C\int_0^{t_n}\|(u - P_h u)_t\|^2_{L^2(\Omega)}\,dt \\
&+ Ck^4\int_0^{t_n}\|u_{ttt}\|^2_{L^2(\Omega)}\,dt + Ch^4\int_0^{t_n}\|u_t\|^2_X\,dt \\
&+ Ch^4\left(1 + \frac{1}{|\log h|}\right)^2\int_0^{t_n}\left[\|u\|^2_X + \|g\|^2_{H^2(\Gamma)}\right] \\
\leq\;& C\left[\|z^0\|^2_{L^2(\Omega)} + \|z^1\|^2_{L^2(\Omega)}\right] + Ck^4\int_0^{t_n}\|u_{ttt}\|^2_{L^2(\Omega)}\,dt \\
&+ Ch^4\left(1 + \frac{1}{|\log h|}\right)^2\int_0^{t_n}\left[\|u\|^2_X + \|u_t\|^2_X + \|g\|^2_{H^2(\Gamma)}\right]\,dt \quad (3.4.40)
\end{aligned}
$$

where use is made of (3.3.22) and (3.4.4) in the above inequalities. We have, from

(3.4.40) with $U_h^0 = \pi_h u_0$,

$$
\begin{aligned}
\|u^n - U_h^n\|_{L^2(\Omega)}^2 &\leq 2\|u^n - P_h u^n\|_{L^2(\Omega)}^2 + \|z^n\|_{L^2(\Omega)}^2 \\
&\leq C\|u^1 - U_h^1\|_{L^2(\Omega)}^2 + Ck^4\|u_{ttt}\|_{L^2(0,t_n;L^2(\Omega))}^2 \\
&\quad + Ch^4 \left(1 + \frac{1}{|\log h|}\right)^2 \left\{\|u_0\|_X^2 + \|u^n\|_X^2 + \|u\|_{L^2(0,t_n;X)}^2 \right. \\
&\quad \left. + \|u_t\|_{L^2(0,t_n;X)}^2 + \|g\|_{L^2(0,t_n;H^2(\Gamma))}^2\right\} \quad (3.4.41)
\end{aligned}
$$

To obtain the same order of accuracy, U_h^1 could be obtained using Taylor's series

$$
U_h^1 = u(0) + ku_t(0) = u_0 + k\left[\nabla \cdot (a(x,u_0)\nabla u_0) + f(x,u_0)\right] \quad (3.4.42)
$$

(3.4.36) is obtained from (3.4.41) and (3.4.42).

From (3.4.41)

$$
\begin{aligned}
\sum_{n=2}^{M} k\|u^n - U_h^n\|_{L^2(\Omega)}^2 &\leq Ch^4 \left(1 + \frac{1}{|\log h|}\right)^2 \left\{\sum_{n=2}^{M} k\|u_0\|_X^2 + \sum_{n=2}^{M} k\|u^n\|_X^2 \right. \\
&\quad \left. + \sum_{n=2}^{M} k \int_0^{t_n} \|u\|_X^2 + \|u_t\|_X^2 + \|g\|_{H^2(\Gamma)}^2 \, dt\right\} \\
&\quad + Ck^4 \sum_{n=2}^{M} k \int_0^{t_n} \|u_{ttt}\|_{L^2(\Omega)}^2 \, dt \\
&\leq Ch^4 \left(1 + \frac{1}{|\log h|}\right)^2 \left\{kM\|u_0\|_X^2 + \int_0^T \|u\|_X^2 \, dt \right. \\
&\quad \left. + kM \int_0^T \|u\|_X^2 + \|u_t\|_X^2 + \|g\|_{H^2(\Gamma)}^2 \, dt\right\} \\
&\quad + Ck^4 kM \int_0^T \|u_{ttt}\|_{L^2(\Omega)}^2 \, dt \\
&\leq Ch^4 \left(1 + \frac{1}{|\log h|}\right)^2 \left\{\|u_0\|_X^2 + \int_0^T \left(\|u\|_X^2 + \|u_t\|_X^2 \right.\right. \\
&\quad \left.\left. + \|g\|_{H^2(\Gamma)}^2\right) \, dt\right\} + Ck^4 \|u_{ttt}\|_{L^2(0,T;L^2(\Omega))}^2 \quad (3.4.43)
\end{aligned}
$$

By a simple calculation (see Appendix A),

$$
\|u - U_{hk}\|_{L^2(0,T;L^2(\Omega))} \leq Ck^2\|u_{tt}\|_{L^2(0,T;L^2(\Omega))} + C\left(\sum_{n=2}^{M} k\|u^n - U_h^n\|_{L^2(\Omega)}^2\right)^{1/2}
$$

$$
(3.4.44)
$$

(3.4.37) follows from (3.4.43) and (3.4.44).

Next we present examples to verify the error estimate (3.4.32).

3.4.4 Two-Step Numerical Experiment

The 2-step iterative scheme for (3.1.1) could be expressed as

$$(\frac{3}{2}U_h^n - 2U_h^{n-1} + \frac{1}{2}U_h^{n-2}, v_h) + k(a(x,U_h^n)\nabla U_h^n, \nabla v_h)_h$$

$$= k(f(x,U_h^n), v_h)_h + k\langle g_h, v_h\rangle_{\Gamma_h} \quad (3.4.45)$$

$v_h \in S_h$, $n = 2, 3, \ldots$.

Implementation of (3.4.45) will result to a system of nonlinear algebraic equations due to the presence of $a(x, U_h^n)$ and $f(x, U_h^n)$. To avoid this difficulty, we use predictor-corrector method. For $n = 2, 3, \ldots$,

$$\begin{cases} (\frac{3}{2}X_h^n - 2U_h^{n-1} + \frac{1}{2}U_h^{n-2}, v_h) + k(a(x,U_h^{n-1})\nabla X_h^n, \nabla v_h)_h \\ \quad = k(f(x,U_h^{n-1}), v_h)_h + k\langle g_h, v_h\rangle_{\Gamma_h} \qquad v_h \in S_h \\ (\frac{3}{2}U_h^n - 2U_h^{n-1} + \frac{1}{2}U_h^{n-2}, v_h) + k(a(x,X_h^n)\nabla U_h^n, \nabla v_h)_h \\ \quad = k(f(x,X_h^n), v_h)_h + k\langle g_h, v_h\rangle_{\Gamma_h} \qquad v_h \in S_h \end{cases} \quad (3.4.46)$$

To obtain U_h^1 we use (3.4.42), another alternative is the use of one-step method discussed in Section 3.4.1.

Example 4 We present the solution of Example 1 using the 2-step implicit scheme.

Errors in L^2-norm at $t = 5$ for various step size h time step k are presented in Table 3.7.

The data presented in Table 3.7 indicate that

$$\|\text{Error}\|_{L^2(\Omega)} = O\left(k^{2.397} + h^{2.047}\left(1 + \frac{1}{|\ln h|}\right)\right)$$

These numerical results match the convergence rate as given in Theorem 3.5.
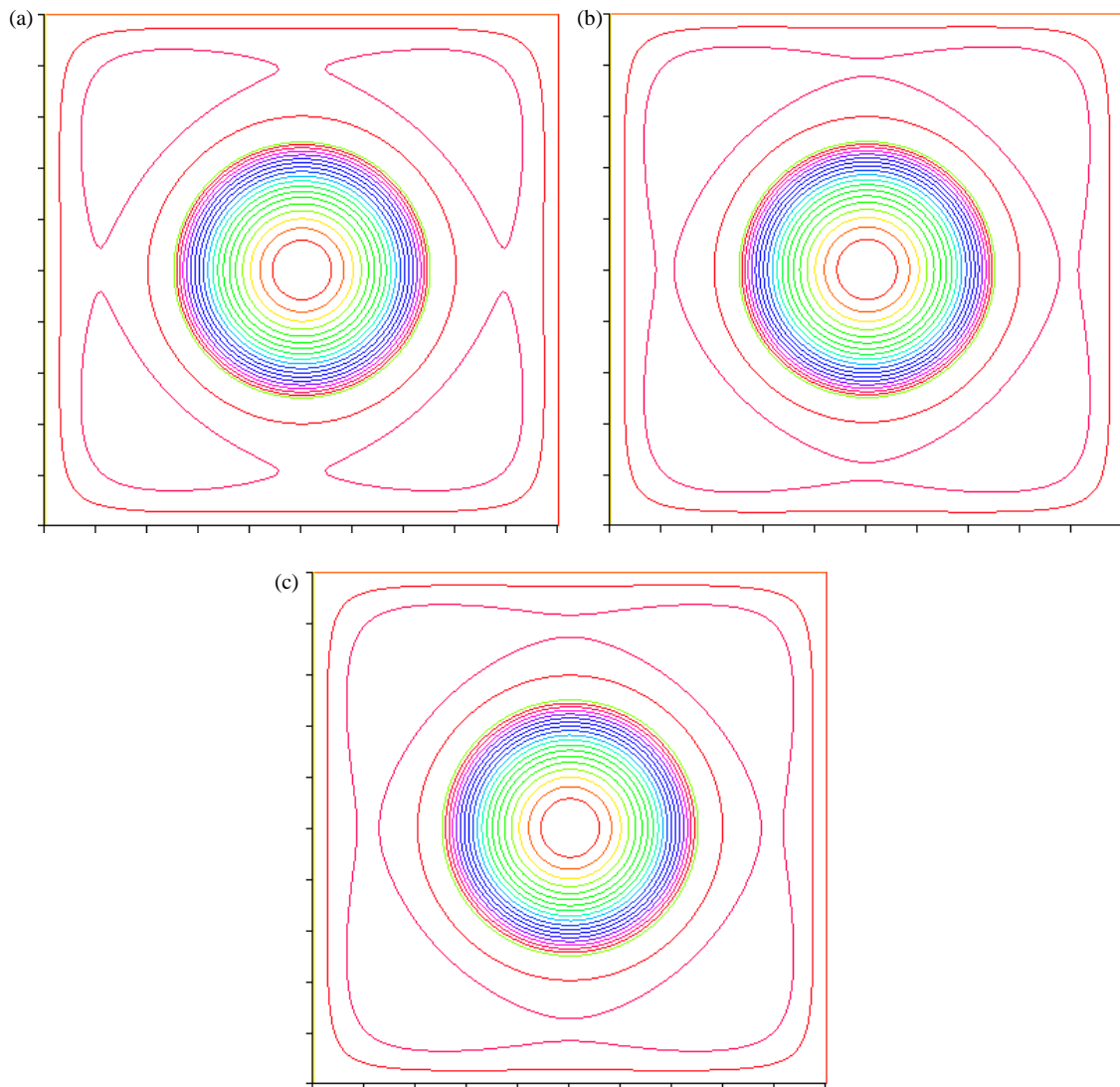
Figure 3.9: (a) Contour plot of the finite element solution of Example 5 at $t = 4$, with $h = 0.0326587$ and $k = 0.0625$ using 1-step implicit scheme. (b) Contour plot of the finite element solution of Example 5 at $t = 4$, with $h = 0.0326587$ and $k = 0.0625$ using 2-step implicit scheme. (c) Contour plot of the exact solution of Example 5.

Comparing (a) and (b) with (c) in Fig 3.9, it is seen that 2-step implicit scheme gives a better approximation than the 1-step scheme.

Example 5 We present the solution of Example 2 using the 2-step implicit scheme.

Errors in L^2-norm at $t = 5$ for various step size h time step k are presented in Table 3.8.

The data presented in Table 3.8 indicate that

$$\|\text{Error}\|_{L^2(\Omega)} = O\left(k^{2.615} + h^{2.013}\left(1 + \frac{1}{|\ln h|}\right)\right)$$

These numerical results match the convergence rate as given in Theorem 3.5.

3.5 Four-Step Linearised FEM-BDS

We propose and analyse a fully discrete scheme based on four-step backward difference approximation. Almost optimal order error estimate in $L^2(\Omega)$-norm is analysed.

The interval [0,T] is divided into M equally spaced (for simplicity) subintervals:

$$0 = t_0 < t_1 < \ldots < t_M = T$$

with $t_n = nk$, $k = T/M$ being the time step. Let $I_n = (t_{n-1}, t_n]$ be the nth subinterval and let

$$u^n = u(x, t_n) \quad \text{and} \quad g^n = g(x, t_n) .$$

For a given sequence $\{w_n\}_{n=0}^M \subset L^2(\Omega)$, we have the backward difference quotients defined by

Table 3.7: Error estimates in L^2-norm for Example 4

h	Error ($k = 0.01$)	k	Error ($h = 0.0606786$)
0.404061	2.90393×10^{-2}	0.125	1.31134×10^{-3}
0.217242	7.14693×10^{-3}	0.1	8.91514×10^{-4}
0.113497	1.74197×10^{-3}	0.05	4.85279×10^{-4}
0.0711493	7.76256×10^{-4}	0.01	4.28527×10^{-4}
0.0606786	4.28527×10^{-4}	0.005	4.27536×10^{-4}

Table 3.8: Error estimates in L^2-norm for Example 5

h	Error ($k = 0.0625$)	k	Error ($h = 0.037129$)
0.205602	1.07997×10^{-1}	0.5	9.14821×10^{-2}
0.110793	2.49325×10^{-2}	0.25	1.95877×10^{-2}
0.0724138	1.09788×10^{-2}	0.2	1.11376×10^{-2}
0.0569736	5.83350×10^{-3}	0.125	3.13144×10^{-3}
0.037129	2.40172×10^{-3}	0.0625	2.40172×10^{-3}

$$\partial^1 w^n = \frac{w^n - w^{n-1}}{\tau_1} \qquad n = 1, 2, \ldots, M$$

$$\partial^2 w^n = \frac{3w^n - 4w^{n-1} + w^{n-2}}{2\tau_2} \qquad n = 2, 3, \ldots, M$$

$$\partial^3 w^n = \frac{11w^n - 18w^{n-1} + 9w^{n-2} - 2w^{n-3}}{6\tau_3} \qquad n = 3, 4, \ldots, M$$

$$\partial^4 w^n = \frac{25w^n - 48w^{n-1} + 36w^{n-2} - 16w^{n-3} + 3w^{n-4}}{12k} \qquad n = 4, 6, \ldots, M$$

The fully discrete finite element approximation to (1.5) is defined as follows:
Let $U_h^0 = \pi_h u_0$, find $U_h^n \in S_h$, such that

$$(\partial^1 U_h^1, v_h)_h + A_h(U_h^0 : U_h^1, v_h) = (f(U_h^0, x), v_h)_h + \langle g_h^1, v_h \rangle_{\Gamma_h} \quad \forall\, v_h \in S_h \quad (3.5.1)$$

$$(\partial^2 U_h^2, v_h)_h + A_h(2U_h^1 - U_h^0 : U_h^2, v_h)$$
$$= (f(2U_h^1 - U_h^0, x), v_h)_h + \langle g_h^2, v_h \rangle_{\Gamma_h} \quad \forall\, v_h \in S_h \quad (3.5.2)$$

$$(\partial^3 U_h^3, v_h)_h + A_h(3U_h^2 - 3U_h^1 + U_h^0 : U_h^3, v_h)$$
$$= (f(3U_h^2 - 3U_h^1 + U_h^0, x), v_h)_h + \langle g_h^3, v_h \rangle_{\Gamma_h} \quad \forall\, v_h \in S_h \quad (3.5.3)$$

$$(\partial^4 U_h^n, v_h)_h + A_h(4U_h^{n-1} - 6U_h^{n-2} + 4U_h^{n-3} - U_h^{n-4} : U_h^n, v_h)$$
$$= (f(4U_h^{n-1} - 6U_h^{n-2} + 4U_h^{n-3} - U_h^{n-4}, x), v_h)_h + \langle g_h^n, v_h \rangle_{\Gamma_h}$$
$$\forall\, v_h \in S_h \quad n = 4, 5, \ldots, M \quad (3.5.4)$$

The scheme $(3.5.1) - (3.5.4)$ is zero-stable. To see this, we obtain the first characteristic polynomials as follows

$$\rho_1(y) = y - 1$$
$$\rho_2(y) = \frac{3}{2}y^2 - 2y + \frac{1}{2}$$
$$\rho_3(y) = \frac{11}{6}y^3 - 3y^2 + \frac{3}{2}y - \frac{1}{3}$$
$$\rho_4(y) = \frac{25}{12}y^4 - 4y^3 + 3y^2 - \frac{4}{3}y + \frac{1}{4}$$

101

The roots of these polynomials have modulli less than one and the roots with modulus one are simple. See Appendix C.

The analysis of this work is done with the assumption that $\frac{\partial^i u}{\partial t^i}$ exist for$(i = 1, \ldots, 5)$. It can be shown using Taylor expansion that

$$\begin{cases} \|U_h^n - 2U_h^{n-1} + U_h^{n-2}\|_{L^2(\Omega)} & \leq & (\Delta t)^2 \lambda_0 \\ \|U_h^n - 3U_h^{n-1} + 3U_h^{n-2} - U_h^{n-3}\|_{L^2(\Omega)} & \leq & (\Delta t)^3 \lambda_1 \\ \|U_h^n - 4U_h^{n-1} + 6U_h^{n-2} - 4U_h^{n-3} + U_h^{n-4}\|_{L^2(\Omega)} & \leq & (\Delta t)^4 \lambda_2 \end{cases} \qquad (3.5.5)$$

We have the following stability result:

Lemma 3.11 Suppose the conditions of Assumption 1.1 are satisfied, there exists a constant C independent of h and k such that for the solution of $(3.5.1) - (3.5.4)$

$$\|U_h^n\|_{L^2(\Omega)}^2 + k\|\nabla U_h^n\|_{L^2(\Omega)}^2 \leq C \left[(1+k)\|U_h^0\|_{L^2(\Omega)}^2 + k \sum_{i=1}^n \left\{ \|g_h^i\|_{H^{1/2}(\Gamma)}^2 \right\} \right] \qquad (3.5.6)$$

Proof We take $\tau_1 = \tau_2 = \tau_3 = k$. Let $v_h = U_h^1$ in (3.5.1), then

$$\|U_h^1\|_{L^2(\Omega)}^2 + \mu_1 k \|\nabla U_h^1\|_{L^2(\Omega)}^2 \leq \|U_h^1\|_{L^2(\Omega)}\|U_h^0\|_{L^2(\Omega)} + \mu_3 k \|U_h^0\|_{L^2(\Omega)}\|U_h^1\|_{L^2(\Omega)}$$
$$+ k\|g_h^1\|_{H^{1/2}(\Gamma_h)}\|U_h^1\|_{L^2(\Omega)}$$

By Young's inequality, there exists a constant C such that

$$(1-k)\|U_h^1\|_{L^2(\Omega)}^2 + k\|\nabla U_h^1\|_{L^2(\Omega)}^2 \leq C \left[(1+k)\|U_h^0\|_{L^2(\Omega)}^2 + k\|g_h^1\|_{H^{1/2}(\Gamma)}^2 \right]$$

There exists a constant $C = \dfrac{1}{1 - k_0}$ such that

$$1 \leq (1-k)^{-1} \leq (1 + Ck) \leq C$$

for $0 < k \leq k_0 < 1$ and therefore

$$\|U_h^1\|_{L^2(\Omega)}^2 + k\|\nabla U_h^1\|_{L^2(\Omega)}^2 \leq C \left[(1+k)\|U_h^0\|_{L^2(\Omega)}^2 + k\|g_h^1\|_{H^{1/2}(\Gamma)}^2 \right] \qquad (3.5.7)$$

Let $v_h = U_h^2$ in (3.5.2)

$$\frac{1}{k}\|U_h^2\|_{L^2(\Omega)}^2 + \mu_1\|\nabla U_h^2\|_{L^2(\Omega)}^2 \leq \frac{1}{k}\|U_h^2\|_{L^2(\Omega)}\|U_h^1\|_{L^2(\Omega)}$$
$$+\frac{1}{2k}\|U_h^2\|_{L^2(\Omega)}\|U_h^2 - 2U_h^1 + U_h^0\|_{L^2(\Omega)}$$
$$+ \mu_3\|2U_h^1 - U_h^0\|_{L^2(\Omega)}\|U_h^2\|_{L^2(\Omega)}$$
$$+ \|g_h^2\|_{H^{1/2}(\Gamma)}\|U_h^2\|_{L^2(\Omega)}$$
$$\leq \frac{1}{k}\|U_h^2\|_{L^2(\Omega)}\|U_h^1\|_{L^2(\Omega)} + \frac{\lambda_0 k}{2}\|U_h^2\|_{L^2(\Omega)}$$
$$+\mu_3\|U_h^2\|_{L^2(\Omega)}^2 + \lambda_0\mu_3 k^2\|U_h^2\|_{L^2(\Omega)}$$
$$+ \|g_h^2\|_{H^{1/2}(\Gamma)}\|U_h^2\|_{L^2(\Omega)}$$

By Young's inequality, we have

$$\frac{1}{2}\left[1 - (1 + 3\mu_3)\,k\right]\|U_h^2\|_{L^2(\Omega)}^2 + k\mu_1\|\nabla U_h^2\|_{L^2(\Omega)}^2$$
$$\leq \frac{1}{2}\|U_h^1\|_{L^2(\Omega)}^2 + k\|g_h^2\|_{H^{1/2}(\Gamma)}^2 + \frac{1}{4}k^3\lambda_0^2 + \frac{1}{2}\mu_3 k^5$$

For $0 < k < \dfrac{1}{1+3\mu_3}$, there is a $C > 0$ such that

$$\|U_h^2\|_{L^2(\Omega)}^2 + k\|\nabla U_h^2\|_{L^2(\Omega)}^2 \leq C\left[\|U_h^1\|_{L^2(\Omega)}^2 + k\|g_h^2\|_{H^{1/2}(\Gamma)}^2 + k^3\right]$$

By (3.5.7), we have

$$\|U_h^2\|_{L^2(\Omega)}^2 + k\|\nabla U_h^2\|_{L^2(\Omega)}^2 \leq C\left[(1+k)\|U_h^0\|_{L^2(\Omega)}^2 + k\sum_{i=1}^{2}\left\{\|g_h^i\|_{H^{1/2}(\Gamma)}^2\right\}\right] \quad (3.5.8)$$

By a similar argument to the argument that led to (3.5.8), we obtain

$$\|U_h^3\|_{L^2(\Omega)}^2 + k\|\nabla U_h^3\|_{L^2(\Omega)}^2 \leq C\left[(1+k)\|U_h^0\|_{L^2(\Omega)}^2 + k\sum_{i=1}^{3}\left\{\|g_h^i\|_{H^{1/2}(\Gamma)}^2\right\}\right] \quad (3.5.9)$$

For $n = 4, 5, \ldots,$

$$\frac{1}{k}\|U_h^n\|_{L^2(\Omega)}^2 + \mu_1\|\nabla U_h^n\|_{L^2(\Omega)}^2$$

$$\begin{aligned}
&\leq \frac{1}{k}\|U_h^n\|_{L^2(\Omega)}\|U_h^{n-1}\|_{L^2(\Omega)} \\
&\quad + \frac{1}{4k}\|U_h^n\|_{L^2(\Omega)}\|U_h^n - 4U_h^{n-1} + 6U_h^{n-2} - 4U_h^{n-3} + U_h^{n-4}\|_{L^2(\Omega)} \\
&\quad + \frac{1}{3k}\|U_h^n\|_{L^2(\Omega)}\|U_h^n - 3U_h^{n-1} + 3U_h^{n-2} - U_h^{n-3}\|_{L^2(\Omega)} \\
&\quad + \frac{1}{2k}\|U_h^n\|_{L^2(\Omega)}\|U_h^n - 2U_h^{n-1} + U_h^{n-2}\|_{L^2(\Omega)} + \|U_h^n\|_{L^2(\Omega)}\|g_h^n\|_{H^{1/2}(\Gamma)} \\
&\quad + \mu_3\|4U_h^{n-1} - 6U_h^{n-2} + 4U_h^{n-3} + U_h^{n-4}\|_{L^2(\Omega)}\|U_h^n\|_{L^2(\Omega)} \\
&\leq \frac{1}{k}\|U_h^n\|_{L^2(\Omega)}\|U_h^{n-1}\|_{L^2(\Omega)} + \frac{\lambda_2 k^3}{4}\|U_h^n\|_{L^2(\Omega)} + \frac{\lambda_1 k^2}{3}\|U_h^n\|_{L^2(\Omega)} \\
&\quad + \frac{\lambda_0 k}{2}\|U_h^n\|_{L^2(\Omega)} + \|U_h^n\|_{L^2(\Omega)}\|g_h^n\|_{H^{1/2}(\Gamma)} \\
&\quad + \mu_3\|U_h^n\|_{L^2(\Omega)}^2 + \mu_3\lambda k^4\|U_h^n\|_{L^2(\Omega)}^2
\end{aligned}$$

By Young's inequality,

$$\begin{aligned}
\frac{1}{2}\left[1 - (1+3\mu_3)k\right]\|U_h^2\|_{L^2(\Omega)}^2 + k\mu_1\|\nabla U_h^2\|_{L^2(\Omega)}^2 \\
\leq \frac{1}{2}\|U_h^1\|_{L^2(\Omega)}^2 + k\|g_h^2\|_{H^{1/2}(\Gamma)}^2 + \frac{3}{16}\lambda_2^2 k^7 + \frac{1}{9}\lambda_1^2 k^5 + \frac{3}{4}\lambda_0^2 k^3 + \frac{1}{2}\lambda_2^2 k^9
\end{aligned}$$

For $0 < k \leq k_0 < \dfrac{1}{1+3\mu_3}$, there is a $C > 0$ such that

$$\|U_h^n\|_{L^2(\Omega)}^2 + k\|\nabla U_h^n\|_{L^2(\Omega)}^2 \leq C\left\{\|U_h^{n-1}\|_{L^2(\Omega)}^2 + k\|g_h^n\|_{H^{1/2}(\Gamma)}^2 + k^3\right\}$$

By iteration on n, we obtain

$$\|U_h^n\|_{L^2(\Omega)}^2 + k\|\nabla U_h^n\|_{L^2(\Omega)}^2 \leq C\left[\|U_h^3\|_{L^2(\Omega)}^2 + k\sum_{i=4}^{n}\left\{\|g_h^i\|_{H^{1/2}(\Gamma)}^2\right\} + k^3\right] \quad (3.5.10)$$

(3.5.6) follows from (3.5.9) & (3.5.10).

The result below establishes the convergence of the scheme $(3.5.1) - (3.5.4)$ to the exact solution in the $L^2(\Omega)$-norm.

Theorem 3.6 Let u and U_h^n be the solutions of (3.1.1) and (3.5.4) respectively.

104

Suppose that the conditions of Assumption 1.1 are satisfied for every $a : \Omega \times \mathbb{R} \to \mathbb{R}$, $f : \Omega \times \mathbb{R} \to \mathbb{R}$, $g \in L^2(0, T; H^2(\Gamma) \cap H^{1/2}(\Gamma))$ and $\dfrac{\partial^5 u}{\partial t^5}$ is defined for $\Omega \times [0, T]$. There exists a positive constant C independent of h and k such that

$$\|u - U_h^n\|_{L^2(\Omega)} \leq \left[k^4 + h^2 \left(1 + \frac{1}{|\log h|} \right) \right] C(u_0, u, g)$$

where

$$
\begin{aligned}
C(u_0, u, g) \;=\; & \left[t_n \|u_0\|_{L^2(\Omega)}^2 + \int_0^{t_n} \left(t_n \|g\|_{H^{1/2}(\Gamma)}^2 + \sum_{j=2}^{5} \|\frac{\partial^j u}{\partial t^j}\|_{L^2(\Omega)}^2 \right) dt \right. \\
& \left. + \|u_0\|_X^2 + \int_0^{t_n} \left(\|u\|_X^2 + \|u_t\|_X^2 + \|g\|_{H^2(\Gamma)}^2 \right) dt \right]^{1/2}
\end{aligned}
$$

Proof Let $z^n = P_h u^n - U_h^n$, from (3.1.1) and (3.5.4), we have

$$(\partial^4 z^n, v_h)_h + A_h(z^n, v_h) \;=\; B_{16} + B_{17} + B_{18} \qquad (3.5.11)$$

where

$$
\begin{aligned}
B_{16} \;&=\; (\partial^4 (P_h u^n - u^n), v_h)_h + (\partial^4 u^n - u_t^n, v_h) + (\partial^4 u^n, v_h)_h - (\partial^4 u^n, v_h) \\
B_{17} \;&=\; (f(x, u^n), v_h) - (f^n, v_h)_h + \langle g^n, v_h \rangle_\Gamma - \langle g_h^n, v_h \rangle_{\Gamma_h} \\
B_{18} \;&=\; A_h(4 U_h^{n-1} - 6 U_h^{n-2} + 4 U_h^{n-3} - U_h^{n-4} : P_h u^n, v_h) - A_h(u^n : P_h u^n, v_h)
\end{aligned}
$$

and $f^n = f(x, 4 U_h^{n-1} - 6 U_h^{n-2} + 4 U_h^{n-3} - U_h^{n-4})$.

With $v_h = z^n$, we have

$$
\begin{aligned}
B_{16} \;\leq\; & \|\partial^4 (P_h u^n - u^n)\|_{L^2(\Omega)}^2 + \frac{1}{2} \|z^n\|_{L^2(\Omega)}^2 + \|\partial^4 u^n - u_t^n\|_{L^2(\Omega)}^2 \\
& + \gamma C h^4 \|\partial^4 u^n\|_X^2 + \frac{1}{4\gamma} \|z^n\|_{H^1(\Omega)}^2 \qquad (3.5.12)
\end{aligned}
$$

Using Lemma 3.4, Lemma 3.7, Lemma 3.8 with the fact that $D^\alpha z^n = 0$ for $|\alpha| = 2$, we have

$$
\begin{aligned}
B_{17} &\leq Ch\|u^n\|_{H^1(\Omega_h^\star)}\|z^n\|_{H^1(\Omega_h^\star)} + \mu_3\|u^n - U_h^n\|_{L^2(\Omega)}\|z^n\|_{L^2(\Omega)} \\
&\quad + Ch^{3/2}\|g^n\|_{H^2(\Gamma)}\|z^n\|_{H^1(\Omega_h^\star)} \\
&\quad + \mu_3\|U_h^n - (4U_h^{n-1} - 6U_h^{n-2} + 4U_h^{n-3} - U_h^{n-4})\|_{L^2(\Omega)}\|z^n\|_{L^2(\Omega)} \\
&\leq Ch^2\|u^n\|_X\|z^n\|_{H^1(\Omega)} + \left(\mu_3 + \frac{1}{2}\right)\|z^n\|_{L^2(\Omega)}^2 + C\|P_h u^n - u^n\|_{L^2(\Omega)}^2 \\
&\quad + Ch^2\|g^n\|_{H^2(\Gamma)}\|z^n\|_{H^1(\Omega)} + Ck^4\|U_h^n\|_{L^2(\Omega)}\|z^n\|_{L^2(\Omega)} \\
&\leq C(\gamma)h^4\left(1 + \frac{1}{|\log h|}\right)^2 \left(\|u^n\|_X^2 + \|g^n\|_{H^2(\Gamma)}^2\right) + \frac{1}{2\gamma}\|z^n\|_{H^1(\Omega)}^2 \\
&\quad + C\|z^n\|_{L^2(\Omega)}^2 + Ck^8\|U_h^n\|_{L^2(\Omega)}^2 \qquad\qquad\qquad (3.5.13)
\end{aligned}
$$

Let $\|P_h u^n\|_{L^\infty(\Omega)} = \beta$. For B_{18}, we have

$$
\begin{aligned}
B_{18} &\leq \beta\mu_3\|(4U_h^{n-1} - 6U_h^{n-2} + 4U_h^{n-3} - U_h^{n-4}) - u^n\|_{L^2(\Omega)}\|z^n\|_{H^1(\Omega)} \\
&\leq \beta\mu_3\|(4U_h^{n-1} - 6U_h^{n-2} + 4U_h^{n-3} - U_h^{n-4}) - U_h^n\|_{L^2(\Omega)}\|z^n\|_{H^1(\Omega)} \\
&\quad + \beta\mu_3\|U_h^n - u^n\|_{L^2(\Omega)}\|z^n\|_{H^1(\Omega)} \\
&\leq C\mu_3 k^4\|U_h^n\|_{L^2(\Omega)}\|z^n\|_{H^1(\Omega)} + \beta\mu_3\|P_h u^n - u^n\|_{L^2(\Omega)}\|z^n\|_{H^1(\Omega)} \\
&\quad + \beta\mu_3\|z^n\|_{L^2(\Omega)}\|z^n\|_{H^1(\Omega)} \\
&\leq \gamma\beta^2\mu_3^2\|z^n\|_{L^2(\Omega)}^2 + \frac{3}{4\gamma}\|z^n\|_{H^1(\Omega)}^2 + Ch^4\left(1 + \frac{1}{|\log h|}\right)^2\|u^n\|_X^2 \\
&\quad + Ck^8\|U_h^n\|_{L^2(\Omega)}^2 \qquad\qquad\qquad\qquad\qquad (3.5.14)
\end{aligned}
$$

Substituting $(3.5.12) - (3.5.14)$ into $(3.5.11)$, we have, for $c_1 > 0$,

$$
\begin{aligned}
\frac{1}{k}\|z^n\|_{L^2(\Omega)}^2 + \mu_1\|z^n\|_{H^1(\Omega)}^2 &\leq \frac{C}{k}\left(\|z^n\|_{L^2(\Omega)}\|z^{n-1}\|_{L^2(\Omega)} + \|z^n\|_{L^2(\Omega)}\|z^{n-2}\|_{L^2(\Omega)}\right. \\
&\quad \left. + \|z^n\|_{L^2(\Omega)}\|z^{n-3}\|_{L^2(\Omega)} + \|z^n\|_{L^2(\Omega)}\|z^{n-4}\|_{L^2(\Omega)}\right) \\
&\quad + \|\partial^4(P_h u^n - u^n)\|_{L^2(\Omega)}^2 + C_0\|z^n\|_{L^2(\Omega)}^2 \\
&\quad + \|\partial_k u^n - u_t^n\|_{L^2(\Omega)}^2 + Ch^4\|\partial^4 u^n\|_X^2 \\
&\quad + Ch^4\left(1 + \frac{1}{|\ln h|}\right)^2\left(\|u^n\|_X^2 + \|g^n\|_{H^2(\Gamma)}^2\right) \\
&\quad + \frac{1}{\gamma}\|z^n\|_{H^1(\Omega)}^2 + Ck^8\|U_h^n\|_{L^2(\Omega)}^2
\end{aligned}
$$

106

where $C_0 = \dfrac{1}{2} + \mu_3 + \gamma\beta^2\mu_3^2$. With $\gamma = \dfrac{1}{\mu_1}$, we obtain

$$(1 - C_0 k)\, \|z^n\|_{L^2(\Omega)}^2$$

$$
\begin{aligned}
\leq\ & C\left(\|z^{n-1}\|_{L^2(\Omega)}^2 + \|z^{n-2}\|_{L^2(\Omega)}^2 + \|z^{n-3}\|_{L^2(\Omega)}^2 + \|z^{n-4}\|_{L^2(\Omega)}^2\right) \\
& + C\left[k\|\partial^4(P_h u^n - u^n)\|_{L^2(\Omega)}^2 + k\|\partial^4 u^n - u_t^n\|_{L^2(\Omega)}^2 + kh^4\|\partial^4 u^n\|_X^2\right] \\
& + Ch^4 k\left(1 + \frac{1}{|\ln h|}\right)^2\left(\|u^n\|_X^2 + \|g^n\|_{H^2(\Gamma)}^2\right) + Ck^9\|U_h^n\|_{L^2(\Omega)}^2
\end{aligned}
$$

For $0 < k < \min\left\{1, \dfrac{1}{C_0}\right\}$, there is a $C > 0$ such that $(1 - C_0 k)^{-1} \leq C$, and therefore

$$
\begin{aligned}
\|z^n\|_{L^2(\Omega)}^2 \leq\ & C\left[\|z^{n-1}\|_{L^2(\Omega)}^2 + \|z^{n-2}\|_{L^2(\Omega)}^2 + \|z^{n-3}\|_{L^2(\Omega)}^2 + \|z^{n-4}\|_{L^2(\Omega)}^2\right. \\
& + k\|\partial^4(P_h u^n - u^n)\|_{L^2(\Omega)}^2 + k\|\partial^4 u^n - u_t^n\|_{L^2(\Omega)}^2 + kh^4\|\partial^4 u^n\|_X^2 \\
& \left. + Ch^4 k\left(1 + \frac{1}{|\ln h|}\right)^2\left(\|u^n\|_X^2 + \|g^n\|_{H^2(\Gamma)}^2\right) + Ck^9\|U_h^n\|_{L^2(\Omega)}^2\right.
\end{aligned}
$$

for $n = 4, \ldots, M$.

By iteration on n, we have

$$
\begin{aligned}
\|z^n\|_{L^2(\Omega)}^2 \leq\ & C\left[\|z^0\|_{L^2(\Omega)}^2 + \|z^1\|_{L^2(\Omega)}^2 + \|z^2\|_{L^2(\Omega)}^2 + \|z^3\|_{L^2(\Omega)}^2\right] \\
& + Ck\sum_{j=4}^{n}\|\partial^4(u^j - P_h u^j)\|_{L^2(\Omega)}^2 + Ck^9\sum_{j=4}^{n}\|U_h^j\|_{L^2(\Omega)}^2 \\
& + Ch^4 k\left(1 + \frac{1}{|\ln h|}\right)^2\sum_{j=4}^{n}(\|u^j\|_X^2 + \|g^j\|_{H^2(\Gamma)}^2) \\
& + Ck\sum_{j=4}^{n}\|\partial^4 u^j - u_t^j\|_{L^2(\Omega)}^2 + Ch^4 k\sum_{j=4}^{n}\|\partial^4 u^j\|_X^2
\end{aligned}
$$

After a simple calculation, we have

$$
\begin{aligned}
\|z^n\|_{L^2(\Omega)}^2 \;\leq\; & C\left[\|z^0\|_{L^2(\Omega)}^2 + \|z^1\|_{L^2(\Omega)}^2 + \|z^2\|_{L^2(\Omega)}^2 + \|z^3\|_{L^2(\Omega)}^2\right] \\
& + C\int_0^{t_n}\|(u - P_h u)_t\|_{L^2(\Omega)}^2\,dt + Ck^8\int_0^{t_n}\|\frac{\partial^5 u}{\partial t^5}\|_{L^2(\Omega)}^2\,dt \\
& + Ch^4\left(1 + \frac{1}{|\ln h|}\right)^2\int_0^{t_n}\left[\|u\|_X^2 + \|u_t\|_X^2 + \|g\|_{H^2(\Gamma)}^2\right]\,dt \\
& + Ck^9\sum_{j=4}^n \|U_h^j\|_{L^2(\Omega)}^2 \\
\leq\; & C\left[\|z^0\|_{L^2(\Omega)}^2 + \|z^1\|_{L^2(\Omega)}^2 + \|z^2\|_{L^2(\Omega)}^2 + \|z^3\|_{L^2(\Omega)}^2\right] \\
& + Ch^4\left(1 + \frac{1}{|\log h|}\right)^2\int_0^{t_n}\left[\|u\|_X^2 + \|u_t\|_X^2 + \|g\|_{H^2(\Gamma)}^2\right]\,dt \\
& + Ck^8\int_0^{t_n}\|\frac{\partial^5 u}{\partial t^5}\|_{L^2(\Omega)}^2\,dt + Ck^9\sum_{j=4}^n \|U_h^j\|_{L^2(\Omega)}^2 \qquad (3.5.15)
\end{aligned}
$$

Let $z^1 = P_h u^1 - U_h^1$, from (3.1.1) and (3.5.1), we have

$$
\begin{aligned}
(\partial^1 z^1, v_h)_h + A_h(z^1, v_h) \;=\; & (\partial^1(P_h u^1 - u^1), v_h)_h + (\partial^1 u^1 - u_t^1, v_h) \\
& + (\partial^1 u^1, v_h)_h - (\partial^1 u^1, v_h) \\
& + A_h(U_h^0 : P_h u^1, v_h) - A_h(u^1 : P_h u^1, v_h) \\
& + (f(x, u^n), v_h) - (f(x, U_h^0), v_h)_h + \langle g^1, v_h\rangle_\Gamma - \langle g_h^1, v_h\rangle_{\Gamma_h}
\end{aligned}
$$

With $v_h = z^1$, we have

$$
\begin{aligned}
\frac{1}{\tau_1}\|z^1\|_{L^2(\Omega)}^2 + \mu_1\|z^1\|_{H^1(\Omega)}^2 \;\leq\; & \frac{1}{\tau_1}\|z^0\|_{L^2(\Omega)}\|z^1\|_{L^2(\Omega)} + \|\partial^1(P_h u^1 - u^1)\|_{L^2(\Omega)}^2 \\
& + \left(\frac{1}{2} + \mu_1\right)\|z^1\|_{L^2(\Omega)}^2 + \|\partial^1 u^1 - u_t^1\|_{L^2(\Omega)}^2 + Ch^4\|\partial^1 u^1\|_X^2 \\
& + Ch^4\|g^1\|_{H^2(\Gamma)}^2 + \frac{1}{\gamma}\|z^1\|_{H^1(\Omega)}^2 + \gamma\beta^2\mu_3^2\|U_h^0 - u^1\|_{L^2(\Omega)}^2 \\
\leq\; & \frac{1}{\tau_1}\|z^0\|_{L^2(\Omega)}\|z^1\|_{L^2(\Omega)} + \|\partial^1(P_h u^1 - u^1)\|_{L^2(\Omega)}^2 \\
& + \left(\frac{1}{2} + \mu_1 + \gamma\beta^2\mu_3^2\right)\|z^1\|_{L^2(\Omega)}^2 + \|\partial^1 u^1 - u_t^1\|_{L^2(\Omega)}^2 \\
& + Ch^4\|\partial^1 u^1\|_X^2 + Ch^4\|g^1\|_{H^2(\Gamma)}^2 + \frac{1}{\gamma}\|z^1\|_{H^1(\Omega)}^2 \\
& + C\tau_1\|U_h^1\|_{L^2(\Omega)}^2 + Ch^4\left(1 + \frac{1}{|\ln h|}\right)^2 \|u^1\|_X^2
\end{aligned}
$$

With $\gamma = \dfrac{1}{\mu_1}$, we obtain

$$
\begin{aligned}
(1 - C_0\tau_1)\|z^1\|_{L^2(\Omega)}^2 \;\leq\; & \|z^0\|_{L^2(\Omega)}^2 + \tau_1\|\partial^1(P_h u^1 - u^1)\|_{L^2(\Omega)}^2 + \tau_1\|\partial^1 u^1 - u_t^1\|_{L^2(\Omega)}^2 \\
& + C\tau_1 h^4\|\partial^1 u^1\|_X^2 + C\tau_1^2\|U_h^1\|_{L^2(\Omega)}^2 \\
& + \tau_1 Ch^4\left(1 + \frac{1}{|\ln h|}\right)^2\left(\|u^1\|_X^2 + \|g^1\|_{H^2(\Gamma)}^2\right)
\end{aligned}
$$

For $0 < \tau_1 < \min\left\{1, \dfrac{1}{C_0}\right\}$, there is a $C > 0$ such that $(1 - C_0\tau_1)^{-1} \leq C$, therefore,

$$
\begin{aligned}
\|z^1\|_{L^2(\Omega)}^2 \;\leq\;& C\Big[\|z^0\|_{L^2(\Omega)}^2 + \tau_1\|\partial^1(P_h u^1 - u^1)\|_{L^2(\Omega)}^2 + \tau_1\|\partial^1 u^1 - u_t^1\|_{L^2(\Omega)}^2 \\
&\qquad +\tau_1 h^4\|\partial^1 u^1\|_X^2 + \tau_1 h^4\left(1 + \frac{1}{|\ln h|}\right)^2\left(\|u^1\|_X^2 + \|g^1\|_{H^2(\Gamma)}^2\right) \\
&\qquad + \tau_1^2\|U_h^1\|_{L^2(\Omega)}^2\Big] \\
\leq\;& C\|z^0\|_{L^2(\Omega)}^2 + C\int_0^{t_1}\|(u - P_h u)_t\|_{L^2(\Omega)}^2\,dt + C\tau_1^2\int_0^{t_1}\|u_{tt}\|_{L^2(\Omega)}^2\,dt \\
&\quad +Ch^4\left(1 + \frac{1}{|\ln h|}\right)^2\int_0^{t_1}\Big[\|u\|_X^2 + \|u_t\|_X^2 + \|g\|_{H^2(\Gamma)}^2\Big]\,dt \\
&\quad + C\tau_1^2\|U_h^1\|_{L^2(\Omega)}^2 \\
\leq\;& C\|z^0\|_{L^2(\Omega)}^2 + C\tau_1^2\int_0^{t_1}\|u_{tt}\|_{L^2(\Omega)}^2\,dt + C\tau_1^2\|U_h^1\|_{L^2(\Omega)}^2 \\
&\quad +Ch^4\left(1 + \frac{1}{|\log h|}\right)^2\int_0^{t_1}\Big[\|u\|_X^2 + \|u_t\|_X^2 + \|g\|_{H^2(\Gamma)}^2\Big]\,dt \quad (3.5.16)
\end{aligned}
$$

By similar arguments to the one that led to (3.5.16), we have

$$
\begin{aligned}
\|z^2\|_{L^2(\Omega)}^2 \;\leq\;& C\Big[\|z^0\|_{L^2(\Omega)}^2 + \|z^1\|_{L^2(\Omega)}^2\Big] + C\tau_2^4\int_0^{t_2}\|u_{ttt}\|_{L^2(\Omega)}^2\,dt \\
&\quad +Ch^4\left(1 + \frac{1}{|\log h|}\right)^2\int_0^{t_2}\Big[\|u\|_X^2 + \|u_t\|_X^2 + \|g\|_{H^2(\Gamma)}^2\Big]\,dt \\
&\quad + C\tau_2^4\|U_h^2\|_{L^2(\Omega)}^2 \qquad\qquad\qquad\qquad (3.5.17) \\
\|z^3\|_{L^2(\Omega)}^2 \;\leq\;& C\Big[\|z^0\|_{L^2(\Omega)}^2 + \|z^1\|_{L^2(\Omega)}^2 + \|z^2\|_{L^2(\Omega)}^2\Big] + C\tau_3^6\int_0^{t_3}\|u_{tttt}\|_{L^2(\Omega)}^2\,dt \\
&\quad +Ch^4\left(1 + \frac{1}{|\log h|}\right)^2\int_0^{t_3}\Big[\|u\|_X^2 + \|u_t\|_X^2 + \|g\|_{H^2(\Gamma)}^2\Big]\,dt \\
&\quad + C\tau_3^6\|U_h^3\|_{L^2(\Omega)}^2 \qquad\qquad\qquad\qquad (3.5.18)
\end{aligned}
$$

From $(3.5.15) - (3.5.18)$ with $\tau_1 \leq k^4$, $\tau_2 \leq k^2$ and $\tau_3 \leq k^{4/3}$ we have

$$
\begin{aligned}
\|z^n\|_{L^2(\Omega)}^2 \leq\ & C\|z^0\|_{L^2(\Omega)}^2 + Ck^8 \int_0^{t_n} \left\{ \sum_{j=2}^5 \|\frac{\partial^j u}{\partial t^j}\|_{L^2(\Omega)}^2 \right\} dt \\
& + Ch^4 \left(1 + \frac{1}{|\log h|} \right)^2 \int_0^{t_n} \left[\|u\|_X^2 + \|u_t\|_X^2 + \|g\|_{H^2(\Gamma)}^2 \right] dt \\
& + k^9 \sum_{j=1}^n \|U_h^j\|_{L^2(\Omega)}^2
\end{aligned}
\tag{3.5.19}
$$

Now, from Lemma 3.11,

$$
\begin{aligned}
k \sum_{j=1}^n \|U_h^j\|_{L^2(\Omega)}^2 =\ & Ck \sum_{j=1}^n \left[(1+k)\|U_h^0\|_{L^2(\Omega)}^2 + k \sum_{i=1}^j \left\{ \|g_h^i\|_{H^{1/2}(\Gamma)}^2 \right\} \right] \\
\leq\ & Ck \sum_{j=1}^n \left[(1+k)\|U_h^0\|_{L^2(\Omega)}^2 + \int_0^{t_j} \|g\|_{H^{1/2}(\Gamma)}^2\, dt \right] \\
\leq\ & Ct_n \left[(1+k)\|\pi u_0\|_{L^2(\Omega)}^2 + \int_0^{t_n} \|g\|_{H^{1/2}(\Gamma)}^2\, dt \right]
\end{aligned}
\tag{3.5.20}
$$

From $(3.5.19)$ and $(3.5.20)$,

$$
\begin{aligned}
\|z^n\|_{L^2(\Omega)}^2 \leq\ & C\|z^0\|_{L^2(\Omega)}^2 + Ck^8 \int_0^{t_n} \left\{ \sum_{j=2}^5 \|\frac{\partial^j u}{\partial t^j}\|_{L^2(\Omega)}^2 + t_n\|g\|_{H^{1/2}(\Gamma)}^2 \right\} dt \\
& + Ch^4 \left(1 + \frac{1}{|\log h|} \right)^2 \int_0^{t_n} \left[\|u\|_X^2 + \|u_t\|_X^2 + \|g\|_{H^2(\Gamma)}^2 \right] dt \\
& + Ct_n k^8 (1+k)\|u_0\|_{L^2(\Omega)}^2
\end{aligned}
\tag{3.5.21}
$$

Now, from Lemma 3.8 and $(3.5.21)$

$$
\|u^n - U_h^n\|_{L^2(\Omega)}^2
$$

$$
\begin{aligned}
\leq\ & 2\|u^n - P_h u^n\|_{L^2(\Omega)}^2 + 2\|z^n\|_{L^2(\Omega)}^2 \\
\leq\ & Ck^8 \left[t_n\|u_0\|_{L^2(\Omega)}^2 + \int_0^{t_n} \left(t_n\|g\|_{H^{1/2}(\Gamma)}^2 + \sum_{j=2}^5 \|\frac{\partial^j u}{\partial t^j}\|_{L^2(\Omega)}^2 \right) dt \right] \\
& + Ch^4 \left(1 + \frac{1}{|\log h|} \right)^2 \left\{ \|u_0\|_X^2 + \int_0^{t_n} \left[\|u\|_X^2 + \|u_t\|_X^2 + \|g\|_{H^2(\Gamma)}^2 \right] dt \right\}
\end{aligned}
$$

The result follows immediately.

Remark 3.3 The initial three steps of the scheme are constructed using low order time discretisation scheme, however, this does not affect the convergence rate since they are used once. Moreover, in the error analysis, the step sizes of these low order discretisation are chosen to be sufficiently small to guarantee the convergence rate.

3.5.1 Four-Step Numerical Experiment

Example 6 We present the solution of Example 1 using the four-step linearised scheme $(3.5.1) - (3.5.4)$.

Errors in L^2-norm at $t = 12$ for various step size h time step k are presented in Table 3.9.

The data presented in Table 3.9 indicate that

$$\|\text{Error}\|_{L^2(\Omega)} = O\left(k^{3.954} + h^{1.991}\left(1 + \frac{1}{|\ln h|}\right)\right)$$

These numerical results match the convergence rate as given in Theorem 3.6.

Example 7 We present the solution of Example 2 using the linearised scheme.

Errors in L^2-norm at $t = 5$ for various step size h time step k are presented in Table 3.10.

The data presented in Table 3.10 indicate that

$$\|\text{Error}\|_{L^2(\Omega)} = O\left(k^{4.900} + h^{1.982}\left(1 + \frac{1}{|\ln h|}\right)\right)$$

These numerical results match the convergence rates as given in Theorem 3.6.

Example 8 We present the solution of Example 3 using the linearised scheme.

Errors in L^2-norm at $t = 4$ for various step size h time step k are presented in Table 3.11.

The data presented in Table 3.11 indicate that

$$\|\text{Error}\|_{L^2(\Omega)} = O\left(k^{3.341} + h^{1.980}\left(1 + \frac{1}{|\ln h|}\right)\right)$$

These numerical results match the convergence rates as given in Theorem 3.6.

Table 3.9: Error estimates in L^2-norm for Example 6

h	Error ($k = 0.04$)	k	Error ($h = 0.0633621$)
0.287138	2.56400×10^{-2}	0.4	1.28272×10^{-1}
0.181985	9.42931×10^{-3}	0.08	2.39792×10^{-2}
0.0950432	2.33584×10^{-3}	0.04	1.02274×10^{-3}
0.0633621	1.02274×10^{-3}	0.02	1.02271×10^{-3}
0.0475216	5.62814×10^{-4}	0.004	1.02271×10^{-3}

Table 3.10: Error estimates in L^2-norm for Example 7

h	Error ($k = 0.03125$)	k	Error ($h = 0.0285903$)
0.205602	1.08564×10^{-1}	0.5	7.17604×10^{-2}
0.110793	2.54235×10^{-2}	0.25	3.22750×10^{-2}
0.0568736	6.28146×10^{-3}	0.0625	1.60550×10^{-3}
0.037129	2.80833×10^{-3}	0.03125	1.58868×10^{-3}
0.0285903	1.58868×10^{-3}	0.0125	1.58764×10^{-3}

Table 3.11: Error estimates in L^2-norm for Example 8

h	Error ($k = 0.01$)	k	Error ($h = 0.048928$)
0.179911	2.54014×10^{-2}	0.05	3.12546×10^{-2}
0.0957657	6.43713×10^{-3}	0.025	7.27635×10^{-3}
0.0749228	4.20417×10^{-3}	0.016	3.27310×10^{-3}
0.0636832	2.95527×10^{-3}	0.01	1.71333×10^{-3}
0.048928	1.71333×10^{-3}	0.005	1.64282×10^{-3}

Chapter 4

APPROXIMATION BY SEM

In the previous chapter, we approximated the problem $(3.1.1) - (3.1.3)$ using piecewise linear functions on the elements with three nodes. In this chapter, we propose the use of higher order polynomials on the elements. Higher order polynomials require additional nodes on the elements. The additional nodes are selected in a way that prevents Runge phenomenon as the polynomial degree increases. The position of the interface is also put under consideration.

The error generated by the finite element method is directly connected to the regularity of the exact solution, thus, when the regularity of the solution is very low, the result obtained from spectral element method might not be different from other low-order methods (Timmermans *et al.*, 1994). We shall assume that the unknown function $u(t) \in X_d$, for $t \in (0, T)$ where

$$X_d = H^d(\Omega) \cap H^{d+1}(\Omega_1) \cap H^{d+1}(\Omega_2)$$

endowed with the norm

$$\|v\|_{X_d} = \|v\|_{H^d(\Omega)} + \|v\|_{H^{d+1}(\Omega_1)} + \|v\|_{H^{d+1}(\Omega_2)} \qquad \forall\, v \in X_d$$

$d \in \mathbb{N}$ is the degree of the polynomial. We write $X_1 = X$. We have the regularity estimate

Lemma 4.1 Suppose that the conditions of Assumption 1.1 are satisfied for every

$a : \Omega \times \mathbb{R} \to \mathbb{R}$, $f : \Omega \times \mathbb{R} \to \mathbb{R}$ and $g \in L^2(0, T; H^{1/2}(\Gamma) \cap H^{d+1}(\Gamma))$, there exists a constant C depending on μ_1, μ_2, μ_3, T and Ω such that for $u \in L^2(0, T; X_d)$,

$$\|u\|_{L^2(0,T;X_d)} \leq C \left(\|g\|_{L^2(0,T;H^{1/2}(\Gamma))} + \|u_0\|_{L^2(\Omega)} \right) \qquad d = 1, 2, \ldots, n_0 \qquad (4.0.1)$$

Proof The case has been proved for $d = 1$ (see Lemma 3.2). We use mathematical induction on d for the case $d > 1$. We need to show that

$$\|u\|_{L^2(0,T;H^{d+1}(\Omega_i))} \leq C \left[\|g\|_{L^2(0,T;H^{1/2}(\Gamma))} + \|u_0\|_{L^2(\Omega)} \right] \qquad i = 1, 2. \qquad (4.0.2)$$

For $d = 1$,

$$\|u\|_{L^2(0,T;H^2(\Omega_1))} \leq C \left[\|g\|_{L^2(0,T;H^{1/2}(\Gamma))} + \|u_0\|_{L^2(\Omega)} \right]$$

We assume (4.0.2) is true for $d = n$, i.e.

$$\|u\|_{L^2(0,T;H^{n+1}(\Omega_1))} \leq C \left[\|g\|_{L^2(0,T;H^{1/2}(\Gamma))} + \|u_0\|_{L^2(\Omega)} \right] \qquad (4.0.3)$$

Now,

$$
\begin{aligned}
\|u\|^2_{L^2(0,T;H^{n+2}(\Omega_1))} &= \int_0^T \int_{\Omega_1} \sum_{|\alpha| \leq n+2} |\partial^\alpha u|^2 \ dx \ dt \\
&= \int_0^T \int_{\Omega_1} \sum_{|\alpha| \leq n+1} |\partial^\alpha u|^2 + \sum_{|\alpha| = n+2} |\partial^\alpha u|^2 \ dx \ dt \\
&= \|u\|^2_{L^2(0,T;H^{n+1}(\Omega_1))} \\
&\quad + \int_0^T \int_{\Omega_1} \sum_{|\alpha| = n+1} \nabla(\partial^\alpha u) \cdot \nabla(\partial^\alpha u) \ dx \ dt \\
&= \|u\|^2_{L^2(0,T;H^{n+1}(\Omega_1))} \\
&\quad + \frac{1}{\mu_1} \int_0^T \int_{\Omega_1} \sum_{|\alpha| = n+1} a\nabla(\partial^\alpha u) \cdot \nabla(\partial^\alpha u) \ dx \ dt \qquad (4.0.4)
\end{aligned}
$$

Using (3.1.7) in (4.0.4), we have

$$
\begin{aligned}
\|u\|^2_{L^2(0,T;H^{n+2}(\Omega_1))} &= \|u\|^2_{L^2(0,T;H^{n+1}(\Omega_1))} + \frac{1}{\mu_1} \left[\int_0^T \int_{\Omega_1} f(x, \partial^\alpha u) \partial^\alpha u \right. \\
&\quad \left. - \int_{\Omega_1} (\partial^\alpha u_t)(\partial^\alpha u) + \int_\Gamma g\partial^\alpha u \ dt \right] \qquad |\alpha| = n + 1 \\
&\leq C \left(\|u\|^2_{L^2(0,T;H^{n+1}(\Omega_1))} + \|g\|^2_{L^2(0,T;H^{1/2}(\Gamma))} \right) \\
&\quad \|\partial^\alpha u_t\|_{L^2(0,T;H^{-1}(\Omega_1))} + \frac{1}{4} \|u\|^2_{L^2(0,T;H^{n+2}(\Omega_1))} \qquad (4.0.5)
\end{aligned}
$$

We have made use of integration by parts, Cauchy and Young's inequalities in the last inequality with $|\alpha| = n$.

Using (3.1.5) and (4.0.3) in (4.0.5), we have

$$\|u\|_{L^2(0,T;H^{n+2}(\Omega_1))}^2 \leq C\left(\|g\|_{L^2(0,T;H^{1/2}(\Gamma))}^2 + \|u_0\|_{L^2(\Omega_1)}\right) \qquad (4.0.6)$$

Following a similar procedure as above,

$$\|u\|_{L^2(0,T;H^{n+2}(\Omega_2))}^2 \leq C\left(\|g\|_{L^2(0,T;H^{1/2}(\Gamma))}^2 + \|u_0\|_{L^2(\Omega_2)}\right) \qquad (4.0.7)$$

(4.0.1) follows from (3.1.2), (4.0.6) and (4.0.7).

4.1   Spectral Element Discretisation

$\mathfrak{T}_h$ denotes a partition of Ω into disjoint triangles K with Gauss-Lobatto-Legendre collocation points. Let $\mathfrak{T}_h^\star$ denote the set of all elements that are intersected by the interface Γ;

$$\mathfrak{T}_h^\star = \{K \in \mathfrak{T}_h : K \cap \Gamma \neq \phi\}$$

$K \in \mathfrak{T}_h^\star$ is called an interface element and we write $\Omega_h^\star = \bigcup_{K \in \mathfrak{T}_h^\star} K$.

The triangulation $\mathfrak{T}_h$ of the domain Ω satisfies the following conditions

(i) $\bar{\Omega} = \bigcup_{K \in \mathfrak{T}_h} \bar{K}$

(ii) If $\bar{K}_1, \bar{K}_2 \in \mathfrak{T}_h$ and $\bar{K}_1 \neq \bar{K}_2$, then either $\bar{K}_1 \cap \bar{K}_2 = \emptyset$ or $\bar{K}_1 \cap \bar{K}_2$ is a common vertex or a common edge.

(iii) For any triangle $K \in \mathfrak{T}_h^\star$, we assume that Γ intersects K at most twice, and it intersects each (open) edge at most once. For $d \geq 2$, we assume some of the nodes fall on the interface (see Fig 4.1). However, if the triangulation could be fitted to the interface, then each $K \in \mathfrak{T}_h$ is either in Ω_1^h or Ω_2^h, and has at most two vertices lying on Γ_h (see Fig 4.2).

(iv) For each element $K \in \mathfrak{T}_h$, let r_K and $\bar{r}_K$ be the diameters of its inscribed and circumscribed circles respectively. It is assumed that, for some fixed $h_0 > 0$, there exists two positive constants C_0 and C_1, independent of h, such that

$$C_0 r_K \leq h \leq C_1 \bar{r}_K \quad \forall\, h \in (0, h_0)$$

For any interface element $K \in \mathfrak{T}_h^\star$, let $K_1 = K \cap \Omega_1$ and $K_2 = K \cap \Omega_2$, it was shown by Chen & Zou (1998) that

$$\text{either} \quad \text{meas}(K_1) \leq C h_K^3 \quad \text{or} \quad \text{meas}(K_2) \leq C h_K^3$$

It is clear from Fig 4.1 that the polynomial approximation of the interface function is one degree less than the polynomial approximation of the unknown function u on each element. However the polynomial approximation of the interface function is of the same degree with the polynomial approximation of the unknown function u on an element when the elements can be fitted exactly to the interface.

Let S_h^d denote the space of continuous piecewise polynomial functions of order $d \in \mathbb{N}$ on $\mathfrak{T}_h$ which vanish on $\partial\Omega$. S_h^d contains dth order Lagrangian polynomial through Gauss-Lobatto-Legendre (GLL) collocation points on each $K \in \mathfrak{T}_h$. The GLL points are clustered near the boundary, therefore Runge phenomenon is avoided. We ensure that the number of interpolation nodes per element is equal to that required to make dth degree polynomial with all the terms in x and y. This is necessary to ensure continuity across the element edges. See (Oden & Reddy 1976) for the details about our choice.

Let $\Pi_h : C(\bar{\Omega}) \to S_h^d$ be the Lagrange interpolation operator corresponding to the space S_h^d. As the solutions concerned are in $H^1(\Omega)$ globally, one cannot apply the standard interpolation theory directly. Thus for the interpolation Π_h, we have

Lemma 4.2 Let $\Pi_h : C(\bar{\Omega}) \to S_h^d$ be the interpolation operator, then for $m = 0, 1, \ldots, d$, $d \in \mathbb{N}$, $n \in \mathbb{R}^+$ $0 < h < d$, we have

$$\|u - \Pi_h u\|_{H^m(\Omega)} \leq C d \left(\frac{h}{d^n} \right)^{d+1-m} \left(1 + \frac{1}{|\ln \frac{h}{d}|} \right)^{1/2} \|u\|_{X_d} \qquad (4.1.1)$$

117
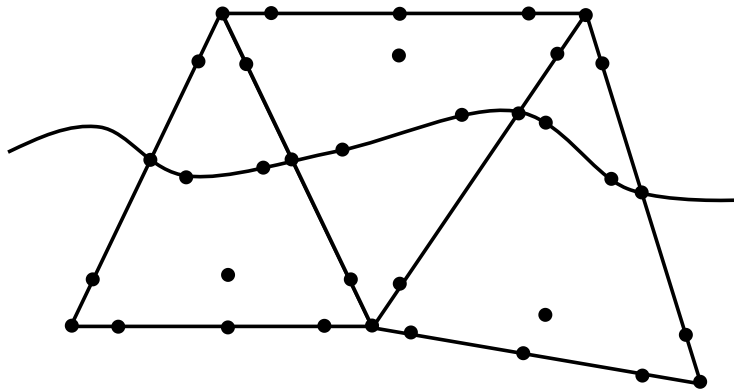
Figure 4.1: Typical unfitted interface elements
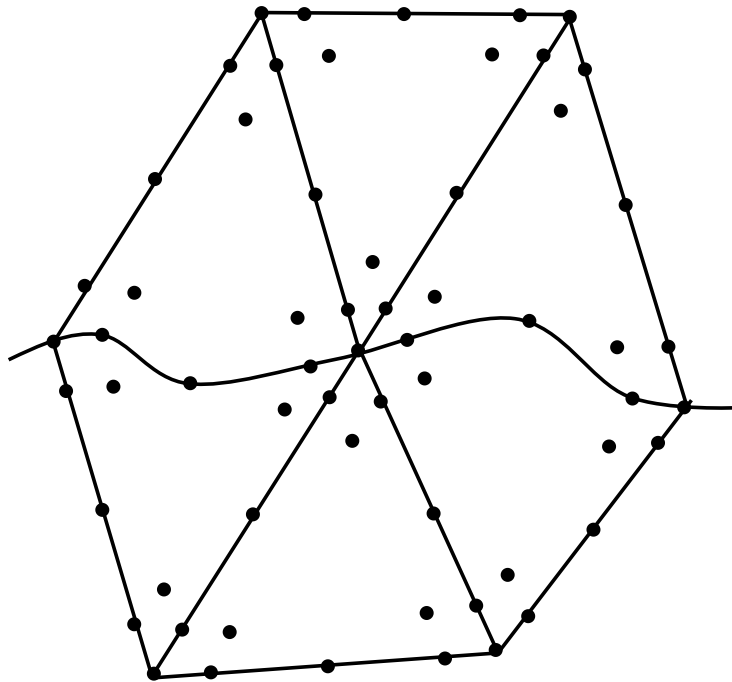
Figure 4.2: Typical interface elements with curved edges

118

Proof For any $u \in X_d$, let u_i be the restriction of u on Ω_i ($i = 1, 2$). As the interface is of class C^{d+1}, by extension theorem (Stein 1971 and Evans 1997), we can extend the function $u_i \in H^{d+1}(\Omega_i)$ onto the whole of Ω, and obtain the function $\tilde{u}_i \in H^{d+1}(\Omega)$ such that $\tilde{u}_i = u_i$ on Ω_i and

$$\|\tilde{u}_i\|_{H^{d+1}(\Omega)} \leq C \|u_i\|_{H^{d+1}(\Omega_i)} \qquad\qquad i = 1, 2 \qquad\qquad (4.1.2)$$

In the proof of Theorem 1.4,

$$|x_e^N - x| \leq h$$

where x_e^N is an interpolation point in the element while x is a variable point. However, without loss of generality, we can take x as a variable point in the h_d−neighbourhood of x_e^N such that

$$|x_e^N - x| \leq h_d$$

where h_d is the minimum distance between a node and its surrounding nodes. For any $K \in \mathfrak{T}_h \backslash \mathfrak{T}_h^*$, we have

$$\|u - \Pi_h u\|_{W^{m,p}(K)} \leq C \left(\frac{h}{d^n} \right)^{d+1-m} \|u\|_{W^{d+1,p}(K)}, \quad m = 0, 1, \ldots, d, \quad p \geq 1$$

$$(4.1.3)$$

The last inequality follows from (1.8.1) using the fact that $h_d \propto \dfrac{h}{d^n}$.

Now, for any element $K \in \mathfrak{T}_h^*$, using Hölder's inequality and the fact that $meas(K_1) \leq Ch^3$, we have

$$\|u - \Pi_h u\|_{H^m(K_1)}^2 \leq \sum_{|\alpha| \leq m} \|D^\alpha (u - \Pi_h u)\|_{L^2(K_1)}^2$$

$$\leq \left(\sum_{|\alpha| \leq m} \|D^\alpha (u - \Pi_h u)\|_{L^2(K_1)}^{2q'} \right)^{1/q'} [meas(K_1)]^{\frac{q'-1}{q'}}$$

Taking $p = 2q'$, we obtain

$$\|u - \Pi_h u\|^2_{H^m(K_1)} \leq [meas(K_1)]^{\frac{p-2}{p}} \left(\sum_{|\alpha| \leq m} \|D^\alpha(u - \Pi_h u)\|^p_{L^2(K_1)} \right)^{2/p}$$

$$\leq Ch^{3\left(\frac{p-2}{p}\right)} \left(\sum_{|\alpha| \leq m} \|D^\alpha(u - \Pi_h u)\|^p_{L^2(K_1)} \right)^{2/p} \quad \text{for} \quad p > 2$$

Therefore

$$\|u - \Pi_h u\|_{H^m(K_1)} \leq Ch^{3\left(\frac{p-2}{2p}\right)} \|u - \Pi_h u\|_{W^{m,p}(K_1)} \tag{4.1.4}$$

$$\leq Ch^{3\left(\frac{p-2}{2p}\right)} \|u - \Pi_h u\|_{W^{m,p}(K)}$$

Using (4.1.3),

$$\|u - \pi_h u\|_{H^m(K_1)} \leq Ch^{\frac{3p-6}{2p}} \left(\frac{h}{d^n} \right)^{d-m} \|u\|_{W^{d,p}(K)}, \quad \text{for any} \ p > 2, \ m = 0, 1, \ldots, d,$$

Recall the Sobolev embedding inequality for two dimensions [Ren & Wei (1994)]

$$\|\phi\|_{L^p(\Omega_i)} \leq Cp^{1/2} \|\phi\|_{H^1(\Omega_i)} \quad \forall \ p > 2, \ \phi \in H^1(\Omega_i), \ i = 1, 2$$

therefore,

$$\|u - \Pi_h u\|_{H^m(K_1)} \leq Ch^{\frac{3p-6}{2p}} \left(\frac{h}{d^n} \right)^{d-m} p^{1/2} \|u\|_{H^{d+1}(K)} \quad \text{for any} \ p > 2, \ m = 0, 1, \ldots, d$$

$$\tag{4.1.5}$$

By means of extensions (4.1.2),

$$\|u - \Pi_h u\|_{H^m(K_2)} \leq \|u - \Pi_h u\|_{H^m(K)}$$

$$\leq C \left(\frac{h}{d^n} \right)^{d+1-m} \|u\|_{H^{d+1}(K)}, \quad m = 0, 1, \ldots, d \tag{4.1.6}$$

It follows from (4.1.5) and (4.1.6) that

$$\sum_{K \in \mathcal{T}_h^*} \|u - \pi_h u\|^2_{H^m(K)} \leq C \left(\frac{h}{d^n} \right)^{2d+2-2m} \left[1 + pd^2 h^{1-6/p} \right] \|u\|^2_{X_d} \tag{4.1.7}$$

120

From (4.1.3) and (4.1.7), we have for $m = 0, 1, \ldots, d$ and $p > 2$

$$\|u - \Pi_h u\|^2_{H^m(\Omega)} \leq C \left(\frac{h}{d^n} \right)^{2d+2-2m} \|u\|^2_{X_d} + C \left(\frac{h}{d^n} \right)^{2d+2-2m} pd^2 h^{1-6/p} \|u\|^2_{X_d}$$

Since $p > 2$, we take

$$p = 2 \left(1 + \frac{1}{|\ln \frac{h}{d}|} \right) > 2 \qquad \text{for} \ \ 0 < h < d, \quad d \in \mathbb{N}$$

and (4.1.1) follows.

It was assumed in the proof of the above theorem that the triangulation does not fit the interface, however, it is possible to have a triangulation that fit (perfectly or almost perfectly) the interface. This could be achieved using curve interface elements or by making the interface elements small enough such that $\Omega^\star \subset \Omega_0$ (where Ω_0 is some neighbourhood of Γ). We therefore have

Remark 4.1 It was assumed that $u \in X_d$ in Lemma 4.2. However if
$u \in X_d \cap W^{d,\infty}(\Omega_0 \cap \Omega_1) \cap W^{d,\infty}(\Omega_0 \cap \Omega_2)$, then we have for $d \in \mathbb{N}$, $0 < h < d$, and
$m = 0, 1, \ldots, d$

$$\|u - \Pi_h u\|_{H^m(\Omega)} \leq Cd \left(\frac{h}{d^n} \right)^{d+1-m} \left\{ \|u\|_{X_d} + \|u\|_{W^{d,\infty}(\Omega_0 \cap \Omega_1)} + \|u\|_{W^{d,\infty}(\Omega_0 \cap \Omega_2)} \right\}$$
$$(4.1.8)$$

Proof For any element $K \in \mathfrak{T}_h^*$, using Hölder's inequality and the fact that $meas(K_2) \leq Ch^2$, we have

$$
\begin{aligned}
\|u - \Pi_h u\|^2_{H^m(K_2)} &\leq \sum_{|\alpha| \leq m} \|D^\alpha(u - \Pi_h u)\|^2_{L^2(K_2)} \\
&\leq [meas(K_2)]^{\frac{p-2}{p}} \left(\sum_{|\alpha| \leq m} \|D^\alpha(u - \Pi_h u)\|^p_{L^2(K_2)} \right)^{2/p} \\
&\leq Ch_\star^{2\left(\frac{p-2}{p}\right)} \left(\sum_{|\alpha| \leq m} \|D^\alpha(u - \Pi_h u)\|^p_{L^2(K_2)} \right)^{2/p} \qquad \text{for} \ \ p > 2
\end{aligned}
$$

Where $h_\star = \max_{K \in \mathfrak{T}_h^\star} h_K$. Therefore

$$\|u - \Pi_h u\|_{H^m(K_2)} \leq Ch_\star^{\left(\frac{p-2}{p}\right)} \|u - \Pi_h u\|_{W^{m,p}(K_2)} \qquad (4.1.9)$$

121

From (4.1.3), (4.1.4) and (4.1.9), we have

$$
\begin{aligned}
\|u - \Pi_h u\|^2_{H^m(\Omega)} &\leq C \left(\frac{h}{d^n} \right)^{2d+2-2m} \|u\|^2_{X_d} \\
&\quad + C h_\star^{2-6/p} \left(\frac{h_\star}{d} \right)^{2d-2m} \sum_{K \in \mathfrak{T}_h^*} \left\{ h_\star \|u\|^2_{W^{d,p}(K_1)} + h_\star^{2/p} \|u\|^2_{W^{d,p}(K_2)} \right\} \\
&\leq C \left(\frac{h}{d^n} \right)^{2d+2-2m} \|u\|^2_{X_d} \\
&\quad + C h_\star^{2-6/p} \left(\frac{h_\star}{d} \right)^{2d-2m} \sum_{K \in \mathfrak{T}_h^*} \left\{ h_\star \|u\|^2_{W^{d,p}(K \cap \Omega_1)} + h_\star^{2/p} \|u\|^2_{W^{d,p}(K \cap \Omega_2)} \right\} \\
&\leq C d^2 \left(\frac{h}{d^n} \right)^{2d+2-2m} \Big[\|u\|^2_{X_d} \\
&\quad + h_\star^{-6/p} \left(h_\star \|u\|^2_{W^{d,p}(\Omega_h^* \cap \Omega_1)} + h_\star^{2/p} \|u\|^2_{W^{d,p}(\Omega_h^* \cap \Omega_2)} \right) \Big] \\
&\leq C d^2 \left(\frac{h}{d^n} \right)^{2d+2-2m} \Big[\|u\|^2_{X_d} \\
&\quad + h_\star^{-6/p} \left(h_\star \|u\|^2_{W^{d,p}(\Omega_0 \cap \Omega_1)} + h_\star^{2/p} \|u\|^2_{W^{d,p}(\Omega_0 \cap \Omega_2)} \right) \Big]
\end{aligned}
$$

For $h_\star$ sufficiently small such that $\Omega_h^* \subset \Omega_0$,

$$
\begin{aligned}
\|u - \Pi_h u\|^2_{H^m(\Omega)} &\leq C d^2 \left(\frac{h}{d^n} \right)^{2d+2-2m} \Big[\|u\|^2_{X_d} \\
&\quad + h_\star^{-4/p} \left(\|u\|^2_{W^{d,p}(\Omega_0 \cap \Omega_1)} + \|u\|^2_{W^{d,p}(\Omega_0 \cap \Omega_2)} \right) \Big] \quad (4.1.10)
\end{aligned}
$$

For $i = 1, 2$,

$$
\begin{aligned}
\|u\|^p_{W^{d,p}(\Omega_0 \cap \Omega_i)} &= \sum_{|\alpha| \leq d} \|D^\alpha u\|^p_{L^p(\Omega_0 \cap \Omega_i)} \\
&\leq \sum_{|\alpha| \leq d} meas(\Omega_0 \cap \Omega_i) \|D^\alpha u\|^p_{L^\infty(\Omega_0 \cap \Omega_i)} \\
&\leq meas(\Omega_0 \cap \Omega_i) \sum_{|\alpha| \leq d} \max_{|\alpha| \leq d} \|D^\alpha u\|^p_{L^\infty(\Omega_0 \cap \Omega_i)} \\
&= meas(\Omega_0 \cap \Omega_i) \|u\|^p_{W^{d,\infty}(\Omega_0 \cap \Omega_i)} \\
\therefore \|u\|_{W^{d,p}(\Omega_0 \cap \Omega_i)} &\leq C^{1/p} \|u\|_{W^{d,\infty}(\Omega_0 \cap \Omega_i)}
\end{aligned}
$$

122

This together with (4.1.10) implies that

$$
\begin{aligned}
\|u - \Pi_h u\|^2_{H^m(\Omega)} \quad \leq \quad & Cd^2 \left(\frac{h}{d^n} \right)^{2d+2-2m} \Big[\|u\|^2_{X_d} \\
& + C^{2/p} h_\star^{-4/p} \left(\|u\|^2_{W^{d,\infty}(\Omega_0 \cap \Omega_1)} + \|u\|^2_{W^{d,\infty}(\Omega_0 \cap \Omega_2)} \right) \Big]
\end{aligned}
$$

(4.1.8) follows as $p \to \infty$.

For computational simplicity, we present the analysis and computation for the case where the spatial discretisation can be fitted exactly to the interface with the use of interface elements with curved edges along the interface (see Fig 4.2). Similar estimates could be obtained for unfitted spatial discretisation.

4.2 Convergence Rate

The time discretisation is based on backward difference approximations. We obtain an error estimate of optimal order in the L^2-norm.

The interval [0,T] is divided into M equally spaced (for simplicity) subintervals:

$$
0 = t_0 < t_1 < \ldots < t_M = T
$$

with $t_n = nk$, $k = T/M$ being the time step. Let the function U_h^n be defined by $U_h^n = U_h(x, t_n)$, $\forall\ t_n \in (0, T]$, $n = 1, 2, \ldots, M$. For a given sequence $\{w_n\}_{n=0}^M \subset L^2(\Omega)$, we have the backward difference quotient defined by

$$
\partial_k w^n = \frac{w^n - w^{n-1}}{k}
$$

The linearized fully discrete spectral element approximation to (3.1.1) is defined as follows:

Let $U_h^0 = \Pi_h u_0$, find $U_h^n \in S_h^d$, for $n = 1, 2, \ldots, M$, such that

$$
(\partial_k U_h^n, v_h)_h + A(U_h^{n-1} : U_h^n, v_h) = (f(x, U_h^{n-1}), v_h) + \langle g_h^n, v_h \rangle_\Gamma \quad \forall\ v_h \in S_h^d \quad (4.2.1)
$$

The main result of this chapter is stated below:

Theorem 4.1 Let u and U_h^n be the solutions of (3.1.1) and (4.2.1) respectively. Suppose that the conditions of Assumption 1.1 are satisfied for every $a : \Omega \times \mathbb{R} \to \mathbb{R}$, $f : \Omega \times \mathbb{R} \to \mathbb{R}$ and $g \in L^2(0, T; H^{d+1}(\Gamma))$. There exists a positive constant C independent of h and k such that

$$
\|u - U_h^n\|_{L^2(\Omega)} \leq \left[d \left(\frac{h}{d^n} \right)^{d+1} + k \right] C(u, g)
$$

where

$$
C(u, g) = \left\{ B(u_0) + \int_0^{t_n} \left(B(u) + B(u_t) + \|u_{tt}\|_{L^2(\Omega)}^2 + \|g\|_{H^{d+1}(\Gamma)}^2 \right) dt \right\}^{1/2}
$$

The proof of this result requires some necessary preparations.

Lemma 4.3 Assume that $g \in H^{1+d}(\Gamma)$, $\nu_h, \omega_h \in S_h^d$ for $t \in (0, T]$. Then we have

$$
|\langle g, v_h \rangle_\Gamma - \langle g_h, v_h \rangle_\Gamma| \leq Cd \left(\frac{h}{d^n} \right)^{d+1} \|g\|_{H^{d+1}(\Gamma)} \|v_h\|_{L^2(\Omega)} \quad (4.2.2)
$$

$$
|A(u : \nu_h, \omega_h) - A(u_h : \nu_h, \omega_h)| \leq \mu_3 \|\nabla \nu_h\|_{L^\infty(\Omega)} \|u - u_h\|_{L^2(\Omega)} \|\omega_h\|_{H^1(\Omega)} \quad (4.2.3)
$$

$$
|(f(x, u), v_h) - (f(x, u_h), v_h)| \leq \mu_3 \|u - u_h\|_{L^2(\Omega)} \|v_h\|_{L^2(\Omega)} \quad (4.2.4)
$$

Proof Since g_h is the interpolant of g along the interface, we can use (4.1.8)

$$
\begin{aligned}
|\langle g, v_h \rangle_\Gamma - \langle g_h, v_h \rangle_\Gamma| &= |\langle g - g_h, v_h \rangle_\Gamma| \\
&\leq \|g - g_h\|_{L^2(\Gamma)} \|v_h\|_{L^2(\Gamma)} \\
&\leq Cd \left(\frac{h}{d^n} \right)^{d+1} \|g\|_{H^{d+1}(\Gamma)} \|v_h\|_{L^2(\Omega)}
\end{aligned}
$$

For (4.2.3), we have

$$
\begin{aligned}
|A(u : \nu_h, \omega_h) - A(u_h : \nu_h, \omega_h)| &\leq \sum_{K \in \mathfrak{T}_h} \int_K |a(x, u) - a(x, u_h)| |\nabla \nu_h \cdot \nabla \omega_h| \\
&\leq \mu_3 \sum_{K \in \mathfrak{T}_h} \int_K |u - u_h| |\nabla \nu_h| |\nabla \omega_h| \\
&\leq \mu_3 \|\nabla \nu_h\|_{L^\infty(\Omega)} \|u - u_h\|_{L^2(\Omega)} \|\nabla \omega_h\|_{L^2(\Omega)} \\
&\leq \mu_3 \|\nabla \nu_h\|_{L^\infty(\Omega)} \|u - u_h\|_{L^2(\Omega)} \|\omega_h\|_{H^1(\Omega)}
\end{aligned}
$$

124

For (4.2.4), we have

$$
\begin{aligned}
|(f(x,u),v_h) - (f(x,u_h),v_h)| &\leq \sum_{K\in\mathfrak{T}_h} \int_K |f(x,u) - f(x,u_h)||v_h| \\
&\leq \mu_3 \sum_{K\in\mathfrak{T}_h} \int_K |u - u_h||v_h| \\
&\leq \mu_3 \|u - u_h\|_{L^2(\Omega)} \|v_h\|_{L^2(\Omega)}
\end{aligned}
$$

Let $R_h : X \cap H^1(\Omega) \to S_h^d$ be the elliptic projection of the exact solution u in S_h^d defined by

$$A(u : R_h\nu - \nu, \phi) = 0 \quad \forall\, \phi \in S_h^d,\ t \in [0,T] \tag{4.2.5}$$

For this projection, we have

Lemma 4.4 Let u be a smooth function in $\Omega \times T$ and $a = a(x,u)$ satisfies Assumption 1.1. Assume that $u \in X \cap H_0^1$ and let $R_h u$ be defined as in (4.2.5), then

$$\|R_h u - u\|_{L^2(\Omega)} + \frac{h}{d^n}\|R_h u - u\|_{H^1(\Omega)} \leq d\left(\frac{h}{d^n}\right)^{d+1} C(u)$$

Proof By the definition of R_h, we have

$$
\begin{aligned}
\mu_1 \|R_h u - u\|_{H^1(\Omega)}^2 &\leq A(u : R_h u - u, R_h u - u) \\
&= A(u : R_h u - u, R_h u - \phi) + A(u : R_h u - u, \phi - u), \quad \phi \in S_h^d \\
&\leq \mu_2 \|R_h u - u\|_{H^1(\Omega)} \|\phi - u\|_{H^1(\Omega)}
\end{aligned}
$$

Using (4.1.8) with $\phi = \Pi_h u$, we have

$$\|R_h u - u\|_{H^1(\Omega)} \leq Cd\left(\frac{h}{d^n}\right)^d \left\{ \|u\|_{X_d} + \|u\|_{W^{d,\infty}(\Omega_0\cap\Omega_1)} + \|u\|_{W^{d,\infty}(\Omega_0\cap\Omega_2)} \right\} \tag{4.2.6}$$

Now consider the dual problem

$$-\nabla \cdot (a(x,u)\nabla\psi) = R_h u - u \qquad \text{in } \Omega,\ \psi = 0 \text{ on } \partial\Omega$$

whose weak form is

$$A(u : \psi, \phi) = (R_h u - u, \phi) \quad \forall\, \phi \in H_0^1(\Omega) \tag{4.2.7}$$

Now, it follows from (4.2.5) that

$$
\begin{aligned}
\|R_h u - u\|_{L^2(\Omega)}^2 &= A(u : R_h u - u, \psi) \\
&= A(u : R_h u - u, \psi - \phi) + A(u : R_h u - u, \phi) \quad \phi \in S_h^d \\
&\leq C\|P_h u - u\|_{H^1(\Omega)}\|\psi - \phi\|_{H^1(\Omega)}
\end{aligned}
$$

Take $\phi = \Pi_h \psi$ and use (4.1.8)

$$\|R_h u - u\|_{L^2(\Omega)}^2 \leq d\left(\frac{h}{d^n}\right)^{d+1} D_d(u) D_1(\psi) \tag{4.2.8}$$

but

$$D_1(\psi) \leq C\|R_h u - u\|_{L^2(\Omega)} \tag{4.2.9}$$

See Appendix B for (4.2.9).

Lemma 4.4 follows from (4.2.6), (4.2.8)

Lemma 4.5 Let u be a smooth function in $\Omega \times T$ and $a = a(x, u)$ satisfies Assumption 1.1. Assume that $u \in X \cap H_0^1$ and let $R_h u$ be defined as in (4.5), then

$$\|(R_h u - u)_t\|_{L^2(\Omega)} + \frac{h}{d^n}\|(R_h u - u)_t\|_{H^1(\Omega)} \leq d\left(\frac{h}{d^n}\right)^{d+1} [D_d(u) + D_d(u_t)]$$

Proof Let $\xi = R_h u - u$, and assume that a_t is uniformly bounded. Following the argument of Thomme (2006), we have

$$
\begin{aligned}
\rho\|\xi_t\|_{H^1(\Omega)}^2 &\leq A(u : \xi_t, \xi_t) \\
&= A(u : \xi_t, \phi - u_t) + A(u : \xi_t, (R_h u)_t - \phi) \\
&= A(u : \xi_t, \phi - u_t) + \int_\Omega \left[\frac{\partial}{\partial t}(a\nabla\xi) - \frac{\partial a}{\partial t}\nabla\xi\right] \cdot \nabla((R_h u)_t - \phi)\, dx \\
&\leq \|\xi_t\|_{H^1(\Omega)}\|\phi - u_t\|_{H^1(\Omega)} + \|\xi\|_{H^1(\Omega)}\|(R_h u)_t - \phi\|_{H^1(\Omega)}
\end{aligned}
$$

Take $\phi = \Pi_h u_t$. Using Lemma 4.5 and Young's inequality, we obtain

$$\|(P_h u - u)_t\|_{H^1(\Omega)} \leq d\left(\frac{h}{d^n}\right)^d [D_d(u) + D_d(u_t)] \tag{4.2.10}$$

126

Following the duality argument $(4.2.7) - (4.2.9)$, we have

$$\|(P_h u - u)_t\|^2_{L^2(\Omega)} \leq d \left(\frac{h}{d^n}\right)^{d+1} [D_d(u) + D_d(u_t)]$$

Proof of Theorem 4.1 We establish this using error splitting technique.
Let $z^n = R_h u^n - U_h^n$, then

$$
\begin{aligned}
(\partial_k z^n, v_h) &+ A(U_h^{n-1} : z^n, v_h) \\
&= (\partial_k R_h u^n, v_h) - (\partial_k U_h^n, v_h) + A(U_h^{n-1} : R_h u^n, v_h) - A(U_h^{n-1} : U_h^n, v_h) \\
&= (\partial_k R_h u^n, v_h) - (f(x, U_h^{n-1}), v_h) - \langle g_h^n, v_h \rangle_\Gamma + A(U_h^{n-1} : R_h u^n, v_h) \\
&\quad - A(u^n : R_h u^n - u^n, v_h) \\
&= (\partial_k R_h u^n, v_h) + A(U_h^{n-1} : R_h u^n, v_h) - A(u^n : R_h u^n, v_h) \\
&\quad + (f(x, u^n), v_h) - (f(x, U_h^{n-1}), v_h) + \langle g^n, v_h \rangle_\Gamma - \langle g_h^n, v_h \rangle_\Gamma \\
&\quad - (u_t^n, v_h) \\
&= (\partial_k(R_h u^n - u^n), v_h) + A(U_h^{n-1} : R_h u^n, v_h) - A(u^n : R_h u^n, v_h) \\
&\quad + (f(x, u^n), v_h) - (f(x, U_h^{n-1}), v_h) + \langle g^n, v_h \rangle_\Gamma - \langle g_h^n, v_h \rangle_\Gamma \\
&\quad + (\partial_k u^n - u_t^n, v_h) \\
&= D_1 + D_2 + D_3 \quad\quad\quad\quad\quad\quad\quad\quad\quad\quad\quad\quad\quad (4.2.11)
\end{aligned}
$$

where

$$
\begin{aligned}
D_1 &= (\partial_k(R_h u^n - u^n), v_h) + (\partial_k u^n - u_t^n, v_h) \\
D_2 &= A(U_h^{n-1} : R_h u^n, v_h) - A(u^n : R_h u^n, v_h) \\
D_3 &= (f(x, u^n), v_h) - (f(x, U_h^{n-1}), v_h) + \langle g^n, v_h \rangle_\Gamma - \langle g_h^n, v_h \rangle_\Gamma
\end{aligned}
$$

Now, using Young's inequality with $v_h = z^n$, we obtain

$$
\begin{aligned}
D_1 &\leq \|\partial_k(R_h u^n - u^n)\|_{L^2(\Omega)}\|z^n\|_{L^2(\Omega)} + \|\partial_k u^n - u_t^n\|_{L^2(\Omega)}\|z^n\|_{L^2(\Omega)} \\
&\leq 2\|\partial_k(P_h u^n - u^n)\|^2_{L^2(\Omega)} + \frac{1}{4}\|z^n\|^2_{L^2(\Omega)} + 2\|\partial_k u^n - u_t^n\|^2_{L^2(\Omega)} \quad (4.2.12)
\end{aligned}
$$

Using Young's inequality, and Lemma 4.3, we obtain

$$
\begin{aligned}
D_2 \;\leq\;& \mu_3 \|\nabla R_h u^n\|_{L^\infty(\Omega)} \|U_h^{n-1} - u^n\|_{L^2(\Omega)} \|z^n\|_{H^1(\Omega)} \\
\leq\;& C\|z^{n-1}\|_{L^2(\Omega)} \|z^n\|_{H^1(\Omega)} + C\|R_h u^{n-1} - u^{n-1}\|_{L^2(\Omega)} \|z^n\|_{H^1(\Omega)} \\
& + C\|u^{n-1} - u^n\|_{L^2(\Omega)} \|z^n\|_{H^1(\Omega)} \\
\leq\;& \gamma C \left(\|z^{n-1}\|_{L^2(\Omega)}^2 + \|R_h u^{n-1} - u^{n-1}\|_{L^2(\Omega)}^2 + k^2 \|\partial_k u^n\|_{L^2(\Omega)}^2 \right) \\
& + \frac{3}{8\gamma} \|z^n\|_{H^1(\Omega)}^2 \tag{4.2.13}
\end{aligned}
$$

Using Lemma 4.3,

$$
\begin{aligned}
D_3 \;\leq\;& \mu_3 \|u^n - U_h^{n-1}\|_{L^2(\Omega)} \|z^n\|_{L^2(\Omega)} + Cd \left(\frac{h}{d^n} \right)^{d+1} \|g^n\|_{H^{d+1}(\Gamma)} \|z^n\|_{L^2(\Omega)} \\
\leq\;& C \left(\|z^{n-1}\|_{L^2(\Omega)}^2 + \|R_h u^{n-1} - u^{n-1}\|_{L^2(\Omega)}^2 + k^2 \|\partial_k u^n\|_{L^2(\Omega)}^2 \right) \\
& + Cd^2 \left(\frac{h}{d^n} \right)^{2d+2} \|g^n\|_{H^{d+1}(\Gamma)}^2 + \frac{1}{4} \|z^n\|_{L^2(\Omega)}^2 \tag{4.2.14}
\end{aligned}
$$

Substituting $(4.2.12) - (4.2.14)$ into $(4.2.11)$, we have

$$
\begin{aligned}
\frac{1}{k} \|z^n\|_{L^2(\Omega)}^2 + \mu_1 \|\nabla z^n\|_{L^2(\Omega)}^2 \;\leq\;& \frac{1}{k} \|z^n\|_{L^2(\Omega)} \|z^{n-1}\|_{L^2(\Omega)} + 2\|\partial_k(R_h u^n - u^n)\|_{L^2(\Omega)}^2 \\
& + \frac{1}{2} \|z^n\|_{L^2(\Omega)}^2 + C\|z^{n-1}\|_{L^2(\Omega)}^2 + 2\|\partial_k u^n - u_t^n\|_{L^2(\Omega)}^2 \\
& + C \left(\|R_h u^{n-1} - u^{n-1}\|_{L^2(\Omega)}^2 + k^2 \|\partial_k u^n\|_{L^2(\Omega)}^2 \right) \\
& + \frac{3}{8\gamma} \|z^n\|_{H^1(\Omega)}^2 + Cd^2 \left(\frac{h}{d^n} \right)^{2d+2} \|g^n\|_{H^{d+1}(\Gamma)}^2
\end{aligned}
$$

With $\gamma = \dfrac{3}{8\mu_1}$, we obtain

$$
\begin{aligned}
(1 - Ck)\|z^n\|_{L^2(\Omega)}^2 \;\leq\;& C\|z^{n-1}\|_{L^2(\Omega)}^2 + C \Big[k\|\partial_k(R_h u^n - u^n)\|_{L^2(\Omega)}^2 \\
& + k\|\partial_k u^n - u_t^n\|_{L^2(\Omega)}^2 + k\|R_h u^{n-1} - u^{n-1}\|_{L^2(\Omega)}^2 \\
& + k^3 \|\partial_k u^n\|_{L^2(\Omega)}^2 \Big] + Ckd^2 \left(\frac{h}{d^n} \right)^{2d+2} \|g^n\|_{H^{d+1}(\Gamma)}^2
\end{aligned}
$$

For k sufficiently small, there exist a constant C such that $(1 - ck)^{-1} \leq C$ and therefore,

$$
\begin{aligned}
\|z^n\|_{L^2(\Omega)}^2 \quad \leq \quad & C\|z^{n-1}\|_{L^2(\Omega)}^2 + C\Big[k\|\partial_k(R_h u^n - u^n)\|_{L^2(\Omega)}^2 \\
& + k\|\partial_k u^n - u_t^n\|_{L^2(\Omega)}^2 + k\|R_h u^{n-1} - u^{n-1}\|_{L^2(\Omega)}^2 \\
& + k^3\|\partial_k u^n\|_{L^2(\Omega)}^2\Big] + Ckd^2\left(\frac{h}{d^n}\right)^{2d+2}\|g^n\|_{H^{d+1}(\Gamma)}^2
\end{aligned}
$$

for $n = 1, \ldots, M$.

By iteration on n, we have

$$
\begin{aligned}
\|z^n\|_{L^2(\Omega)}^2 \quad \leq \quad & C\|z^0\|_{L^2(\Omega)}^2 + Ck\sum_{j=1}^{n}\|\partial_k(R_h u^j - u^j)\|_{L^2(\Omega)}^2 \\
& + Cd^2\left(\frac{h}{d^n}\right)^{2d+2}k\sum_{j=1}^{n}\left(\|g^j\|_{H^{d+1}(\Gamma)}^2\right) + Ck^3\sum_{j=1}^{n}\|\partial_k u^j\|_{L^2(\Omega)}^2 \\
& + Ck\sum_{j=1}^{n}\left(\|\partial_k u^j - u_t^j\|_{L^2(\Omega)}^2 + \|R_h u^{j-1} - u^{j-1}\|_{L^2(\Omega)}^2\right) \\
\leq \quad & C\|z^0\|_{L^2(\Omega)}^2 + Ck\sum_{j=1}^{n}\Big[\|\partial_k(R_h u^j - u^j)\|_{L^2(\Omega)}^2 + \|\partial_k u^j - u_t^j\|_{L^2(\Omega)}^2 \\
& + k^2\|\partial_k u^j\|_{L^2(\Omega)}^2 + d^2\left(\frac{h}{d^n}\right)^{2d+2}\left(B(u^{j-1}) + \|g^j\|_{H^{d+1}(\Gamma)}^2\right)\Big] \\
\leq \quad & C\|z^0\|_{L^2(\Omega)}^2 + C\int_0^{t_n}\Big[\|(R_h u - u)_t\|_{L^2(\Omega)}^2 + k^2\|u_{tt}\|_{L^2(\Omega)}^2 \\
& + k^2\|u_t\|_{L^2(\Omega)}^2 + d^2\left(\frac{h}{d^n}\right)^{2d+2}\left(B(u) + \|g\|_{H^{d+1}(\Gamma)}^2\right)\Big]\,dt
\end{aligned}
$$

Where $B(\xi) = \|\xi\|_{X_d}^2 + \|\xi\|_{W^{d,\infty}(\Omega_0 \cap \Omega_1)}^2 + \|\xi\|_{W^{d,\infty}(\Omega_0 \cap \Omega_2)}^2$. Therefore

$$
\begin{aligned}
\|z^n\|_{L^2(\Omega)}^2 \quad \leq \quad & C\|z^0\|_{L^2(\Omega)}^2 + C\int_0^{t_n}\Big[k^2\left(\|u_t\|_{L^2(\Omega)}^2 + \|u_{tt}\|_{L^2(\Omega)}^2\right) \\
& + d^2\left(\frac{h}{d^n}\right)^{2d+2}\left(B(u) + B(u_t) + \|g\|_{H^{d+1}(\Gamma)}^2\right)\Big]\,dt
\end{aligned}
$$

With $U_h^0 = \Pi_h u_0$, we have

$$
\begin{aligned}
\|z^n\|_{L^2(\Omega)}^2 \;\leq\; & Ck^2 \int_0^{t_n} \left(\|u_t\|_{L^2(\Omega)}^2 + \|u_{tt}\|_{L^2(\Omega)}^2 \right) dt \\
& + Cd^2 \left(\frac{h}{d^n} \right)^{2d+2} \left[B(u_0) + \int_0^{t_n} \left(B(u) + B(u_t) + \|g\|_{H^{d+1}(\Gamma)}^2 \right) dt \right]
\end{aligned}
$$

Theorem 4.1 follows using triangle inequality.

4.2.1 SE Numerical Experiment

The result of the spectral element error estimate is verified using globally continuous piecewise polynomials on the quasi-uniform triangulation described in section 4.1. The mesh parameter $h = \max_{K \in \mathfrak{T}_h} h_K$ where h_K is the longest side of an element $K \in \mathfrak{T}_h$.

We represent the solution as $u_h(x,t) = \sum_{j=1}^{N_h} \alpha_j(t)\phi_j(x)$, where each basis function ϕ_j, $(j = 1, 2, \ldots, N_h)$ is a polynomial function with unit height and zeros at GLL points.

For the approximation $g(x,t)$, let $\{z_j\}_{j=1}^{n_h}$ be the set of all nodes of the triangulation $\mathfrak{T}_h$ that lie on the interface Γ and $\{\psi_j\}_{j=1}^{n_h}$ be the Legendre polynomials corresponding to GLL points $\{z_j\}_{j=1}^{n_h}$ in the space S_h^d.

The iterative scheme for (4.2.1) could be expressed as

$$
(U_h^n - U_h^{n-1}, v_h) + k(a(x, U_h^{n-1})\nabla U_h^n, \nabla v_h) = k(f(x, U_h^{n-1}), v_h) + k\langle g_h, v_h \rangle_\Gamma
$$
$$
v_h \in S_h^d, \; n = 1, 2, \ldots
$$
$$
(4.2.15)
$$

The mesh generation and computation are done in Nektar++ (Cantwell *et al.*, 2015) environments.

Example 1 We consider the Advection-Diffusion equation

$$
\frac{\partial u}{\partial t} = \nabla \cdot (D\nabla u) - \nabla \cdot (\vec{v}u) + R \tag{4.2.16}
$$

where

u = the variable of interest which could be mass transfer (for species concentration) or temperature (for heat transfer)

D = mass diffusivity (for particle motion) or thermal diffusivity (for heat transfer)

$\vec{v}$ = the average velocity of the quantity. For example, where u is the concentration of the salt in a river, then $\vec{v}$ would be the velocity of the water flow.

R = the sources or sinks of the quantity u. For heat transfer for example, $R > 0$ means the thermal energy is being generated (possibly by friction).

Obviously, (4.2.16) is a PDE of practical interest and of the form (1.5.1). Consider (4.2.16) in $\Omega = (-1, 1) \times (-1, 1)$. The interface $\Gamma = \bar{\Omega}_1 \cap \bar{\Omega}_2$ occurs at $y = 0$ where $\Omega_1 = (-1, 1) \times (-1, 0)$, $\Omega_2 = (-1, 1) \times (0, 1)$. We choose a problem with a known solution as follows:

$$u = \begin{cases} e^{-0.1t} \sin \pi x \sin \pi y & \text{in} \quad \Omega_1 \times (0, 10] \\ e^{-0.01t} \sin \pi x \sin \pi y & \text{in} \quad \Omega_2 \times (0, 10] \end{cases} \qquad (4.2.17)$$

The source function f, interface function g and the initial data u_0 are determined from the choice of u with

$$D = \begin{cases} \dfrac{1}{20\pi^2} & \text{in} \quad \Omega_1 \times (0, 10] \\ \dfrac{1}{200\pi^2} & \text{in} \quad \Omega_2 \times (0, 10] \end{cases} \qquad (4.2.18)$$

131

Table 4.1: Error estimates in L^2-norm for the test problem $(4.2.16) - (4.2.18)$.

d	$h = \sqrt{2}$	$h = \dfrac{1}{2}\sqrt{2}$
6	3.78356×10^{-5}	3.78356×10^{-6}
8	9.37908×10^{-7}	8.18879×10^{-9}
10	1.63671×10^{-8}	4.20808×10^{-11}
12	2.10014×10^{-10}	2.12807×10^{-12}

Errors in L^2-norm at $t = 2$ for various step size h and polynomial order d are presented in Table 4.1.

The data presented in Table 4.1 indicate that

$$\|u - u_h\|_{L^2(\Omega)} \cong 1.81 \times 10^{-12} + 7.14786 \times 10^{-3}d \left(\frac{\sqrt{2}}{d^{0.754174}}\right)^{d+1} \quad \text{for } h = \sqrt{2} \quad (4.2.19)$$

and

$$\|u - u_h\|_{L^2(\Omega)} \cong 1.79 \times 10^{-12} + 1.83985 \times 10^{-2}d \left(\frac{\sqrt{2}}{2d^{0.727628}}\right)^{d+1} \quad \text{for } h = \frac{\sqrt{2}}{2} \quad (4.2.20)$$

These numerical results match the convergence rates as given in Theorem 4.1.
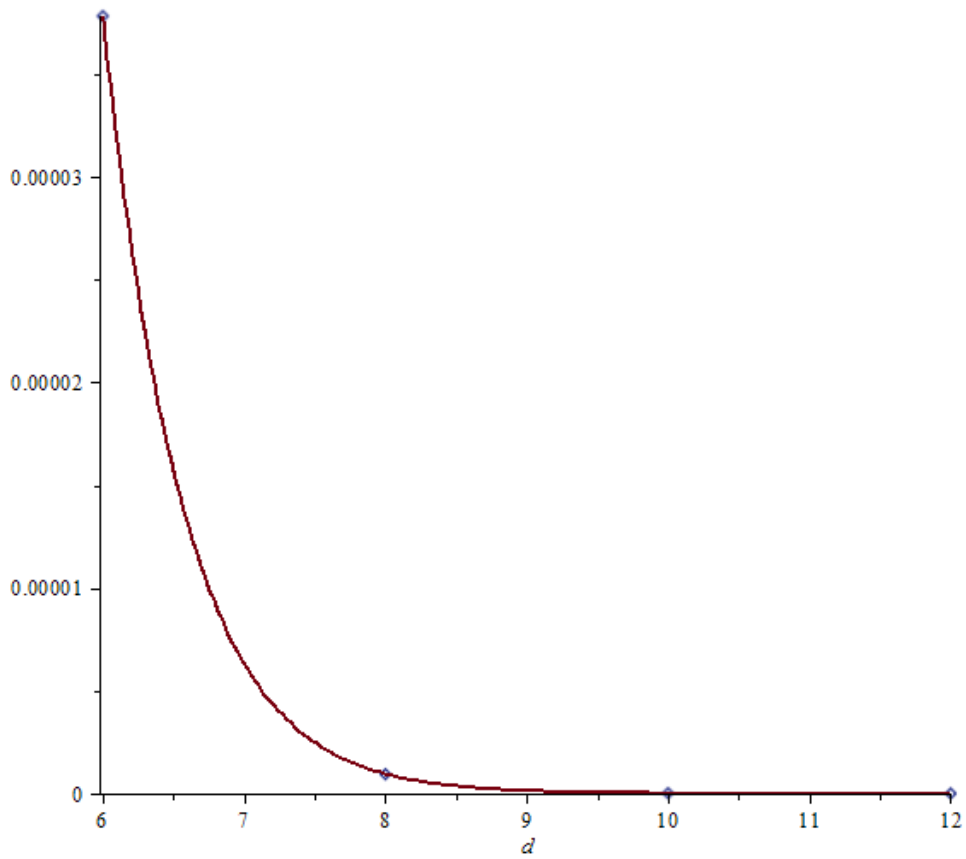
Figure 4.3: The errors, for $h = \sqrt{2}$, in Table 4.1 and the graph of (4.2.19)

134
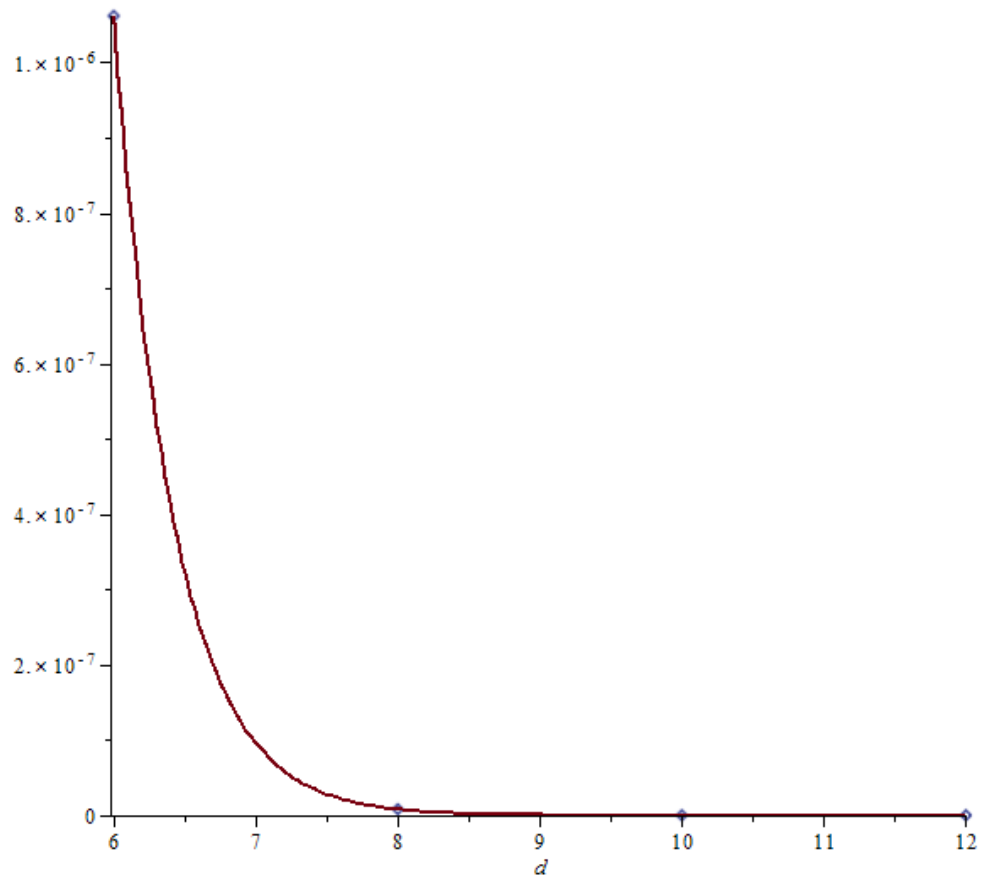
Figure 4.4: The errors, for $h = \dfrac{\sqrt{2}}{2}$, in Table 4.1 and the graph of (4.2.20)

Chapter 5

DISCUSSION OF RESULTS

In contrast with the four-step FEM-BDM, Backward Euler scheme behaves anomalously as t becomes large. This behaviour can be controlled by using very small time step k and small mesh parameter h, however the four-step linearised scheme is more efficient in this case. For instance, when $t = 40$ in Example 2, the convergence of the Backward Euler scheme (see Table 5.1) behaves irregularly with constant mesh parameter. We demonstrated same in Table 5.2 with constant time step.

We also give a comparison of the schemes with the one proposed by Yang (2015) in Tables $5.1 - 5.3$. The two-step implicit scheme gives a better approximation than the method proposed by Yang (2015) but computationally slower.

The proposed 4-step FEM-BDM gives a better accuracy. However to achieve the same accuracy using the backward Euler scheme or 2-step implicit scheme, the step size k has to be very small which could be computationally time consuming. This is also demonstrated in Table 5.3 with all computations done on a laptop with 2G RAM and 500G hard-drive. In the analysis, it was assumed that $\frac{\partial^5 u}{\partial t^5}$ exists, however if the regularity of the solution with respect to time is very low, the result obtained from the method may not be different from other low-order time discretisation methods (such as the two-step implicit scheme or the backward

Euler scheme).

Improving on the spatial discretisation by SEM is rewarding when the regularity of the unknown is very high. In Example 3, where the regularity of the unknown is low, the result of using high degree polynomial is not different from using low degree polynomial (see Table 5.4).

Due to the low regularity of the unknown function across the interface, reduction of error by increasing the polynomial degree may not be achieved.

5.1   Conclusion

Solution of a second order nonlinear parabolic interface problem by finite element method and spectral element method was discussed. The convergence of the finite element solution to the exact solution on a two-dimensional convex polygonal domain is analysed. In our study, the linear theories of interface and non-interface problems, Sobolev imbedding inequality were used to obtain a priori estimates of the weak solution and approximation of the linear interpolation operator. The linear interpolation operator was later used to estimate the clearly defined projection operators in L^2 and H^1 norms.

The spatial discretisation was done using quasi-uniform triangular elements with the unknown function approximated using Legendre polynomials. Discretisation in time was based on backward difference scheme.

For FEM, we showed that almost optimal order of convergence rate in $L^2(0, T; H^1(\Omega))$-norm and $L^2(0, T; L^2(\Omega))$-norm could be obtained for the approximation of a nonlinear parabolic interface problem when the integrals involved in the method are evaluated by numerical quadrature and the mesh cannot be fitted to the interface. The numerical experiment was implemented using predictor-corrector method because of the nonlinear terms. A four-step linearised FEM-BDS was proposed and analysed to ease the computational stress and improve the accuracy of the time-descretisation. The method was shown to be numerically

Table 5.1: Comparison, in L^2-norm error, of the numerical schemes with $h = 0.0463597$

k	Backward Euler	2-step implicit	linearised 4-step	Yang
0.4	1.09686	1.14329	1.09535	1.099700
0.2	7.82985×10^{-2}	4.92450×10^{-2}	7.04749×10^{-3}	4.92897×10^{-2}
0.1	4.85658×10^{-2}	1.06354×10^{-2}	6.24596×10^{-3}	1.09047×10^{-2}

Table 5.2: Comparison, in L^2-norm error, of the numerical schemes with $k = 0.2$

h	Backward Euler	2-step implicit	linearised 4-step	Yang
0.217242	1.87077×10^{-1}	1.88643×10^{-1}	1.91605×10^{-1}	1.82463×10^{-1}
0.108621	4.19731×10^{-2}	4.08319×10^{-2}	4.35048×10^{-2}	5.48989×10^{-2}
0.0550215	1.93533×10^{-2}	9.85728×10^{-3}	9.45986×10^{-3}	4.89246×10^{-2}
0.0273063	2.08968×10^{-2}	1.06763×10^{-2}	7.10719×10^{-3}	5.14151×10^{-2}

Table 5.3: Comparison of the numerical schemes with $t = 20, k = 0.125$, $h = 0.0550215$

	Backward Euler	2-step implicit	linearised 4-step	Yang
$\|\text{Error}\|_{L^2}$	6.2998×10^{-2}	1.07111×10^{-2}	1.11134×10^{-2}	1.60784×10^{-2}
$\|\text{Error}\|_{H^1}$	3.68037×10^{-1}	1.50167×10^{-1}	1.50011×10^{-1}	1.74212×10^{-1}
Time	11.94 min	12.12 min	6.71 min	6.06 min

Table 5.4: Comparison, in L^2-norm error, with polynomials of different degrees

	$d = 1$	$d = 2$	$d = 3$	$d = 4$
Error	1.87077×10^{-1}	1.88643×10^{-1}	1.91605×10^{-1}	1.82463×10^{-1}

stable and that higher order accuracy in time could be obtained for k sufficiently small.

On spectral elements, the formulation was based on Legendre polynomials evaluated at Gauss-Lobatto-Legendre points. The integrals involved were evaluated by numerical quadrature. We analysed a spectral convergence rate for spectral element approximation under certain regularity assumptions on the input data.

5.2   Contribution to Knowledge

In this work,

- Convergence rates of almost optimal order for the FE solution of a nonlinear parabolic interface problem under certain regularity assumptions that guarantee uniqueness and boundedness of solution were established

- A two-step implicit scheme with implementation by predictor-corrector approach due to the presence of nonlinearity was proposed. The scheme was shown to be stable for small time-step k and its convergence was also confirmed.

- A four-step linearised FEM-BDS was proposed and analysed to ease the computational stress and improve on the accuracy of the time-descretisation. The stability and convergence of the scheme were established. Numerical examples were given to confirm the theoretical results and to show the effectiveness of the methods over the existing one by Yang (2015).

- A theoretical framework for the convergence rate of spectral element solution of the problem in L^2-norm was given and spectral convergence of the scheme was established.

5.3   Further Research

Future work includes

- Extension of the results to domain in $\mathbb{R}^3$

- Investigation of FE and SE solutions of parabolic interface problems with other types of nonlinearities.

- The maximum principle of the scheme $(3.5.1) - (3.5.4)$ is a good area of interest. This is possible in view of Farago *et al.* (2010).

- Investigation of FE and SE solutions of nonlinear hyperbolic interface problems

- Extension of the work to integral and integro-differential equations with interfaces

References

Adams, R.A. 1975. *Sobolev Spaces. Pure and Applied Mathematics*, New York: Academic Press.

Argyris, J.H. 1960. *Energy theorems and structure analysis. A generalised discuss with applications on energy principles of structure analysis including the effects and non-linear stress-strain relations*, Butterworths, London.

Atkinson, K. and Han, W. 2009. *Theoretical numerical analysis; A functional analysis framework.* Third Edition, Springer.

Babuska, I. 1970. The finite element method for elliptic equations with discontinuous coefficients. *Computing*, $5 : 207 - 213$.

Babuska, I. 1994. *Courant element: before and after, in: M. Krizek, P. Neittaanmaki, R. Stenberg (Eds), finite element methods: fifty years of the Courant element, Decker, New York.*

Barrett, J.W. and Elliot, C.M. 1987. Fitted and unfitted finite element methods for elliptic equations with smooth interfaces. *IMA J. Numer. Anal.* $7 : 283 - 300$.

Bodard, N., Bouffanais, R. and Deville, M.D. 2008. Solution of moving-boundary problems by the spectral element method. *Applied Numerical Mathematics*, $58.7 : 968 - 984$.

Boyd, J.P. 1999. *Chebychev and Fourier spectral methods. Dover Publications, Inc. 31 East 2nd Street, Mineola, New York 11501.*

Brenner, S.C. and Scott, L.R. 2008. *The mathematical theory of finite element methods. Text in Applied Mathematics 15, Springer.*

Cantwell, C. D., Moxey, D., Comerford, A., Bolis, A., Rocco, G., Mengaldo, G., De Grazia, D., Yakovlev, S., Lombard, J-E., Ekelschot, D., Jordi, B., Xu, H., Mohamied, Y., Eskilsson, C., Nelson, B., Vos, P., Biotto, C., Kirby, R. M., and Sherwin, S. J. 2015. Nektar++: An open-source spectral/hp element framework, *Computer Physics Communications*, $192 : 205 - 219$.

Canosa, J. 1973. On a nonlinear diffusion equation describing population growth. *IBM J. Res Develop.* $17 : 307$.

Chen, Z. and Zou, J. 1998. Finite element methods and their convergence for elliptic and parabolic interface problems. *Numerical Math.* $79 : 175 - 202$.

Ciarlet, P.G. 1978. *The finite element methods for elliptic problems. Amsterdam: North Holland.*

Ciarlet, P.G. 1991. *Basic error estimates for elliptic problems, in P.G. Ciarlet and J.L. Lions edited Handbook of Numerical Analysis, Vol II, North Holland, Amsterdam.*

Claus, S., Cantwell C.D. and Phillips T.N. 2015. Spectral/hp element methods for plane Newtonian extrudated swell. *Journal of Computers and Fluids*, $116 : 105 - 117$.

Debnath, L. 2012 *Nonlinear partial differential equations for scientists and engineers. Third Edition Springer New York Dordrecht Heidelberg London.*

Dehghan, M. and Sabouri, M. 2013. A Legendre spectral element method on a large spatial domain to solve the predator-prey system modeling interacting populations. *Journal of Applied Mathematical Modelling*, $37 : 1028 - 1038$.

Deka, B. and Ahmed T. 2012. Semidiscrete finite element method for linear and semilinear parabolic problems with smooth interfaces: Some new optimal error estimates. *Numer. Functional Analysis and Optimization*, $33.4 : 1 - 21$.

Deng, S. and Cai, W. 2005. Analysis and application of an orthogonal nodal basis on triangles for discontinuous spectral element methods. *Appl. Numerical Anal. Comp. Math.* $2.3 : 326 - 345$.

Dutt, P., Husain, A., Murthy, A.S.V. and Upadhyay C.S. 2014. *h-p* spectral element methods for three dimensional elliptic problems on non-smooth domains. *Journal of Applied Mathematics and Computation*, $234 : 13 - 35$.

Evans, L.C. 1997. *Partial differential equations. Graduate studies in Mathematics.* American Mathematical Society. $251 - 270$.

Farago, I., Karatson, J., and Korotov, S. 2010. Discrete maximum principles for the FEM solution of some nonlinear parabolic problems. *Electronic Transaction on Numerical Analysis*, $36 : 149 - 167$. ISSN $1068 - 9613$.

Feistauer, M. and Sobotiková, V. 1990. Finite element approximation of nonlinear elliptic problems with discontinuous coefficients. *RAIRO Model. Math. Anal. Numer.* $24.4 : 457 - 500$.

Fisher, R.A. 1936. The wave of advance of advantageous genes. *Ann. of Eugen* $7 : 355$.

Germain, N. 2001. The effect of numerical integration in finite element methods for nonlinear parabolic equations. *Appl. Math. J. Chinese Univ. Ser. B.* $16.2 : 219 - 230$

Gerritsma, M., Bars, R., Maerscalck, B., Koren, B. and Deconinck, H. 2008. Least squares spectral element method applied to the Euler equations. *International Journal for Numerical methods in Fluids*, $57.9 : 1371 - 1395$.

143

Gockenbach, M.S. 2006. *Understanding and implementing the finite element method. SIAM.* Chapter 2, $15 - 27$.

Gupta, K.K. and Meek, J.L. 1996. A Brief History of the Beginning of the Finite Element Method. *International Journal for Numerical Methods in Engineering* $39 : 3761 - 3774$.

Haberman, R. 2005. *Applied partial differential equations; with Fourier series and boundary value problems*, Fourth Edition (ISBN 0-13-065243-I). Pearson Education Asia Limited and China Machine Press (English reprint edition).

Hansbo, A. and Hansbo, P. 2002. An unfitted finite element method based on Nitche's method, for elliptic interface problems. *Computational Methods Appl. Mech. Eng.*, $191 : 5537 - 5552$.

Hecht, F. 2012. New development in FreeFEM++. *J. Numer. Math.*, $20 : 251 - 265$.

Ja, R.V. 1966. On an estimate of the rapidity of convergence of homogenous difference schemes for elliptical and parabolic equations with discontinuous coefficients. *Problems Math. Anal., Boundary Value Problems, Integr. Equations*, $110 - 119$.

Munjiza, A. 2004. The combine finite-discrete element method. *John Wiley & Sons, Ltd.* Chapter $1 : 1 - 32$.

Johnson, C. 1987. *Numerical solutions of partial differential equations by the finite element method.* Cambridge University Press. Chapter $1:10 - 11$.

Kantorovich, L.V. and Krylov, V.I. 1958. Approximate methods in higher analysis, *Interscience, New York.*

Karatson, J. and Korotov, S. 2005. Discrete maximum principles for finite element solutions of nonlinear elliptic problems with mixed boundary conditions. *Numer. Math.*, $99 : 669 - 698$.

Karatson J. and Korotov S. 2009. Discrete maximum principles for FEM solutions of some nonlinear elliptic interface problems *Int. Jour. of Numerical Analysis and Modeling.* $6.1 : 1 - 16$.

Knabner, P. and Angermann L. 2002. Numerical methods for elliptic and parabolic partial differential equations. *Texts in Applied Mathematics. Springer.* $46 - 82$.

Komatitsch, D., Vilotte, J.,Vai, R., Castillo-Covarrubias, J.M. and Sanchez-Sesma, F.J. 1999. The spectral finite element method for elastic wave equations-application to 2-D and 3-D seismic problems. *International Journal of Numerical Methods in Engineering*, $45 : 1139 - 1164$.

Kumar, M. and Joshi, P. 2012. Some numerical techniques for solving elliptic interface problems. *Numerical Methods for Partial Differential Equations*, $28.1 : 94 - 114$.

Ladyzhenskaya, O.A., Ja, R.V. and Ural'ceva, N.N. 1966. The classical solvability of diffraction problems. *Trudy Mat. Inst. Steklov*, $92 : 116 - 146$. Translated in Proceedings of the Steklov Institute of Math., no. 92, Boundary value problems of mathematical physics IV, Am. Math. Soc.

Lambert, J.D. 1973. Computational methods in ordinary differential equations. *John Wiley & Sons Ltd.* Reprinted in April 1977. Chapter $1:11 - 40$.

Li, Z., Lin T. and Wu X. 2003. New cartesian grid methods for interface problems using the finite element formulation. *Numer. Math.*, $96 : 61 - 98$.

Liquan, M. 1999. Spectral finite element method for a unsteady transport equation. *Appl. Math. Journal of Chinese Univ. Ser B.* $14.4 : 381 - 388$.

Meng, S., Li, X.K. and Evans, G. 2003. Spectral element method for viscoelastic flows in a planar contraction channel. *International Journal for Numerical methods in Fluids*, $42:323 - 348$.

145

Mu, L., Wang, J., Wei, G., Ye, X. and Zhao S. 2013. Weak Galerkin methods for second order elliptic interface problems. *Journal of Computational Physics* $250 : 106 - 125$

Oden, J.T. and Reddy, J.N. 1976. *An introduction to the mathematical theory of finite elements.* Pure and Applied Science Mathematics, a Wiley-Interscience Publication.

Olshanskii, M.A. and Reusken, A. 2004. A Stokes interface problem: stability, finite element analysis and a robust solver. *European Congress on Computational Methods in Applied Sciences and Engineering ECCOMAS 2004.*

Pasquetti, R. and Rapetti, F. 2004. Spectral element methods on triangles and quadrilaterals: comparisons and applications. *Journal of Computational Physics*, $198 : 349 - 362$.

Patera, A.T. 1984. A spectral element method for fluid dynamics laminar flow in a channel expansion. *Journal of Computaional Physics* $54 : 468 - 488$.

Payne, V.F., Adewole, M.O. and Ajibola S.A. 2012. A finite element method and its convergence for an elliptic interface problem. *Pioneer Journal of Advances in Applied Mathematics*, $6.1 : 25 - 44$.

Polyanin, A.D. and Zaitsev V.F. 2012. Handbook of nonlinear partial differential equations. *Chapman & Hall/CRC, Boca Raton*, $367 - 377$.

Pozrikidis, C. 2014. *Introduction to finite and spectral element methods using MATLAB*®. CRC Press Taylor & Francis Group. ISBN $13 : 978 - 1 - 4822 - 0916 - 7$(eBook - PDF).

Ren, X. and Wei, J. 1994. On a two-dimensional elliptic problems with large exponent in nonlinearity. *Trans. AM Math. Soc.*, $343 : 749 - 763$.

Ronquist, E.M. and Patera, A.T. 1987. A Legendre spectral element method for the Stefan problem. *International Journal for Numerical Methods in Engineering*, 24 : 2273 − 2299

Sabouri, M. and Dehghan, M. 2015. An efficient implicit spectral element method for time-dependent nonlinear diffusion equation by evaluating integrals at one quadrature point. *Journal of Computers and Mathematics with Applications*, 70 : 2513 − 2541.

Shin, B. and Jung, J. 2011. Spectral collocation and radial basis function methods for one-dimensional interface problems. *Applied Numerical Mathematics*, 61.8 : 911 − 928.

Siddiqi, A.H. 2004. *Applied functional analysis: numerical methods, wavelet methods and image processing.* Marcel Dekker, Inc. New York.

Sinha, R.K. and Deka, B. 2005. Optimal error estimates for Linear Parabolic Problems with Discontnuous Coeficients. *SIAM J. Numer. Anal.* 43.2 : 733 − 749.

Sinha, R.K. and Deka, B. 2006. A priory error estimates in finite element methods for non-selfadjoint elliptic and parabolic problems. *Calcodo*, 43 : 253 − 278.

Sinha, R.K. and Deka, B. 2007. An unfitted finite element method for elliptic and parabolic problems. *IMA Jour. Numer. Anal.* 27 : 529 − 549.

Sinha, R.K. and Deka, B. 2009. Finite element method for semilinear elliptic and parabolic interface problems. *Applied Numerical Mathematics* 59 : 529 − 549.

Stein, E.M. 1971. Singular integrals and differential properties of functions. *Princeton NJ: Princeton University Press.* 180 − 183.

Taylor, M., Tribbia, J. and Iskandarani, M. 1997. The spectral element method for the shallow water equations on the sphere. *Journal of Computational Physics* 130 : 92 − 108.

Thomee, V. 2001. From finite difference to finite elements. A short history of numerical analysis of partial differential equations. *Journal of Computational and Applied Mathematics* $128 : 1 - 54$.

Thomee, V. 2006. *Galerkin Finite Element Methods for Parabolic Problems.* Springer Series in Computational Mathematics. Second Edition.

Timmermans, L.J.P., Van De Vosse, F.N. and Minev, P.D. 1994. Taylor-Galekin-based spectral element methods for convection-diffusion problems. *International Journal for Numerical Methods in Fluids*, $18 : 853 - 870$.

Turner, M.J., Clough, R.W., Martin, H.C. and Topp L.J. 1956. Stiffness and deflection analysis of complex structures. *Journal of Aero Sci*, $23:805 - 823$.

Wang, J. and Ye, X. 2013. A weak Galerkin finite element method for second order elliptic problems, *Journal of Comput. Appl. Math.* $241 : 103 - 115$.

Yang, C. 2015. Convergence of a linearized second-order BDF-FEM for nonlinear parabolic interface problems. *Computers and Mathematics with applications* $70 : 265 - 281$.

Yoseph, P.B., Moses, E., Zrahia U. and Yarin, A.L. 1995. Space-time spectral element methods for one-dimensional nonlinear advection-diffusion problems. *Journal of Computational Physics*, $119 : 62 - 74$.

Zhang, Z., Yu, X. 2015. Local discontinuous Galerkin method for parabolic interface problems. *Acta Mathematicae Applicatae Sinica, English Series.* $31.2 : 453 - 466$.

Zienkiewicz, O.C. and Cheung, Y.K. 1965. Finite elements in the solution of field problems. *The Engineer*, $220:507 - 510$.

Zienkiewicz, O.C. and Cheung, Y.K. 1965. *The finite element method in continuum and structural mechanics.* McGraw-Hill, New York.

Zienkiewicz, O.C. and Taylor, R.L. 1989. *The finite element method. Vol I. Basic Formulation and Linear Problems*, 4th edition. McGraw-Hill, New York.

Zienkiewicz, O.C. and Taylor, R.L. 1991. *The finite element method. Vol II. Solid and Fluid Mechanics, Dynamics and Non Linearity.* McGraw-Hill, New York.

Ženíśek, A. 1990. The finite element method for nonlinear equations with discontinuous coefficients. *Numer. Math.* $58:51-77$.

Zlamal, M. 1968. On the finite element method. *Numer Math* $12:394-409$.

Appendices

Here, we give the explanation of the components of proofs of some results as well as computer codes that produced the graphs and tables.

Appendix A

$$
\begin{aligned}
\|u - U_{hk}\|^2_{L^2(0,T;L^2(\Omega))} &= \sum_{n=1}^{M} \int_{t_{n-1}}^{t_n} \|u - U_h^n\|^2_{L^2(\Omega)} \, ds \\
&\leq 2 \sum_{n=1}^{M} \int_{t_{n-1}}^{t_n} \|u - u^n\|^2_{L^2(\Omega)} + \|u^n - U_h^n\|^2_{L^2(\Omega)} \, ds \\
&= 2 \sum_{n=1}^{M} \int_{t_{n-1}}^{t_n} \|u - u^n\|^2_{L^2(\Omega)} \, ds + 2 \sum_{n=1}^{M} k \|u^n - U_h^n\|^2_{L^2(\Omega)} \\
&\leq Ck^4 \|u_{tt}\|^2_{L^2(0,T;L^2(\Omega))} + 2 \sum_{n=1}^{M} k \|u^n - U_h^n\|^2_{L^2(\Omega)}
\end{aligned}
$$

Therefore,

$$
\|u - U_{hk}\|_{L^2(0,T;L^2(\Omega))} \leq Ck^2 \|u_{tt}\|_{L^2(0,T;L^2(\Omega))} + C \left[\sum_{n=1}^{M} k \|u^n - U_h^n\|^2_{L^2(\Omega)} \right]^{1/2}
$$

Appendix B

By Sobolev Embedding Theorem 1.13,

$$
W^{1,\infty}(\Omega_i \cap \Omega_0) \hookrightarrow C(\Omega_i \cap \Omega_0) \quad i = 1, 2
$$

therefore there exist $c, C > 0$ such that

$$
c\|v\|_{W^{1,\infty}(\Omega_i \cap \Omega_0)} \leq \|v\|_{C(\Omega_i \cap \Omega_0)} \leq C\|v\|_{W^{1,\infty}(\Omega_i \cap \Omega_0)} \quad \forall \, v \in W^{1,\infty}(\Omega_i \cap \Omega_0)
$$

Since $C(\Omega_i \cap \Omega_0)$ is dense in $L^2(\Omega_i \cap \Omega_0)$ for $i = 1, 2$, we have

$$\|v\|_{W^{1,\infty}(\Omega_i \cap \Omega_0)} \le C\|v\|_{L^2(\Omega_i \cap \Omega_0)} \qquad \forall\, v \in W^{1,\infty}(\Omega_i \cap \Omega_0)$$

Thus,

$$
\begin{aligned}
D_1(\psi) &\le C\{\|\psi\|_X + \|\psi\|_{L^2(\Omega_1 \cap \Omega_0)} + \|\psi\|_{L^2(\Omega_2 \cap \Omega_0)}\} \\
&\le C\|\psi\|_X
\end{aligned}
\tag{5.3.1}
$$

(5.3.1) follows from the fact that

$$\|\psi\|_{L^2(\Omega_i \cap \Omega_0)} \le \|\psi\|_{L^2(\Omega)} \le \|\psi\|_X$$

Following the argument that led to (3.3.19), we have

$$D_1(\psi) \le C\|u\|_X \le C\|R_h u - u\|_{L^2(\Omega)}$$

Appendix C

Definition Consider the linear multistep method

$$\sum_{j=0}^{k} \alpha_j y_{n+j} = h \sum_{j=0}^{k} \beta_j f_{n+j} \tag{5.3.2}$$

where α_j and β_j are constants with $\alpha_k \ne 0$ and that not both α_0 and β_0 are zero. (5.3.2) is said to be zero-stable if no root of the first characteristic polynomial has modulus greater than one, and every root with modulus one is simple.

More information on zero-stability can be found in Lambert (1973).

Appendix D The FreeFEM++ code that produced Tables $3.1 - 3.2$ and Figure 3.4

border a(t=-1.0,1.0){x=t; y=-1; label=1;};
border b(t=-1.0,1.0){x=1; y=t; label=2;};

```
border c(t=-1.0,1){x=-t; y=1; label=3;};
border d(t=-1.0,1){x=-1; y=-t;label=4;};
border aa(t=0,2*pi){x=0.5*cos(t); y=0.5*sin(t); label=5;};
real n=1 ;
mesh Th = buildmesh (a(14*n) + b(14*n) + c(14*n) + d(14*n)+ aa(40*n) );
plot(Th,wait=1);
func u0 = 0 ;
real T=5, dt=0.01 ;
real L2error, H1error;
func uexact = (5*(0.125-0.5*x^2-0.5*y^2)*sin(T)*(x^2+y^2<=0.25))+
((x^2-1)*(-y^2+1)*(x^2+y^2-.25)*sin(2*T))*(x^2+y^2>0.25);
real t;
func f = ((5*(.125-.5*x^2-.5*y^2))*cos(t)-(250*(0.125-0.5*x ^2-0.5*y^2))
*sin(t)^3 *x^2/(1+25*(.125-.5*x^2-.5*y^2)^2*sin(t)^2) +6250*(.125-.5*x^2-.5*y^2)^3
*sin(t)^5 *x^2/(1+25*(.125-.5*x^2-.5*y^2)^2*sin(t)^2)^2
+250*(.125-.5*x^2-.5*y^2)^2 *sin(t)^3/(1+25*(.125-.5*x^2-.5*y^2)^2*sin(t)^2)
-(250*(.125-.5*x^2-.5*y^2)) *sin(t)^3*y^2/(1+25*(.125-.5*x^2-.5*y^2)^2*sin(t)^2)
+6250*(.125-.5*x^2-.5*y^2)^3 *sin(t)^5*y^2/(1+25
*(0.125-.5*x^2-.5*y^2)^2*sin(t)^2)^2 )*(x^2+y^2<=0.25)
+((2*(x^2-1))*(-y^2+1)*(x^2+y^2-0.25)*cos(2*t)+(1.0*(2*x*(-y^2+1)
*(x^2+y^2-.25)*sin(2*t)+(2*(x^2-1))*(-y^2+1)*x*sin(2*t)))*((4*(x^2-1))
*(-y^2+1)^2 *(x^2+y^2-.25)^2*sin(2*t)^2*x+4*(x^2-1)^2*(-y^2+1)^2*(x^2+y^2-
.25)*sin(2*t)^2*x)/(1+(x^2-1)^2*(-y^2+1)^2*(x^2+y^2-.25)^2
*sin(2*t)^2)^2-(1.0*((2*(-y^2+1))*(x^2+y^2-.25)*sin(2*t)+8*x^2*(-y^2+1)
*sin(2*t)+(2*(x^2-1))*(-y^2+1)*sin(2*t)))/(1+(x^2-1)^2*(-y^2+1)^2
*(x^2+y^2-.25)^2*sin(2*t)^2)+(1.0*(-(2*(x^2-1)) *y*(x^2+y^2-.25)*sin(2*t)
+(2*(x^2-1))*(-y^2+1)*y*sin(2*t)))*(-4*(x^2-1)^2*(-y^2+1)*(x^2+y^2-.25)^2
*sin(2*t)^2*y+4*(x^2-1)^2*(-y^2+1)^2*(x^2+y^2-.25)*sin(2*t)^2*y)/(1+(x^2-1)^2*(-
y^2+1)^2*(x^2+y^2-.25)^2*sin(2*t)^2)^2-(1.0*(-(2*(x^2-1))*(x^2+y^2-.25)*sin(2*t)-
```

(8*(x^2-1))*y^2*sin(2*t)+(2*(x^2-1))*(-y^2+1)*sin(2*t)))/(1+(x^2-1)^2*(-y^2+1)^2

(x^2+y^2-.25)^2*sin(2*t)^2))*(x^2+y^2>0.25) ;

func g1 = 0;

fespace Vh(Th,P1);

Vh u=u0,v,uold,uu ;

Vh h = hTriangle; // get the size of all triangles

problem ther(uu,v)= int2d(Th)(uu*v/dt + ((uold^2/(1+uold^2))*(x^2+y^2<=0.25)

+ ((1/(1+uold^2))*(x^2+y^2>0.25))) *(dx(uu) * dx(v) + dy(uu) * dy(v)))

- int2d(Th)(uold*v/dt)-int2d(Th)(f*v) + on(aa,uu=0) + on(a,uu=0) + on(b,uu=0)

+on(c,uu=0)+ on(d,uu=0);

problem the(u,v)= int2d(Th)(u*v/dt + ((uu^2/(1+uu^2))*(x^2+y^2<=0.25) +

((1/(1+uu^2))*(x^2+y^2>0.25))) *(dx(u) * dx(v) + dy(u) * dy(v)))

- int2d(Th)(uold*v/dt)-int2d(Th)(f*v) + on(aa,u=0) + on(a,u=0)

+ on(b,u=0)+on(c,u=0)+ on(d,u=0);

ofstream ff("ther.dat");

for(t=dt;t<=T;t+=dt){

ther; // here solve the thermic problem

the; uold=uu; uu=u; // }

plot(u);

L2error= sqrt(int2d(Th)((u-uexact)^2));

Vh uuu = uexact;

plot(uuu) ;

H1error = sqrt(L2error^2 + int2d(Th)((dx(u)-dx(uuu))^2 + (dy(u)-dy(uuu))^2

));

cout ≪ "h = "≪ h[ ].max ≪ endl;

cout ≪ "L2 error = "≪ L2error ≪ endl;

cout ≪ "H1 error = "≪ H1error ≪ endl;

Appendix E The FreeFEM++ code that produced Tables $3.3 - 3.4$ and Figures

153

3.6&3.7

```
border a(t=-1.0,1.0){x=t; y=-1; label=1;};
border b(t=-1.0,1.0){x=1; y=t; label=2;};
border c(t=-1.0,1){x=-t; y=1; label=3;};
border d(t=-1.0,1){x=-1; y=-t;label=4;};
border aa(t=0,2*pi){x=0.5*cos(t); y=0.25*sin(t); label=5;};
real n=1 ;
mesh Th = buildmesh (a(14*n) + b(14*n) + c(14*n) + d(14*n)+ aa(30*n) );
plot(Th,wait=1);
func u0 = 0 ;
real T=4, dt=0.005 ;
real L2error, H1error;
func uexact = (0.125*(1-4*x^2-16*y^2)*T*exp(sin(T))*(4*x^2+16*y^2<=1)) +
(0.5*(x^2-1)*(y^2-1)*(4*x^2+16*y^2-1)*sin(T))*(4*x^2+16*y^2>1) ;
real t;
func f = ((1/8*(-4*x^2-16*y^2+1))*exp(sin(t+dt))+(1/8*(-4*x^2-16*y^2+1))
*(t+dt)*cos(t+dt)*exp(sin(t+dt))+(25*(t+dt))*exp(sin(t+dt))) *(4*x^2+16*y^2<=1)
+ (-(.5*(-x^2+1))*(-y^2+1)*(-4*x^2-16*y^2+1)*cos(t+dt) +(1.0*x*(-y^2+1)*(-
4*x^2-16*y^2+1)*sin(t+dt)+(4.0*(-x^2+1)) *(-y^2+1)*x*sin(t+dt))*(-((-x^2+1))*(-
y^2+1)^2*(-4*x^2-16 *y^2+1)^2*sin(t+dt)^2*x-4.00*(-x^2+1)^2*(-y^2+1)^2*(-4*x^2
-16*y^2+1)*sin(t+dt)^2*x)/(1+.25*(-x^2+1)^2*(-y^2+1)^2*(-4*x^2-16 *y^2+1)^2
*sin(t+dt)^2)^2-((1.0*(-y^2+1))*(-4*x^2-16*y^2+1) *sin(t+dt)-16.0*x^2*(-y^2+1)
*sin(t+dt)+(4.0*(-x^2+1))*(-y^2+1) *sin(t+dt))/(1+.25*(-x^2+1)^2*(-y^2+1)^2*(-
4*x^2-16*y^2+1)^2 *sin(t+dt)^2)+((1.0*(-x^2+1))*y*(-4*x^2-16*y^2+1)*sin(t+dt)
+(16.0*(-x^2+1))*(-y^2+1)*y*sin(t+dt))*(-(-x^2+1)^2*(-y^2+1) *(-4*x^2-16*y^2
+1)^2 *sin(t+dt)^2*y-16.00*(-x^2+1)^2*(-y^2+1)^2 *(-4*x^2-16*y^2+1)*sin(t+
dt)^2*y)/(1+.25*(-x^2+1)^2*(-y^2+1)^2 *(-4*x^2-16*y^2+1)^2*sin(t+dt)^2)^2-
((1.0*(-x^2+1))*(-4*x^2-16 *y^2+1)*sin(t+dt)-(64*(-x^2+1))*y^2*sin(t+dt)+(16
*(-x^2+1)) *(-y^2+1)*sin(t+dt))/(1+.25*(-x^2+1)^2*(-y^2+1)^2*(-4*x^2-16*y^2
```

+1)^2*sin(t+dt)^2))*(4*x^2+16*y^2>1);

func g1 = 0;

fespace Vh(Th,P1);

Vh u,v,uu,uold=u0;

Vh h = hTriangle; // get the size of all triangles

problem thermicc(uu,v)= int2d(Th)(uu*v/dt + (5*(4*x^2+16*y^2<=1)

+ ((1/(1+ (uold)^2))*(4*x^2+16*y^2>1))) *(dx(uu) * dx(v) + dy(uu) * dy(v)))

- int2d(Th)(uold*v/dt) - int2d(Th)(f*v) + on(aa,uu=0) + on(a,uu=0) + on(b,uu=0)

+on(c,uu=0)+ on(d,uu=0);

problem themic(u,v)= int2d(Th)(u*v/dt + (5*(4*x^2+16*y^2<=1)

+ ((1/ (1+(uu)^2))*(4*x^2+16*y^2>1))) *(dx(u) * dx(v) + dy(u) * dy(v)))

- int2d(Th)(uold*v/dt) - int2d(Th)(f*v) + on(aa,u=0) + on(a,u=0)

+ on(b,u=0)+on(c,u=0)+ on(d,u=0);

ofstream ff("thermic.dat");

for(t=dt;t<=T;t+=dt){

thermicc; // here solve the thermic problem

themic; uold=uu; uu=u; // }

plot(u);

L2error= sqrt(int2d(Th)((u-uexact)^2));

Vh uuu = uexact;

plot(uuu) ;

H1error = sqrt(L2error^2 + int2d(Th)((dx(u)-dx(uuu))^2 + (dy(u)-dy(uuu))^2

));

cout ≪ "h = "≪ h[ ].max ≪ endl;

cout ≪ "L2 error = "≪ L2error ≪ endl;

cout ≪ "H1 error = "≪ H1error ≪ endl;

Appendix F The FreeFEM++ code that produced Tables $3.5 - 3.6$ and Figure
3.8

```
border a(t=-1.0,1.0){x=t; y=-1; label=1;};
border b(t=-1.0,1.0){x=1; y=t; label=2;};
border c(t=-1.0,1){x=-t; y=1; label=3;};
border d(t=-1.0,1){x=-1; y=-t;label=4;};
border e(t=-1.0,1){x=-t; y=t; label=5;};
real n=1;
mesh Th = buildmesh (a(16*n) + b(16*n) + c(16*n) +d(16*n) + e(40*n));
plot(Th,wait=1);
func u0 = 0;
real T=10, dt=0.0125 ;
real L2error, H1error;
func uexact = (T*(1+x)*(1+y)*(x+y))*(x+y<=0)+(T*(1-x)*(1-y)*(x+y))*(x+y>0);
real t;
func g = 0;
func f = ((1+x)*(1+y)*(x+y)+((t+dt)*(1+y)*(x+y)+(t+dt)*(1+x)*(1+y))
*(2*(t+dt)^2*(1+x)*(1+y)^2*(x+y)^2+2*(t+dt)^2*(1+x)^2*(1+y)^2
*(x+y))/(1+(t+dt)^2 *(1+x)^2*(1+y)^2*(x+y)^2)^2-2*(t+dt)*(1+y)/(1+(t+dt)^2
*(1+x)^2*(1+y)^2 *(x+y)^2)+((t+dt)*(1+x)*(x+y)+(t+dt)*(1+x)*(1+y))
*(2*(t+dt)^2*(1+x)^2*(1+y) *(x+y)^2+2*(t+dt)^2*(1+x)^2*(1+y)^2*(x+y))
/(1+(t+dt)^2*(1+x)^2*(1+y)^2 *(x+y)^2)^2-2*(t+dt)*(1+x)/(1+(t+dt)^2
*(1+x)^2*(1+y)^2*(x+y)^2))*(x+y<=0) +((1-x)*(1-y)*(x+y)+2*x*y^2*(-(t+dt)
*(1-y)*(x+y)+(t+dt)*(1-x)*(1-y)) +(2*(-x^2*y^2+1))*(t+dt)*(1-y)+2*x^2*y*(-
(t+dt)*(1-x)*(x+y) +(t+dt)*(1-x)*(1-y))+(2*(-x^2*y^2+1))*(t+dt)*(1-x))*(x+y>0);
fespace Vh(Th,P1);
Vh u,v,uu,uold=u0;
Vh h = hTriangle; // get the size of all triangles
problem thermicc(uu,v)= int2d(Th)(uu*v/dt + (1/(1+uold^2)*(x+y<=0) + (1-
x^2*y^2)*(x+y>0))*(dx(uu) * dx(v) + dy(uu) * dy(v))) - int2d(Th)(uold*v/dt)
- int2d(Th)(f*v) + on(e,uu=0) + on(a,uu=0) + on(b,uu=0) +on(c,uu=0)+ on(d,uu=0);
```

problem themic(u,v)= int2d(Th)(u*v/dt + (1/(1+uu^2)*(x+y<=0) + (1-x^2*y^2)
(x+y>0))(dx(u) * dx(v) + dy(u) * dy(v))) - int2d(Th)(uold*v/dt)
- int2d(Th)(f*v) + on(e,u=0) + on(a,u=0) + on(b,u=0)+on(c,u=0)+ on(d,u=0);

ofstream ff("thermic.dat");

for(t=dt;t<=T;t+=dt){

thermicc; // here solve the thermic problem

themic; uold=uu; uu=u; }

plot(u);

L2error= sqrt(int2d(Th)((u-uexact)^2));

Vh uuu = uexact;

plot(uuu) ;

H1error = sqrt(L2error^2 + int2d(Th)((dx(u)-dx(uuu))^2 + (dy(u)-dy(uuu))^2
));

cout ≪ "h = "≪ h[ ].max ≪ endl;

cout ≪ "L2 error = "≪ L2error ≪ endl;

cout ≪ "H1 error = "≪ H1error ≪ endl;

Appendix G The FreeFEM++ code that produced Table 3.7

border a(t=-1.0,1.0){x=t; y=-1; label=1;};

border b(t=-1.0,1.0){x=1; y=t; label=2;};

border c(t=-1.0,1){x=-t; y=1; label=3;};

border d(t=-1.0,1){x=-1; y=-t;label=4;};

border aa(t=0,2*pi){x=0.5*cos(t); y=0.5*sin(t); label=5;};

real n= 1;

mesh Th = buildmesh (a(14*n) + b(14*n) + c(14*n) + d(14*n)+ aa(40*n));

plot(Th,wait=1);

func u0 = 0 ;

real T=12, dt=0.01 ;

real L2error, H1error;

func uexact = (5*(0.125-0.5*x^2-0.5*y^2)*sin(T)*(x^2+y^2<=0.25)) +((x^2-1)*(-y^2+1)*(x^2+y^2-0.25)*sin(2*T)) *(x^2+y^2>0.25);

real t;

func f = ((5*(.125-.5*x^2-.5*y^2))*cos(t)-(250*(0.125-0.5*x ^2-0.5*y^2)) *sin(t)^3 *x^2/(1+25*(.125-.5*x^2-.5*y^2)^2*sin(t)^2) +6250*(.125-.5*x^2-.5*y^2)^3 *sin(t)^5 *x^2/(1+25*(.125-.5*x^2-.5*y^2)^2*sin(t)^2)^2 +250*(.125-.5*x^2-.5*y^2)^2 *sin(t)^3/(1+25*(.125-.5*x^2-.5*y^2)^2*sin(t)^2) -(250*(.125-.5*x^2-.5*y^2)) *sin(t)^3*y^2/(1+25*(.125-.5*x^2-.5*y^2)^2*sin(t)^2) +6250*(.125-.5*x^2-.5*y^2)^3 *sin(t)^5*y^2/(1+25 *(0.125-.5*x^2-.5*y^2)^2*sin(t)^2)^2)*(x^2+y^2<=0.25) +((2*(x^2-1))*(-y^2+1)*(x^2+y^2-0.25)*cos(2*t)+(1.0*(2*x*(-y^2+1) *(x^2+y^2-.25)*sin(2*t)+(2*(x^2-1))*(-y^2+1)*x*sin(2*t)))*((4*(x^2-1)) *(-y^2+1)^2 *(x^2+y^2-.25)^2*sin(2*t)^2*x+4*(x^2-1)^2*(-y^2+1)^2*(x^2+y^2-.25)*sin(2*t)^2*x)/(1+(x^2-1)^2*(-y^2+1)^2*(x^2+y^2-.25)^2 *sin(2*t)^2)^2-(1.0*((2*(-y^2+1))*(x^2+y^2-.25)*sin(2*t)+8*x^2*(-y^2+1) *sin(2*t)+(2*(x^2-1))*(-y^2+1)*sin(2*t)))/(1+(x^2-1)^2*(-y^2+1)^2 *(x^2+y^2-.25)^2*sin(2*t)^2)+(1.0*(-(2*(x^2-1)) *y*(x^2+y^2-.25)*sin(2*t) +(2*(x^2-1))*(-y^2+1)*y*sin(2*t)))*(-4*(x^2-1)^2*(-y^2+1)*(x^2+y^2-.25)^2 *sin(2*t)^2*y+4*(x^2-1)^2*(-y^2+1)^2*(x^2+y^2-.25)*sin(2*t)^2*y)/(1+(x^2-1)^2*(-y^2+1)^2*(x^2+y^2-.25)^2*sin(2*t)^2)^2-(1.0*(-(2*(x^2-1))*(x^2+y^2-.25)*sin(2*t)-(8*(x^2-1))*y^2*sin(2*t)+(2*(x^2-1))*(-y^2+1)*sin(2*t)))/(1+(x^2-1)^2*(-y^2+1)^2 (x^2+y^2-.25)^2*sin(2*t)^2))*(x^2+y^2>0.25) ;

func g1 = 0;

fespace Vh(Th,P1);

Vh u=u0,v,uold,uu, uold1 ;

Vh h = hTriangle; // get the size of all triangles

for(t=dt;t<2*dt;t+=dt){

solve Poisson1(uold1,v,solver=LU) = int2d(Th)(uold1*v/dt + ((uold^2/(1+uold^2)) *(x^2+y^2<=0.25) + ((1/(1+(uold)^2))*(x^2+y^2>0.25))) *(dx(uold1)*dx(v) +

dy(uold1)*dy(v))) - int2d(Th)(f*v + uold*v/dt) + on(a,uold1=0) + on(b,uold1=0)
+ on(c,uold1=0) + on(d,uold1=0) + on(aa,uold1=0) ; }

problem termicc(uu,v)= int2d(Th)(1.5*uu*v/dt + ((((2*uold1-uold)^2)/(1+
(2*uold1-1*uold)^2))*(x^2+y^2<=0.25) + ((1/(1+(2*uold1-uold)^2))
*(x^2+y^2>0.25))) *(dx(uu) * dx(v) + dy(uu) * dy(v))) - int2d(Th)(2*uold1*v/dt)
+ int2d(Th)(0.5*uold*v/dt) -int2d(Th)(f*v) + on(aa,uu=0) + on(a,uu=0)
+ on(b,uu=0)+on(c,uu=0)+ on(d,uu=0);

problem temic(u,v)= int2d(Th)(1.5*u*v/dt + (((uu^2)/(1+(uu)^2))*(x^2+y^2<=0.25)
+ ((1/(1+(uu)^2))*(x^2+y^2>0.25)))*(dx(u) * dx(v) + dy(u) * dy(v)))
- int2d(Th)(2*uold1*v/dt) + int2d(Th)(0.5*uold*v/dt) -int2d(Th)(f*v)
+ on(aa,u=0) + on(a,u=0) + on(b,u=0)+on(c,u=0)+ on(d,u=0);

ofstream ff("ther.dat");

for(t=2*dt;t¡=T;t+=dt){

termicc; // here solve the thermic problem

temic;

uu=u;

uold=uold1;

uold1=u;

}

plot(u);

L2error= sqrt(int2d(Th)((u-uexact)^2));

Vh uuu = uexact;

plot(uuu) ;

H1error = sqrt(L2error^2 + int2d(Th)((dx(u)-dx(uuu))^2 + (dy(u)-dy(uuu))^2
));

cout ≪ "h = "

*ll*h[ ].max≪ endl;

cout ≪ "L2 error = "≪L2error≪ endl;

cout ≪ "H1 error = "≪H1error≪ endl;

Appendix H The FreeFEM++ code that produced Table 3.8

border a(t=-1.0,1.0){x=t; y=-1; label=1;};

border b(t=-1.0,1.0){x=1; y=t; label=2;};

border c(t=-1.0,1){x=-t; y=1; label=3;};

border d(t=-1.0,1){x=-1; y=-t;label=4;};

border aa(t=0,2*pi){x=0.5*cos(t); y=0.25*sin(t); label=5;};

real n=1 ;

mesh Th = buildmesh (a(14*n) + b(14*n) + c(14*n) + d(14*n)+ aa(30*n));

plot(Th,wait=1);

func u0 = 0 ;

real T=4, dt=0.005 ;

real L2error, H1error;

func uexact = (0.125*(1-4*x^2-16*y^2)*T*exp(sin(T))*(4*x^2+16*y^2<=1)) + (0.5*(x^2-1)*(y^2-1)*(4*x^2+16*y^2-1)*sin(T))*(4*x^2+16*y^2>1) ;

real t;

func f = ((1/8*(-4*x^2-16*y^2+1))*exp(sin(t+dt))+(1/8*(-4*x^2-16*y^2+1)) *(t+dt)*cos(t+dt)*exp(sin(t+dt))+(25*(t+dt))*exp(sin(t+dt))) *(4*x^2+16*y^2<=1) + (-(.5*(-x^2+1))*(-y^2+1)*(-4*x^2-16*y^2+1)*cos(t+dt) +(1.0*x*(-y^2+1)*(-4*x^2-16*y^2+1)*sin(t+dt)+(4.0*(-x^2+1)) *(-y^2+1)*x*sin(t+dt))*(-((-x^2+1))*(-y^2+1)^2*(-4*x^2-16 *y^2+1)^2*sin(t+dt)^2*x-4.00*(-x^2+1)^2*(-y^2+1)^2*(-4*x^2 -16*y^2+1)*sin(t+dt)^2*x)/(1+.25*(-x^2+1)^2*(-y^2+1)^2*(-4*x^2-16 *y^2+1)^2 *sin(t+dt)^2)^2-((1.0*(-y^2+1))*(-4*x^2-16*y^2+1) *sin(t+dt)-16.0*x^2*(-y^2+1) *sin(t+dt)+(4.0*(-x^2+1))*(-y^2+1) *sin(t+dt))/(1+.25*(-x^2+1)^2*(-y^2+1)^2*(- 4*x^2-16*y^2+1)^2 *sin(t+dt)^2)+((1.0*(-x^2+1))*y*(-4*x^2-16*y^2+1)*sin(t+dt) +(16.0*(-x^2+1))*(-y^2+1)*y*sin(t+dt))*(-(-x^2+1)^2*(-y^2+1) *(-4*x^2-16*y^2 +1)^2 *sin(t+dt)^2*y-16.00*(-x^2+1)^2*(-y^2+1)^2 *(-4*x^2-16*y^2+1)*sin(t+ dt)^2*y)/(1+.25*(-x^2+1)^2*(-y^2+1)^2 *(-4*x^2-16*y^2+1)^2*sin(t+dt)^2)^2- ((1.0*(-x^2+1))*(-4*x^2-16 *y^2+1)*sin(t+dt)-(64*(-x^2+1))*y^2*sin(t+dt)+(16

```
*(-x^2+1)) *(-y^2+1)*sin(t+dt))/(1+.25*(-x^2+1)^2*(-y^2+1)^2*(-4*x^2-16*y^2
+1)^2*sin(t+dt)^2))*(4*x^2+16*y^2>1);
func g1 = 0;
fespace Vh(Th,P1);
Vh u,v,uu,uold=u0,uold1;
for( t=0;t<=0;t+=dt){
solve Poisson1(uold1,v,solver=LU) = int2d(Th)( uold1*v/dt + (5*(4*x^2+16*y^2<=1)
+ ((1/(1+(uold)^2))*(4*x^2+16*y^2>1))) *(dx(uold1)*dx(v) + dy(uold1)*dy(v)))
- int2d(Th)(f*v + uold*v/dt ) + on(a,uold1=0) + on(b,uold1=0) + on(c,uold1=0)
+ on(d,uold1=0) + on(aa,uold1=0) ; }
Vh h = hTriangle; // get the size of all triangles
problem  thermicc(uu,v)=  int2d(Th)(1.5*uu*v/dt  +  (5*(4*x^2+16*y^2<=1)  +
((1/(1+ (2*uold1-1*uold)^2))*(4*x^2+16*y^2>1))) *(dx(uu) * dx(v) + dy(uu)
* dy(v))) - int2d(Th)(2*uold1*v/dt) + int2d(Th)(0.5*uold*v/dt) -int2d(Th)(f*v)
+ on(aa,uu=0) + on(a,uu=0) + on(b,uu=0)+on(c,uu=0)+ on(d,uu=0);
problem  themic(u,v)=  int2d(Th)(1.5*u*v/dt  +  (5*(4*x^2+16*y^2<=1)  +  ((1/
(1+(uu)^2))*(4*x^2+16*y^2>1))) *(dx(u) * dx(v) + dy(u) * dy(v)))
- int2d(Th)(2*uold1*v/dt) + int2d(Th)(0.5*uold*v/dt) -int2d(Th)(f*v)
+ on(aa,u=0) + on(a,u=0) + on(b,u=0)+on(c,u=0)+ on(d,u=0);
ofstream ff("ther.dat");
for( t=dt;t<T;t+=dt){
thermicc; // here solve the thermic problem
themic;
uu=u;
uold=uold1;
uold1=u; }
plot(u);
L2error= sqrt(int2d(Th)((u-uexact)^2));
Vh uuu = uexact;
```

plot(uuu) ;

H1error = sqrt(L2error^2 + int2d(Th)((dx(u)-dx(uuu))^2 + (dy(u)-dy(uuu))^2

));

cout ≪ "h = "≪h[ ].max≪ endl;

cout ≪ "L2 error = "≪L2error≪ endl;

cout ≪ "H1 error = "≪H1error≪ endl;

Appendix I The FreeFEM++ code that produced Table 3.9

border a(t=-1.0,1.0){x=t; y=-1; label=1;};

border b(t=-1.0,1.0){x=1; y=t; label=2;};

border c(t=-1.0,1){x=-t; y=1; label=3;};

border d(t=-1.0,1){x=-1; y=-t;label=4;};

border e(t=-1.0,1){x=-t; y=t; label=5;};

real n=1;

mesh Th = buildmesh (a(16*n) + b(16*n) + c(16*n) +d(16*n) + e(40*n));

plot(Th,wait=1);

func u0 = 0;

real T=10, dt=0.0125 ;

real L2error, H1error;

func uexact = (T*(1+x)*(1+y)*(x+y))*(x+y<=0)+(T*(1-x)*(1-y)*(x+y))*(x+y>0);

real t;

func g = 0;

func f = ((1+x)*(1+y)*(x+y)+((t+dt)*(1+y)*(x+y)+(t+dt)*(1+x)*(1+y))

(2(t+dt)^2*(1+x)*(1+y)^2*(x+y)^2+2*(t+dt)^2*(1+x)^2*(1+y)^2

*(x+y))/(1+(t+dt)^2 *(1+x)^2*(1+y)^2*(x+y)^2)^2-2*(t+dt)*(1+y)/(1+(t+dt)^2

(1+x)^2(1+y)^2 *(x+y)^2)+((t+dt)*(1+x)*(x+y)+(t+dt)*(1+x)*(1+y))

(2(t+dt)^2*(1+x)^2*(1+y) *(x+y)^2+2*(t+dt)^2*(1+x)^2*(1+y)^2*(x+y))

/(1+(t+dt)^2*(1+x)^2*(1+y)^2 *(x+y)^2)^2-2*(t+dt)*(1+x)/(1+(t+dt)^2

(1+x)^2(1+y)^2*(x+y)^2))*(x+y<=0) +((1-x)*(1-y)*(x+y)+2*x*y^2*(-(t+dt)

162

```
*(1-y)*(x+y)+(t+dt)*(1-x)*(1-y)) +(2*(-x^2*y^2+1))*(t+dt)*(1-y)+2*x^2*y*(-
(t+dt)*(1-x)*(x+y) +(t+dt)*(1-x)*(1-y))+(2*(-x^2*y^2+1))*(t+dt)*(1-x))*(x+y>0);
fespace Vh(Th,P1);
Vh u,v,uu,uold=u0,uold1;
for( t=0;t<=0;t+=dt){
solve Poisson1(uold1,v,solver=LU) = int2d(Th)( uold1*v/dt + (1/(1+uold^2)
*(x+y<=0) + (1-x^2*y^2)*(x+y>0))*(dx(uold1) * dx(v) + dy(uold1) * dy(v))) -
int2d(Th)(f*v + uold*v/dt ) + on(a,uold1=0) + on(b,uold1=0) + on(c,uold1=0)
+ on(d,uold1=0) + on(e,uold1=0) ; }
Vh h = hTriangle; // get the size of all triangles
problem hermicc(uu,v)= int2d(Th)(1.5*uu*v/dt + (1/(1+(2*uold1-uold)^2)
(x+y<=0) + (1-x^2*y^2)*(x+y>0))*(dx(uu) * dx(v) + dy(uu) * dy(v)))-int2d(Th)
(2*uold1*v/dt) + int2d(Th)(0.5*uold*v/dt) -int2d(Th)(f*v) + on(e,uu=0)
+ on(a,uu=0) + on(b,uu=0)+on(c,uu=0)+ on(d,uu=0);
problem hemic(u,v)= int2d(Th)(1.5*u*v/dt + (1/(1+uu^2)*(x+y<=0) +
(1-x^2*y^2)*(x+y>0))*(dx(u) * dx(v) + dy(u) * dy(v))) - int2d(Th)(2*uold1*v/dt)
+ int2d(Th)(0.5*uold*v/dt) -int2d(Th)(f*v) + on(e,u=0) + on(a,u=0) + on(b,u=0)
+on(c,u=0)+ on(d,u=0);
ofstream ff("ther.dat");
for( t=dt;t<T;t+=dt){
hermicc; // here solve the thermic problem
hemic;
uu=u;
uold=uold1;
uold1=u; }
plot(u);
L2error= sqrt(int2d(Th)((u-uexact)^2));
Vh uuu = uexact;
plot(uuu) ;
```

H1error = sqrt(L2error^2 + int2d(Th)((dx(u)-dx(uuu))^2 + (dy(u)-dy(uuu))^2));

cout << "h = "<<h[ ].max<< endl;

cout << "L2 error = "<<L2error<< endl;

cout << "H1 error = "<<H1error<< endl;

Appendix J The FreeFEM++ code that produced Table 3.10

border a(t=-1.0,1.0){x=t; y=-1; label=1;};

border b(t=-1.0,1.0){x=1; y=t; label=2;};

border c(t=-1.0,1){x=-t; y=1; label=3;};

border d(t=-1.0,1){x=-1; y=-t;label=4;};

border aa(t=0,2*pi){x=0.5*cos(t); y=0.5*sin(t); label=5;};

real n= 4 ;

mesh Th = buildmesh (a(16*n) + b(16*n) + c(16*n) + d(16*n)+ aa(40*n));

plot(Th,wait=1);

func u0 = 0 ;

real T=60, dt=0.08 ;

real L2error, H1error;

func uexact = (5*(0.125-0.5*x^2-0.5*y^2)*sin(T)*(x^2+y^2<=0.25))

+((x^2-1)*(-y^2+1)*(x^2+y^2-.25)*sin(2*T))*(x^2+y^2>0.25);

real t;

func f = ((5*(.125-.5*x^2-.5*y^2))*cos(t)-(250*(0.125-0.5*x ^2-0.5*y^2))

*sin(t)^3 *x^2/(1+25*(.125-.5*x^2-.5*y^2)^2*sin(t)^2) +6250*(.125-.5*x^2-.5*y^2)^3

*sin(t)^5 *x^2/(1+25*(.125-.5*x^2-.5*y^2)^2*sin(t)^2)^2

+250*(.125-.5*x^2-.5*y^2)^2 *sin(t)^3/(1+25*(.125-.5*x^2-.5*y^2)^2*sin(t)^2)

-(250*(.125-.5*x^2-.5*y^2)) *sin(t)^3*y^2/(1+25*(.125-.5*x^2-.5*y^2)^2*sin(t)^2)

+6250*(.125-.5*x^2-.5*y^2)^3 *sin(t)^5*y^2/(1+25

*(0.125-.5*x^2-.5*y^2)^2*sin(t)^2)^2)*(x^2+y^2<=0.25)

+((2*(x^2-1))*(-y^2+1)*(x^2+y^2-0.25)*cos(2*t)+(1.0*(2*x*(-y^2+1)

164

*(x^2+y^2-.25)*sin(2*t)+(2*(x^2-1))*(-y^2+1)*x*sin(2*t)))*((4*(x^2-1))
*(-y^2+1)^2 *(x^2+y^2-.25)^2*sin(2*t)^2*x+4*(x^2-1)^2*(-y^2+1)^2*(x^2+y^2-
.25)*sin(2*t)^2*x)/(1+(x^2-1)^2*(-y^2+1)^2*(x^2+y^2-.25)^2
*sin(2*t)^2)^2-(1.0*((2*(-y^2+1))*(x^2+y^2-.25)*sin(2*t)+8*x^2*(-y^2+1)
*sin(2*t)+(2*(x^2-1))*(-y^2+1)*sin(2*t)))/(1+(x^2-1)^2*(-y^2+1)^2
*(x^2+y^2-.25)^2*sin(2*t)^2)+(1.0*(-(2*(x^2-1)) *y*(x^2+y^2-.25)*sin(2*t)
+(2*(x^2-1))*(-y^2+1)*y*sin(2*t)))*(-4*(x^2-1)^2*(-y^2+1)*(x^2+y^2-.25)^2
*sin(2*t)^2*y+4*(x^2-1)^2*(-y^2+1)^2*(x^2+y^2-.25)*sin(2*t)^2*y)/(1+(x^2-1)^2*(-
y^2+1)^2*(x^2+y^2-.25)^2*sin(2*t)^2)^2-(1.0*(-(2*(x^2-1))*(x^2+y^2-.25)*sin(2*t)-
(8*(x^2-1))*y^2*sin(2*t)+(2*(x^2-1))*(-y^2+1)*sin(2*t)))/(1+(x^2-1)^2*(-y^2+1)^2
(x^2+y^2-.25)^2*sin(2*t)^2))*(x^2+y^2>0.25) ;

func g1 = 0;

fespace Vh(Th,P1); Vh u,v,uold=u0,uold1,uold2,uold3;

for(t=dt/4;t<=dt/4;t+=dt){

solve Poisson1(uold1,v,solver=LU) = int2d(Th)(uold1*v/dt + ((uold^2/(1+uold^2))

(x^2+y^2<=0.25) + ((1/(1+(uold)^2))(x^2+y^2>0.25))) *(dx(uold1)*dx(v) +

dy(uold1)*dy(v))) - int2d(Th)(f*v + uold*v/dt) + on(a,uold1=0) + on(b,uold1=0)

+ on(c,uold1=0) + on(d,uold1=0) + on(aa,uold1=0) ; }

for(t=dt/2;t<=dt/2;t+=dt){

solve Poisson2(uold2,v,solver=LU) = int2d(Th)(1.5*uold2*v/dt + ((((2*uold1-

uold)^2)/(1+(2*uold1-uold)^2))*(x^2+y^2<=0.25) + (1/(1+(2*uold1-uold)^2))

(x^2+y^2>0.25))(dx(uold2)*dx(v) + dy(uold2)*dy(v)))

- int2d(Th)(f*v + 2*uold1*v/dt - 0.5*uold*v/dt) + on(a,uold2=0) + on(b,uold2=0)

+ on(c,uold2=0) + on(d,uold2=0) + on(aa,uold2=0) ; }

for(t=3*dt/4;t<=3*dt/4;t+=dt){

solve Poisson3(uold3,v,solver=LU) = int2d(Th)(11*uold3*v/(6*dt) + ((((3*uold2-

3*uold1+uold)^2)/(1+(3*uold2-3*uold1+uold)^2))*(x^2+y^2<=0.25)

+ (1/(1+(3*uold2-3*uold1+uold)^2))*(x^2+y^2>0.25))*(dx(uold3)*dx(v)

+ dy(uold3)*dy(v))) - int2d(Th)(f*v + 3*uold2*v/dt - 1.5*uold1*v/dt

+ uold*v/(3*dt)) + on(a,uold3=0) + on(b,uold3=0)

+ on(c,uold3=0) + on(d,uold3=0) + on(aa,uold3=0) ; }

Vh h = hTriangle ; // get the size of all triangles

problem thermiccc(u,v)= int2d(Th)(25*u*v/(12*dt)

+ ((((4*uold3-6*uold2+4*uold1-uold)^2)/(1+(4*uold3-6*uold2+4*uold1-uold)^2))

*(x^2+y^2<=0.25) + (1/(1+(4*uold3-6*uold2+4*uold1-uold)^2))*(x^2+y^2>0.25)

)*(dx(u) * dx(v) + dy(u) * dy(v))) - int2d(Th)(f*v) + int2d(Th)(-4*uold3*v/dt

+ 3*uold2*v/dt - 4*uold1*v/(3*dt)) + int2d(Th)(uold*v/(4*dt)) + on(aa,u=0)

+ on(a,u=0) + on(b,u=0) + on(c,u=0) + on(d,u=0);

ofstream ff("thermiccc.dat");

for(t=dt;t<=T;t+=dt){

thermiccc; // here solve the therm problem

uold=uold1;

uold1 = uold2;

uold2=uold3;

uold3=u; }

plot(u);

L2error= sqrt(int2d(Th)((u-uexact)^2));

Vh uu = uexact;

plot(uu) ;

Vh zzz = uexact-u;

plot(zzz);

H1error = sqrt(L2error^2 + int2d(Th)((dx(u)-dx(uu))^2 + (dy(u)-dy(uu))^2));

cout << "h = "<<h[].max<< endl;

cout << "L2 error = "<<L2error<< endl;

cout << "H1 error = "<<H1error<< endl;

Appendix K The XML code that produced Table 4.1

<?xml version="1.0" encoding="UTF-8"?>

```
<NEKTAR xmlns:xsi="http://www.w3.org/2001/XMLSchema-instance"
xsi:noNamespaceSchemaLocation="http://www.nektar.info/schema/nektar.xsd">
<GEOMETRY DIM="2" SPACE="2">
<VERTEX>
<V ID="0"> -1.0 -1.0 0.0 </V>
<V ID="1"> 0.0 -1.0 0.0 </V>
<V ID="2"> 1.0 -1.0 0.0 </V>
<V ID="3"> -1.0 0.0 0.0 </V>
<V ID="4"> 0.0 0.0 0.0 </V>
<V ID="5"> 1.0 0.0 0.0 </V>
<V ID="6"> -1.0 1.0 0.0 </V>
<V ID="7"> 0.0 1.0 0.0 </V>
<V ID="8"> 1.0 1.0 0.0 </V>
</VERTEX>
<EDGE>
<E ID="0"> 0 1 </E>
<E ID="1"> 1 2 </E>
<E ID="2"> 0 3 </E>
<E ID="3"> 0 4 </E>
<E ID="4"> 1 4 </E>
<E ID="5"> 1 5 </E>
<E ID="6"> 2 5 </E>
<E ID="7"> 3 4 </E>
<E ID="8"> 4 5 </E>
<E ID="9"> 3 6 </E>
<E ID="10"> 3 7 </E>
<E ID="11"> 4 7 </E>
<E ID="12"> 4 8 </E>
<E ID="13"> 5 8 </E>
```

<E ID="14"> 6 7 </E>

<E ID="15"> 7 8 </E>

</EDGE>

<ELEMENT>

<T ID="0"> 0 4 3 </T>

<T ID="1"> 4 5 8 </T>

<T ID="2"> 1 6 5 </T>

<T ID="3"> 8 13 12 </T>

<T ID="4"> 12 15 11 </T>

<T ID="5"> 7 11 10 </T>

<T ID="6"> 10 14 9 </T>

<T ID="7"> 7 2 3 </T>

</ELEMENT>

<COMPOSITE>

<C ID="0"> T[0,1,2,7] </C>

<C ID="1">T[3,4,5,6] </C>

<C ID="2"> E[0,1,2,6,7,8] </C>

<C ID="3"> E[9,13,14,15,7,8] </C>

</COMPOSITE>

<DOMAIN> C[0]</DOMAIN>

</GEOMETRY>

<EXPANSIONS>

<E COMPOSITE="C[0]" NUMMODES="7" FIELDS="u" TYPE="MODIFIED"
POINTSTYPE="GaussLobattoLegendre"/>

</EXPANSIONS>

<CONDITIONS>

<SOLVERINFO>

<I PROPERTY="EQTYPE" VALUE="UnsteadyAdvectionDiffusion"/>

<I PROPERTY="Projection" VALUE="Continuous"/>

```xml
<I PROPERTY="HOMOGENEOUS" VALUE="1D"/>
<I PROPERTY="DiffusionAdvancement" VALUE="Implicit"/>
<I PROPERTY="AdvectionAdvancement" VALUE="Explicit"/>
<I PROPERTY="TimeIntegrationMethod" VALUE="IMEXOrder2"/>
</SOLVERINFO>
<PARAMETERS>
<P> TimeStep = 0.0001 </P>
<P> FinalTime = 5 </P>
<P> NumSteps = FinalTime/TimeStep </P>
<P> IO_CheckSteps = 1000 </P>
<P> IO_InfoSteps = 1000 </P>
<P> wavefreq = 0 </P>
<P> epsilon = 1/(20*PI∧2) </P>
<P> LZ=0.01</P>
<P>HomModesZ=2</P>
</PARAMETERS>
<VARIABLES>
<V ID="0"> u </V>
</VARIABLES>
<BOUNDARYREGIONS>
<B ID="0"> C[2] </B>
</BOUNDARYREGIONS>
<BOUNDARYCONDITIONS>
<REGION REF="0">
<D VAR="u" USERDEFINEDTYPE="TimeDependent" VALUE="0"/>
</REGION>
</BOUNDARYCONDITIONS>
<FUNCTION NAME="AdvectionVelocity">
<E VAR="Vx" VALUE="0.0"/>
```

```
<E VAR="Vy" VALUE="0.0"/>
<E VAR="Vz" VALUE="0.0"/>
</FUNCTION>
<FUNCTION NAME="InitialConditions">
<E VAR="u" VALUE="sin(PI*x)*sin(PI*y)"/>
</FUNCTION>
<FUNCTION NAME="ExactSolution">
<E VAR="u" VALUE="exp(-FinalTime /10)*sin(PI*x)*sin(PI*y)"/>
</FUNCTION>
</CONDITIONS>
</NEKTAR>


<?xml version="1.0" encoding="UTF-8"?>
<NEKTAR xmlns:xsi="http://www.w3.org/2001/XMLSchema-instance"
xsi:noNamespaceSchemaLocation="http://www.nektar.info/schema/nektar.xsd">
<GEOMETRY DIM="2" SPACE="2">
<VERTEX>
<V ID="0"> -1.0 -1.0 0.0 </V>
<V ID="1"> -0.5 -1.0 0.0 </V>
<V ID="2"> 0.0 -1.0 0.0 </V>
<V ID="3"> 0.5 -1.0 0.0 </V>
<V ID="4"> 1.0 -1.0 0.0 </V>
<V ID="5"> -1.0 -0.5 0.0 </V>
<V ID="6"> -0.5 -0.5 0.0 </V>
<V ID="7"> 0.0 -0.5 0.0 </V>
<V ID="8"> 0.5 -0.5 0.0 </V>
<V ID="9"> 1.0 -0.5 0.0 </V>
<V ID="10"> -1.0 0.0 0.0 </V>
```

```
<V ID="11"> -0.5 0.0 0.0 </V>
<V ID="12"> 0.0 0.0 0.0 </V>
<V ID="13"> 0.5 0.0 0.0 </V>
<V ID="14"> 1.0 0.0 0.0 </V>
<V ID="15"> -1.0 0.5 0.0 </V>
<V ID="16"> -0.5 0.5 0.0 </V>
<V ID="17"> 0.0 0.5 0.0 </V>
<V ID="18"> 0.5 0.5 0.0 </V>
<V ID="19"> 1.0 0.5 0.0 </V>
<V ID="20"> -1.0 1.0 0.0 </V>
<V ID="21"> -0.5 1.0 0.0 </V>
<V ID="22"> 0.0 1.0 0.0 </V>
<V ID="23"> 0.5 1.0 0.0 </V>
<V ID="24"> 1.0 1.0 0.0 </V>
</VERTEX>
<EDGE>
<E ID="0"> 0 1 </E>
<E ID="1"> 1 2 </E>
<E ID="2"> 2 3 </E>
<E ID="3"> 3 4 </E>
<E ID="4"> 0 5 </E>
<E ID="5"> 0 6 </E>
<E ID="6"> 1 6 </E>
<E ID="7"> 1 7 </E>
<E ID="8"> 2 7 </E>
<E ID="9"> 2 8 </E>
<E ID="10"> 3 8 </E>
<E ID="11"> 3 9 </E>
<E ID="12"> 4 9 </E>
```

171

<E ID="13"> 5 6 </E>

<E ID="14"> 6 7 </E>

<E ID="15"> 7 8 </E>

<E ID="16"> 8 9 </E>

<E ID="17"> 5 10 </E>

<E ID="18"> 5 11 </E>

<E ID="19"> 6 11 </E>

<E ID="20"> 6 12 </E>

<E ID="21"> 7 12 </E>

<E ID="22"> 7 13 </E>

<E ID="23"> 8 13 </E>

<E ID="24"> 8 14 </E>

<E ID="25"> 9 14 </E>

<E ID="26"> 10 11 </E>

<E ID="27"> 11 12 </E>

<E ID="28"> 12 13 </E>

<E ID="29"> 13 14 </E>

<E ID="30"> 10 15 </E>

<E ID="31"> 10 16 </E>

<E ID="32"> 11 16 </E>

<E ID="33"> 11 17 </E>

<E ID="34"> 12 17 </E>

<E ID="35"> 12 18 </E>

<E ID="36"> 13 18 </E>

<E ID="37"> 13 19 </E>

<E ID="38"> 14 19 </E>

<E ID="39"> 15 16 </E>

<E ID="40"> 16 17 </E>

<E ID="41"> 17 18 </E>

<E ID="42"> 18 19 </E>

<E ID="43"> 15 20 </E>

<E ID="44"> 15 21 </E>

<E ID="45"> 16 21 </E>

<E ID="46"> 16 22 </E>

<E ID="47"> 17 22 </E>

<E ID="48"> 17 23 </E>

<E ID="49"> 18 23 </E>

<E ID="50"> 18 24 </E>

<E ID="51"> 19 24 </E>

<E ID="52"> 20 21 </E>

<E ID="53"> 21 22 </E>

<E ID="54"> 22 23 </E>

<E ID="55"> 23 24 </E>

</EDGE>

<ELEMENT>

<T ID="0"> 4 5 13 </T>

<T ID="1"> 0 6 5 </T>

<T ID="2"> 6 7 14 </T>

<T ID="3"> 1 8 7 </T>

<T ID="4"> 8 9 15 </T>

<T ID="5"> 2 10 9 </T>

<T ID="6"> 10 11 16 </T>

<T ID="7"> 3 12 11 </T>

<T ID="8"> 17 18 26 </T>

<T ID="9"> 13 19 18 </T>

<T ID="10"> 19 20 27 </T>

<T ID="11"> 14 21 20 </T>

<T ID="12"> 21 22 28 </T>

<T ID="13"> 15 23 22 </T>

<T ID="14"> 23 24 29 </T>

<T ID="15"> 16 25 24 </T>

<T ID="16"> 30 31 39 </T>

<T ID="17"> 26 32 31 </T>

<T ID="18"> 32 33 40 </T>

<T ID="19"> 27 34 33 </T>

<T ID="20"> 34 35 41 </T>

<T ID="21"> 28 36 35 </T>

<T ID="22"> 36 37 42 </T>

<T ID="23"> 29 38 37 </T>

<T ID="24"> 44 52 43 </T>

<T ID="25"> 39 45 44 </T>

<T ID="26"> 45 46 53 </T>

<T ID="27"> 40 47 46 </T>

<T ID="28"> 47 48 54 </T>

<T ID="29"> 41 49 48 </T>

<T ID="30"> 49 50 55 </T>

<T ID="31"> 42 51 50 </T>

</ELEMENT>

<COMPOSITE>

<C ID="0"> T[0-15] </C>

<C ID="1"> T[16-31] </C>

<C ID="2"> E[0,1,2,3,4,12,17,25,26,27,28,29] </C>

<C ID="3"> E[26,27,28,29,30,38,43,51,52,53,54,55] </C>

</COMPOSITE>

<DOMAIN> C[0] </DOMAIN>

</GEOMETRY>

<EXPANSIONS>

```
<E COMPOSITE="C[0]" NUMMODES="7" FIELDS="u" TYPE="MODIFIED"
POINTSTYPE="GaussLobattoLegendre"/>
</EXPANSIONS>
<CONDITIONS>
<SOLVERINFO>
<I PROPERTY="EQTYPE" VALUE="UnsteadyAdvectionDiffusion"/>
<I PROPERTY="Projection" VALUE="Continuous"/>
<I PROPERTY="HOMOGENEOUS" VALUE="1D"/>
<I PROPERTY="DiffusionAdvancement" VALUE="Implicit"/>
<I PROPERTY="AdvectionAdvancement" VALUE="Explicit"/>
<I PROPERTY="TimeIntegrationMethod" VALUE="IMEXOrder2"/>
</SOLVERINFO>
<PARAMETERS>
<P> TimeStep = 0.0001 </P>
<P> FinalTime = 5 </P>
<P> NumSteps = FinalTime/TimeStep </P>
<P> IO_CheckSteps = 1000 </P>
<P> IO_InfoSteps = 1000 </P>
<P> wavefreq = 0 </P>
<P> epsilon = 1/(20*PI^2) </P>
<P> LZ=0.01</P>
<P>HomModesZ=2</P>
</PARAMETERS>
<VARIABLES>
<V ID="0"> u </V>
</VARIABLES>
<BOUNDARYREGIONS>
<B ID="0"> C[2] </B>
</BOUNDARYREGIONS>
```

```
<BOUNDARYCONDITIONS>
<REGION REF="0">
<D VAR="u" USERDEFINEDTYPE="TimeDependent" VALUE="0"/>
</REGION>
</BOUNDARYCONDITIONS>
<FUNCTION NAME="AdvectionVelocity">
<E VAR="Vx" VALUE="0.0"/>
<E VAR="Vy" VALUE="0.0"/>
<E VAR="Vz" VALUE="0.0"/>
</FUNCTION>
<FUNCTION NAME="InitialConditions">
<E VAR="u" VALUE="sin(PI*x)*sin(PI*y)"/>
</FUNCTION>
<FUNCTION NAME="ExactSolution">
<E VAR="u" VALUE="exp(-FinalTime /10)*sin(PI*x)*sin(PI*y)"/>
</FUNCTION>
</CONDITIONS>
</NEKTAR>
```